THE INFLUENCE OF FORCES GENERATED DURING GAIT ON THE CLINICAL APPEARANCE AND PHYSICAL PROPERTIES OF SKIN CALLUS

KATHRYN SPRINGETT

A thesis submitted in partial fulfilment of the requirements
of the University of Brighton for the degree of
Doctor of Philosophy

April 1993

The University of Brighton in collaboration with
Scholl PLC

Abstract

The influence of forces generated during gait in the clinical appearance and physical properties of skin callus.

Plantar skin callus plaques are a common, frequently painful hyperkeratotic condition affecting a number of the population and these hard, dense, yellowish, cutaneous lesions may even be sufficiently severe to limit working practices and social activities. Pathological callus formation is thought, empirically from clinical observation, to be due to excess intermittent pressure during gait, associated frequently with a structural or functional anomaly of the foot and leg.

Studies into callus pathology are relatively few and have been concerned mainly with the structure and ultrastructure of callus tissue. The biomechanical features of plantar skin callus have been studied and results show it behaves differently from normal plantar and hairy skin. The current work extends the understanding of plantar skin calluses, their aetiology and pathology, utilising techniques, with some novel applications, from a number of fields.

The mechanical forces exerted on the callused foot at the time of lesion loading were studied using the Kistler force and Musgrave pressure measurement plates. The duration of loading of the lesion was found to be increased compared with that of a normally functioning foot ($p = 0.05$). It was not possible to attribute reactive forces exerted on the foot at the time of loading to the lesion site, as appropriate technological advances have yet to be made. No predominant force vector was found which could be associated with the clinical appearance of plantar callus plaques. The clinical appearance of the callus lesion cannot therefore be used as an indicator of influential mechanical stresses. There is no relationship between either the dominant side and callus incidence on left or right feet or the different skin ridging patterns (dermatoglyphics) of callus lesions and their viscoelasticity. However, the results from rheological studies of this tissue suggested that the viscoelastic properties of areas of the stratum corneum within the callus plaque may be influential in the formation of the dermatoglyphic patterns found in these lesions.

Fourier Transform Infrared Spectrometry was used to provide fundamental information for the rheological studies on plantar skin callus tissue and also confirmed the clinical assumption that callus tissue had a lower water content than normal plantar skin. A-scan ultrasound skin imaging (Dermal Depth Detector) with which it was hoped to quantify the topographical features of the lesion was not successful, probably due to the limitations of the instrument and transducer in this application, rather than the technique in general. Light microscopical examination of plantar callus sections was in general agreement with previous studies. The most notable feature was the disruption or absence of the granular layer in callus and corns respectively.

A model for callus formation has been proposed partly as a result of the information generated during the course of study. An accelerated transit rate of callus keratinocytes is likely to result in cell immaturity on reaching the stratum corneum since differentiation will not have had time to be completed. Thus a number of differences in plantar callus will be evident, such as altered cell cohesion and desquammation.

The results of this work will provide useful data which may direct further studies into suitable therapeutic modalities, thus extending the range of methods available for treatment of this common condition.

CONTENTS

CHAPTER 6

Discussion of investigations undertaken over scope of thesis

References

Appendices

List of tables

List of figures

Glossary

Acknowledgements

Professor Christopher Marriott, Director of Studies, Head of Department, Pharmacy Department, King's College London has been extra-ordinarily helpful during the entire development and writing of this thesis. His guidance has been invaluable.

The help given by Dr Richard White, Assistant Director, European Clinical Trials, ConvaTec UK Ltd, in providing direction and contacts for the work undertaken in this thesis was essential. His contribution to the content is greatly appreciated, as was the loan, by ConvaTec WHRI, of the Dermascan C.

Dr David Melcher and Mrs Linsay Dixon of the Histology Department, Royal Sussex County Hospital, Brighton kindly lent their knowledge, skills and facilities for the histology work on normal plantar skin and callus.

The use of the facilities in both the Departments of Podiatry and Pharmacy, University of Brighton was central to the the studies undertaken. Especial thanks are due to Mr Michael Potter and Mr Ivan Birch of the Department of Podiatry for their contributions, particularly with the section on gait analysis. The help provided by the Course Resources Officer, Mrs Julia Paul and Resource Assistant, Miss Alison Paul, was totally supportive.

Thanks are also due to Mr Keith Parramore of the Department of Mathematical Sciences, Dr Andrew Lloyd, Dr Howard Dodd and Mrs Heather Duffield of the Pharmacy Department, and to the two Heads of Department involved, Dr Linda Lang and Dr Stephen Denyer.

Discussions on the thesis content with Dr Paul Wilkes, Manager, Clinical Regulatory Affairs, Scholl PLC, proved useful and encouraging, particularly at times of disillusion.

Some un-published work from my students should also be acknowledged, in Laser Doppler Imaging of plantar callus lesions (Miss M. Dowsett), FTIR *in vivo* of plantar skin (Mr J. Jevans), and sweat duct density in callus plaques (Mr S. Spooner, Mr M.Ballard and Miss H. Shepherd).

Finally, thanks are due to my colleagues, in the Department of Podiatry, who have supported and encouraged me throughout.

This work is dedicated to my children, without whose eager, loving help, the thesis would have been completed in half the time.

CHAPTER 1

Skin, plantar forefoot calluses, their formation and management.

1. Introduction

Skin is a remarkable organ and in its normal state forms a tough, pliable, resilient interface with the environment which is also capable of deforming to its contact surface. However, those suffering with a skin disorder frequently complain of difficulty maintaining their normal life style, due to pain or infection (Graham-Brown and Burns 1990). Hard skin (calluses) and corns are minor yet debilitating cutaneous conditions affecting the feet of a large number of people. A survey of employees of a large organisation in the South East of England indicated that 18% of these workers (age range 19 - 65 years) suffered or had suffered with corns or calluses (Whiting 1987). Popular demand for footcare products is such that a number of pharmaceutical companies (for example Scholl and Boots) supply retail outlets with a suitable range of products, intimating these conditions are common. Podiatrists and non-state registered chiropodists[1] spend much of their professional time treating these conditions and unpublished data appears to support this assertion. However a multicentre survey of a large group of people is required to identify, definitively, the prevalence of these conditions across the UK and within different ethnic groups.

Corns and calluses are a problem for a proportion of the working population and such conditions may make a significant, albeit indirect, contribution to time off work. The alteration in walking style (gait) consequential to these lesions invariably causes abnormal stresses on other parts of the body

1
(In recent years the English title "chiropody/chiropodist" has been changing to that used by most countries in the world - podiatry/podiatrist (or derivations such as podologie/podologiste) - to indicate a professional who has expertise in managing conditions of the lower limb and foot and holds a qualification recognised by the State.)

(Neale 1989) resulting in further aches and pains in the load bearing structures of the body. Knee joint pain and low back pain are frequent complaints related to gait anomaly (Root et al 1977). Small changes in gait cause sequential and proportionately greater joint movement as each leg segment becomes involved in compensating for the anomaly in the distal part of the locomotor system (the foot) (Inman et al 1981).

Thus a minor foot problem which causes a small change in foot function can effect relatively large changes in, for example, the sacro-iliac joint. These may manifest as chronic or acute back pain due to sciatic nerve irritation or entrapment or degenerative changes in the sacro-iliac joint. In an occupation which demands physical activity, back pain may make working intolerable and time off work will be consequent. The number of working days lost through back pain is considerable (Stubbs 1982, Abenhaim and Suissa 1987). Though currently there is no published data relating this problem directly to an aetiology of gait anomaly, it is accepted that gait anomaly is associated with low back pain (Root et al 1977).

Mobility in the elderly is essential as opportunities for social interaction are very limited if the individual is confined to one small geographical area. The emotional effects of such isolation are well documented (Kemp and Winkler 1983, Davies 1984). Reluctance to walk any distance to shop or to rely on others can mean that dietary intake is restricted to storable foods, the nutritional quality of which may not be suitably balanced (Davies 1981). For people who suffer with diseases such as diabetes mellitus or rheumatoid arthritis, the development of plantar calluses is particularly important as these lesions may often be a precursor of ulceration (Tappin et al 1980, Adams et al 1989). Development of ulceration is distressing for the

patient as well as being costly in time and dressings (Harkiss 1985, Savage and Jordon 1986).

Children rarely form calluses on their feet, although those who do need early management, otherwise the problem often becomes so severe that it might influence their life considerably. Painful feet can affect the quality of life and choice of occupation.

A healthy individual may also find corns and calluses become a problem. Quality of life involving sport as part of leisure activity is dependent upon having a comfortably functioning locomotor system. Playing squash, for example, pivoting for shots on a painful area of plantar callus is most inhibiting and eventually an alternative, less energetic social activity may be sought (Sperryn and Williams 1982, Yaffe 1986). Thus, lack of physical exercise, which is contrary to the advice offered by the British Heart Foundation and Health Education Council, may be associated, indirectly, with plantar calluses.

1.2 A brief history of the management of plantar calluses

Humans and their ancestors have been bipedal for at least 3.4 million years and fossil footprints in what was volcanic ash at Laetoli, Tanzania, indicate the foot has changed very little since that time (Johanson and Maitland 1981). The primary function of the foot is to provide the body with both support and a method of locomotion (Neale 1989). The sensory and musculo-skeletal systems of the foot are complex, allowing it to accommodate to different contact surfaces, to absorb shock on heel strike with the ground and transform into a rigid lever to permit propulsion at toe-off. The foot must also follow the conditions imposed upon it by the leg

muscles and the rest of the body, yet still provide stable, efficient support when required. Thus during the gait cycle, the foot is required to change function, converting from a loose, shock absorbing structure to a rigid lever and even a few, minor disorders of the locomotor system are sufficient to derange function causing pain and loss of efficiency.

The minor skin complaint of having painful corns and calluses can now be seen to have important repercussions. Treatment of these conditions satisfactorily will block a chain of problems which affect quality of life and cost society in terms of time, money and effort.

Podiatrists, general practitioners and pharmacists may be consulted about the treatment of plantar skin calluses, but alternatively, footcare products are available for purchase in a variety of outlets. The restricted nature of proprietary products obtainable for treatment of corns and calluses may be considered indicative of the relatively limited understanding of these conditions. A combination of protective padding and salicylic acid paste, or each alone, form, in general, the range of available products (no unbiased information is available on the success rate of this form of management, though such studies are being carried out currently). The field of podiatry, which encompasses surgery, medicine, social aspects of care, structure and function of the locomotor system, and skin and its abnormalities, has a wide range of therapies available for the management of plantar calluses and corns. However, selection of treatment option is based, generally, on historical clinical observation and long term demonstration of the worthiness of the technique.

Corns and callus are not a feature of today's society alone and chiropody has been practiced for centuries (Rhodes 1985). Many remedies have

been tried for such lesions, and an extract from a book by Nicholas Laurent Laforest (1782) describes the treatment of that time for calluses:

> (translation from the French).
> "Sometimes sweat and the continuous compression of the shoes causes an excessive heat on the sole of the foot and pain so severe, that often it prevents sleep. In this case one must take:
> Some Green Mousse (the sort which forms around boats)
> Fricassee this Mousse with some Pork Grease
> Apply this under the sole of the foot and it will result in a radical cure."

Currently, the range of therapeutic modalities utilised by podiatrists to manage corns and calluses tends to be based upon "tried and tested" regimes rather than the informed development of treatments based upon an understanding of the pathogenesis of calluses. This is not surprising as investigations into the pathology of this tissue have been relatively few and the information generated commensurate with this lack. The histology of callus, cell kinetics (Thomas et al 1985), and electron-micrographic (EM) structure (Mackenzie 1983) have been reported. Other areas of investigation reported include the effects of hydration on callus (Spencer 1976, Hey et al 1978), the biomechanical characteristics of plantar skin (Ferguson 1980) and biochemical differences in callus compared with normal plantar skin (Lundstrom and Egelrud 1990, Camp 1991). The present study will review the literature relevant to each area of study in the current work, and each will be presented within the appropriate chapter.

In brief, podiatric methods of managing of corns and callus include diagnosing and removing the cause (if possible), removal of the superficial layers of this hyperkeratinised tissue with a scalpel, and enucleation of

corns where appropriate, assessment and management of the mechanical aetiology (Adams et al 1989), application of topical preparations (for example, keratolytics and emollients) and use of physical therapies such as therapeutic ultrasound. Selection of the therapeutic modality is influenced by the patient's systemic or peripheral condition, their requirements and the expectations of treatment. Some therapeutic progress in the management of corns and callus has been made by utilising clinically perceivable characteristics such as the effect of occlusion on callus tissue pliability (Springett 1987).

In the early part of this century, education for chiropodists began to require an academic as well as practical understanding of the conditions affecting the feet and the lower limb, in part to improve the management options available to the patient. Gradually the profession began to acquire the academic acumen required for scientific study, and investigations into subjects of interest and specifically relevant to podiatry are now being undertaken. The present work is directed towards two areas of podiatry, locomotor biomechanics and skin biology, and the investigation of empirical observations on the aetiology of callus formation (Adams et al 1989) which need substantiating. Application of knowledge gained in these studies should advance the currently limited understanding of this common cutaneous podiatric condition and contribute further to the management of plantar calluses.

The forthcoming sections describe the skin's morphology, with particular reference to plantar skin as a precursor to the consideration of the use of ultrasound imaging and histology in investigating callus lesions. A background follows as an introduction to investigations to be carried out in

the present work within which the influence of force vector on callus clinical appearance and viscoelasticity are investigated.

1.3 The human skin, epidermis and stratum corneum

Skin, in its normal state it interacts with the environment, permitting the body to function optimally at all times (Wood and Bladon 1986). Its viscoelastic structure (Vincent 1982) allows the skin to deform under load rather than puncture if traumatised, and it can renew itself to maintain its integrity.

One of the skin's many functions is to protect the rest of the body from trauma, whether it be chemical, thermal, physical or invasion by pathogens. Certain areas of the skin's surface are differentiated to fulfil a specific protective function where the skin is particularly prone to mechanical damage, for example, palmar or plantar skin (Wilkes et al 1973, Ferguson 1980). In some sites, the skin demonstrates variation in surface topography, for example the skin ridging on finger tip to improve grip (Buchholz et al 1988).

The skin is composed of two main layers (figures 1.3.1 and 1.3.2). Outermost is the epidermis which is separated from the deeper layer, the dermis, by the dermo-epidermal junction (DEJ). Beneath the dermis lies the adipose tissue and fascia of the hypodermis. In human skin, the thickness of the layers is not consistent and up- and downward projections of one layer into the other are frequent, particularly in the dermis and adipose tissue. Thickness also varies with site (Wilkes et al 1973, Ferguson 1980).

The dermis provides the main viscoelastic nature of the skin (Vincent 1982). It is sub-divided into two layers, although the interface between the two is

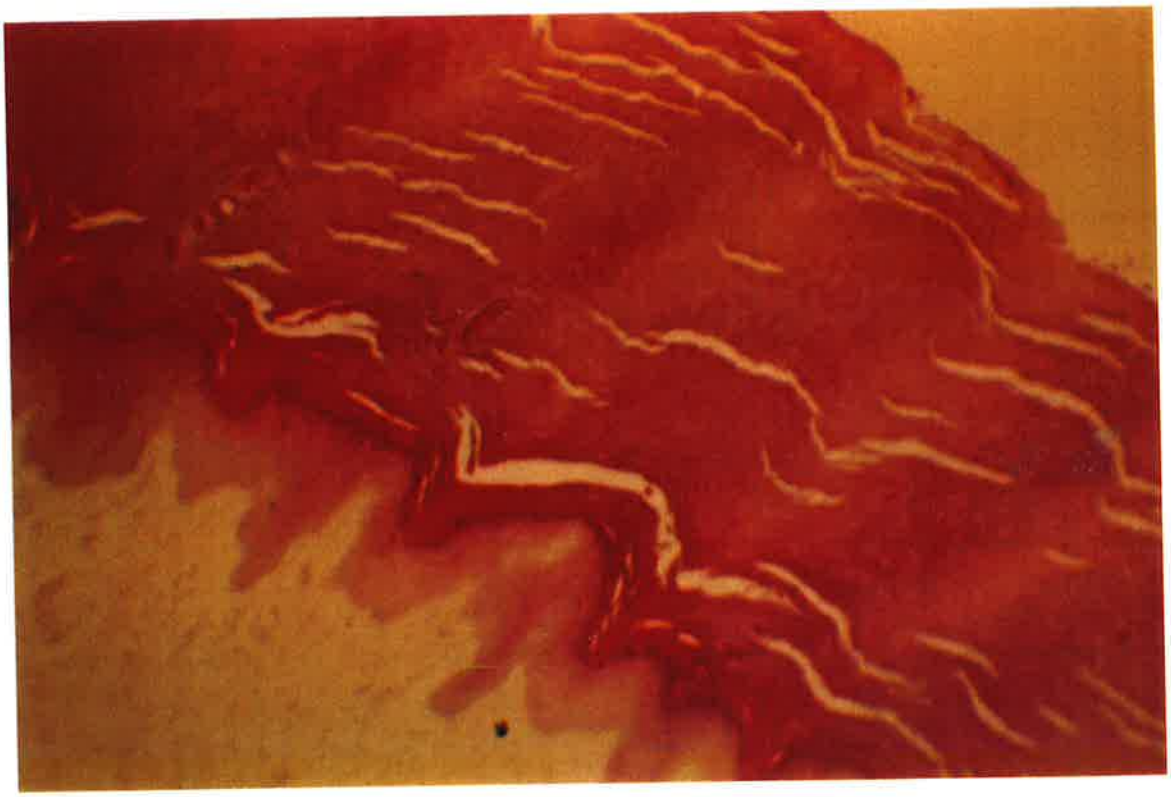

Figure 1.3.1
Light micrograph of normal plantar skin, stained with haematoxylin and eosin. (x 47.)

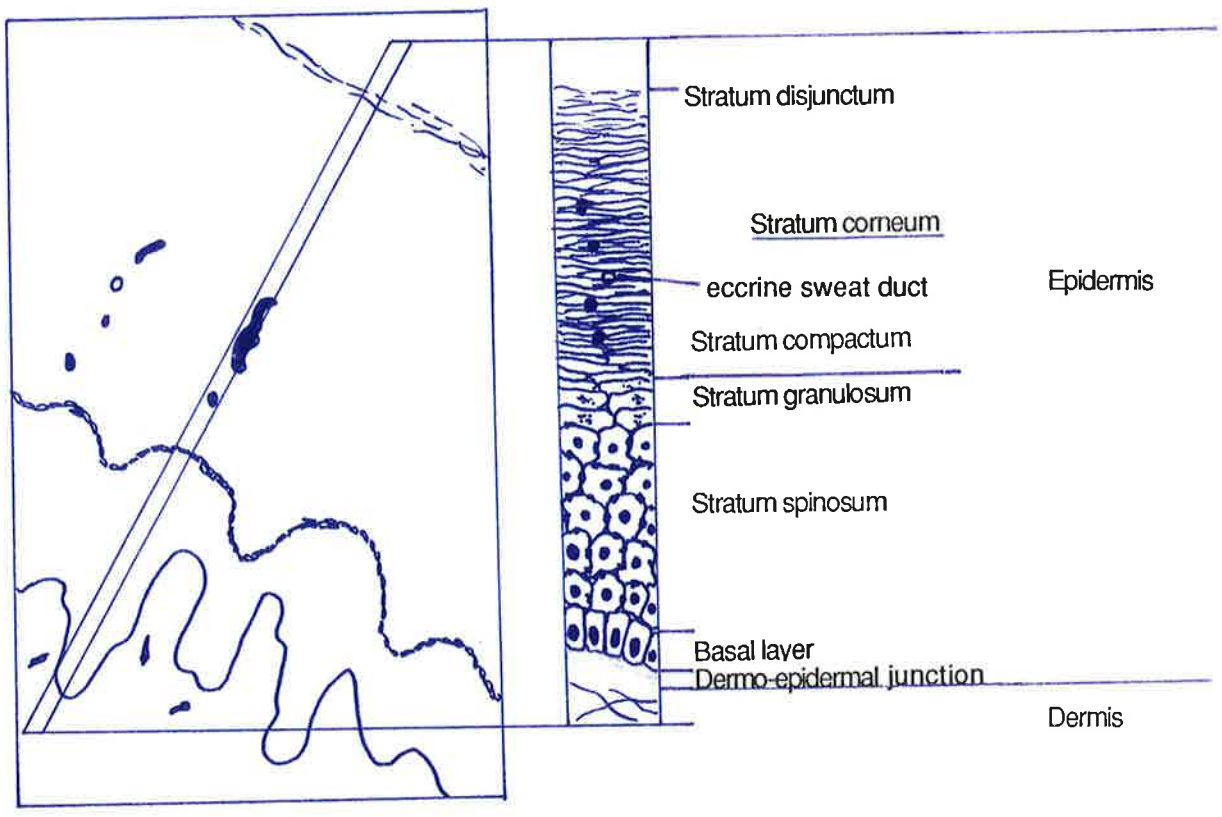

Figure 1.3.2
Diagram of plantar skin and its component layers (not to scale).

not readily distinguishable. The upper, papillary dermis is less fibrous than the lower reticular dermis and is less echodense on ultrasound imaging than the deeper layer. The fibrous components of the dermis include collagen and elastin: the former fibrous protein takes load under stress preventing tearing of the integument, whilst the latter being an elastic protein, permits restoration of normal skin configuration on stress release (Wood and Bladon 1986). These fibrous proteins are supported in an amorphous glycosaminoglycans dermal matrix, along with cells (macrophages, fibrocytes) and structures such as blood vessels and nerve fibres. The dermal morphology changes with age (Lavker et al 1989, Smith 1989) and disease such as diabetes (Graham-Brown and Burns 1990). However, the current work is intended to concentrate on the skin, particularly the epidermis and the local cutaneous pathology of plantar skin calluses in otherwise healthy individuals.

1.3.1 The epidermis

The epidermis is a stratified, keratinised squamous epithelium and includes a number of specialised cells (Merkel, Langerhans cells and melanocytes) within its structure. Its prime function is concerned with formation and preservation of the skin barrier (Potts and Francoeur 1990). As illustrated in figure 1.3.1, the epidermis is sub-divided into four main layers, with the stratum corneum further divided into the lower, younger stratum compactum (stratum lucidum) and the outermost stratum disjunctum where the corneocytes are shed (desquammate). Hairy skin epidermal sections studied under light microscopy (LM) show the stratum corneum to have an artifactual loose appearance (basket weave) whereas palmar and plantar skin stratum corneum appears denser and is sometimes referred to as "brick keratin". The healthy epidermis is a flexible structure capable of deforming to external stresses, yet able to restore to normal configuration

(Wood and Bladon,1986). In skin disorders, this feature is often lost and the break in the skin barrier may result in pain and infection. The need to manage skin pathologies has triggered study of skin morphology, biochemistry and biomechanics so that clinicians may understand skin diseases more fully in order that management may be more effective (Marks et al 1981).

To maintain the skin barrier, the body's primary barrier to the environment, the normal epidermis, is in a continuous state of renewal through the process of keratinisation (Wertz and Downing 1989). The cells of the basal layer have no direct blood supply and nutrient and gas exchange in the papillary plexus must occur via the DEJ.

There appear to be differences in the basal layer cell population of the epidermis according to function (Mackenzie 1983, Wertz and Downing 1989, Bernerd et al 1992). The well-developed projections of the serrated basal cells appear to anchor the epidermis, via the DEJ, into the dermis, whereas non-serrated basal cells (stem cells) contain numerous melanosomes but few tonofilaments and are thought to be the actively dividing cells of the basal layer. The stem cells mitose and remain in the basal layer where their DNA is protected from external noxious stimuli, both by the numerous cells superficial to them and their melanosome content (Wright 1983), while their highly proliferative suprabasal daughter cells amplify the cell division and enter the stratum spinosum.

In the stratum spinosum (prickle cell layer) the desmosomes appear prominent and there is a full complement of cell organelles, and both keratohyaline and membrane coating granules (Odland bodies, cementasomes) become apparent. As the cells of this layer move

superficially, so they flatten and the membrane coating granules (MCG) move to the periphery of the cell.

The cells then enter the granular layer (stratum granulosum) where there is a drastic morphological change. The lamellar contents of the MGC's extrude into the intercellular space and their polar head groups attach to the exterior of the keratinocyte, forming the lipid bilayers or lipid lamellae which surround each squame (keratinocyte) (Wertz and Downing 1989). The formation of the lipid bilayer is essential to the skin barrier formation (Potts and Francoeur 1990) and its presence influential in cell cohesion. At the same time, the cell interior fills with keratin and matrix proteins. The cell organelles break down and involucrin and other proteins are deposited in the interior of the cell membrane to form the cell envelope (Michel et al 1988, Wertz and Downing 1989) creating a physically resistant superficial layer to the squame (Haftek et al 1991). The outer cell membrane consists of hydroxyceramides which probably anchor the cell envelope to the lipid bilayer (Wertz and Downing 1989).

The keratinocytes then enter the stratum corneum and eventually slough off. Normally, epidermal turnover varies from 14 - 21 days (Thomas et al 1985, Wertz and Downing 1989). In hyperproliferative skin diseases such as psoriasis and ichthyosis or traumatised tissue, this time lessens (Marks et al 1982, Graham-Brown and Burns 1990). In plantar skin callus, the transit time for the epidermis is also more rapid than in normal plantar skin (Thomas et al 1985). A steady state system is thought to exist in normal skin where the rate of desquammation equals cell proliferation (Wright 1983) and in skin disorders where desquammation rates are altered (such as in the hyperproliferative disorders), cell cohesion mechanisms become interesting.

The factors influencing cellular cohesion and thence desquammation await elucidation although a number of mechanisms have been identified as an aid to understanding "scaly" skin diseases such as psoriasis. The interdigitation of the convoluted surface of immature corneocytes precludes separation of these cells by mechanical stress (Ferguson 1980); this feature is apparent in psoriasis and ichthyosis (Dawber et al 1972, Heilman 1983). In normal plantar skin, desmosomes can be assumed to have an important function in maintaining the structural integrity of the skin as the desmosomal plaque interacts with intracellular keratin filaments. Therefore the endogenous proteolysis of desmosomal protein (desmoglein 1) which occurs in normal plantar skin is likely to have an influence on cellular cohesion (Lundstrom and Egelrud 1990). The state of maturation of the cell envelope, normally completed within the stratum corneum (Michel et al 1988) may also influence cell cohesion.

The lipid bilayers of the stratum corneum are also important in cellular cohesion (Seddon 1990) and abnormality in these structures will lead to change in cell shedding rates (Steinert and Cantieri 1983), as well as skin biomechanical characteristics. When no lipid bilayer is present, the ceramide molecules of the cell envelope interdigitate in a zipper-like manner (Wertz and Downing 1989) and the epidermis will then be a more rigid structure. The theoretical hypothesis that plantar skin callus is a stiff tissue because of the state of hydration (probably associated with its lipid bilayers) will be investigated using Fourier Transform Infrared Spectrometry (FTIR) and rheological techniques in the current work.

The clinical appearance and biomechanical behaviour of plantar calluses may also be influenced by the ultrastructure of the keratinocyte. Information

extracted from the studies of other workers infers that the keratinocyte, having entered the stratum corneum, is not inert (Leveque et al 1992) even though cell organelles are no longer evident by the time it reaches the stratum corneum. Proteolysis of desmoglein 1 (Lundstrom and Egelrud 1990) is required to degrade desmosomes as part of the desquammation process. Camp et al (1990) reported finding the cytokine interleukin 1 and 8 in skin and Michel et al (1988) reported maturation of the cell envelope was completed within the stratum corneum. It would appear, therefore, that the keratinocyte of the stratum corneum may contribute to the complex cascade of epidermal kinetics and control of growth. The dermal contribution to epidermal kinetics, also complex and convoluted, is mediated by a number of factors including retinoids (Eichner et al 1992), cyclic AMP, possibly cyclic GMP, calcium, steroids and epidermal growth factor (EGF) (Duell and Voorhees 1983), through the stable negative, rather than unstable positive, feedback system (Wright 1983).

The type of keratin found in the stratum corneum keratinocyte varies according to site and may affect the structural integrity and biomechanical behaviour of the skin. There are different cytokeratins (cytoskeletal proteins) in sweat ducts, hair follicles and interfollicular epidermis, despite their common embryological origin (Knapp et al 1986). These latter workers found a large content of cytokeratin no. 9 in human callus-forming epidermis, which was also evident, sparsely, in other tissues, such as keratinocytes peripheral to the acrosyringia of eccrine ducts (Moll and Moll 1991). Orfanos et al (1971) reported callus to be chemically different from normal stratum corneum and suggested that this should be classified with the "hard keratins" of hair and nail. Garson et al (1990) reported X-ray diffraction techniques and suggested that normal human stratum corneum keratin was an alpha keratin whilst that of callus showed a form similar to

wool, hair and nails. However, Steinert and Cantieri (1983) argued convincingly that the soft keratin of human skin forms a coiled alpha-helix.

In normal skin, keratin fibrils, comprising of keratin filaments of many microns length within the corneocyte, are embedded within an amorphous matrix of sulphur-rich proteins, Filaggrin, a histidine-rich basic protein which has the ability to aggregate intermediate-size keratin filaments is one of the matrix proteins (Manabe et al 1991). In skin disease, variations in keratin fibril structure have been noted. Psoriasis, ichthyosis and Darier's disease show major deviations from normal morphology including abnormal keratin filaments (Steinert and Cantieri 1983). Mackenzie (1983) described short keratin fibrils of normal diameter in plantar skin callus. In psoriasis, there is reduced lateral aggregation of keratin into fibrils which are also shorter and wider than normal, while in Darier's disease, filaments are shorter, but narrower (Steinert and Cantieri 1983).

In all these hyperproliferative skin conditions, the migration time of keratinocytes is accelerated by varying rates (Thomas et al 1985, Graham-Brown and Burns 1990), or alternatively the differentiation of cells may be delayed (Bernerd et al 1992), and the importance of this point in plantar skin callus formation will be considered along with the LM histological features of callus.

1.4 The clinical appearance of plantar skin calluses and corns

Plantar skin calluses appear as dense, hard, yellowish, shiny plaques of hard skin on the sole of the foot (figure 1.4.1). Callus lesions may be considered as "physiological calluses" when asymptomatic, and become pathological when excess bulk of keratinised tissue causes pain (Adams et

Figure 1.4.1
A plantar skin callus plaque. This lesion appears shiny and hard compared with adjacent normal plantar skin.

Figure 1.4.2
Corns appear as inverted "cones" of hyperkeratotic tissue and frequently look darker than the callus plaque which is often associated. The size of corns may range from 1mm to 5mm or more in diameter.

al 1989). It is possible to demonstrate the biomechanical behaviour of this stiff tissue *in vivo*; as stress is applied to a callus plaque so adjacent tissues can be seen to deform. For example, torque applied to the callus plaque causes tissue around its periphery to take load and sometimes an erythematous "halo" develops around the lesion.

Corns (figure 1.4.2) appear as more dense, darker coloured keratinised tissue than do calluses, the bulk of which is pushed into the foot by ground reaction forces or shoe pressure. Patients usually complain of a sharp, stabbing pain with these lesions. Although the remit of the present work is limited to consideration of plantar calluses alone, reference will be made, at times, to corns.

The steady-state system (Wright 1983), where epidermal proliferation equals desquammation, appears altered in plantar skin calluses and there is a gradual build-up of keratinised tissue over a period of time which has yet to be identified. This is thought to be a response to excess mechanical stress (Adams et al 1989). Thomas et al (1985) reported some increase in cell proliferation in callus tissue compared with normal plantar skin resulting in build-up in superficial tissue, though mitotic figures were considered to be considerably less than that seen in psoriasis. The present work will propose a model for plantar skin callus formation compiled from studies of other workers.

Callus plaques may be of uniform thickness or may show minor variations in colour, denoting differences in tissue bulk (Adams et al 1989). The changes in density and thickness within the lesion appear to be associated with variation in skin ridging (dermatoglyphics), where the ridges are parallel but wider apart (accentuated) (figure 1.4.3) or disrupted so that

Figure 1.4.3
The skin ridges (dermatoglyphics) in normal plantar skin may become altered under a callus plaque to show an accentuated, flattened or convoluted appearance, or a combination of these features. This lesion demonstrates accentuated dermatoglyphics.

Figure 1.4.4
The linear arrangement of dermatoglyphics has been disrupted within this callus lesion to form a convoluted or tortuous pattern.

parallel ridging is no longer apparent (tortuous/convoluted) (figure 1.4.4). Complete flattening of dermatoglyphics may also be seen clinically, or a combination of all three variations. In normal palmar and plantar skin, the undulations of the dermatoglyphics can be seen on the skin's surface, while in callus lesions, the surface topography may smooth but the dermatoglyphic patterns are still visible through the translucent callus stratum corneum. There is no evidence to suggest the macroscopic undulations of the DEJ form the dermatoglyphics or whether this appearance is influenced by other structures such as the dermis.

The technique of ultrasound skin imaging will be applied to create a contour map of callus lesions, so that the features of the lesion may be defined to aid association of lesion clinical appearance with any aetiological force vector. Should a mechanical aetiology be so identifiable, then the most appropriate management may be selected, such as the most suitable insole material to accommodate the stresses occurring on the foot at the site of lesion formation.

1.5 Plantar calluses, abnormality of foot structure and function and influence of mechanical stresses

Callus and corn formation is frequently associated with foot anomaly, either in function or due to skeletal abnormality (Root et al 1977). Structural and functional abnormality may be congenital, developmental (Lang 1991) or due to a disease process such as the arthroses (particularly osteo- and rheumatoid arthritis). Medical disorders, in which neuropathy and ischaemia feature, (for example diabetes mellitus and peripheral vascular disease) have the potential for altering both gait and foot function and also skin quality, so that resulting excess formation of callus tissue can lead to ulceration (Nakamura et al 1981, Soames et al 1982).

Figure 1.5.1
The most frequent sites of corn and/or callus formation are illustrated on the diagramatic foot.

Common sites of callus formation on the foot are illustrated in figure 1.5.1. The incidence of callus plaques at different sites of the foot often provides an indicator of the locomotor biomechanical abnormality (pathomechanics) which is associated with their formation. For example, callus formation in the centre of the forefoot is usually due to hypermobility of the foot. In this foot type, the first and fifth rays dorsiflex on load-bearing, exposing the second and third metatarsal heads to excessive force while reducing the surface area over which load can be taken. Wear marks on the outer sole of the shoe often show signs of spin as the foot and then the shoe, undergo adbuction in effort to achieve efficient propulsion at toe off. A callus lesion under the 2nd metatarsal head associated with this foot type may therefore show signs of torsion stress, for example in the form of tortuous/convoluted dermatoglyphics.

The size, shape, density and thickness of an area of callus is thought to be influenced by the mechanical stress postulated as being responsible for its development (Adams et al 1989, Soames et al 1982). When excessive mechanical force is applied to an abnormally functioning foot during gait, the tissues in the most affected region will become chronically traumatised. Their morphology appears to change, presumably as tissue proliferation alters in response to stimulated release of inflammatory mediators and growth factors (Wright 1983) by the dermis and epidermis (Leveque et al 1992). The sequence of events leading to the dermal and epidermal changes which are observable clinically in plantar calluses is not well understood. Not only do plantar calluses have different surface appearance and dermatoglyphics when compared with normal plantar skin, but they also exhibit clinical evidence of fibrotic changes in the dermis. The current work will be confined to the consideration and clarification of

plantar epidermal response to intermittent mechanical trauma which occurs with gait anomaly. The biochemical changes which may occur in this tissue, such as release of cytokines will not be investigated. However, findings of other workers will be considered and applied to the current study.

The relationship of the clinical appearance of plantar calluses to force vector exerted on the foot at the time of loading of the callus lesion will be studied in the present work, so that the influence of force vectors in frontal and sagittal planes may be assessed.

Further clinical features of plantar skin calluses will be investigated to clarify their role in determining the appearance and perpetuation of the lesion. The dense nature of the callus plaque tissue, evident clinically, may be due to an altered form of keratin (which will not be investigated in this work), or its water content (Hey et al 1978, Potts and Francoeur 1990). The water content of the skin influences its biomechanical behaviour markedly (Wildnauer et al 1971, van Duzee 1978, Potts et al 1983, Tagami et al 1988) and the current work will investigate the water content of plantar skin stratum corneum and that of callus using FTIR, and the viscoelastic behaviour of this tissue using rheological techniques.

1.6 A summary of the scope of the thesis.

There is a limited understanding of the aetiology of corns and callus and, as described earlier, these lesions are common, often painful conditions. The present work seeks to further knowledge of such conditions so that management options can be re-evaluated. Conclusions drawn from this work may form the basis upon which new therapeutic modalities may be

selected rationally and with some expectation of efficacy. Some novel techniques, which are described fully in the appropriate chapter, will be used to investigate callus lesions and their postulated aetiology of excess mechanical stress (Adams et al 1989). Each area of investigation is considered in detail in separate chapters.

The understanding of the complexities of normal skin biochemistry is far from complete and that of skin pathology is in accord; moreover, a specialist expertise is required to compete in this field. More accessible and potentially successful areas of investigation into callus lesions encompass study of their viscoelasticity and proposed mechanical aetiology. Callus tissue appears less pliable than normal plantar skin and this characteristic will be studied using rheological techniques which may provide an explanation of some of the clinical features associated with these lesions. As water content markedly influences skin viscoelasticity (Tagami et al 1988), the hydration levels of callus will be studied using FTIR. Ultrasound imaging of the lesion may permit quantification of its features. This technique has been applied to plantar skin (Edwards et al 1986, Edwards et al 1989) yet its use has not been validated and this will be carried out by the use of histological sections and light microscopy (LM histology) which may also provide a useful insight into the aetiology of calluses.

A number of workers using a variety of instruments have studied the effects of pressure alone on the foot during stance and gait (Hughes et al 1991, Rose et al 1992). However, the three dimensional force exerted on the foot at the time of lesion loading during gait has not been undertaken previously, and may allow assessment of the influence of predominant force vector (if any) on lesion clinical appearance.

It is hoped that by correlating results of this work with those of other workers in the relevant fields described above, that it will be possible to construct a model for an aetiology of callus formation and its perpetuation.

CHAPTER 2

The influence of mechanical forces generated during gait on the clinical appearance of callus.

2.1 Introduction

It is thought that excess mechanical stress is implicated in the aetiology of plantar callus and that the nature of this stress influences the clinical appearance of these lesions (Adams et al 1989). Measurement of plantar pressures play a key role in the evaluation (and treatment) of foot disorders (Hughes 1988, Cavenagh et al 1992, Rose et al 1992). Measurement of force and pressure exerted on the callused foot during gait therefore may be expected to provide information to support (or otherwise) these empirical assumptions and may identify any predominant force vector associated with a particular callus lesion clinical appearance.

When humans move around, the whole of the body's weight is placed on the feet and each foot in turn will take the entire load during the gait cycle. Should this tiny proportion of the body's anatomy fail to function properly, then our ability to stand, walk and run efficiently is grossly affected. Skin response to load is important especially in disease states such as diabetes. If the skin is subjected to marked, prolonged stress, mechanical damage results to both the skin and soft tissue as blood supply to the tissues is impeded (Nakamura et al 1981). When skin on the sole of the foot (plantar skin) is over-stressed by mechanical force, as occurs in an abnormally functioning foot, a number of conditions will develop including ulceration (Nakamura et al 1981, Soames et al 1982), blistering, cracks (fissuring),

corns and callus (Adams et al 1989). Knowledge of the force vectors occurring during the different phases of normal and abnormal gait may aid prediction of soft tissue and bony reaction to these stresses which will be of use to orthopaedic specialists and orthotists as well as podiatrists when managing foot malfunction. For example optimum selection of insole material may be made utilising information generated by the current work.

Ideally, all forces exerted on the foot during gait should be measured, but as yet, no instrument is available which is capable of allocating three dimensional (3D) forces and torque to a specific section of the foot at an identifiable time, while allowing normal gait. The point of force application on the Kistler force measurement plate can be calculated (Bobbert and Schamhardt 1990), but it is not possible to demonstrate that this point is associated with a particular site on the foot. In the current study, investigating the influence of forces generated during gait on the clinical features and viscoelasticity of plantar skin callus, it is proposed to apply a novel technique to provide a greater insight into the reactive forces exerted on these skin lesions.

Two force plates will be used. A Musgrave pressure measurement plate placed in a cradle attached to a Kistler force measurement plate should permit forces to be transmitted via the Musgrave plate to the Kistler plate so that reactive forces during gait can be recorded simultaneously by these two instruments. The time of forefoot and lesion loading and site of peak vertical pressure can be identified readily using the Musgrave software. The 3D forces and moment exerted on the foot by ground reaction forces

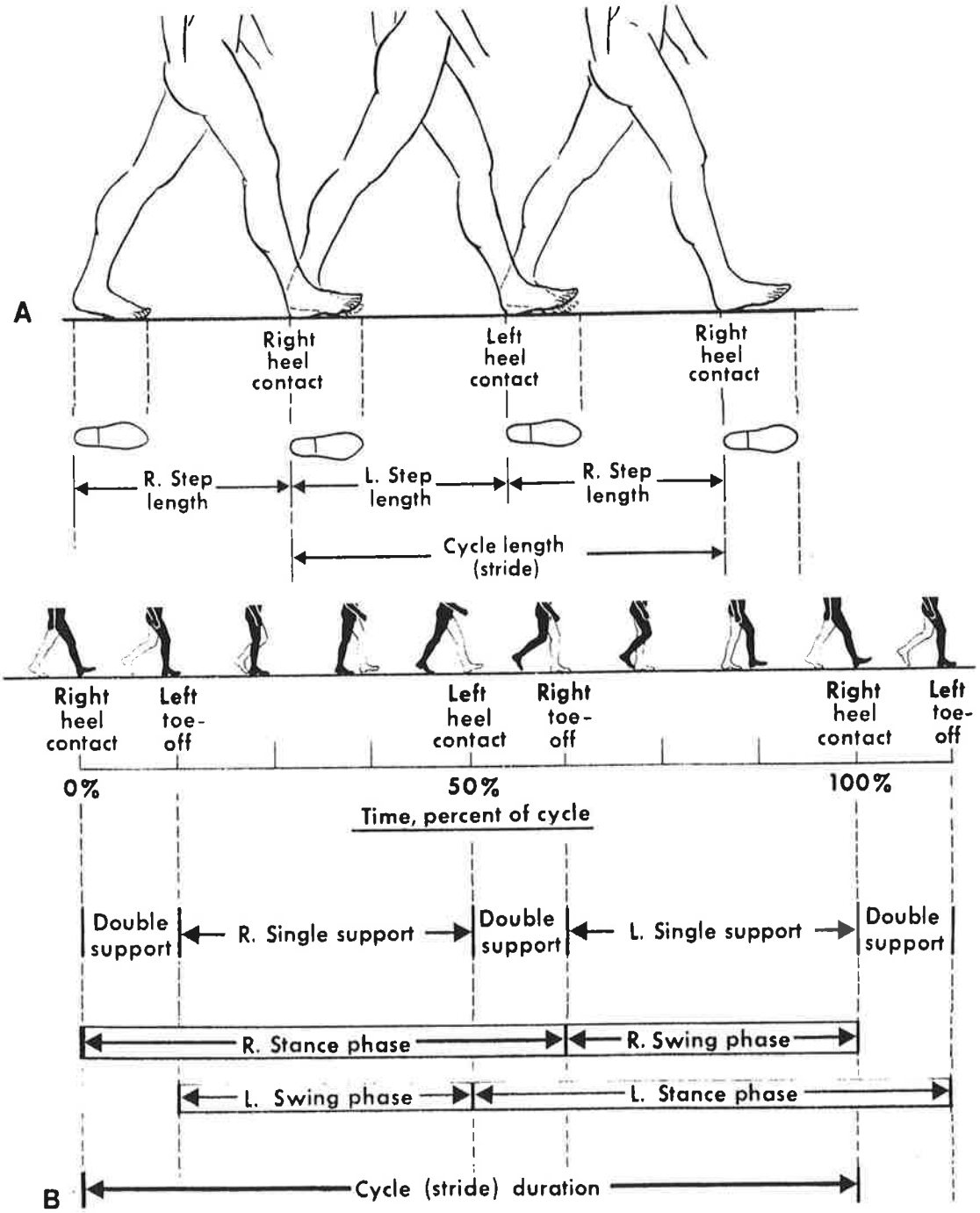

Figure 2.2.1
Human walking divided into step and stride (Inman et al 1981).

during forefoot and lesion loading (the time of which is identified using Musgrave plate data) can be studied using the Kistler force plate facilities.

This combination of the two force plates will be compared with a third, independent system, the Gaitscan, before being used to study the gait and forces exerted on the feet of patients suffering with plantar callus. A number of supporting studies will be carried out, including the influence of dominant side on gait to determine the importance of force loading patterns of either foot in left- or right-side dominance, and demonstration that the population studied in the present work is characteristic of the population as a whole in the South East of England. Each of these studies will be reported under separate headings.

2.2 The Gait Cycle

Detailed kinematics of human gait is outside the remit of the current work and only an outline of relevant information follows. The process of human walking is often referred to as "the gait cycle" and is split into levels of increasing complexity. The "swing phase" of gait refers to the foot which is not weight bearing and "stance phase" refers the foot which is load bearing and undertaking the task of propulsion. Figure 2.2.1 illustrates the concept of stride and step length, terms which are used to describe the parameters of gait.

Each step comprises heel contact, mid-stance and toe-off (Inman et al 1981) permitting the body to progress along the sagittal plane. At heel contact the foot, via the subtalar joint, begins to pronate (in-roll) into its

shock-absorbing mode when it can accommodate to uneven ground. This movement is initiated by the internal rotator muscles of the thigh. Mid-stance sees the end of the pronatory phase and the start of supination, initiated by the external rotator muscles of the thigh, when the foot begins to become a rigid lever for efficient propulsion and toe-off.

In normal stance phase, the point on the transverse plane where force vectors intersect will travel over and outside the foot in the sagittal and frontal planes. Acceleration and deceleration of the foot also occur during gait in the transverse plane.

As the heel contacts the ground, marked deceleration occurs, body's centre of pressure then moves anteriorly swiftly during mid-stance, and as the foot re-supinates this slows again with further acceleration at toe-off (Root et al 1977, Inman et al 1981). The forces exerted on the foot by the forward and backwards movement (Fy), and side to side movement (Fx) of the body's centre of pressure and vertical load through the foot (Fz) can be viewed clinically and quantified using force measurement plates and in-shoe force measurement instruments. However, an individual's gait varies from day to day. It is difficult, therefore to obtain definitive and consistent data for an individual and a wide range of variation must therefore be accepted by the clinician and researcher alike. Variability is also associated with footwear and ground conditions (Bransby-Zachary et al 1990, de Vita and Bates 1988).

Forefoot loading at mid-stance is the sub-phase to be considered in detail for the current work as this is the time during which a forefoot plantar callus

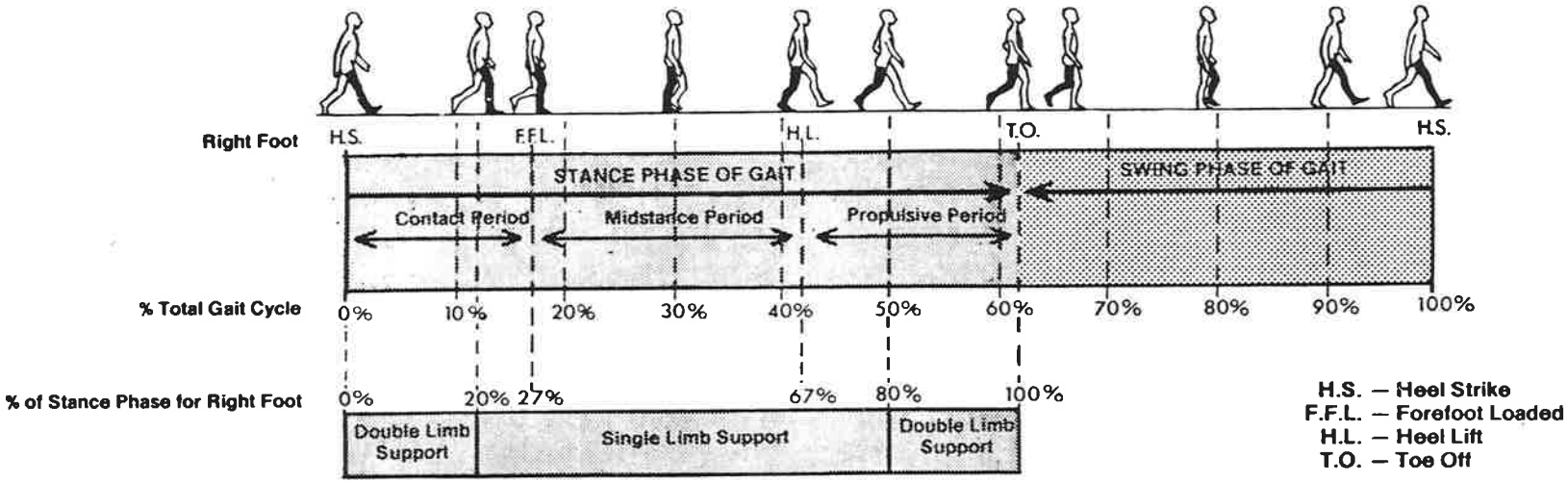

Figure 2.2.2

Normal gait. The stance phase of gait is divided into sub-phases and the duration of normal foot loading is illustrated (Root et al 1977)

lesion takes load. Forefoot loading is taken, in the present work, to refer to the percentage time at which pressure sensitive transducers on the Musgrave monitor relating to the forefoot are seen to take load. Similar criteria are used for the off-loading, taken to indicate the end of this phase of gait. These values are subject to an error +/-9ms as explained later in this chapter. The duration of each portion of the stance phase of gait is illustrated in fig 2.2.2. A wide range of values have been reported for the duration of normal forefoot loading (25% to 85% of total foot contact time) (Scranton and McMaster 1970, Miller and Stokes 1979, Hutton and Dhanedran 1981), with polarised evidence about the influence of age and weight on normal gait characteristics (Nigg and Skleryk 1988, Hughes et al 1991). Variation in interpretation of the onset of forefoot loading, intra- and inter-day variation in an individual's gait (de Vita and Bates 1988), coupled with the difficulty in correlating different force measurement instruments (Stewart and Grove 1989) as well as variation in experimental techniques will all contribute to the range of values reported for forefoot loading times.

Force effects in skin and plantar callus will be difficult to measure because of the skin's composite structure (Vincent 1982) and the morphology of deeper structures. Bones, for example metatarsal shafts, are subject to bending moments which tend to dorsiflex them. If the toes are inactive, the metatarsals are subject to greater bending moment. A reduction in axial load and an increase in metatarsal head loading then occurs (Stokes 1975). Thus foot skeletal morphology will also account for further variation in results.

During the period of forefoot loading, in the normal foot, forces are exerted in three planes (Fx, Fy and Fz), the predominant one being vertical (Fz) (Tappin et al 1980, Roy 1988). Vertical force and pressure (force/area) are parameters measured frequently, as these provide a sensitive method of measuring variation. The forces and pressure exerted on the normal forefoot have been established (Betts et al 1980, de Vita and Bates 1988, Roy 1988, Ranu 1989). The influence of disease and structural abnormality have been considered by some workers (Tappin et al 1980, Hutton and Dhanedran 1981), but there have been no published studies on 3D force vector analysis associated with the formation of plantar callus and its clinical appearance.

2.3 History of instrumentation developed to investigate ground reaction forces

Viewing the pattern of foot to ground contact, both static and dynamic, has been of interest to a variety of researchers, including biomechanists and prostheses designers, footwear manufacturers, surgeons and clinicians for a number of years (Miller and Stokes 1979, Lord 1981, Hutton and Dhanedran 1981, Cavenagh et al 1992). Distribution of load between the soles of the feet and the supporting surface reveals information about the structure and function of not only the foot, but also the locomotor status of the lower limb, and posture (Lord 1981).

Visual analysis of gait and comparison of this form of assessment from one time to another or between individuals has been considered problematical (Messenger and Bowker 1986, Krebs et al 1985, Saleh and Murdoch 1985)

particularly when change is to be quantified. Consequently a number of methods for measuring change in foot function, loading and gait began to be devised. Beeley (cited by Elftman 1930) stood subjects on a thin sack filled with Plaster of Paris. This method succeeded in producing a characteristic foot shape rather than providing information about pressure distribution. Morton (1930, 1935) described one of the earliest techniques developed to record foot-pressure distribution which comprised of a triangular ridged inked rubber mat laid on paper upon which the subject stood. The ridges flattened on load and the width of the inkprint lines were taken to be proportional to the pressure applied.

Harris and Beath (1947) developed this deformable mat concept further to produce a permanent visual record of dynamic or static foot loading. The mat consisted of a rubber gridded surface, each large grid square being filled with progressively shallower and smaller ridges. The mat was covered with duplicating ink and then thin paper, upon which the subject walked or stood. Where high loading occurred the shallow ridges were made to contact the paper and so small grid lines printed on to the paper. This cheap, easy, but messy method of indicating foot loading is still used occasionally to help patients understand their foot problems. However it has a number of disadvantages, for example heavy people flatten the grid lines, only rough calibration is possible and the technique is time consuming.

Grieve (1980) substituted the paper cover of the Harris and Beath (1947) with aluminium foil. Using a rubber mat with upward pyramidal projections, the foil laid over the top and walked on assumed and retained the

indentations which can then be measured, albeit laboriously. Once again, this method is unsuitable for heavy people as the foil ruptures.

Later, direct visualisation techniques were developed permitting real-time viewing of foot loading patterns and photography was employed to record data. The first generation of barographs were simply glass plates with a covering of textured rubber mats which were side-lit. Variations of increasing sophistication eventually lead Arcan and Brull (1976) to use a photoelastic material which, with computer hard- and software and a video camera, became the Pedobarograph.

There are a number of current alternative methods of measuring foot loading, although some are rather bulky and could interfere with normal gait (Messenger and Bowker 1986, Cavenagh et al 1992, Rose et al 1992) influencing pressure distribution and creating artifactual data. These include strain gauges, capacitance transducers (Soames et al 1982), conductive rubber pads, liquid crystals, thermography and Moire fringes (Fok 1988). All these instruments measure pressure as a vertical component of force and the other components are not measured. However the vertical component is usually highest and is a useful indicator of the total force experienced by the foot. However, vertical force is usually the largest force component acting on the foot (Roy 1988) and is therefore a useful indicator of loads (the composite of 3D force vectors) that the foot is sustaining.

A further generation of gait analysis instruments are force measurement plates. These are flat plates which register components of force applied to

the top surface in one, two or three planes. Force plates may rest on the floor or be set flush with its surface. When gait is investigated, the subject must time their step and stride to coincide with the plate, treading on it as normally as possible. Control of cadence (walking rhythm) was considered by some workers (Hughes et al 1991) as being necessary to obtain consistent gait data, whereas others suggested that such control disturbed the gait pattern (Henig and Rosenbaum 1991) and erroneous data would be collected. Patients taking part in the present work remarked on the difficulty in maintaining a "normal" gait if their cadence is dictated, though found a starting point marked on the floor helpful.

Electronic force plate measuring systems such as the Kistler force plate, a well established instrument, use piezoelectric cells to measure these forces. Other instruments, such as the Musgrave, utilise pressure sensitive transducers to measure the applied vertical force. The volume of data generated by such instruments is vast and must be reduced for analysis (Henig and Rosenbaum 1991). A wide variety of methods have been utilised in other studies (Hughes et al 1991, Neville 1991) including sampling data at different time intervals and selection of specific parameters such as time between peaks of vertical force (F_z).

In-shoe systems constituted the next phase of development in force analysis during gait. Henig et al (1982) developed piezoelectric ceramic transducers which were embedded into a 3 - 4mm highly resilient, insulating silicone rubber insole, but few shoes could accommodate this thickness. A similar problem faced the 0.9mm thick beryllium copper

transducers described by Soames et al (1982) and these instruments did not appear to be successful clinically.

Two instruments being developed currently are designed to fit in the shoe to provide true, dynamic information of foot loading. The Tekscan (Rose et al 1992) consists of a paper-thin insole made of two layers of a plastic material between which transducers and their circuitry are sandwiched. The electrical resistance between conducting elements is transduced and digitized and displayed on a monitor as a series of pressure contour lines within the foot's outline. The prototype in-shoe system insoles, available at the time of data collection, were heat sensitive and could only be worn for about 10 minutes each before spurious data was displayed (Potter 1992). Variation in intra-day and inter-day measurements was reported by Rose et al (1992) as being small though values cited (28 to 41.2kPa) would seem to indicate the converse.

The Gaitscan consists of piezoelectric, PVDF transducers inserted in a thin (1.5mm) insole at strategic sites (metatarsal heads, base of the 5th metatarsal and heel) and worn by the patient in their shoe. Both systems necessitate the patient wearing a convertor box on their leg or waist at which coaxial cables from the insole and instrument converge. The patient is often disconcerted by the accoutrements of these instruments and distracted from their normal gait.

Figure 2.4.1.1
The Kistler force plate system in use

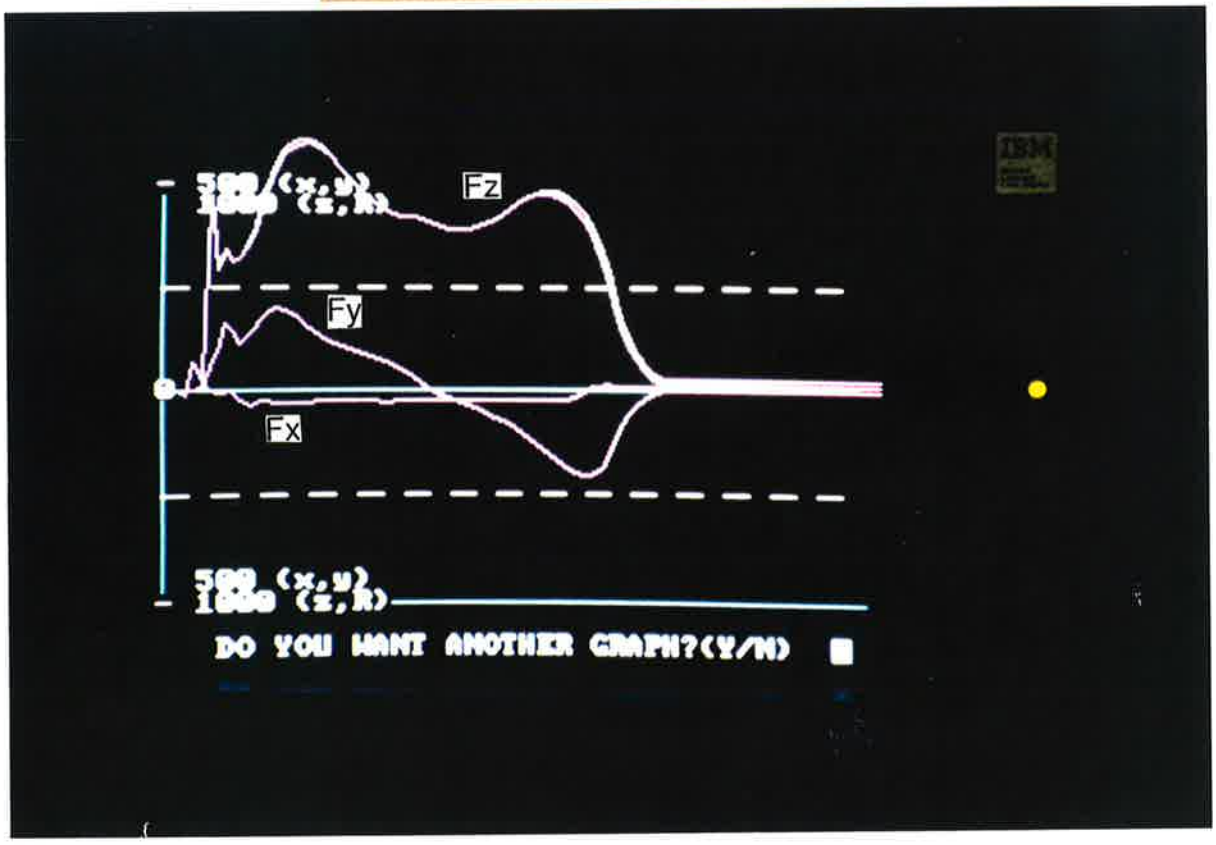

Figure 2.4.1.2
F_{xyz} force plot of normal gait using the Kistler force plate system

2.4. The Kistler and Musgrave plates - the principles of force plate instrumentation

Force measurement instrumentation must satisfy a number of prerequisites (Messenger and Bowker 1986) including durability, reproducibility and accuracy. Measurement should be possible over the entire range of force magnitudes, yet be sensitive enough to record small variations. Normal gait should not be disrupted by the instrument which must also record time accurately.

Currently the most sensitive and reproducible method of measuring loading in three dimensions is the Kistler force plate. However data from this instrument cannot be allocated specifically to a precise time interval of the stance phase of gait (ie: forefoot loading) as required by the current study. Therefore a second instrument (Musgrave pressure plate) was selected and used in conjunction with the Kistler force plate. Patients and clinicians alike can readily allot an area of the foot's plantar surface to features illustrated on the Musgrave monitor so demonstrating the ease of relating a specific area on the foot to that on the monitor image. The time of forefoot loading as identified by the Musgrave can be allocated to the appropriate period of time in the Kistler data which provides information on 3D force vectors and moment. Also the area of callus on the plantar aspect of the forefoot can be seen over the metatarsophalangeal joints (figure 2.4.2.1). The force vectors measured are x (side to side/medial to lateral),y(front to back/anterior to posterior), z (vertical).

2.4.1 The Kistler Force Plate.

The Kistler system is one of a number of commercial force plates all having similar specifications. The Kistler has industrial as well as medical applications, comprises a measurement plate with piezoelectric transducers, a microprocessor, buffer, monitor and printer; a plotter can be added. The Kistler plate must be installed in a solid floor so that its surface is flush and once installed it is immovable (figure 2.4.1.1). It provides three force components and three moments, usually manipulated to yield total force vector, point of intersection with the horizontal plane and moment about the vertical (Mz). Software options permit selection of the time of data collection, and provision of data displayed on the monitor or in digital form.

The piezoelectric effect utilised by the Kistler system was discovered by the Curie brothers in 1880. An electrical charge appears on the surface of certain crystals when they are mechanically stressed. Quartz is an excellent piezoelectric material with high stability and it is this crystal which is cut to produce the Kistler force plate transducers. Depending on the plane in which they are cut out of the quartz crystal, discs obtained are sensitive to compression/tension only or else to shear stress in one direction only. An assembly of these discs with suitable dividing insulators create the Kistler piezoelectric transducer; one of which is placed at each of the four corners of the plate. With the aid of the appropriate hard- and software, this expensive system provides information on a number of parameters of gait including time, 3D forces and moment (torque). Software options permit selection of the force to be studied. Copious data on vertical (Fz), side to side (Fx) and back to front (Fy) forces and moment are generated by this instrument over a one minute sampling period. A wide variation in data of forces exerted on the normal forefoot has been reported by different workers (Betts et al 1980, de Vita et al 1988, Roy 1988, Ranu 1989) using the same and other

instruments which is generally considered unavoidable given the inevitable variation in biological systems and the different physical principles used by each variety of instrument (Cavenagh et al 1992).

When interpreting Kistler data, both forms of presentation, digital and plot data are used. Clinicians tend to view visual data of the pattern of the forces and relative motion of the centre of pressure recorded and plotted by the Kistler initially. Visual assessment of data can enable a reasonable specific allocation of, for example, the normality of gait within the wide ranges reported (figure 2.4.1.2), before resorting to the digital data provided by the instrument.

Figure 2.4.1.2 illustrates the predominance of vertical force (Fz) during gait. The spike at heel contact with the Kistler plate on the Fz trace may be considered a function of the modifying action of the quadriceps muscle (Raden et al 1987), and of footwear and gait style. This spike has also been considered as a possible result of a reverberating characteristic of the plate (Roy 1988). The position of the Fx curve plotted on the monitor display (figure 2.4.1.2), either side of the x axis indicates side to side sway. The negative values and curve indicate a sway to the right. The movement of the Fy plot across the x axis indicates acceleration and deceleration. At heel strike, the foot pushes down (Fz) and forwards against the surface of the plate in deceleration (seen as the positive curve of the x axis in figure 2.4.1.2). At toe-off the foot pushes backwards against the plate to accelerate (Fy).

2.4.2 The Musgrave pressure measurement plate.

The Musgrave system utilises pressure sensitive transducers housed within a flat plate to measure applied vertical force, and is linked to a microprocessor, monitor and printer.

The Musgrave plate used in the current study, consisted of a grid of 65 pressure sensitive transducers under its black, vinyl-covered surface. With the aid of a microprocessor and appropriate software, static or dynamic variations in vertical force and the vertical components of other forces acting on the foot during gait can be identified. Values recorded by each transducer are converted by the instrument into digital form and displayed on the monitor in a number of formats as dictated by software option choice. For example, areas of peak pressure may be displayed on the monitor in the form of uncalibrated different coloured squares according to pressure (figure 2.4.2.1). The time taken from start to completion of one scan of all transducers and start of the next scan sequence, is 18ms.

Further options include selection of duration of loading of identified transducers and percentage of weight taken by each of these transducers. Data is stored on disc and a screen dump command allows a paper copy of the monitor display. The site of peak pressure can be identified on the monitor and readily attributed to a specific region on the plantar surface of the foot by both the clinician and the patient.

Although instruments designed to record in-shoe pressures are being developed, study of three dimensional forces exerted on the foot still eludes technology. Mounting the Musgrave force plate on top of the Kistler force plate is a novel technique adopted for the present study, whereby the 3D reactive forces and moment generated during gait can be elucidated for a

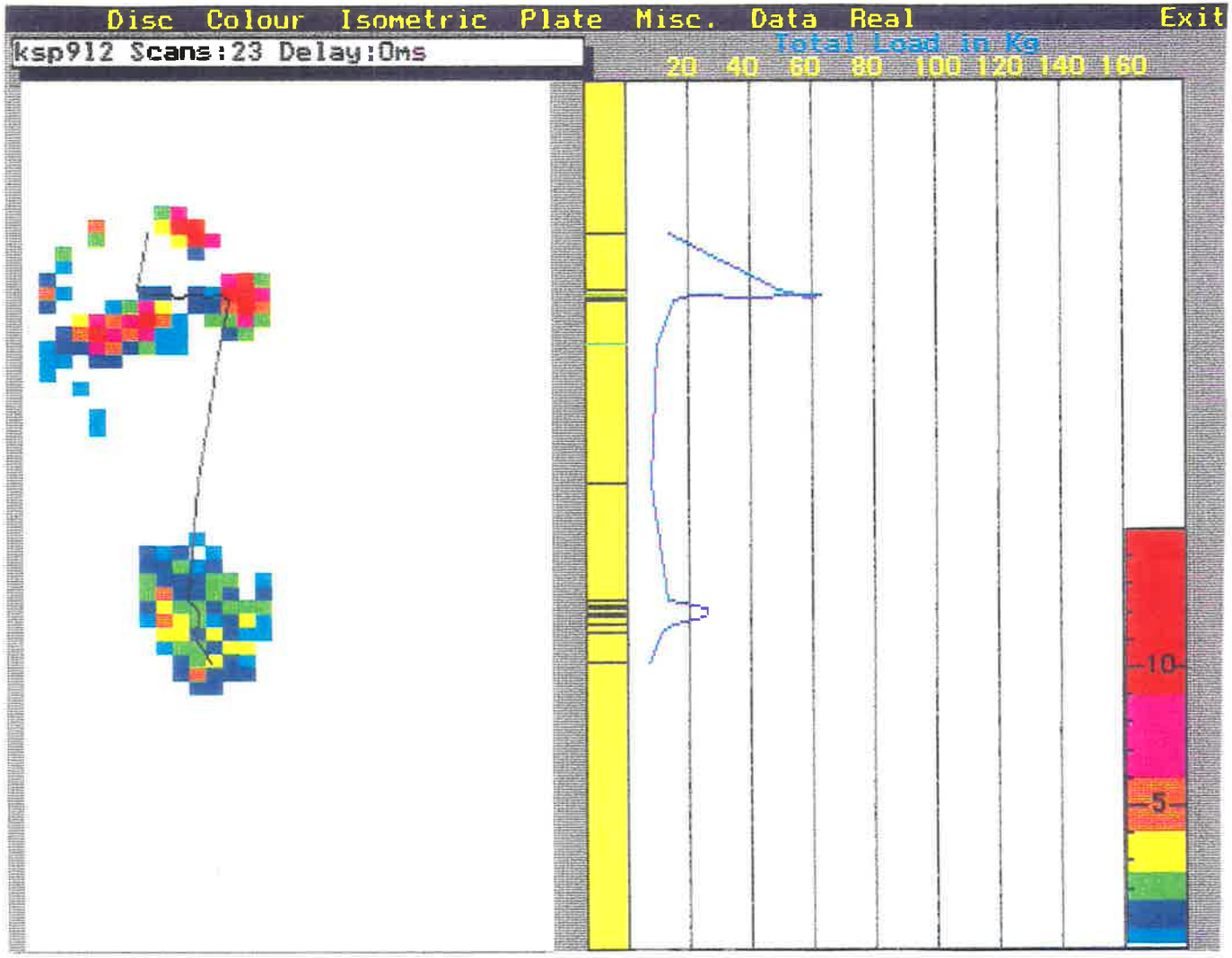

Figure 2.4.2.1
The monitor of the Musgrave pressure plate displays the dynamic pressure loading pattern of the foot. Vertical load and the vertical components of other force vectors are recorded by the instrument.

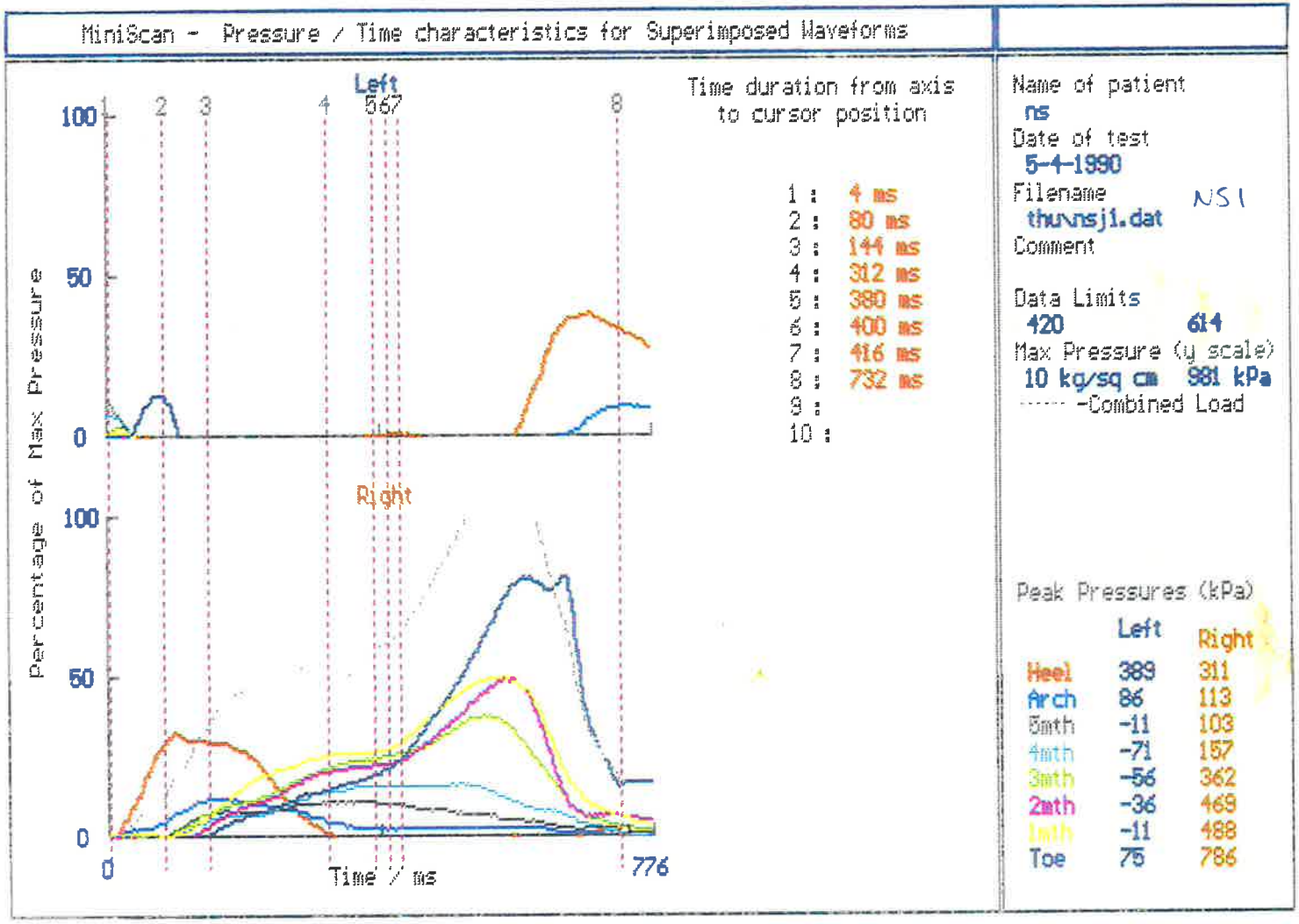

Figure 2.5.1
Data presentation from the Gaitscan, an in-shoe pressure measuring instrument, allows pressure:time analysis and provides data on the loads taken by the metatarsal heads and heel. The Gaitscan was used in the current study when comparing the Musgrave and Kistler plates.

specific time of forefoot loading. Before being used to investigate the foot loading characteristics of patients with plantar callus, this technique was compared with a third prototype-type in-shoe force measuring instrument, the Gaitscan.

2.5 Materials and instrumentation

Kistler force plate, Kistler, Switzerland (see section 2.4.1)

Musgrave pressure measurement plate, WM Automation, Ireland (see section 2.4.2)

Dewar flask filled with liquid nitrogen

Cryotubes, Nunc Cryosystems, Denmark

Medical Eye camera (Zenith), with fixed focal length.

Walkway constructed around the force measurement plates, 7cm thick ethyl vinyl acetate sheets.

The clinical facilities of the Dept of Podiatry, University of Brighton

Gaitscan, University of Kent.

This instrument was in its developmental infancy (Neville 1991) at the time of data collection for the present study and comprised of a series of PVDF transducers inserted into an insole at strategic points, namely first toe, all metatarsal heads, base of the 5th metatarsal and heel, and a microprocessor with specific software. The Gaitscan was capable of measuring pressure which was displayed graphically on the monitor screen or as a print out (figure 2.5.1). Time of loading of each transducer was also recorded by the instrument and had a potential error of +/- 4ms.

The insole was 2mm thick and the transducers set flush with its surface. To obtain foot loading data, the subject wore the insole in their shoe, and a number of cables from the insole and the microprocessor converged at a connector attached at the subject's waist or leg.

2.6 The influence of laterality on plantar callus distribution on left and right feet

People, when walking, generally lead (start off) with their dominant (preferred) foot. Their proprioceptive capabilities are enhanced on the preferred side and they feel safer, more sure of themselves using that foot. The dominant side tends to be more dexterous while the non-dominant foot is used for initial propulsion and may be accompanied by concurrent increase in limb muscle bulk (Peters and Durding 1979). It is possible that one foot may be favoured and thus show the effects of the subsequent, long-term extra stress in many ways including the formation of corns and calluses (Nakamura et al 1981, Soames et al 1982).

A history of injury, congenital asymmetry, disease and neurological disorders will affect laterality (use of the preferred/dominant side). Gait will be affected by such conditions and a change in preferred side loading can be expected to be a sequel to this, demonstrable clinically as a limp, foot ulceration or less severely, callus and corn formation (Adams et al 1989).

Sighted people have a tendency to lean towards their right side (Cernacek and Jagr 1972) as invariably in right-side motor preference, it is the left eye which is dominant for verticality and posture position perception. It is thought that the lean towards the right brings the dominant left eye more in line with the body's centre of pressure. Possible increased loading of the

preferred side and asymmetrical acceleration and deceleration demands (Stokes 1975) may result in unequal work being done by one side of the body. A long-term asymmetry of this nature may cause chronic minor changes manifesting for example as corns and callus on the feet. These lesions may therefore be used as long-term indicators of the influence of laterality on gait. A survey of forefoot callus sufferers was undertaken for the current work to establish association (if any) of laterality and callus formation. Kaliszer et al (1989) reported significant differences in normal gait between right and left dominance, but suspected this result may have been influenced by the layout of the two force measurement plates used in their study. Differences in gait parameters between right and left feet in normal individuals were also studied to assess the influence of laterality on foot loading.

To demonstrate that patients selected for the current study were typical of callus sufferers in the local population as a whole, data obtained from this group was to be compared with that collated by Whiting (1987) of employees of one of Eastbourne's largest organisations. However, retirement of women at 60 years and men at 65 years from this employed group made direct comparison with a more elderly patient group difficult. Whiting (1987) also carried out a survey of the patients of the Department of Podiatry, University of Brighton who were suffering with corns and callus but the survey parameters did not include everything that was required for the current work, such as record of dominant side, thus necessitating a smaller, specific survey to support the present study.

To assess the influence of laterality in normal callus-free subjects, the gait of adults of varying ages was studied using the Kistler force plate. West (1987) intimated that as little as two steps acceleration were required before

characteristic gait over a force plate was achieved in normal gait. This technique was adopted for the current work to minimise subject confusion, lack of coordination and time taken for each force plate loading and data collection.

2.6.1 Methods

Instrumentation

(see section 2.5)

A group of 319 non-smoker patients (from the Department of Podiatry, University of Brighton) who suffered with plantar forefoot callus were questioned and assessed to establish their age, preferred side and duration of callus plaques. Note was made of the site of the forefoot callus and the lesion diameter was measured using a ruler. Patients who smoked or had an obvious body asymmetry were excluded from this group, as were those who had a medical condition or drug therapy (such as steroid or retinoid drugs administered topically or systemically). Medical conditions which may affect skin morphology include peripheral vascular disease, rheumatoid arthritis, disorders of nutrition and endocrine disorders such as diabetes mellitus.

The influence of laterality on normal gait was assessed in 50 randomly selected healthy people, (23 male, 27 female), age range 20 - 63 years, who were free of pain or discomfort in their feet and legs, had no obvious callus plaques or body asymmetry. Kistler data on total contact time of the foot with the plate and the ratio of body weight to peak vertical force were studied.

A number of practice walk-overs were made by each subject until both the clinician and subject considered their gait was normal for them. The starting

point for each patient was marked on the floor. Kistler loading parameters were set at 1000N (Fz) and at 500N for Fx and Fy with a one minute data collection period. The Kistler loading data for one foot was recorded, stored on disc, and the process repeated for the other foot, each three times. The subject was allowed two steps to accelerate so that the foot to be studied contacted the Kistler within a gait cycle characteristic for that subject.

Note was made of the subjects' dominant side at the end of the study period so that the reply to the clinician about use of one foot or the other did not influence their gait inadvertently.

2.6.2 Results

Of the 319 patients suffering with plantar forefoot callus, 230 (72%) were female and 89 (28%) male and 270 (84.3%) of the total group had a right side motor preference. This proportion of right and left preference is similar to that found by other workers (Heylings 1988). None of the group were truly ambidextrous though some (5) could use either hand and foot for non-dexterous tasks.

	Left foot callus	Right foot callus	Both feet callus	Total
Left dominant side	n %	n %	n %	n %
Female	7 (2.19)	4 (1.25)	14 (4.37)	25 (7.83)
Male	10 (3.14)	5 (1.57)	9 (2.82)	24 (7.53)
Right dominant side				
Female	31 (9.72)	29 (9.09)	145 (45.46)	205 (64.24)
Male	18 (5.64)	17 (5.33)	30 (9.4)	65 (20.37)
Male and female	66 (20.65)	55 (17.24)	198 (62.07)	319 (100)

Female chi-squared $_{(0.05)(2)}$ = 2.29
Male chi-squared $_{(0.05)(2)}$ = 7.66
Total group chi-squared $_{(0.05)(2)}$ = 1.58
Critical value chi-squared $_{(0.05)(2)}$ = 5.991

Table 2.6.2.1 Callus incidence on left, right and both feet in relation to right and left dominant side and sex.

A non-parametric chi-squared two-sample test was selected as this can be used to compare more than two pairs of proportions. This test may be considered analogous to the F test in analysis of variance (Armitage 1980). Its use permitted statistical evaluation of the independence of left and right side dominance with callus incidence. A 95% confidence limit (0.05) has been selected to determine level of significance.

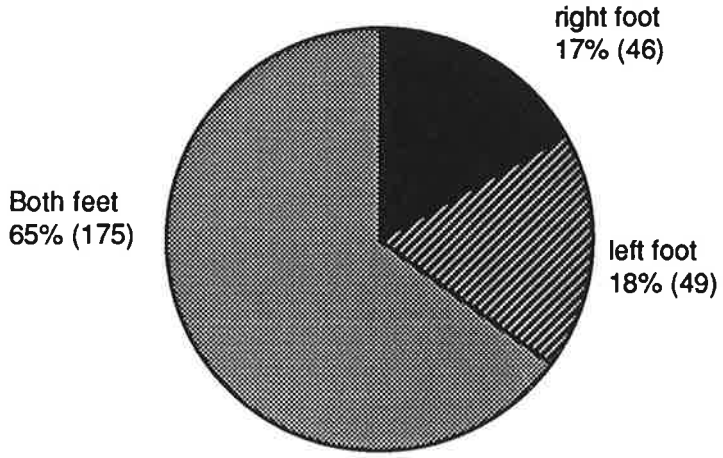

Right side dominant

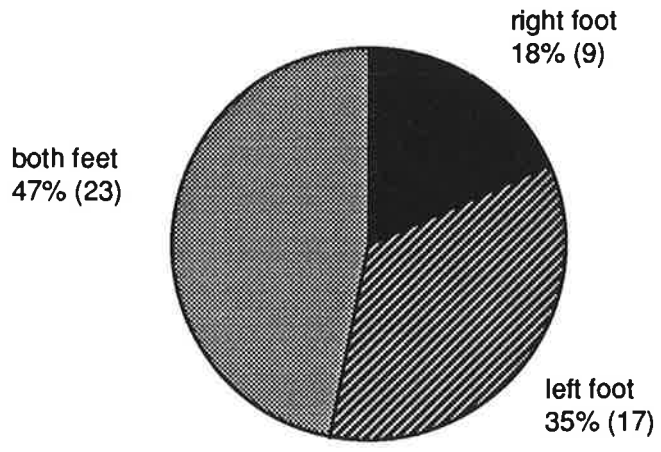

Left side dominant

Figure 2.6.2.1
Incidence of left, right and both feet forefoot callus (male and female) in left and right side dominant.

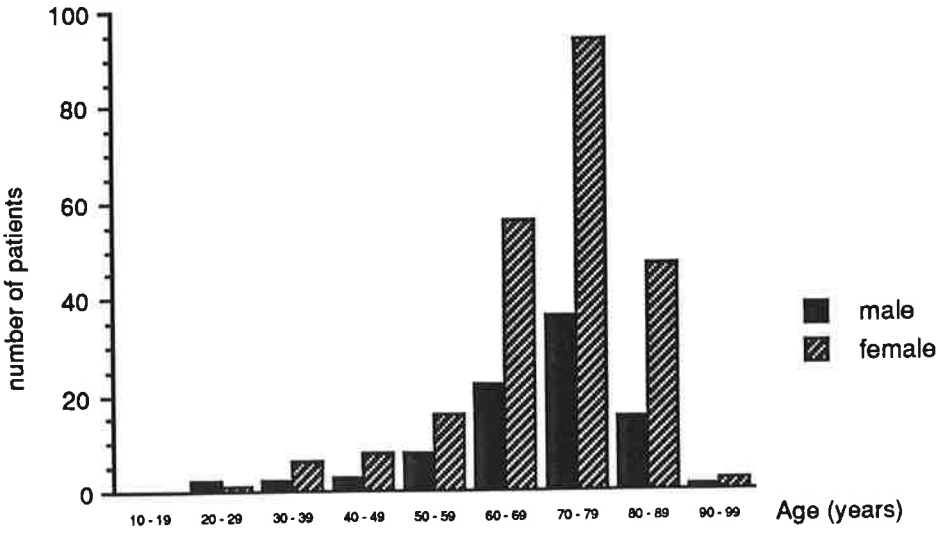

Figure 2.6.2.2
The age and sex distribution of patients suffering from forefoot plantar callus in this survey.

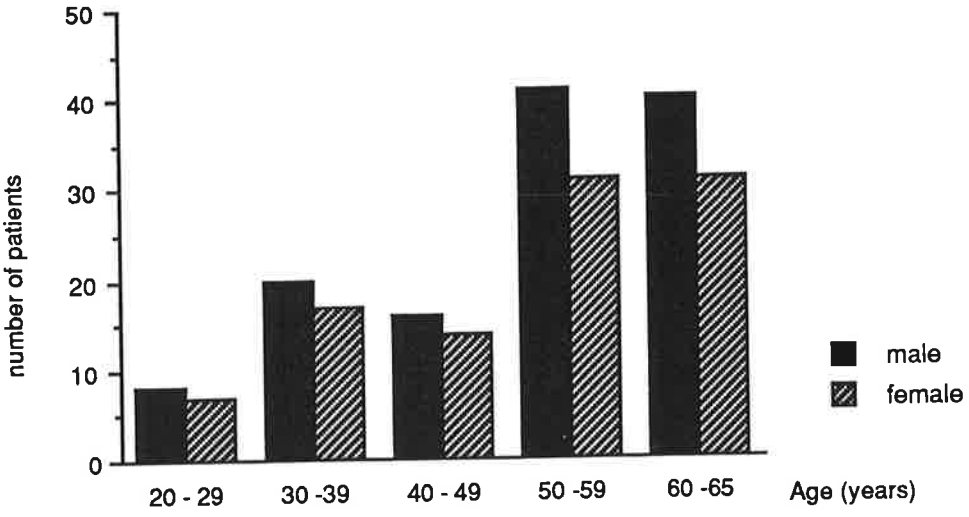

Figure 2.6.2.3
The distribution of sex of callus sufferers in the group of employed people surveyed by Whiting (1987).

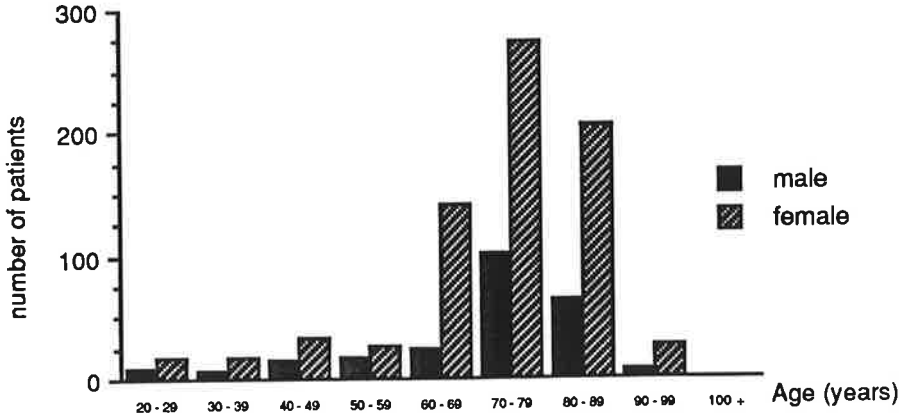

Figure 2.6.2.4
The age and sex distribution of patients surveyed by Whiting (1987).

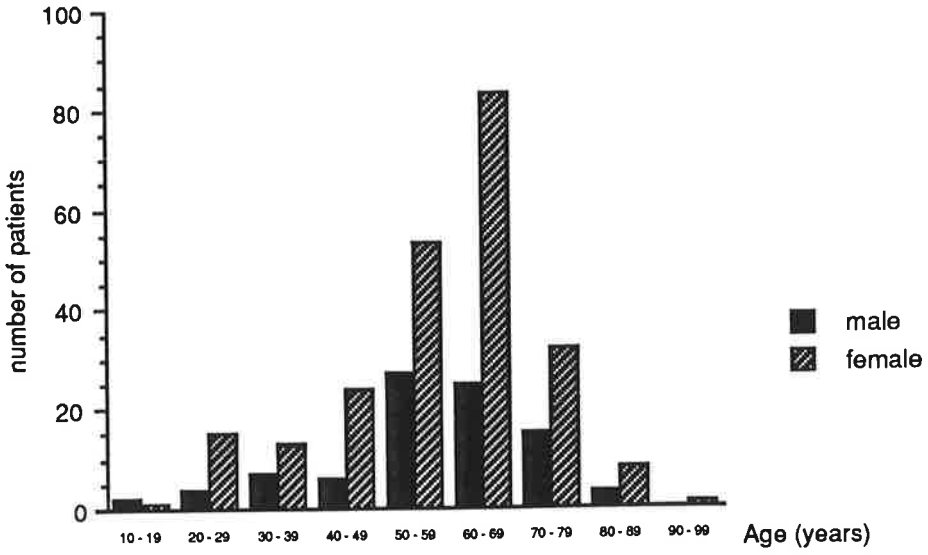

Figure 2.6.2.5
The age of onset of callus formation in patients surveyed for this study.

In the right dominant side group, 29 (9%) of the women had plantar forefoot callus only on the right foot, 31 (9.7%) had callus only on the left foot and 145 (45.5%) had callus on both feet. In this same group 17 (5.3%) of the men had plantar forefoot calluses on the right foot, 18 (5.6%) on the left foot and 30 (9.4%) on both feet (table 2.6.2.1 and figure 2.6.2.1).

There is no statistically significant association between right, left, and both feet callus formation and dominant (or preferred) side in the total group of patients surveyed for the current study (table 2.6.2.1). However, statistical analysis of the male group given in table 2.6.2.1 indicates that there is a significant association with right, left and both feet callus formation and dominant side, though this result may not be justifiable since some cells within the test contingency table (not given here) had values of less than 5.

Relevant information extracted from the raw data of surveys undertaken by Whiting (1987) was studied in conjunction with the data obtained to support the current work. The age and sex distribution of patients with plantar callus surveyed as part of the current work is illustrated in figure 2.6.2.2 and can be compared with that for the employed group (figure 2.6.2.3) and patients surveyed by Whiting (1987) (figure 2.6.2.4). Information on the patients' mode age at which callus formation became a complaint is illustrated in figure 2.6.2.5.

Data extracted from the surveys undertaken by Whiting (1987) concurs with that collected in the current work (figures 2.6.2.2, 2.6.2.3, and 2.6.2.4). There was no significant difference (ANOVA) in age of onset of pathological callus formation in the employed and two patient groups surveyed in the current study (table 2.6.2.2). Thus it may be assumed the group of patients selected

for the current study are similar and characteristic of callus sufferers in the local population as a whole.

	DEB employees	Patients (Whiting 1987)	Patients (current study)
Age range	20 - 65 yrs	20-100 yrs	20-90 yrs
Callus formation: sex ratio	1M : 4F	1M : 3F	1M : 2.6F
Incidence of forefoot callus	1M : 3.5F	not known	1M : 2.6F
Age (mode) at which callus became a complaint	50-60 yrs M* 60-65 yrs F*	70-79 yrs M 70-79 yrs F	50-59 yrs M 60-69yrs F

("yrs" denotes years)
(* retirement age for men 65 years, for women 60 years)

ANOVA of age of onset of callus formation
Male group $F = 2.343$ $p = 0.12$
Female group $F = 2.476$ $p = 0.108$
($F_{alpha\ (0.05)(2,23)} = 3.422$)

Table 2.6.2.2. Data extracted from the survey of employed people (DEB) and patient group (Whiting 1987) and the patient group surveyed to support the current study. Analysis of variance has been carried out on data concerning age at onset of pathological callus formation.

Gait parameters (table 2.6.2.3) for the 50 normal subjects walking over the Kistler force plate were within the wide range reported by other workers (Greer et al 1988, Kaliszer et al 1989). There was a slight difference in the duration of right and left foot contact time between males and females.

Analysis of variance (ANOVA) is a method of analysing the way in which the mean value of a variable is affected by classifications of the data (Armitage 1980). The critical value (F alpha (0.05)) selected was at the 95% confidence level, with degrees of freedom (n, n).

The t-test permitted comparison of the means of small group sizes where the mean and variation of a normal population were not known (Armitage 1980). Significance was tested at the 95% confidence level (alpha 0.05).

Statistical analysis of results showed there was a small, but significant difference in the left foot total contact times between males and females ($t = 1.72$, $p = 0.056$), however, right foot total contact times showed no significant difference between males and females ($t = 0.77$, $p = 0.22$). Females also showed a wider range in contact times for both feet than males.

	Total contact time (ms)		
	mean	SD	range
Male R dominant			
RF (n = 18)	64.45	5.82	54 - 78
LF	64.46	4.65	56 - 72
Male L dominant			
RF (n = 5)	61.0	4.24	58 - 64
LF	61.5	4.94	58 - 65
Female R dominant			
RF (n = 21)	60.73	7.23	43 - 72
LF	59.45	6.2	48 - 70
Female L dominant			
RF (n = 6)	79.1	11.79	66 - 89
LF	69.13	7.77	63 - 78

Table 2.6.2.3 Parameters of normal foot loading during gait over the Kistler force plate. Total contact time (s) and time between peaks of the resultant are noted. Of 44 subjects, 11 were left side dominant.

The association of left and right foot contact times with dominant side (table 2.6.2.4) was investigated using Kistler data to assess the influence of laterality on gait. In right foot contact times, there was a significant difference in data for left and right side dominance (ANOVA, different sample sizes) ($F = 6.37$, $p = 0.012$). There is a significant difference also in left foot contact times in left and right side dominance ($F = 4.29$, $p = 0.01$).

The ratio of body mass to vertical reactive force was calculated from Kistler data of normal individuals so that the relationship of loading characteristics

(Fz first and second peaks (figure 2.4.1.2)) of left and right feet with dominant side could be determined. There was an insignificant difference between right and left foot loading (Fz) in left and right side dominant people (table 2.6.2.4) where the right foot, in both left and right side dominant people, took slightly less load than the left foot. Analysis of variance (F (alpha (0.05) = 2.758) showed no significant difference between left and right side dominance with left and right foot ratio of vertical loading to body weight; 1st peak force F = 0.227, p = 0.877 and 2nd peak force F = 0.969, p = 0.41. Regression analysis of left and right foot loading at the first peak of the Fz trace (y = 0.99 + 1.045y) correlated closely (r^2 = 0.91), as did data obtained for the second Fz peak (y = 1.03 + -26.15, r^2 = 0.95).

	Ratio of peak force to body weight		
	Mean	SD	Range
Left side dominant			
First peak (Fz)			
Left foot	11.04	2.08	9.5 - 14.6
Right foot	10.34	0.53	9.9 - 11.1
Second peak (Fz)			
Left foot	11.42	1.95	9.5 - 14.72
Right foot	11.0	0.8	10.2 - 12.1
Right side dominant			
First peak (Fz)			
Left foot	10.9	1.3	6.1 - 15.2
Right foot	10.9	1.2	6.1 - 13.3
Second peak (Fz)			
Left foot	10.86	1.09	5.9 - 12.5
Right foot	10.76	1.08	5.8 - 12.7

Table 2.6.2.4. Calculated ratio of body mass of normal subjects to force at the first and second peaks (Fz) during foot loading over the Kistler force plate.

2.6.3 Discussion

The incidence of forefoot callus does not appear to be related to dominant side for the total group studied, though there is a significant association between dominant side and callus formation in men. Although the numbers of women studied predominate (72% of the total group), it was not possible to extend numbers or match sexes as the accessible patient population had been exhausted. Explanations for the significant association of callus and dominant side in men are not obvious as the influence of laterality is likely to affect both sexes equally. It is unlikely that the occupation and leisure pursuits of all 69 men studied are sufficiently similar to cause indentical callus formation on each foot.

As reported by other workers (Greer et al 1988, Kaliszer et al 1989), a wide range in gait analysis parameters for left and right feet was displayed by normal subjects studied for the present work. Laterality did not appear to influence gait parameters temporally, but there was insignificant difference between loading (Fz) characteristics and dominant side. Data collected in the current work is unable therefore in general, to support that reported by Cernacek and Jagr (1972). Callus incidence does not appear to be influenced by laterality. In both right and left side dominance, the left foot takes a slight, though statistically insignificantly greater vertical load than the right foot. Peters and Durding (1979) reported inconsistency of motor behaviour in left side dominant people and these results from the current study may be a further example.

For women patients surveyed in the current study, the age for onset of callus formation was most frequent at 60-69 years, and for men at 50-59 years of age, which corresponds with that established by Whiting (1987) for an

employed group of healthy people. Leveque et al (1984) reported that ageing effects in female skin become apparent about 10 years before that for men. If callus formation were age-related, then the age at onset would therefore be expected to be the reverse of that reported here.

The potential for over-stressing plantar structures with enhanced physical activity leading to callus formation is unlikely to increase with age. However, changes in the musculo-skeletal system occur with increasing age, whereby joint range of motion reduces (Nigg and Skerlyk 1988) and opportunity for distribution of stress evenly over the plantar surface of the foot also reduces. Thus small areas of the plantar aspect are required to take loads which may normally be spread over a larger area. The consequent increase in load as well as increased duration of loading may result in mechanical damage to the keratinocytes and the cycle proposed in the present work (section 3.12.2) for callus formation is entered.

Statistical analysis of total numbers in most groups studied in the current work to assess the influence of laterality illustrated a significant difference only in left and right side dominance and vertical loading. However, to minimise any potential variation in results, the gait of either right or left side dominant people should be studied.

2.7 Investigation of reactive force vectors exerted on the forefoot during gait

The present study requires a method of relating three dimensional force and moment generated during gait to an area of the foot. In this way locomotor pathomechanics giving rise to specific force vectors acting on a particular area of the forefoot may be related to plantar callus physical characteristics and viscoelastic behaviour.

The vast majority of published papers describe instruments that have been developed to gather foot to ground contact data (Simkin and Stokes 1982, Fok 1988, Rose et al 1992, Cavenagh et al 1992). The difficulties for patients using these instruments and consequent influence on data obtained have been discussed (Messenger and Bowker 1986). Quantifiable, clinical data has been reported on whole- and forefoot loading by a few workers (Bransby-Zachary et al 1990, Ranu 1989, Hughes et al 1991) all of which consider vertical force, or pressure (force divided by area) only at specific areas on the foot. Measurement of shear stress at these sites would be helpful but this has proved technically difficult, particularly with in-shoe measurement instruments (section 2.3).

Subject variation, as well as calculation and manipulation of force plate data may lead to error. Hutton and Dhanedran (1981) recorded a +/-25% variation in data when analysing data, probably for these reasons. Studies on the validity of data provided by in-shoe instruments such as the Tekscan and the Gaitscan are few as these instruments are comparitively new developments. (Such instruments were insufficiently advanced at the time of data collection for the current study to be available for use with patients.)

As discussed in section 2.3, the Kistler force plate is an established instrument providing information on 3D force vectors and moment. It is utilised frequently in the study of reactive forces generated during gait and its foible of influencing gait by causing the patient to change walking style and cadence to strike the plate are acknowledged. Roy (1988) attempted to equate Kistler force plate data with stages of the stance phase of gait but as yet no instrument is available which is capable of attributing 3D forces and moment (torque) to a specific area of the foot at an identifiable time.

The force(s) acting on the foot during gait will be studied using the Kistler force plate data, this will be related to foot biomechanics, clinical characteristics of the lesion and callus viscoelastic behaviour. The Musgrave plate will be placed above and attached to the Kistler plate so that data generated by reactive forces during foot contact can be collected simultaneously by each instrument. Thus the intra- and inter-day differences in gait reported (de Vita and Bates 1988, Rose et al 1992) need not be considered. Any temporal effects of one plate being placed on the other will be evaluated by comparing time data with that of a third instrument, the Gaitscan (Neville 1991).

It is possible to measure forces exerted on the foot in three dimensions (3D) at the time of lesion loading but not, with currently available instrumentation, at the site of lesion loading. Although there will be a point of intersection of all forces with the force plate, it cannot be predicted that this will fall within the margins of the foot (Roy 1988). To determine the point of force intersection with the Kistler plate and then allocate this to a small region of

the Musgrave plate (from which the site of lesion loading is identifiable) requires engineering and software development outside the remit of this work. Although Bobbert and Schamhardt (1990) reported an improved method of calculating the point of intersection of force vectors with the Kistler force plate, transfer of this data to the Musgrave plate is fraught with difficulty and in-shoe force measurement instruments are therefore an attractive alternative for technological advance.

2.7.1 Comparison of use of two linked force plates (Musgrave and Kistler) with a third force measurement instrument (Gaitscan)

As the influence of the Musgrave plate on the performance of the Kistler is not known, the temporal performance of the two plates was therefore compared with a third (in-shoe) pressure measurement instrument, the Gaitscan (Neville 1991).

2.7.1.1 Methods

Instrumentation

The Kistler and Musgrave plates, and Gaitscan (see section 2.5)

Kistler force plate parameters are variable and can be used to amplify forces if required. These were set to be sensitive within the range normal for walking, with data collection over a one minute period:

Vertical (Fz) 1000N

Side to side (Fx) 500N

Front to back (Fy) 500N

Figure 2.7.1.1
A walkway was erected around the linked force plates so that subjects did not have to step up onto the raised surface of the Musgrave plate.

Kistler data collection was initiated by contact with the force plate surface, processed using instrument-specific software and stored on disc.

The Musgrave plate was set in a cradle bolted to the Kistler force plate. A walkway 7cm thick, was erected around the Musgrave plate so that the patient did not have to step up onto the Musgrave force plate (figure 2.7.1.1). Musgrave force plate data collection was initiated by contact of the patient's foot with the plate and stored on disc.

The Gaitscan insole was inserted into the subject's shoe and cables connected to the patient and microprocessor. Continuous data collection was initiated and stored on disc.

One subject was chosen to walk over the three linked force measurement systems. After a series of practice walk-overs when the clinician and subject were satisfied that a near to normal gait had been achieved, all force measuring instruments were prepared for data collection as described above. The subject was shod only for this study, all other data collected was for barefoot gait.

2.7.1.2 Results and discussion

The time recorded by the Musgrave force plate for foot loading was found to be consistently inaccurate against times recorded by both the Kistler and Gaitscan. This was an unexpected finding as previous studies by other workers (Heylings 1988, Kaliszer et al 1989) had not described this anachronism and the instrument manufacturers were apparently unable to

correct the problem. It was necessary to apply a factor of correction (2.015) to Musgrave data, which then correlated well with Kistler data ($r^2 = 0.974$, t = 0.031, p = 0.9753). However, it was elected that values recorded by the Musgrave and Kistler plates be converted into percentages for convenience of comparison of values in the current work and with those of other workers (Inman et al 1981, Rose et al 1992). Table 2.7.1.1 shows the foot loading times (milliseconds) recorded by the Musgrave and Kistler force plates. The slight variation in values given in table 2.7.1.1 probably represent the potential error of +/-9ms for the Musgrave plate.

Data obtained (table 2.7.1.2) for total foot loading times using the three force measurement instruments simultaneously showed no significant difference at the 95% confidence level between instruments (ANOVA ($F_{alpha\ (0.05)(2,22)}$ = 3.44, F = 0.4, p = 0.67).

	Musgrave contact time (ms)	Kistler contact time (ms)	Musgrave: Kistler contact ratio
Mean	336.6	676	2.015
SD	83.46	159.39	0.06
Range	216 - 468	460 - 940	1.94 - 2.13

Table 2.7.1.1 Total foot contact loading times recorded simultaneously by the Musgrave and Kistler force plates.

	Musgrave (corrected times) (ms)	Kistler (ms)	Gaitscan (ms)
Mean	740.57	737.14	736.00
SD	28.66	17.05	16.49
Range	725 - 798	720 - 780	719 - 763

(n = 8)

Table 2.7.1.2 Comparison of total contact times for Musgrave (corrected data), Kistler force plates and the Gaitscan.

2.8 Forces exerted on the forefoot of normal subjects and patients with plantar callus studied using the Kistler and Musgrave plates.

It has been assumed from empirical evidence that excess mechanical force is implicated in the aetiology of corn and callus formation. Intermittent pressure has been mooted as the predominant aetiological factor (Adams et al 1989). There is no doubt that excess pressure is influential in the formation of ulcers on the sole of the foot (Tappin et al 1980, Nakamura et al 1981) in patients where the viability of peripheral tissues is questionable. However patients studied in the current work were otherwise healthy, and as demonstrated previously, were characteristic of the local population.

The formation of callus on the sole of the foot may indicate areas of excess loading (Soames et al 1982), however the nature of this overload has not been established, nor has the postulated increased duration of contact in patients with plantar callus been studied. Therefore the temporal parameters of forefoot and lesion loading will be studied in normal subjects

and those with plantar callus. Reactive forces other than vertical pressure may be influential in the aetiology of these lesions. The majority of studies by other workers consider the measurement of pressure only during gait (Cavenagh et al 1987, Hughes et al 1991, Henig and Rosenbaum 1991), which may be a reflection of the difficulties in technological development of methods for measuring forces in other planes. Shear stress and friction have proved difficult to measure on the sole of the foot (Tappin et al 1980, Neville 1991, Rose et al 1992) as transducers created were too thick to permit unperturbed gait or thinner materials delaminated with use. Forces exerted of the forefoot of normal subjects and patients in the current study, will be sampled at normalised intervals and compared. Data so obtained will extend the information available on force loading during the forefoot contact period and may help to explain some of the clinical features of callus.

The time of forefoot and lesion loading can be isolated using a Musgrave software option. The forces exerted on the foot at the time of lesion loading can be identified by merging Kistler and Musgrave data. Thus a study of reactive forces exerted on the forefoot during the time of loading of a callus lesion can be made. Unfortunately, as other instruments measure force per unit area (pressure), direct comparison with Kistler data (force) is difficult (table 2.8.1).

Metatarsal heads					Force measurement instrument
1st	2nd	3rd	4th	5th	
.....96.4 - 43.1.....			.....92.9 - 28.1 kPa....		in-shoe (Bransby-Zachary et al 1990)
420	400	380	250	180kPa	in shoe (Soames et al 1982)
163	212	197	160	97N/mm^2	foil pedobarography (Grieve and Rashdi 1984)
270	330	300	**	130kPa	in-shoe (Gross and Bunch 1988)
314	**	380	**	215kPa	capacitive pressure distribution platform (Henig and Rosenbaum 1991)
210	250	240	180	140kPa	pedobarograph (Hughes et al 1991)

** not reported

Table 2.8.1 The range of loads measured by other workers under the forefeet of subjects using a variety of instruments.

2.8.1 Materials and methods

(see sections 2.5. and 2.7.1.1)

Fifteen subjects (7 male and 8 female) who had no obvious body asymmetry, evidence or history of foot or leg complaints and were in good general health were selected for the "normal" group. All were right side dominant, age range 19 - 35 years.

The few patients who satisfied inclusion criteria were selected from the patient population of the Dept of Podiatry, University of Brighton. Patients

who had forefoot plantar calluses and agreed to take part were required to have good general health, no obvious body asymmetry, able to walk over the force measurement plates in a normal manner and be able to stand for a number of minutes while each force measurement instrument was made ready. All were right side dominant, age range 30 - 84 years (14 male 13 female).

Both force measurement data collection and US measurements were made at this time. Also callus was removed from the patient's forefoot prior to walking over the force measurement plates as the lesion(s) were often very painful when walking, particularly when barefoot. The callus sections were stored in liquid nitrogen for later investigation. Callus removal, force measurement and US measurement took no less than one and a half hours for each patient.

When making force measurements, two acceleration steps were taken by each subject before stepping onto the force plates (West 1987). After an initial practice period walking over the linked force plates in the walkway, data collection by each instrument was initiated by foot contact with the plates. Three sets of data were recorded for each subject. Differences in results obtained for all left foot and then all right foot loadings were calculated. Data from both instruments of force vector and moment were stored on disc for later processing. The same procedure was adopted for the patient group, but the number of "walk-overs" was reduced to two for this group as many found the time taken for data processing too tiring or too painful.

The time of forefoot loading was identified from the Musgrave plate data. Once the time of the start and end of forefoot loading had been obtained as a percentage of total contact time, this data was applied to Kistler data times. Using Kistler data at the times dictated by Musgrave data, 3D reactive forces and moment during forefoot loading were identified. To reduce the volume of data, sampling was carried out at incremental intervals of 20% for the forefoot contact time for each subject. This method was necessary as forefoot contact time varied for each subject and sampling at proportionate times was required. Statistical analysis was carried out on force data (Fxyz, moment resultant) for normal subjects and patients.

2.8.2 Results

The forefoot loading period, identified using Musgrave data and applied to Kistler data, can now be allocated for forefoot plantar callus patients and normal subjects and is illustrated in figure 2.8.2.1.

Both patients and normal subjects showed a wide range in values for same whole foot, and forefoot loading times, with normal subjects having the smaller variation values (table 2.8.2.1). Insufficient data on total and forefoot contact times for same foot and opposite feet for normal subjects and patients precludes further analysis.

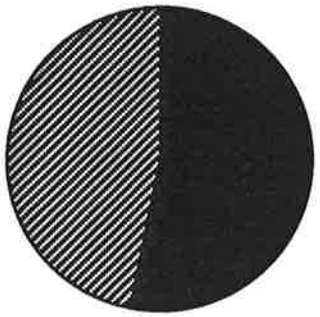

forefoot contact
time 53% (0.36s)

Normal subjects

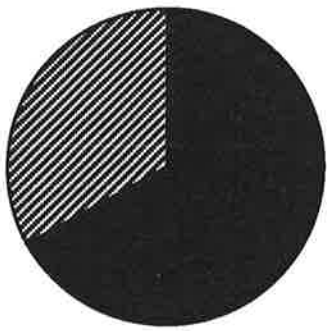

forefoot contact
time 67% (0.53s)

Patients

Figure 2.8.2.1
Proportion of forefoot to total foot contact time in normal subjects and patients with plantar forefoot callus.

	Differences in time of same foot loading			
	Mean	SD	Range	Coefficient of variation
Foot loadings for Normal subjects n = 15 Forefoot contact differences	0.03	0.001	0 - 0.08	111.55%
Foot loadings for patients n = 42 Forefoot contact differences	0.113	0.251	0 - 0.08	221.96%

Table 2.8.2.1. Same foot loadings for normal subjects and patients. Values given are the differences in time (seconds) between same foot loadings.

Figure 2.8.2.2 illustrates the onset of forefoot loading for normal subjects and patients during total foot loading (table 2.8.2.2). Figure 2.8.2.3 illustrates the proportion of forefoot contact to total contact time for both normal subjects and patients with plantar forefoot callus respectively. The duration of forefoot loading for normal subjects is 53% of the total contact time and for patients, the duration of forefoot loading is 67% total contact time. Statistical analysis of forefoot loading times (ANOVA different sample sizes) shows a significant difference between results for normal subjects and patients ($F_{alpha\ (0.05)} = 4.08$, $F = 14.38$, $p = 0.37^{-04}$), correlation is poor ($r^2 = 0.1299$), and the difference in loading times illustrated in figure 2.8.2.2 would indicate a marked difference between forefoot loading times in normal subjects and patients.

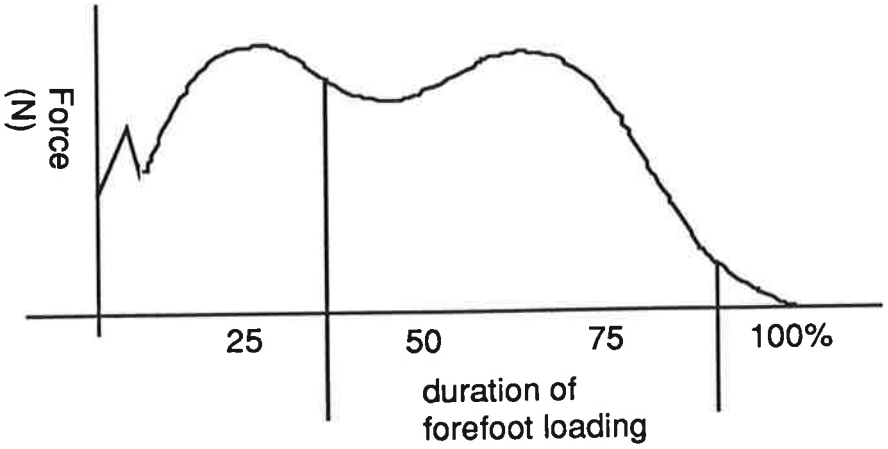

Figure 2.8.2.2
Typical F resultant indicating mean position of normal forefoot loading during the stance phase of gait

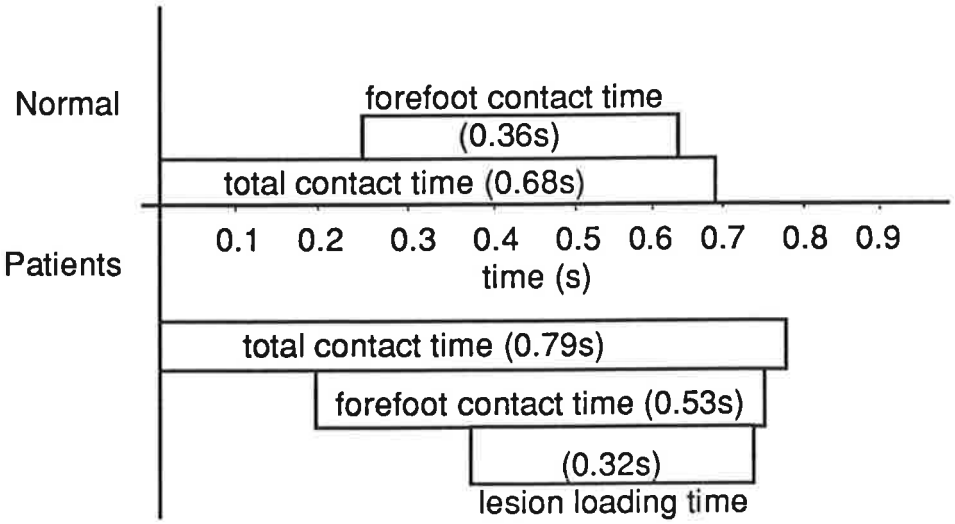

Figure 2.8.2.3
Forefoot contact and total foot contact time in patients and normal subjects.

	Time (s) Mean	SD	Range
Total foot contact time normal subjects			
Start of loading	0		
End of loading	0.68	0.05	0.6 - 0.77
(n = 15)			
Forefoot loadings for normal subjects			
Start of loading	0.27	0.07	0.12 - 0.38
End of loading	0.63	0.059	0.52 - 0.72
Total foot contact time, patients			
Start of loading	0		
End of loading	0.79	0.107	0.56 - 0.99
(n = 42)			
Forefoot loadings for patients			
Start of loading	0.22	0.131	0.03 - 0.68
End of loading	0.75	0.11	0.53 - 0.96

Table 2.8.2.2. Total and forefoot loading times (in seconds) of normal subjects and patients with plantar forefoot callus.

Comparison of body weight (t-test) indicates that there is no significant difference between normal subjects and patients ($t = 3.0068$, $p = 4.1$). Therefore the ratio of Fz values to body weight need not be calculated when comparing normal subjects' and patients' gait parameters in general terms rather than in matched individuals.

Comparison of F x,y,z and moment resultant (Mr) measured during forefoot loading in normal people and those with plantar forefoot calluses (appendix 2 and table 2.8.2.3) showed no significant differences, except for movement in Fy (forward and backward) between 40% and 80% of forefoot loading for

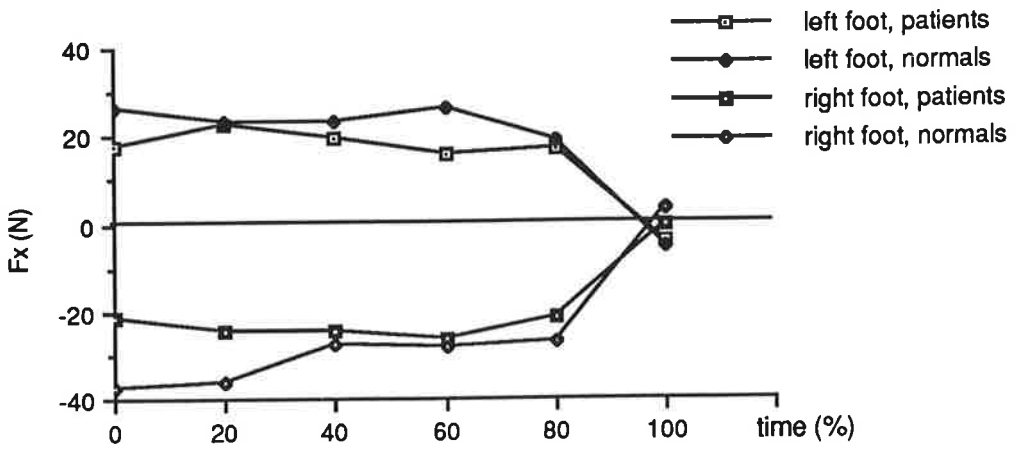

Figure 2.8.2.4
Plot of Fx (N) mean at 20% incremental intervals
of forefoot contact time in normal subjects and patients.

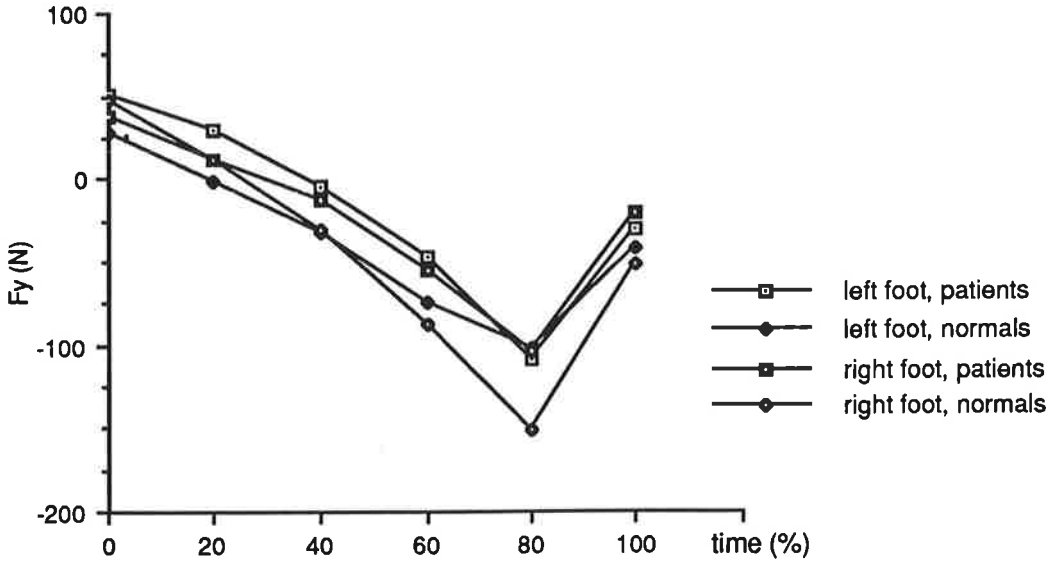

Figure 2.8.2.5
Plot of Fy (N) mean at 20% incremental intervals of
forefoot contact time in normal subjects and patients.

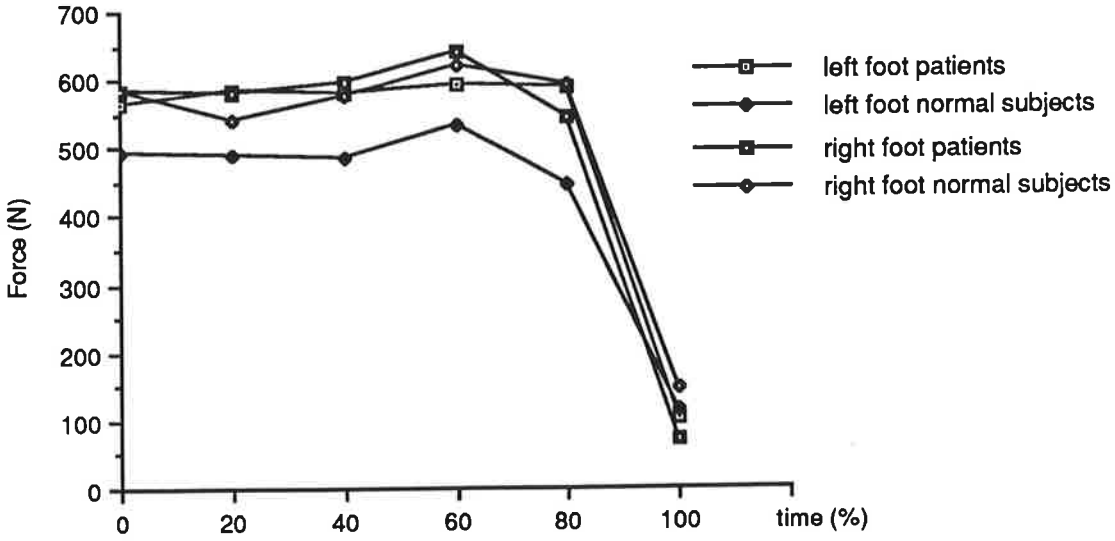

Figure 2.8.2.6
Plot of Fz (N) mean at 20% incremental intervals of forefoot contact time in normal subjects and patients, left and right feet.

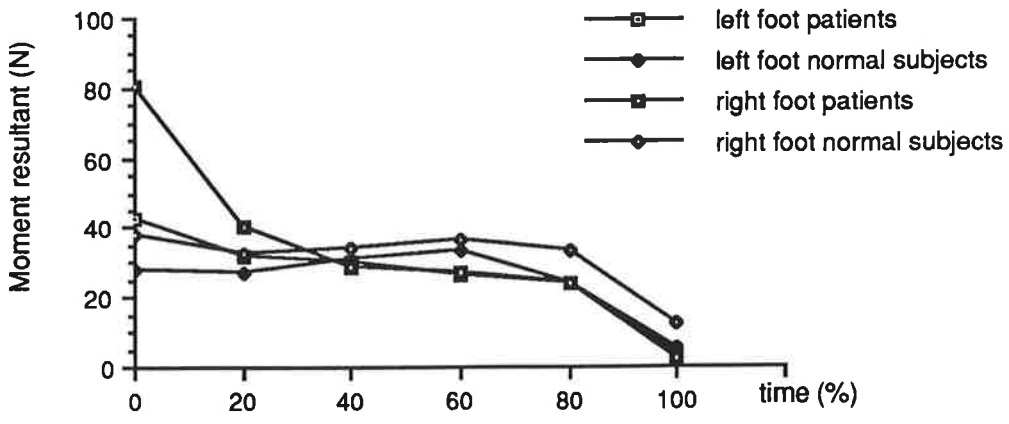

Figure 2.8.2.7
Plot of mean of moment resultants at 20% incremental intervals of forefoot contact time in normal subjects and patients, left and right feet.

normal subjects and patients, and no significant difference in vertical force (Fz) at 20% forefoot loading. Figures 2.8.2.4, 2.8.2.5, 2.8.2.6 and 2.8.2.7 illustrate the mean for each of these forces. (Mr is the resultant of moments in the x, y and z planes.)

The range of values for Fxyz and Mr is invariably greater for patients than for normal subjects, and when comparing data on reactive forces in normal subjects and patients, no specific force vector or moment appears predominant. For patients generally, reactive forces have a longer duration than in normal gait, reflecting an increase in contact time for the forefoot (figure 2.8.2.1).

Comparison of normal subjects and patients
(ANOVA different sample sizes)

Percentage time of forefoot contact	Fx				Fy	
	left foot		right foot		both feet	
	F	p	F	p	F	p
0%	0.721	0.404	3.986	0.0562	0.692	0.561
20%	0.907^{-03}	0.951	2.035	0.1648	2.395	0.0786
40%	0.343	0.563	0.186	0.6695	4.217	0.97^{-03}
60%	2.64	0.1178	0.48	0.8276	5.83	1.63^{-03}
80%	0.081	0.7787	0.423	0.5213	3.81	0.015
100%	0.05	0.0824	1.118	0.2996	2.626	0.0924
Critical value F alpha(0.05)	4.22		4.25		4.25	

	Fz		Mr			
	both feet		right foot		left foot	
	F	p	F	p	F	p
0%	0.849	0.473	1.035	0.319	0.684	0.417
20%	2.95	0.04	0.215	0.6474	0.794	0.382
40%	1.748	0.168	0.011	0.9193	0.828	0.372
60%	1.95	1.32	0.799	0.38	2.762	0.1107
80%	1.643	0.191	0.1^{-04}	0.98	2.124	0.1598
100%	1.946	0.134	0.484	0.494	50.8	3.79^{-03}
Critical value F alpha (0.05)	2.75		4.22			4.25

Table 2.8.2.3 Statistical comparison (ANOVA different sample sizes) between patients and normal subjects for each force at each section of time is given, with the critical value (F alpha 0.05).

2.8.3 Discussion

In the past, it has been difficult to identify the components of the stance phase of gait which contribute to the resultant trace from the Kistler force plate. However, data generated in the current study allow a section of the Kistler resultant trace to be attributed to forefoot loading time for normal subjects and patients (figures 2.8.3.1 and 2.8.3.2) which confirms the assumptions made by Roy (1988).

Variability is associated with all human performance (de Vita and Bates 1988) as manifested in the gait of both normal subjects and patients. The current study was not designed to detect variation in same and opposite foot loading, however data obtained for other aspects of gait analysis (reactive force vector analysis) show a trend towards slight variability in same foot loading in normal subjects, whereas those for patients are markedly different. The variation in reactive force results in the current study is commensurate with those found by other workers (Kaliszer et al 1989, Hughes et al 1991). The extent of the influence of laterality is not clear without further data collected specifically to investigate this issue.

It is difficult to speculate, without a longitudinal study being undertaken, whether the variability in gait parameters demonstrated by patients results from a mechanism developed by them to avoid loading an uncomfortable or painful plantar callus, whether the variation is a prelude to development of the lesions, or this variability is due to some other, more obscure reason.

It is disappointing that no particular reactive force vector appears prevalent during forefoot loading in patients when compared with normal subjects; to manage the effects of one parameter would be much easier than dealing with a variety of aetiological factors. However, as gross averages were considered this is perhaps not surprising, and force analysis associated with lesion type is considered in the next section of this chapter. The loading of the forefoot in patients is of significantly longer duration than for normal subjects (figure 2.8.2.2). Comparison of Fy values in patients and normal subjects shows a significant difference between 40% and 80% of forefoot contact time which coincides with the mean onset of lesion loading (section 2.9). As the patient group was older than the normal subject group, age may have influenced their cadence (Nigg and Skleryk 1988) and consequently foot contact time, however this relationship is disputed by Hughes et al (1991).

Whilst there is no statistical difference between reactive forces measured for normal subjects and patients, (except for Fy at 40%, 60%, and 80% of forefoot contact) figures 2.8.2.4, 2.8.2.5, 2.8.2.6 and 2.8.2.7 illustrate a slight variation in gait patterns. It appears that patients move less from side to side (Fx), and do not accelerate or decelerate (Fy) with the alacrity of normal subjects (figure 2.8.2.5). The culmination of these small variations coupled with a significantly increased duration in forefoot loading in patients (table 2.8.2.1) may be that force application on the plantar forefoot will be spread over a smaller surface region. The same force would then be received by a smaller region, or conversely, it would receive a proportionately larger force, possibly sufficient to initiate the cycle of callus formation.

As shown in table 2.8.1 comparison of vertical force (Fz) measurement with those of other studies is difficult as the units of measurement are not directly compatible. However, the results of the current work concur generally with those of other workers (Soames et al 1982, Gross and Bunch 1988, Hughes et al 1991, Rose et al 1992). Measurement of force Fx and Fy have been reported rarely (Tappin et al 1980). The novel method reported in the present work, of using two force plates in conjunction, has produced data on side to side and front to back reactive forces during forefoot loading. It has also been shown that there is no statistical difference in overall forefoot vertical reactive force (Fz) in normal subjects and patients during the time of forefoot loading (although the Musgrave plate data illustrates a site of peak pressure over the lesion site in all patients) (figure 2.9.2.2).

Normal forefoot loading time was calculated to be 53% of total stance time compared with 68% (Scranton and McMaster 1970), and 25 - 53% (Miller and Stokes 1979). A functionally abnormal forefoot was reported by Miller and Stokes (1979) to take 21 - 54% of total foot contact time, compared with that of 67% for patients' forefoot contact demonstrated in the current study. The differences in values reported are most likely to represent the variability in data collection techniques, instrumentation and intra- and inter-day variation reported by other workers (Heylings 1988, de Vita and Bates 1988, Stewart and Grove 1989) as well as the different foot conditions studied. The volume of data generated by the Kistler and Musgrave force measurement plates was vast and the data reduction (Henig and Rosenbaum 1991), coupled with a potential error of +/-9ms in the Musgrave plate may have lead to some unavoidable minor inaccuracies. Linking two force plates, utilising two different principles of force measurement, may

introduce error (Stewart and Grove 1979) and this method of measurement must be considered crude once in-shoe instruments have been developed which are capable of measuring shear stress as well as vertical force.

The time taken for data collection in the current work distressed some patients and the consequent physical tiredness and drain on their ability to concentrate may also have influenced results to the extent that some of the later force plate loading data had to be discarded as giving totally uncharacteristic, aberrant results. Refusal of the Musgrave microprocessor to accept and reload stored data led to a loss of some information (7 sets of data). Also the Kistler microprocessor became prone, with aging, to idiosyncratic retrieval of files due to a faulty brake on the hard disc again leading to loss of data. Thus the quantity and pattern of data collated for analysis was not as expected.

2.8.4 Conclusion

It would appear from results of the present work, that duration of forefoot contact with the ground is increased in patients with forefoot plantar callus. The summation of insignificantly less side to side (Fx) and back to front movement (Fy) in patients may result in a smaller area of symptomatic forefeet of patients being subjected to forces, leading to over-stressing of the area. The empirical assumption that pressure alone is implicated in the formation of callus would therefore appear to be erroneous and the surmised increased duration of forefoot loading in patients has been confirmed in this work. Application of this information to the mechanical management of callus lesions will require, for example, insole materials to

absorb vertical stress as well as shear; and pressure redistribution alone is inadequate. The effects of the increased duration of lesion contact compared with a normal foot, established in the present work, may also be applied to the formation of ulcers in non-viable tissue and mechanical management should be pursued accordingly.

It should be recalled that pressure (force/area) as measured by the Musgrave is more than simply comprised of vertical force, it is an aggregate of a predominant vector (Fz) and probably values in the other planes which the Musgrave cannot measure. However, when using the Kistler force plate, the force vector can be resolved into Fx, y and z.

2.9 The relationships between force vector, pathomechanics, clinical appearance and callus viscoelasticity

It is possible to see variations from the normal dermatoglyphics under the translucent hyperkeratotic tissue of a callus plaque. Clinically, these appear flattened, accentuated or tortuous (figures 2.9.1, 2.9.2 and 2.9.3). It had been considered that these variations may indicate predominance of one particular force vector. While studying the sequence of force loading on the forefoot of patients suffering with plantar forefoot calluses, it has become clear that an increase in duration of forefoot contact, compared with that for normal subjects, is involved in the aetiology and clinical features of these lesions. However it is interesting to pursue the loading characteristics at the time of individual lesions to see whether a pattern of force vectors emerges associated with flat, accentuated or tortuous dermatoglyphics in a callus plaque.

Figure 2.9.1
Plantar skin callus showing flattened dermatoglyphics

Figure 2.9.2
Plantar skin callus showing accentuated dermatoglyphics

Figure 2.9.3
Plantar skin callus showing tortuous dermatoglyphics

2.9.1 Materials and methods

Instrumentation

(as described in section 2.5)

Data from patients with forefoot callus studied in the previous section (2.8) were used to study the reactive forces during the time of lesion loading.

The period of lesion loading was identified in the manner described previously when identifying forefoot contact time using data from the Musgrave and Kistler force plates. Data sampling was made at 40, 60, 80 and 100% forefoot contact time, so that a profile of force loading could be generated enabling identification of any prevalent force vector associated with lesion type.

2.9.2 Results

The duration of callus lesion loading (table 2.9.2.1) is illustrated in figures 2.8.2.1. There is a wide range in times for both the start and end of lesion loading, however it is evident that the callus lesion loads for a considerable period of forefoot contact time. In patients, forefoot loading time as a proportion of total foot loading, is generally more prolonged than in normal subjects.

lesion loading	Mean	SD	range
start	0.39	0.166	0.15 - 0.83 seconds
end	0.74	0.112	0.53 - 0.98

Table 2.9.2.1. Time (s) of lesion loading during total foot contact time (patients) (n = 42)

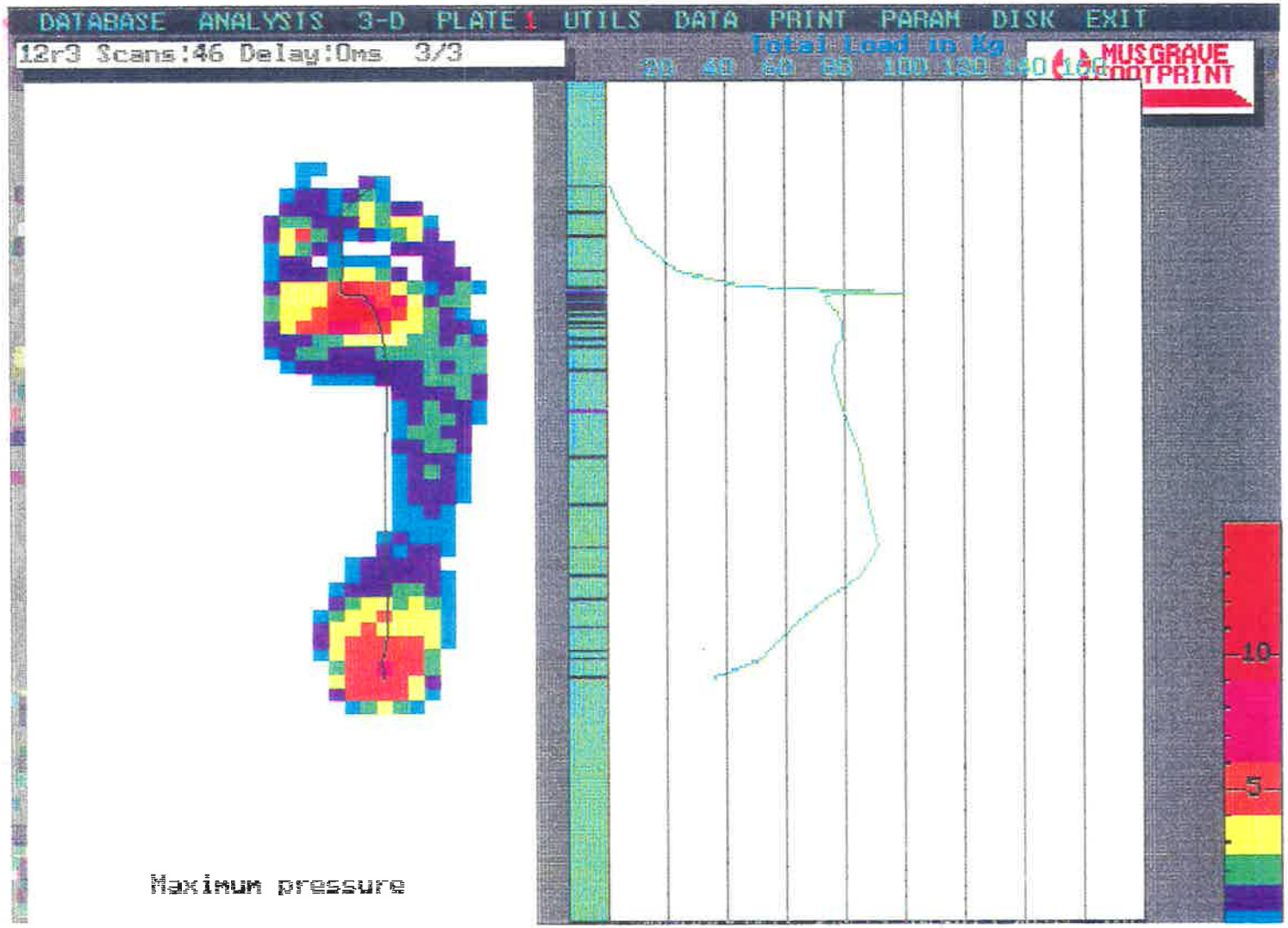

Figure 2.9.2.2
Forefoot loading pattern obtained using the Musgrave plate. The site of plantar forefoot callus coincides with the peak pressure as demonstrated by the red-coloured squares. Thus the peak pressure seen on the heel is equal to that under the centre of the forefoot. The central green bar indicates duration of pressure and the speed of progression of the body's centre of pressure.

It was shown that there was no significant difference in duration of lesion loading and callus lesion clinical appearance when considering all lesion types (accentuated, flattened or a combination of these patterns) (ANOVA different sample sizes $F_{alpha\ (0.05)} = 3.315$, $F = 1.28$, $p = 0.2911$).

It is clear from the Musgrave data, that the site of the lesion takes a greater load than surrounding skin (figure 2.9.2.1), possibly because the contour of the lesion creates a specific point of contact. It is not possible to segregate the different reactive forces acting on the lesion itself. However, there is no significant difference in vertical reactive force (Fz) between normal subjects and patients during the time of lesion loading (appendix 1 and table 2.8.2.3.2) as measured by the Musgrave and Kistler force plates combined.

The reactive forces at the time of each lesion loading (appendix 2) were studied so that a profile of predominant force (if any) could be demonstrated. This was then related to the callus clinical appearance where dermatoglyphics were seen to be accentuated, flattened, tortuous or a combination of these (table 2.9.2.2). There was a significant difference (ANOVA different sample sizes) in all parameters measured at the start of lesion loading and at 40% of forefoot contact time (table 2.9.2.2 and appendix 2). Thereafter no significant difference in parameters measured was evident between lesion types, except in Fx and Fy at 60% forefoot contact time, which corresponds to forefoot loading data (tables 2.8.2.3.1 and 2.8.2.3.2).

40%	Fx	Fy	Fz	Mr
F	3.55	7.44	4.2	2.57
p	0.023	4.85^{-04}	0.0115	0.0681
60%				
F	2.91	4.167	0.679	0.25
p	0.0468	0.012	0.5706	0.8608
80%				
F	2.797	3.173	1.934	2.299
p	0.0531	0.0531	0.1406	0.0929
100%				
F	0.233	2.103	1.3	0.969
p	0.8727	0.116	0.2884	0.4174

Table 2.9.2.2 Comparison of all the different callus lesion types investigated in the current work (accentuated, flattened, tortuous or a combination of these). Data sampling was taken at 40, 60, 80 and 100% intervals of forefoot contact time. Statistical analysis was carried out (ANOVA) and values are given ($F_{alpha\ (0.05)} = 2.83$)

2.9.3 Discussion

While innovative identification of the reactive forces exerted on the foot during the time of forefoot and lesion loading has been possible in the current work, the original intention that forces exerted on a plantar forefoot lesion be investigated has not been fulfilled. The engineering and software development required to calculate the location of force intersection (Bobbert and Schamhardt 1990) with the linked Musgrave and Kistler force plates (if feasible) which would be equated this with a site on the load-bearing foot, are outside the remit of the current study.

The total vertical force (Fz) exerted on the forefoot during forefoot and lesion loading is statistically similar for both patients and normal subjects studied in

the present work. However, there is an uneven spread of load across the forefoot in patients as demonstrated by the Musgrave display (figure 2.9.2.1). Variations in loading of an area within the normal forefoot (table 2.8.1) have been reported and sites of overload have been described in people with foot pathologies (Miller and Stokes 1979, Nakamura et al 1981, Soames et al 1982).

The empirically held hypothesis that callus shape and size may be indicative of the forces acting upon it (Adams et al 1989) has not been confirmed, by the current work. The forces acting on the foot during the time of lesion loading have been related to each callus lesion clinical characteristic (accentuated, flattened, tortuous dermatoglyphics, or a combination of these). In lesions where dermatoglyphics are accentuated, flattened or a combination of these features there is an increase in Fx and Fy in the early stages of lesion loading, suggesting that shear stress may be implicated in relation to the type of lesion. However, otherwise there is no significant difference for each of these lesion types.

It would appear therefore, that callus dermatoglyphics may be influenced by early increases in force in Fx and Fy planes, but further association of clinical appearance with force vectors is tenuous. Other factors which are probably influential in the aetiology and appearance of plantar calluses include history of the duration of the lesion (which was not studied), the effect of change in joint range of motion and bending resistance of bone with age, the skin biomechanics and extent of dermal fibrosing. It is unlikely that even in-shoe pressure and shear stress measuring instruments will be able to provide definitive data in view of this list of variables.

Water content of callus tissue and therefore its viscoelastic behaviour may influence its interaction with dermal tissue giving rise to the dermatoglyphics described. The viscoelasticity of callus tissue is probably intimately related to its water content (Wildnauer et al 1971, Potts and Breuer 1981, Tagami et al 1988), this in turn to the presence and quality and quantity of the stratum corneum lipid lamellae (Mackenzie 1983, Phillips 1992) and thence its biomechanical behaviour is influenced. This concept is discussed further in section 5.4.

It is possible to see patches of parakeratosis and orthokeratosis in callus histological sections (figure 3.12.2.3) , though it is difficult to equate these with the clinical, macroscopic appearance as histological section preparation distorts these features. Areas of parakeratosis, indicative of incomplete keratinisation, may also have incomplete formation of the lipid lamellae (Mackenzie 1983). In corns, where parakeratosis is invariably present, the lipid lamellae appear absent (Phillips 1992). Should this premise be correct, then the duration and magnitude of force vectors will be only one of the factors influential in callus dermatoglyphic variation. Cell division in the basal layer is slightly increased in callused skin (Dykes 1992) which might cause further undulation of the DEJ.

On weight-bearing, a transient ischaemia of the superficial blood plexus occurs, and in disease states this is sufficient to cause ulcer formation (Nakamura et al 1981). Preliminary laser doppler imaging of callus lesions show changes in superficial plexus flow at rest and just after walking. These early results show marked changes in flux in the foot after removal of the

callus tissue (see figures 2.9.3.1 and 2.9.3.1). The presence of callus tissue causes attenuation of pulses so that no useful data can be obtained. Further studies are required to assess the influence of blood flow and the effect of ischaemia on weight bearing which occurs with the prolonged loading of the forefoot in plantar callus sufferers. Further studies are also required in all the hyperkeratoses (psoriasis, ichthyosis, callus), to determine whether diffusion of nutrients from the superficial blood plexus into the epidermis may affect the epidermal transit time and keratinisation of squames. It would be interesting to pursue studies into the duration of the transient ischaemia of plantar skin on load bearing and relate this to release of dermal cytokines.

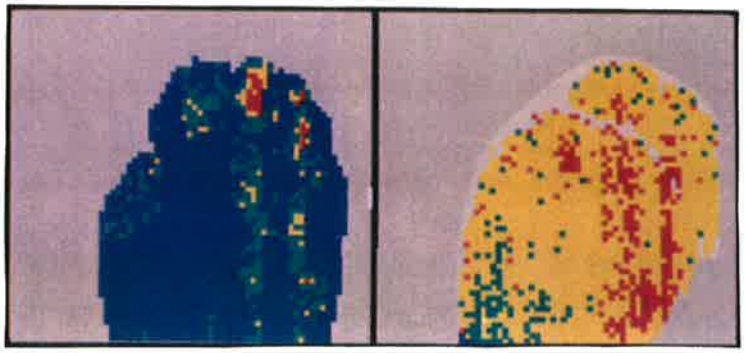

a b

Plantar callus lesion sites

Figure 2.9.3.2
Laser doppler flow image of blood flux under a callus plaque at rest (a) and after walking (b). The thickness of the callus precludes satisfactory reception of echoes from the superficial plexus.
Blue and green denote slow flow, yellow and red faster flow respectively.

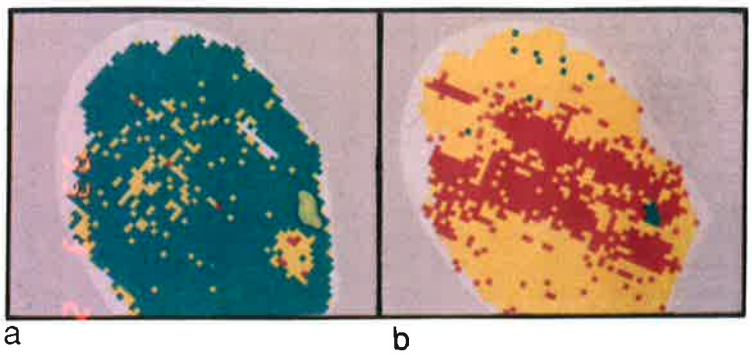

a b

Figure 2.9.3.3
Laser doppler flow image of blood flux under the same callus plaque after removal of the callus tissue, at rest (a) and immediately after walking (b). Removal of the callus tissue minimises pulse attenuation and useful data on superficial plexus blood flux can be obtained. A change in flow under the most severe lesion, 5th metatarsal head, at rest (a) and after walking (b) is evident.

2.10 Summary

The reactive force vectors, Fx and Fy, are significantly different only during the early stages of lesion loading, otherwise all other parameters measured are not significantly different for patients and normal subjects. The Musgrave data demonstrate the lesion site invariably takes an increased load compared with adjacent structures. The increased duration of loading in patients may be indirectly influential in causing changes in the rate of epidermal proliferation and differentiation during keratinisation. These changes may be due in part to a more prolonged but still intermittant trauma to the epidermal and dermal structures resulting in release of cytokines such as epidermal growth factor (Steinert and Cantieri 1983) and TGFβ (McKay and Leigh 1991). Excess and over-prolonged mechanical stress may also stimulate keratinocytes to release cytokines such as Interleukin 1 (Camp 1990) which will stimulate epidermal cell proliferation and possibly increase cell transit rate leading to hyperkeratinisation of areas of the plantar surface of the foot.

The rapid transit rate of squames in callus may preclude formation of mature lipid bilayers, and histologically it is possible to see patches of parakeratosis. Thus potential exists for formation of areas of different hydration levels within the stratum corneum of callus and consequent variation in tissue stiffness (chapter 5).

Further studies should be directed to more detailed consideration of single lesion types and force analysis, so that a useful method of lesion categorisation may be developed.

CHAPTER 3

Quantification of the characteristics of plantar calluses

3.1 Introduction

Plantar callus lesions have characteristics which are difficult to quantify and the margins of the callus plaque are not always definite. It is thought that the clinical appearance of the dermatoglyphics may provide an insight into the mechanical aetiology of callus (Adams et al 1989), therefore it will be useful to define these features. Methods which permit non-invasive measurement of the thickness of skin calluses on the plantar surface of the foot may allow development of a lesion contour map to facilitate the description of lesion characteristics in preparation for studies investigating aspects of the aetiology of calluses. Non-invasive techniques were considered essential to avoid the prolonged healing which resulted on the sole of the foot post-biopsy (Thomas 1987).

3.2 Non-invasive methods of measuring skin thickness

Non-invasive techniques available for skin thickness measurement are relatively limited and include magnetic resonance imaging (MRI) and xeroradiography.

The MRI technique described by Querleux et al (1986) provided an interesting comparison with ultrasound measurements on skin, but owing to the very different nature of instrument signal output, results could not be compared directly. Leveque et al (1991) reported detailed imaging of skin using MRI and also implied this technique would have a useful future in this field. Sadly MRI systems are few in number, not readily available due to high cost, and those with resolution suitable for skin are particularly scarce.

Xeroradiography of the skin described by Tan et al (1981) requires specialist instrumentation and expertise. Ultrasound measurement of skin, validated by Tan et al (1982) and Dines et al (1984), was adopted by a number of centres since it was readily available, totally non-invasive, and relatively inexpensive. Payne (1988) reviewed the role of ultrasound (US) in skin thickness measurement and concluded that it was the method of choice. Edwards et al (1986) using an appropriate range of transducer probes, suggested it possible to measure the depth of the component skin layers in normal plantar skin and hyperkeratotic areas such as corns and callus.

The method of US measurement was therefore selected for the current study to measure callus depth non-invasively and it was considered that it may be possible to map the visible dermatoglyphics within the callus plaque, to provide a quantifiable definition of these features.

Ultrasound measurement of full skin thickness has become an accepted technique, however identification of the position of the base of the epidermis and the DEJ continues to be contentious. The non-invasive identification of the position of the DEJ and the visible dermatoglyphics within a callus plaque is important to the current study. It was decided therefore, to pursue the US investigation of the DEJ position using initially A-scan (amplitude), and later B-scan (brightness) instrumentation and compare these US measurements with the histological studies.

3.3 Ultrasound in skin imaging

Ultrasound is used by animals (for example bats and porpoises) for echo-location and characterisation of objects both in air and under water (Fleischer

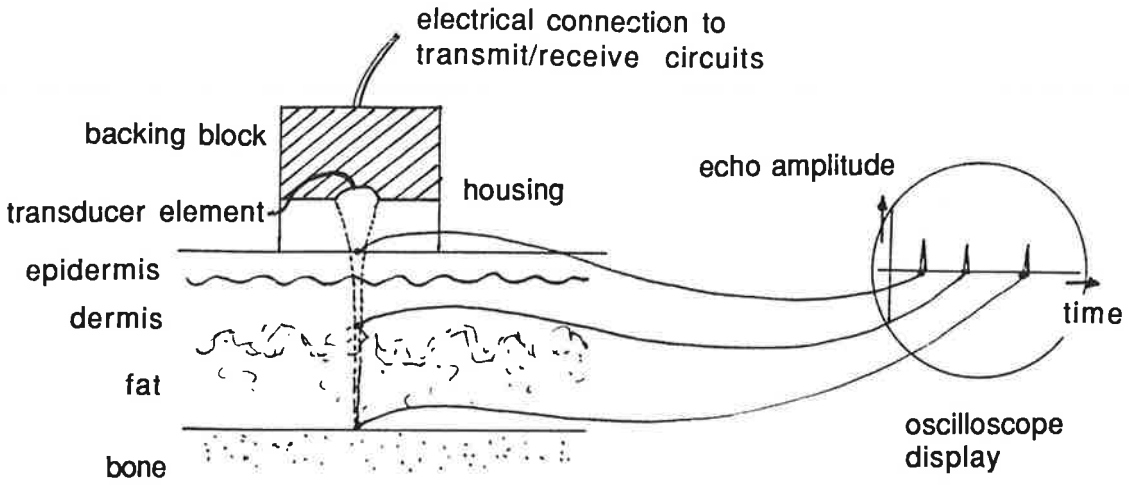

A-scan

B-scan

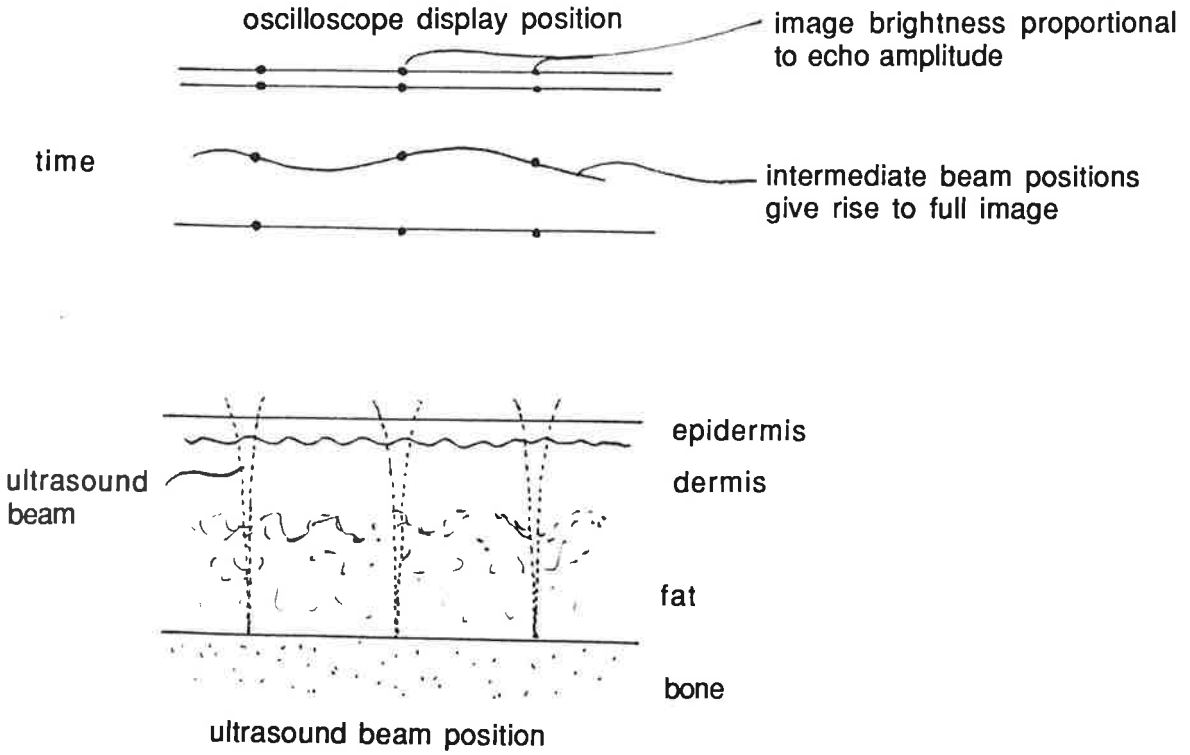

Figure 3.3.1
Diagram illustrating the relationship between A-and B-scan ultrasound imaging systems.

and James, 1980). In medicine, US has therapeutic uses, mostly at frequencies of 1 - 3MHz, as well as being used to obtain US images of body structures. US imaging techniques are now well established with foetal imaging being perhaps the most widely used application, but it is only relatively recently that the technique has been applied to dermatological studies. Non-invasive investigation is obviously attractive to the patient and ultrasound skin imaging has the potential for obviating biopsy in skin disease as well as in differential diagnosis of malignant and benign melanoma (Nessi et al 1991). Unfortunately the apparatus used in existing instruments for imaging body structures cannot be applied directly to ultrasound measurement of the skin since the transducer frequencies are inappropriate.

Current skin ultrasound imaging systems still require some refinement. Information about skin thickness is converted by the instrument into a linear amplitude scan (A-scan) on an oscilloscope screen or with use of appropriate software into a B-scan image (brightness scan) on a monitor. The A-scan oscilloscope trace requires practice to interpret, whilst the B-scan image is of poor quality and is reliant on the most appropriate gain ("intensity of picture") being selected. Initially A-scan instruments were utilised (Payne 1985) and applied to clinical investigations (Tan et al 1981, Mandy 1988). More recently B-scan ultrasound imaging has been utilised in clinical investigation with some success (Nessi et al 1991) and programs for three dimensional C-scan images have been written recently (al Gammal 1991). The relationship between A- and B-scan systems is illustrated in figure 3.3.1 (Payne 1985).

It is possible, when the time base of the A-scan trace is expanded, to detect a quiet region within the thin skin entry/exit echo waveforms. This region in the A-scan trace may be interpreted as indicating a change in the quality of tissue from one relatively homogeneous tissue to another, *viz* the minor interface

between the stratum corneum and viable epidermis or the DEJ. Identification of the structural region within the epidermis from which this quiet region of the A-scan originates may be feasible, but even amongst those who accept its existence, it is still a subject of controversy and research. It is also within the remit of the current work to investigate also the relationship of the quiet area in this waveform to skin structures.

3.4 Principles of ultrasound in skin thickness measurement

Ultrasound waves are compressional waves produced by the push-pull of the source, normally a transducer, in which the vibrating element is a piezoelectric ceramic or plastic material driven by an appropriate voltage signal (Evans et al 1989). The frequency range of transducers used in skin measurement is 10MHz - 50MHz.

At a discontinuity of medium (interface), scattering, absorption, reflection or refraction of the ultrasound beam may occur. Attenuation includes absorption (the process of conversion of US wave energy into heat) and reflection of US waves, and figure 3.4.1 illustrates the ways in which it occurs in skin. Attenuation is marked in plantar skin in which the the stratum corneum has a large number of interfaces where is can occur.

There would appear to be no explanation for the echogenicity in stratum corneum which, for the purposes of acoustic propagation, can be considered almost as a solid (Edwards 1989). The acoustic impedance, the resistance to the propagation of US waves, is imaged in the stratum corneum as an echodense region, easily perceived in a brightness modulated image (B-scan). In thick plantar skin, the echoes received from skin structures are reduced and the image obtained of plantar callus can be particularly difficult

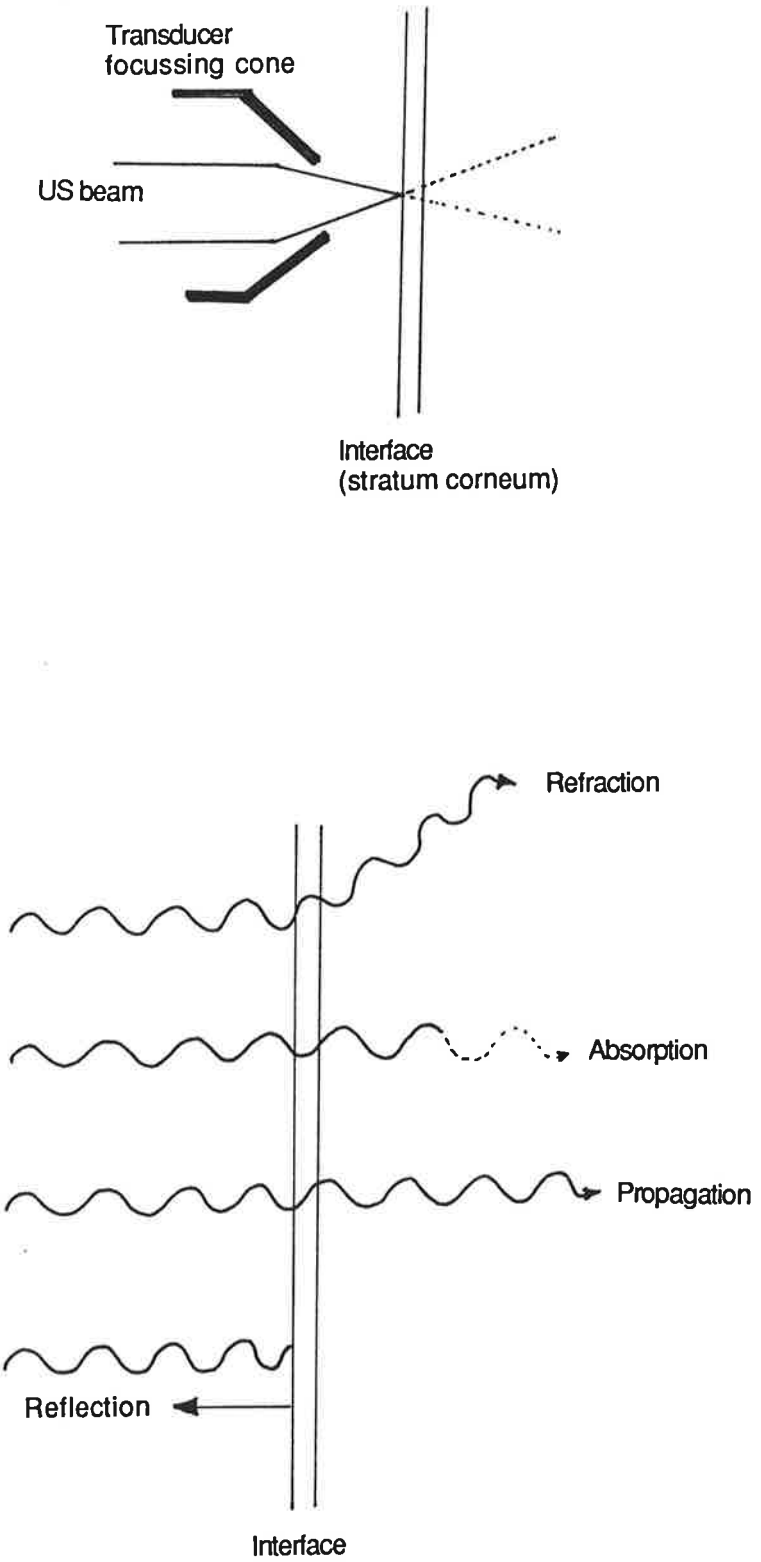

Figure 3.4.1
Attenuation of ultrasound waves in the skin (from Fleischer and James 1980).

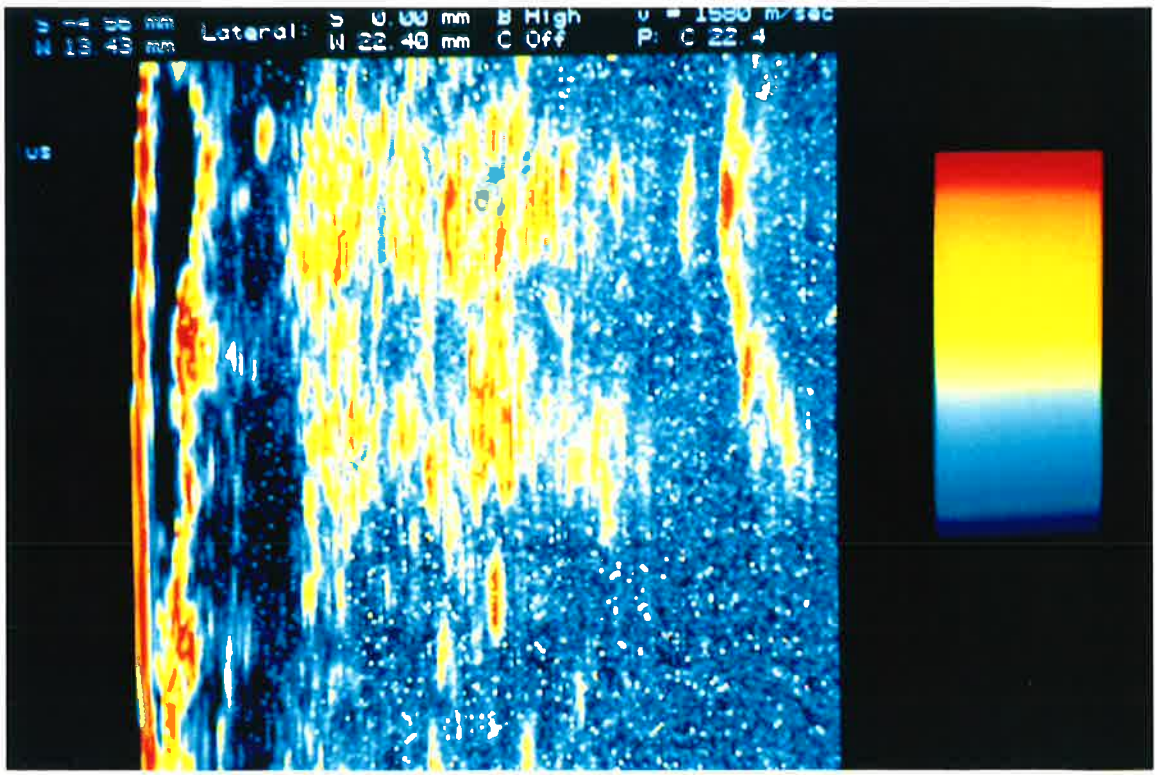

Figure 3.4.2
B-scan image of callus and adjacent normal plantar skin obtained using the Dermascan C. The upper part of the image shows good detail of deep structures imaged through normal plantar skin. Attenuation of US pulses through callus in the lower part of the image results in little or no echo reception and a blank image.

to interpret (figure 3.4.2) unless the superficial callus is removed first. This is probably due to attenuation and the stratum corneum resistance to US propagation (Edwards 1989).

Pulsed A-scan ultrasound is used to measure skin thickness over a range of about 0.5mm to 20mm (it may be possible to measure structures from 0.15mm thick). A short duration US pulse (<20ms) from a transducer, echoing from an interface is converted into electrical voltages which are amplified by a receiver and displayed on an oscilloscope giving rise to A-scan data (Wells 1979). The time delay between output and reception of signals is converted by the instrument into distance using equation 3.4.1.

$$d = vt/2 \qquad \text{Equation 3.4.1}$$

where d denotes distance (mm)
v denotes velocity (m/s)
t denotes time (ms).

It is possible to select the points of interest on the A-scan trace using cursors and the distance in millimeters between them is calculated by the instrument which will have a pre-set conductive velocity value (usually 1580m/s for skin (Edwards 1986). Thus skin thickness can be measured. The velocities of US through different materials and tissues are listed in table 3.4.1.

	velocity (m/s)
Air	331
Pure water	1430
Metal	5000
Fat	1450
Muscle	1585
Skull	4085

Table 3.4.1 The conductive velocity of US through some materials and tissues (Fleischer and James 1980)

To summarise, the A-scan trace provides a sequence of ultrasound pulsed echoes received from the skin's surface and deeper tissues. Interpretation may vary depending upon the echogenicity, acoustic impedance and conductive velocity characteristics of the tissue being measured, as well as the transducer frequency and the instrument used.

3.5 Interpretation of A- and B scan US data

US echoes from the skin's surface are seen on the A-scan oscilloscope trace as waveforms on the left side of the screen. The final waveforms on the right are echoes from deeper tissues, such as blood vessels, deep fascia or bone. The entry:exit echo for the stratum corneum is in the form of marked waveforms on the A-scan trace and is created by the interface between the water transmission and stratum corneum surface (figure 3.5.1).

In thick skin a relatively echo-lucent area exists between the entry and exit echoes, indicating a homogeneous layer with few if any, interfaces (figure 3.5.2). This may correspond either to the stratum corneum alone or the entire epidermis.

In thin skin the entry and exit echoes tend to form a continuous series of waves before merging into papillary dermis echoes on the oscilloscope screen. However if the time base is extended, it is possible to identify a quiet region in thin skin (Edwards 1989), which may correspond to the wider, homogeneous region perceivable in thick skin. Part of the current study intends to clarify this confusion. As discussed previously, it is postulated that this region may be attributable either to the base of the epidermis or just the stratum corneum. The hydration gradient (Bomannan 1990) within the stratum corneum creates a gradual change in water content, therefore an

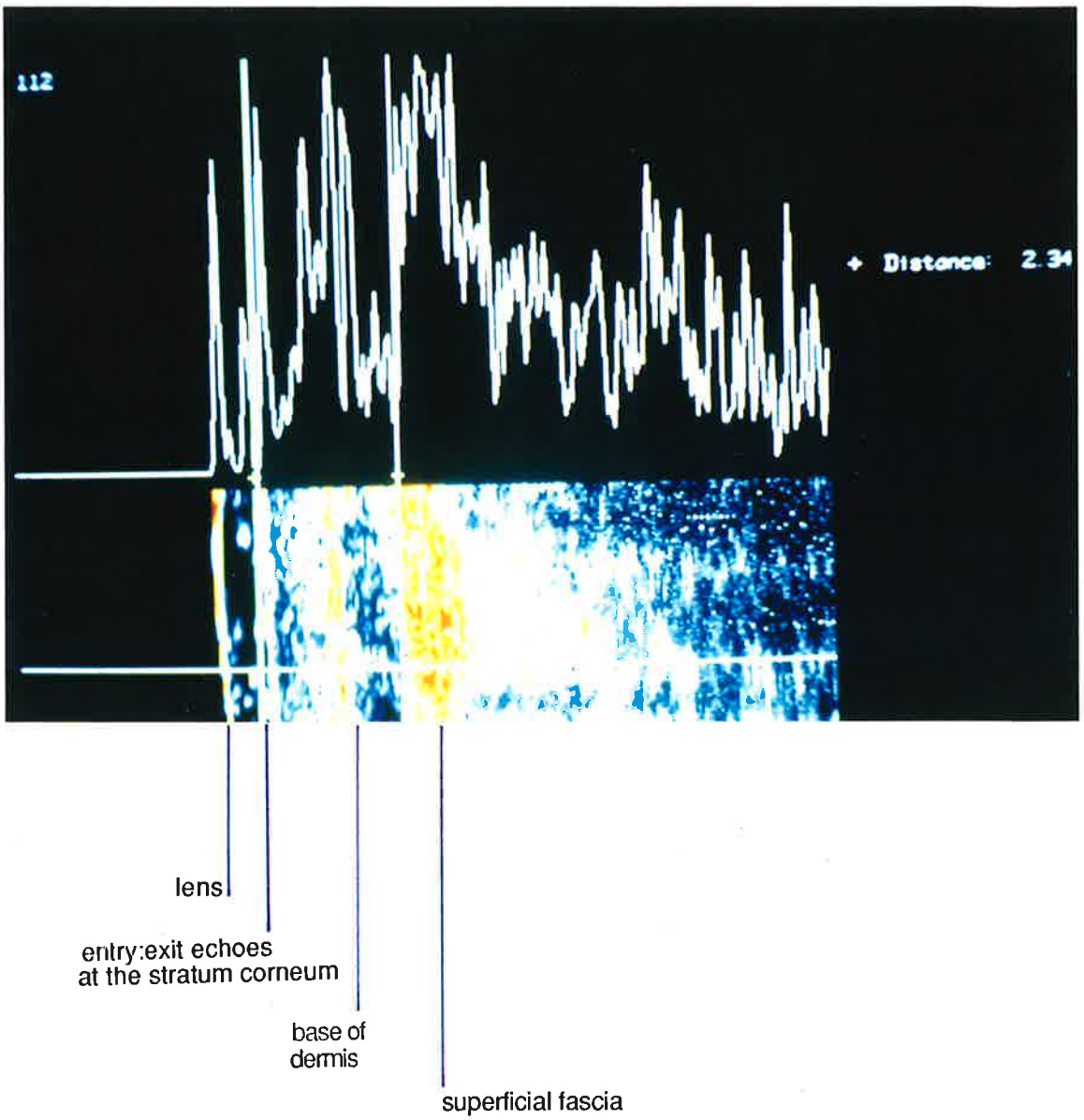

Figure 3.5.1
The position of A-scan waveforms and B-scan image in relation to skin structures using the Dermascan C.

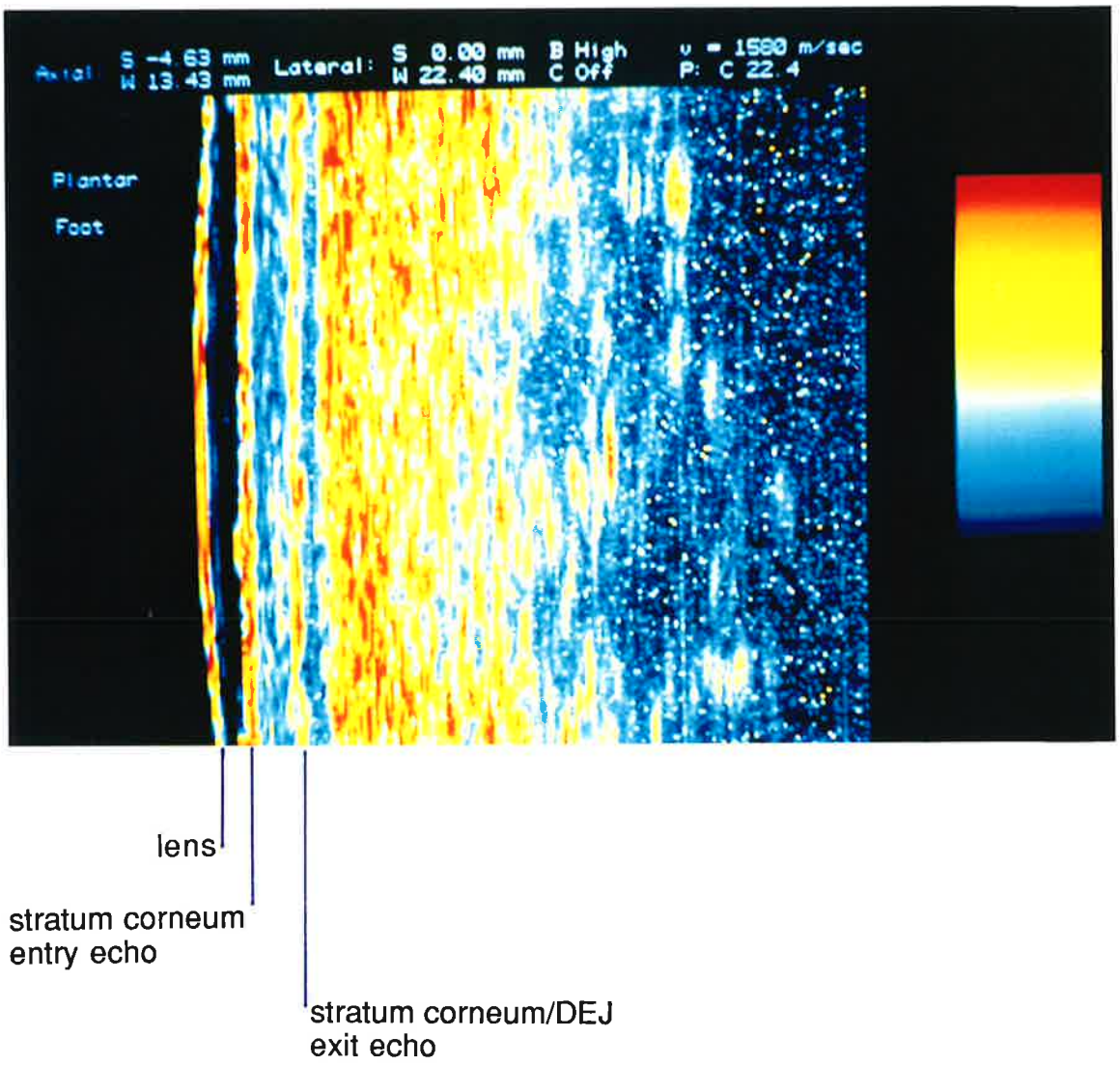

Figure 3.5.2

Dermascan C monitor B-scan image of plantar skin, showing US entry:exit echoes. The quiet, homogeneous region, which may correspond to the thick plantar stratum corneum or entire epidermis can be seen.

interface between the base of the stratum corneum and stratum granulosum will not be marked. It is more likely that the change in echogenicity identifies the position of the DEJ (Edwards 1989).

The base of the dermis can be determined particularly easily in a real time A-scan. Compression and release of pressure on the tissues with the instrument transducer head causes narrowing and movement of the A-scan waveforms towards the right side of the oscilloscope screen since this movement compresses and releases sub-dermal adipose tissue. The point where this movement no longer occurs on the oscilloscope display indicates the position of the base of the dermis. The dermis A-scan echo pattern behaves in a different manner from that of adipose tissue under compression. Within the dermis region, variations in wave amplitude oscillation are visible which which are thought to indicate the quieter papillary dermis and the noisier, more collagen rich, reticular dermis. It is possible also to identify echoes from blood vessel walls, tendons, peri-articular structures and bone providing these are not beyond the range of the instrument.

A number of aspects of US measurement require investigation and validation before the technique can be applied to plantar skin callus. For example, temperature will influence US velocity (Duck 1990), as will hydration of skin tissue. US velocity alters with differing materials (Fleischer and James 1980) and its value through callus has not been calculated. These variables will therefore be studied prior to validation of US use in plantar skin callus measurement.

3.6 Materials and methods

3.6.1 Instrumentation

A calibrated thermistor with needle probe.

A ratchet micrometer (0.1mm divisions).

Facilities of the Brighton Health Authority Histology Laboratory - microtome, histological dyes and fixing processes

Medical Eye single lens reflex camera, with constant focal length.

A light microscope (Weiss, W Germany) was used for skin section histology measurements. (The microscope eye piece graticule was calibrated with a stage micrometer.)

The Dermal Depth Detector* (DDD) (Cutech, Stiefel, UK) (figure 3.6.1).

This instrument was used to measure skin thickness. It utilises real time A-scan ultrasound and consists of a transducer, signal convertor and oscilloscope to display the A-scan echo waveforms. The oscilloscope time base was set at 2 div/ms. Two movable cursors on the oscilloscope screen can be used to identify regions of interest and the distance between these is calculated by the instrument software in millimeters using equation no. 3.4.1.

The externally focused polyvinylidine (PVDF) transducer used had a centre frequency of 14MHz providing an axial and lateral resolution of 0.5mm and 0.1mm respectively with a depth measurement range of 0.5mm to 20mm. It is connected to the skin's surface by a Perspex cone filled with de-ionised,

(* *This instrument is no longer available from Cutech, Stiefel*)

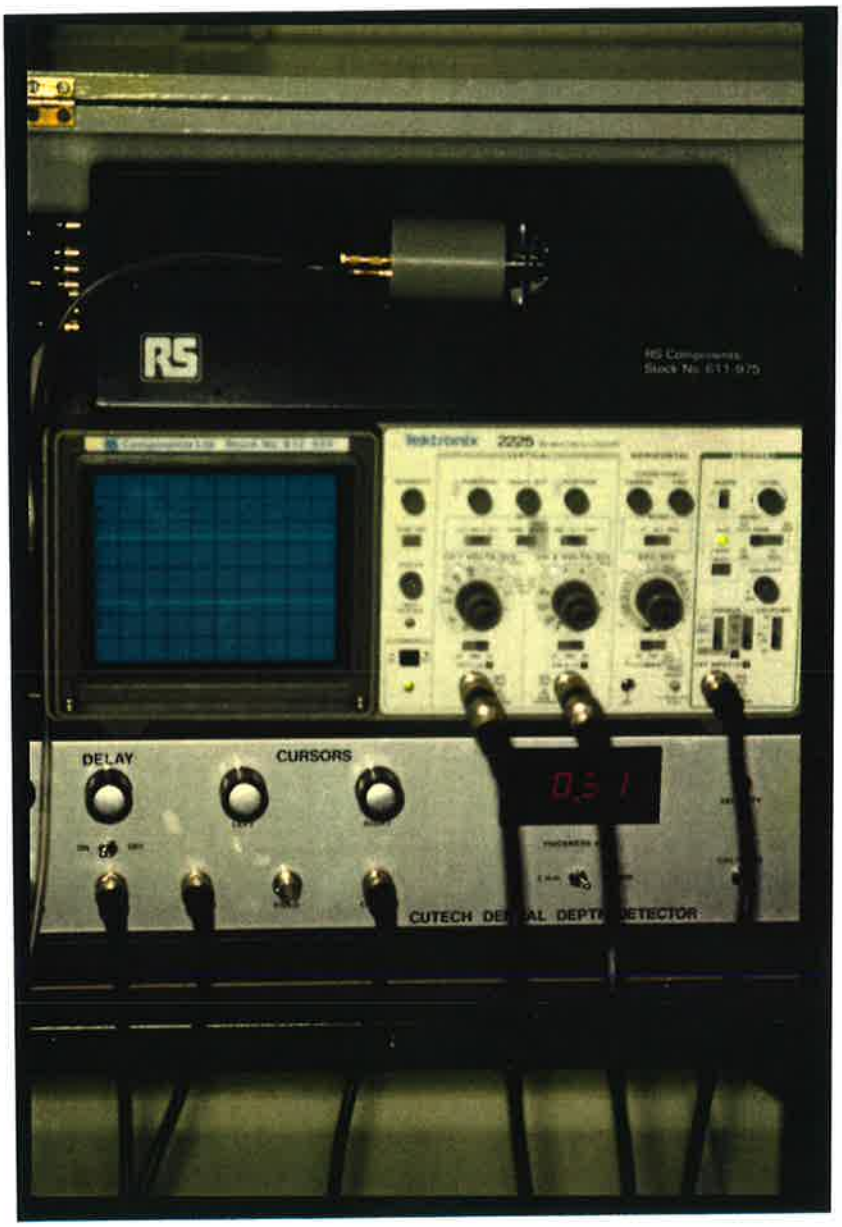

Figure 3.6.1
The Dermal Depth Detector

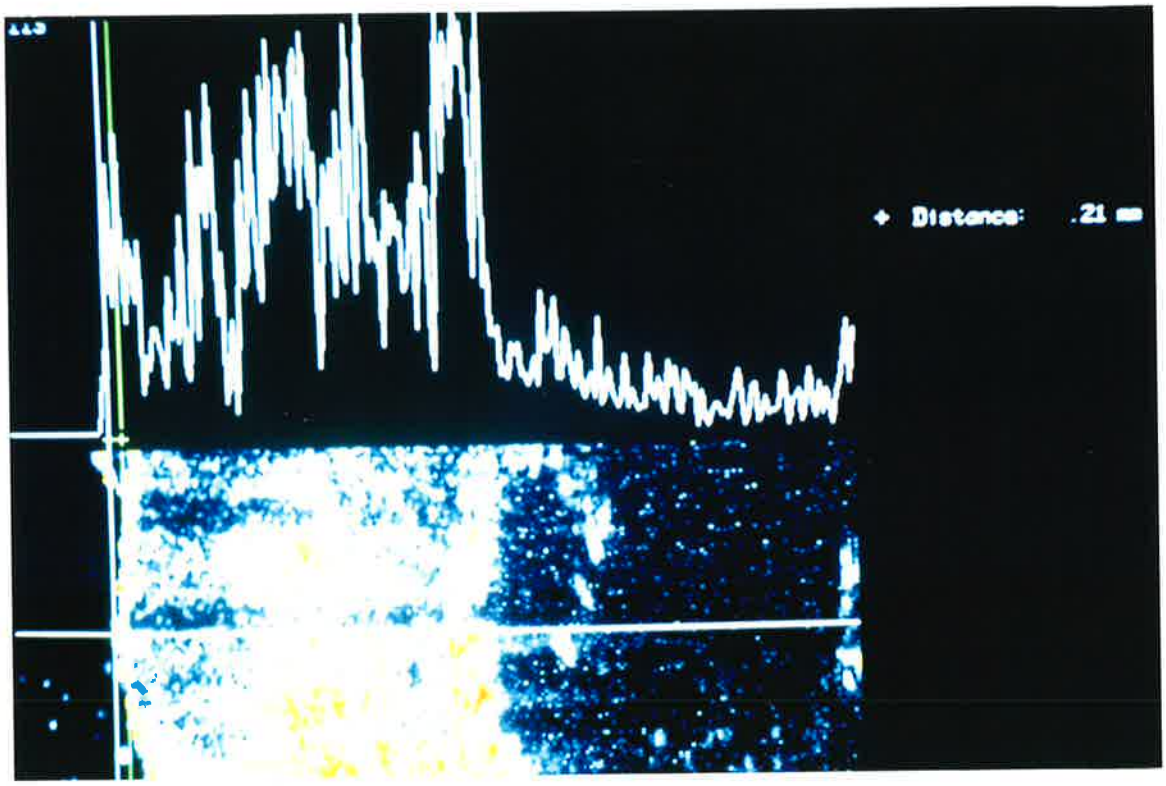

Figure 3.6.2
Dermascan C monitor display of A- and B-scan image of abdomen skin. The cursors are aligned to measure possible epidermal thickness.

degassed water. The separation of the transducer from the skin permits external focusing of the ultrasound. A contact medium of water (some US instruments use an aqueous contact gel) reduces attenuation at the skin's surface, permitting maximal output and pulse reception.

The second US instrument used, the Dermascan C (Cortex, Denmark), utilises the same principles as the DDD. A linear A-scan is carried out by the instrument and the time interval between pulsed A-scan echoes is calculated and converted by the software into a B-scan image on a monitor screen. Cursors can be used to measure distances between echoes (figure 3.6.2).

3.7 Influence of temperature and hydration on ultrasound conductivity.

When making ultrasound measurements of the skin a number of variables must be considered. Temperature fluctuation will affect conductivity of ultrasound, for example surface temperature and that of the transducer water transmission column may rise resulting in an increase in the conductive velocity (Duck 1990). However, the surface temperature range of plantar skin *in vivo* in healthy humans, regardless of season, ranges from 27º - 34ºC, and within biological variation its effect on the rate of ultrasound conductivity can be expected to be marginal.

The most widely used method of ultrasound measurement is that of pulsed transmission (Duck 1990). US energy converts to heat within the tissues but being pulsed, the energy transmitted into the tissues is negligible. However, ultrasound may affect the temperature of the transmission substance (water) and therefore the temperature of the water column of the DDD transducer was recorded.

3.7.1 Methods

The DDD transducer cone was filled with de-ionised and degassed water in a room of temperature 24°C. The transducer water column temperature was measured by inserting a thermistor probe into the transducer cone, before the instrument was switched on and at 5 minute intervals over a 30 minute period during which skin thickness measurements were made. These temperature measurements were repeated five times.

3.7.2 Results and discussion

The mean (22.29°C, SD 0.27) temperature of the DDD transducer water column during skin thickness measurement over a 30 minute period shows little variation (range 21.9 - 22.6°C). There was a mean increase in temperature of the water column of 0.48°C and maximum increase of 0.7°C.

The rise in temperature of the water column from 21.9°C to 22.6°C, the conductive velocity of ultrasound measured with the DDD will increase by a maximum of 23m/s or a mean of 8m/s. Since the foot skin surface temperature varies from 27°C to 33°C, and the DDD water column temperature varied by only 0.7 °C, no correction for velocity of ultrasound due to temperature changes in the transducer water transmission column was considered necessary.

3.8 The influence of skin hydration on ultrasound measurement

Skin stratum corneum hydrates either when in contact with water or when it is occluded and this is particularly the case with plantar callus (Hey 1978). When making ultrasound skin thickness measurements using the DDD, the water transmission column comes in direct contact with the surface of the

skin. Invariably, instantaneous data collection cannot take place while the transducer is positioned optimally for skin depth measurement and errors may be introduced as the skin hydrates with water contact (skin hydration also occurs with the aqueous transmission gels used with other ultrasound instruments). The contact of water with the lipids of the stratum corneum enlarges the hydration shells round the hydrophillic headgroups of the lipid bilayer molecules, which separate resulting in swelling of these structures (Seddon 1990). Also the presence of water and H_{II}-forming lipids in the bilayer may modify many of its properties other than thickness, such as permeability, bending stiffness (deformability) and elastic modulus (Seddon 1990).

3.8.1 Materials and methods

Instrumentation (see section 3.6)

Twenty non-smoker volunteers, age range 18-30 years, took part in this study to investigate the influence of hydration on skin US measurements. None of the subjects had any medical disorder or was taking any medication which might affect their skin (section 2.6.1), but each subject had a painful, mechanically-induced plantar skin callus. Callus sections were removed from subjects using a scalpel and the thickness was measured using both the DDD and a ratchet micrometer. Measurements were carried out at ambient temperature (range 22°C - 25°C) immediately after the callus had been removed from the foot to minimise inaccuracies caused by drying of this tissue on exposure to the environment.

The thickness was first measured using the micrometer and the callus sample was then placed on top of the vertically positioned transducer with the outer surface in contact with the water column. Ultrasound measurements were

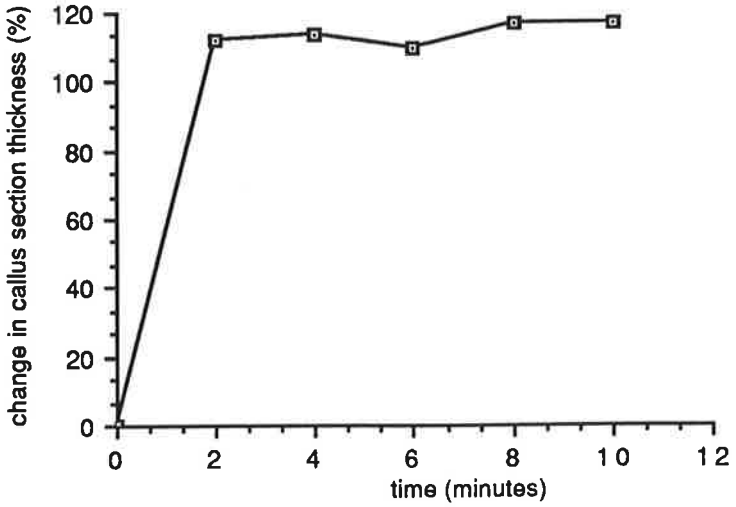

Figure 3.8.2.1
Change in skin callus section thickness on hydration, measured by DDD (normalised values).

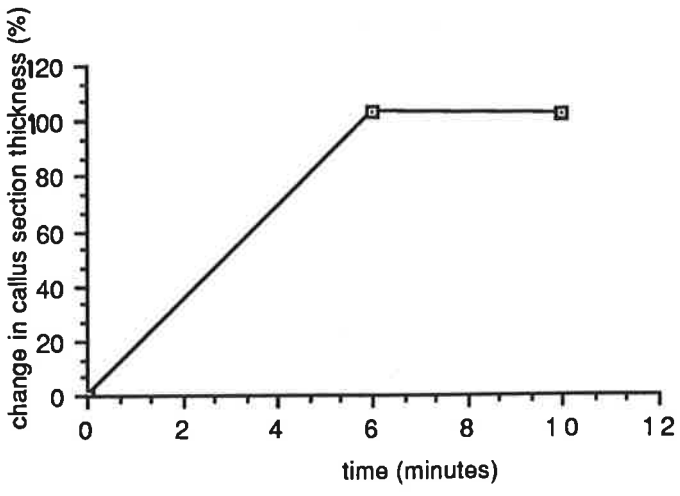

Figure 3.8.2.2
Change in skin callus section thickness on hydration measured by means of a micrometer (normalised values).

made at 0, 2, 4, 6, 8 and 10 minutes. Sections were re-measured with the micrometer at 6 and 10 minutes. The callus sections were dried carefully on paper tissue prior to each micrometer measurement.

3.8.2 Results and discussion

Skin callus sample thicknesses measured using the DDD and micrometer (table 3.8.2.1) are plotted in figures 3.8.2.1 and 3.8.2.2 and illustrate changes in callus section thickness as a function of the time it was in contact with water.

	Microm.	DDD	DDD	DDD	Microm.	DDD	DDD	Microm.	DDD
Minutes	0		2	4	6		8	10	
Mean	0.42	0.46	0.51	0.51	0.43	0.5	0.53	0.44	0.5
SD	0.1	0.09	0.07	0.07	0.11	0.08	0.06	0.11	0.06
Range	0.26-0.62	0.29-0.62	0.36-0.62	0.37-0.62	0.31-0.65	0.31-0.65	0.14-0.63	0.22-0.61	0.4-0.65

(microm. denotes micrometer)

Table 3.8.2.1 Changes in skin callus thickness (*in vitro*) on hydration, measured using a ratchet micrometer and the Dermal Depth Detector.

A 10% increase in callus sample thickness was observed between 0 and 2 minutes (figure 3.8.2.1). Changes thereafter show a very slight linear increase in thickness, shown by regression analysis of data between 2 and 10 minutes ($y = 110.06 + 0.628x$, $r^2 = 0.016$) (figure 3.8.2.1). The average sample thickness of 0.46mm can be calculated to increase to 0.51mm after contact with water for two minutes. Therefore in order to minimise errors in measurement, the measurement of plantar skin thickness must either be made immediately or a non-aqueous contact medium be used (for example silicone oil). Alternatively, water may be left in contact with the skin for 2

minutes prior to measurement by ultrasound techniques. The majority of published papers validating the measurement of skin thickness by ultrasound (Tan et al 1981, Dines et al 1984) utilise water as the transmission medium, and as the DDD employs this approach then it was adopted.

The change in callus sample thickness measured at 6 minutes (figure 3.8.2.2) meant regression analysis of the change in thickness was inappropriate. This feature could be explained by increased plasticity on contact with water (Hey 1978) resulting in progressively greater compression of the callus section during measurement with the micrometer.

3.9 Variation in conductive velocity of ultrasound in skin from different sites

The conductive velocity of ultrasound in skin is a contentious issue. Since the preset velocity in an ultrasound measurement instrument can be varied in order to minimise errors, the most appropriate velocity must be selected for the tissue type. Alternatively the data, once collected, must be corrected for the appropriate velocity retrospectively.

There is variation in published values for conductive velocity of ultrasound in the skin as listed in table 3.9.1. With the earlier type of transducers which tended to generate heat, the data recorded may have been affected by temperature fluctuation as discussed previously. Also, the level of skin hydration will alter the conductive velocity of ultrasound. These factors may account for some of these variations in conductive velocity reported in the present study (table 3.9.1).

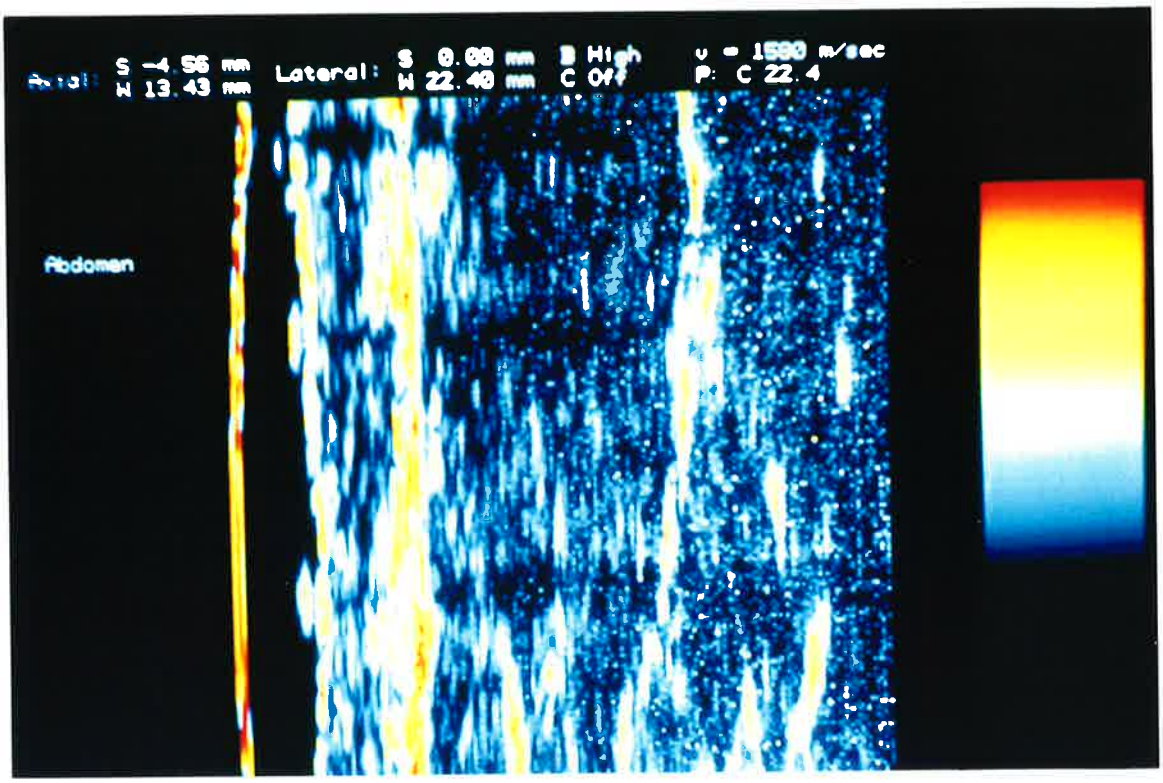

Figure 3.9.1

B-scan US image of abdominal skin with the gain set appropriately for low density core skin.

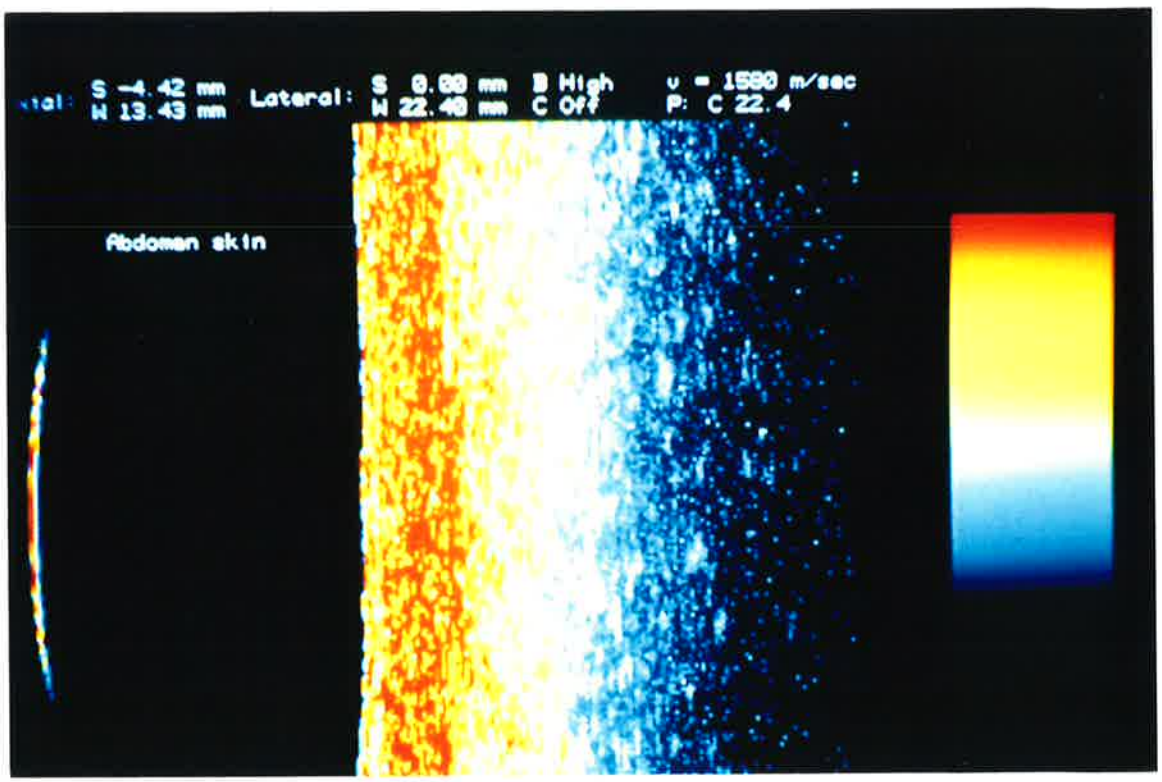

Figure 3.9.2
B-scan image (Dermascan C) of abdomen skin with the instrument's gain set to provide a useful image of calf skin. No structure is evident.

1518m/s	Daly and Wheeler 1971 (skin from an unspecified area)
1600m/s	Escoffier and Leveque 1989 (forearm skin)
1580m/s	Edwards et al 1986 (calculated mean of values for skin taken from a number of different sites)

Table 3.9.1 Values given for velocities of ultrasound through the skin

The variation in values obtained by these workers may also be due to differences in skin density (Serup 1991) at different body sites, which is particularly noticeable in humans (Rippon et al 1991). Density variation with site is probably best demonstrated in figures 3.9.1 and 3.9.2.

The semi-crystalline nature of normal stratum corneum (Morris and Shamos 1967) may be enhanced in plantar callus so that the conductive velocity will be greater than that averaged for normal human skin. Callus has been shown, in the current work, to have a lower water content than normal plantar skin (chapter 4) and it may therefore be more crystalline and conduct ultrasound more readily than normal plantar skin. However callus is certainly more echo-dense than normal plantar skin, and the ultrasound acoustic impedance means that propagation of the US pulses and reception of echoes will be reduced. It can be surmised that callus being thicker and having an abnormal lipid bilayer (Mackenzie 1983) and immature squames may have an increased number of interfaces compared with normal plantar skin, thus marked attenuation will occur in such tissue. The acoustic characteristics of callus, therefore, may be expected to be different from that of normal glabrous or plantar skin and require investigation before US measurement techniques can be applied in the current study.

3.9.1 Materials and methods

Instrumentation (section 3.6)

Twenty, healthy, consenting subjects with an age range of 18 - 30 years, took part in this study. None of the subjects had a medical disorder or were on a therapy (section 2.6.1) which might be expected to affect skin but each subject had a painful mechanically induced plantar skin callus.

Plantar callus samples removed (using a scalpel) from each subject were each measured 10 times each, using the micrometer and the DDD. The callus sections were placed vertically over the transducer and the distance between the entry and exit echoes displayed on the A-scan oscilloscope trace were recorded. The conductive velocity of these callus samples was calculated by counting the oscilloscope graticule divisions (set at a time base of 2 microseconds) and applying equation no. 3.4.1 rearranged as equation no. 3.9.1.

$$V = d / (t/2) \qquad \text{Equation 3.9.1}$$

where V denotes velocity (m/s)
d denotes mean value of micrometer measurements (mm)
t denotes two way transit time (ms).

All measurements were made in an environment with a temperature range of 22 - 25°C and variation in conductive velocity within this temperature range has been demonstrated to be small.

3.9.2 Results and discussion

The mean velocity was calculated as 2593m/s (SD = 490m/s, range 1800 - 3333m/s). This would appear unlikely as the velocity of US in Perspex (a

medium through which ultrasound transmission is rapid) is 2700m/s. As this value is obviously incorrect, regression analysis was carried out ($y = 0.14 + 2.052x$, $r^2 = 0.7$) to produce a value for the conductive velocity of ultrasound in callus of 2052m/s.

The calculated value for the conductive velocity of ultrasound through skin callus is faster than that reported for normal stratum corneum (1578m/s (Edwards 1986)), and consequently when measuring hyperkeratotic tissue (callus, psoriatic plaque) either the DDD preset (1580m/s) value will need to be altered or the data corrected retrospectively, (the correction factor is 0.77).

The range of conductive velocities obtained, 2593 - 3333m/s, is wide and may be due to experimental variation such as, compression of the callus section during measurement with the micrometer, the surfaces of the callus sections being uneven or unparallel, or less likely, system errors, for example, variation in A-scan pulse thickness or oscilloscope calibration.

It is apparent that skin callus is more echo-dense than normal stratum corneum so the attenuation of US pulses which occurs in this tissue is marked. However, it is not clear what structures within the stratum corneum cause its echogenicity (Edwards 1989), but it could be due to callus having a lower water content (chapter 4) and being more crystalline in structure than normal stratum corneum.

3.10 Validation of non-invasive ultrasound measurement of plantar skin and skin calluses

The studies described above indicate the suitability of the ultrasound techniques for skin thickness measurement. They also demonstrate:

a) the correction factors which need to be applied to measurements, ie: that the instrument preset conductive velocity must be reset to 2052m/s when measuring callus,

b) the variables which may affect the accuracy and interpretation of measurements, such as temperature.

To support the use of US *in vivo* to measure the dermatoglyphics in plantar calluses, the predicted success of the technique of ultrasound measurement in plantar skin (Edwards 1986) should be validated, since previous studies (Tan et al 1981, 1982, Dines et al 1984) used sites other than plantar skin. With the Brighton Coroner's permission, full thickness skin samples of cadaver plantar callus and adjacent normal skin were resected for histological comparison with ultrasound measurements.

Unfortunately, it was not possible to use techniques such as xeroradiography (Tan et al 1981) to provide comparative data. However, a second ultrasound instrument (Dermascan C) was used to aid comparison of ultrasound thickness measurements of skin with the histology. Although called the "Dermascan C", this instrument's software converts A-scan data into a B-scan image. Dermascan C measurements are made using the A-scan data and the values so obtained were compared with the A-scan values obtained using the DDD in the present study.

Body tissue increases in thickness and shrinks in diameter on excision *in vivo* (Tan et al 1981) due to removal of tension across the organ's surface. Generally the histological fixation process causes the tissue sample to shrink (Ross and Romrell 1989), so it is difficult to compare final histological and ultrasound measurements directly. Therefore, skin thickness was measured *in situ* using ultrasound and after excision to permit assessment of the extent of skin thickening on excision. To confirm previous work (Tan et al 1982) and to validate the use of ultrasound measurement in plantar skin, both epidermal and full-skin thickness were measured using US and histological techniques. Since human tissue is scarce and should not be abused, the number of full skin samples removed from cadavers was restricted.

3.10.1 Methods

Instrumentation (see section 3.6)

Five full skin callus sections were studied as well as samples excised from other body sites. These were resected from people over 60 years of age, who had died from acute conditions, had been dead no longer than four days, and on whom a post mortem examination was to be carried out. The non-callus skin sections resected were removed from the abdomen, forearm, thigh, calf and the dorsum of the foot.

The clinical appearance of the plantar forefoot calluses was recorded photographically and the thickness measured using the DDD. Superficial callus tissue was removed from the lesion surface using a scalpel prior to ultrasound measurement to ease the later microtoming of this tough tissue.

A grid was drawn over the callus which extended over adjacent normal skin. Indian ink was used since this should penetrate through the surface of the

Figure 3.10.1
A grid was drawn over callus and adjacent normal skin in indian ink which should penetrate into the skin's surface, surviving the fixation process and aid identification of the site of US measurements made *in situ* . The gaps in the grid indicate the site where US measurement was to be made.

skin, stain it, and withstand histological fixation processes (figure 3.10.1). Thus, a reference line was made for microtome sections and the site where US measurements were made *in situ* could be identified on the histology slides as spaces between the lines. An orientation mark was made on the skin to facilitate labeling of microtomed sections.

The DDD transducer was positioned so that measurement was made through the spaces in the grid and the epidermal and full skin thickness was measured in millimeters. The thickness of normal epidermal and full skin adjacent to the lesion were also measured. US measurements were made *in situ* and then the callus plaque with a periphery of normal tissue was excised to the superficial fascia. Post-excision epidermal, full skin and adjacent normal skin thickness were again measured using the DDD so any change in tissue thickness on excision could be identified and compared with the effects of histological processing. The skin sample was immersed in 10% formalin to await paraffin embedding, staining with haematoxylin and eosin dye (H and E) and sectioning using a microtome along the grid lines so that they were visible on the histological section.

It was intended to measure the thickness of the callus by means of a light microscope at the sites where the US measurements had been made *in situ.* However, experimental problems necessitated an alternative approach since the ink grid lines marked on intact cadaver skin were not visible then sectioned and viewed under LM as the indian ink had not penetrated into the callused skin sufficiently.

The measurements made using LM which were intended to be made at the same site as the US measurements were therefore made at 2mm intervals along the skin section and the mean thickness calculated. These values

were then compared with those made *in vivo* by ultrasound (DDD) after the correcting factor for conductive velocity of ultrasound through callus had been applied.

There was an unavoidable delay between taking US measurements and the histology sections becoming available for measurement. Consequently, the tissue was fixed and prepared but not sectioned.

Tables 3.10.1, 3.10.2 and 3.10.3 show the pre- and post-excision measurements made by US on plantar skin tissue and the results of the statistical analysis (paired t-test). Direct measurements of the histological sections are also included in the table.

Ultrasound measurements (in mm)
(Abdomen, thigh, forearm, dorsal foot and calf)

	Epidermis		**Full skin**	
	pre-excision	post-excision	pre-excision	post-excision
mean	0.27	0.24	1.41	1.32
SD	0.093	0.076	0.12	0.075
Range	0.16 - 0.43	0.2 - 0.39	1.2 - 1.5	1.16 - 1.4

change in epidermal thickness on excision, $t = 1.16$, $p = 0.147$
change in full skin thickness on excision, $t = 4.25$, $p = 3.99$

Direct measurements of skin sections using light microscopy (in mm)

Epidermis	Mean	0.16	Full skin	Mean	1.64
	SD	0.08		SD	0.36
	Range	0.1 - 0.33		Range	1.11 - 2.03

Table 3.10.1 Pre- and post excision real-time A-scan measurements (using the DDD) of normal skin thickness of different body sites measured in millimeters and compared with those obtained using histological sections of the same tissue sample. (n = 8)

US measurements (in mm)
(Heel and metatarsophalangeal joint regions of the foot)

	Epidermis		Full skin	
	pre-excision	post-excision	pre-excision	post-excision
mean	0.173	0.163	2.49	2.48
SD	0.049	0.034	0.2	0.33
Range	0.13 - 0.25	0.14 - 0.23	2.15 - 2.8	2.0 - 2.9

change in epidermal thickness $t = 0.35$, $p = 0.37$
change in full skin thickness $t = 0.1$, $p = 0.46$

Direct measurements using light microscopy (in mm)

Epidermis.	Mean	1.0	Full skin	Mean	2.8
	SD	0.2		SD	0.35
	Range	0.8 - 1.2		Range	2.5 - 3.3

Table 3.10.2 Pre- and post excision real-time A-scan measurements (using the DDD) of normal skin thickness of the heel and plantar forefoot measured in millimeters and compared with those obtained using histological sections of the same tissue sample.
(n = 8)

US measurements (in mm)
(Plantar skin callus lesions)

	Epidermis		Full skin	
	Pre-excision	Post-excision	Pre-excision	Post-excision
mean	0.2	0.21	1.69	1.78
SD	0.064	0.053	0.364	0.435
Range	0.11 - 0.29	0.13 - 0.29	1.13 - 2.3	1.18 - 2.44

change in epidermal thickness $t = 0.22$, $p = 0.41$
change in full skin thickness $t = 1.25$, $p = 0.119$

Direct measurements (in mm)

Epidermis	Mean	2.49	Full skin	Mean	3.98
	SD	0.81		SD	0.61
	Range	1.6 - 3.6		Range	3.14 - 4.6

Table 3.10.3 Pre- and post excision real-time A-scan measurements (using the DDD) of normal skin thickness of plantar calluses measured in millimeters and compared with those obtained using histological sections of the same tissue sample. (n = 9). Callus skin sections were shown to be considerably thicker than both hairy skin and normal plantar skin.

Significant reduction occurred in full skin thickness of hairy skin samples, insignificant thinning occurred in all tissues with the exception of plantar callus where insignificant tissue thickening occurred (tables 3.10.1, 3.10.2 and 3.10.3).

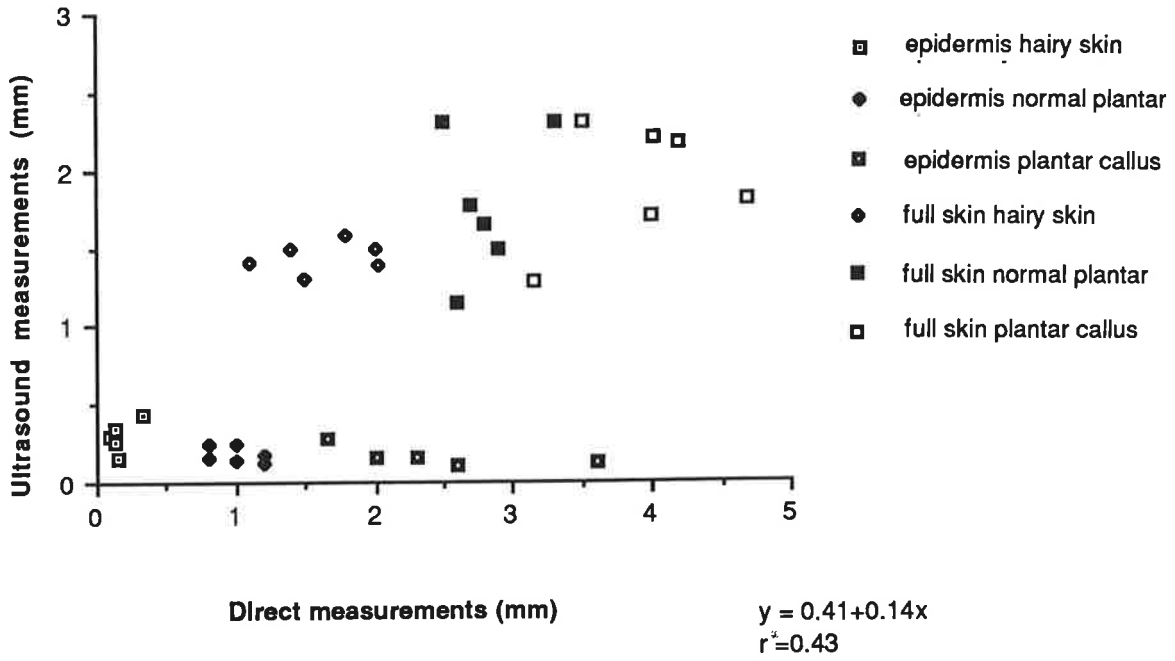

Figure 3.10.2
Scatterplot of ultrasound and direct measurements of different skin sites

Skin thickness measurements (in mm)

	DDD (A-scan) epidermis	DDD (A-scan) full skin	Dermascan (B-scan) epidermis	Dermascan (B-scan) full skin	Direct measurement epidermis	Direct measurement full skin
Mean	0.24	1.49	0.31	1.51	0.5	2.11
SD	0.074	0.229	0.21	0.45	0.549	0.859
Range	0.13-0.36	1.2-1.95	0.1-0.72	1.03-2.47	0.01-1.6	1.1-3.9
	n = 8	n = 8	n = 9	n = 9	n = 9	n = 9

Table 3.10.4. Direct (light microscopy) and US measurements (DDD and Dermascan C) of epidermal and full skin thickness of samples from different body sites, measured in millimeters. Body sites measured - anterior thigh, outer and inner forearm, abdomen, calf, dorsal foot, normal plantar and forefoot callused skin and corn.

Direct measurements were compared with both DDD and Dermascan C measurements obtained for the same skin sections (table 3.10.4, figure 3.10.2). Analysis of variance (ANOVA) indicated there was no significant difference between values obtained for the US and direct measurements of the epidermis ($F = 1.3$, $p = 0.28$), and a small but significant difference was found in those of full skin ($F = 3.2$, $p = 0.05$) (Rippon et al 1991). Scatter plots of epidermal and full skin thickness measured using the Dermascan C and direct measurement (tables 3.10.1, 3.10.2, 3.10.3 and 3.10.4, and figure 3.10.2) illustrate the variation in measurements obtained. ANOVA of callus sections shows there is a statistically significant difference between US measurements and the direct measurement (epidermal measurements, $F_{alpha\ (0.05)} = 3.23$, $F = 60.76$, $p = 1.4^{-12}$, full skin measurements $F = 20.52$, $p = 9.06^{-07}$). Some skin sections were not studied as they were too slippery to hold in place over the DDD. Also, it was evident that histological preparation distorted some samples grossly, there was marked separation of layers of the stratum corneum or folds in the processed tissue and so measurements of these were worthless.

3.10.3 Discussion

The effect of tissue thickening on excision is observable clinically as living skin gapes on incision. However, the hairy full skin from cadavers used in this study showed insignificant thinning on excision, rather than thickening, and this is in direct contrast to previous studies (Bamber et al 1979, Tan et al 1981, Dines et al 1984). These workers, using skin biopsies found differences in thickness between US measurement *in vivo* and direct measurements, and while precise figures are not cited, the anecdotal evidence implies that there is variation in their data. This difference in the measurements was attributed to the effects of tissue expansion on excision which occurred *in vivo* . As plantar skin samples showed insignificant changes in thickness on excision, in the present study, it was considered unnecessary to apply a correction factor to direct measurements when comparing values with those made by US. Hairy skin was shown to be thinner than normal plantar skin and callused plantar skin, as expected (Thomas et al 1985).

The most likely explanation for thinning of the sample on excision is that loss of tone on death meant tissues were no longer constrained and placed under tension. Thus, change in tissue configuration had already taken place and histological fixation resulted in shrinkage. Formation of gas bubbles within dead tissue might affect US measurement, but attenuation has been shown to be minimal between 20° and 40°C (Bamber et al 1979), well within the temperature range at which *in vivo* US measurements were made in the current study. It is unlikely therefore that the US measurements will have been affected by this factor.

Errors introduced by variation in the histological fixation process will affect results, although the histology sections selected for measurement showed

minimal artifacts. Poor interpretation of US A-scan traces and selection of an inappropriate conductive velocity will also cause variation in results. The cadavers studied had been washed but not dried, so uneven hydration of skin tissue could have occurred and this might have affected US measurements (section 3.7). One or a combination of these variables may be responsible for the range in values obtained.

3.11 Conclusion to investigations of ultrasound measurement of plantar skin and calluses

It is generally accepted that study of biological systems will not provide definitive, repeatable data as, for example, engineering design usually does. A wider margin of variation occurs frequently in biological measurements when compared with those made of a non-organic structure. This being the case, the use of US measurement would appear acceptable for clinical purposes. In the absence of a more accurate, readily available, non-invasive technique this method of measurement may be considered suitable for study of the skin for scientific purposes. However, a greater consistency than that obtained in this study is desirable but not possible at present.

Although it is possible to identify the ultrasound entry and exit echoes in the epidermis, the precise region to which the exit echo is attributable cannot be identified, although the DEJ has been cited as a likely structure (Edwards 1989). The current study shows that although the DEJ may be identifiable, since this exit echo shows inconsistency when compared with direct measurement of histological sections, the technique must be considered unreliable for the determination of the DEJ position. To complicate matters further, attenuation of US in thick callus plaques precludes further investigation of undebrided callus lesions using the DDD with a transducer frequency of 14MHz. An improvement in both axial resolution of A- and B-

scan skin imaging and the use of high frequency transducers may permit identification of structures within the epidermis, but no instrument currently available fulfils these specifications. The Dermascan A and Dermascan C have a higher decibel output than the DDD and echo reception using these instruments may provide improved data. Although non-invasive US imaging of skin has become an accepted technique, practice is required in interpreting A- and B-scan data.

Cadaver plantar skin does not expand significantly on excision but the thickness of cadaver hairy skin dermis would appear to decrease on histological fixation, contrary to expectations. In the present study, direct measurement of histological sections is used as the reference for US skin thickness measurements, although the tissue fixation process may lead to creation of artifacts (Skerrow and Skerrow 1985). A more definitive method of comparison may become available using high resolution MRI (Salter et al 1992). The variability in the contours of the DEJ and hypodermis in a histological section and US B-scan image may lead to further errors in measurement when comparing US with histology measurement. Although the position of the base of the dermis has been validated (Tan et al 1982) and data obtained in this study finds this to be reproducible, adipose tissue incursion into the dermis creates variability.

There is still controversy over the conductive velocity of ultrasound in skin as described in section 3.3. If an inappropriate conductive velocity for a particular tissue were selected, the distance calculated by the instrument would be wrong. The instrument's pre-set conductive velocity of 1580m/s was used in this study and a factor of correction (0.77) for ultrasound conductive velocity through callus (2052m/s) was applied to DDD measurements of plantar callus plaques. However, a slight variation in the

or tortuous DEJ in plantar skin callus plaques. However, the cost of this instrument is prohibitive and is not readily accessible.

3.12 Histology of normal plantar skin and calluses

Plantar skin morphology is distinctly different from that of hairy "basket weave" skin, the latter is well documented (Schuster et al 1975, Smith 1989, Graham-Brown and Burns 1990), whilst for the former it is relatively limited (Thomas et al 1985). The present study intends to concentrate on the stratum corneum and its viscoelastic properties but mention will also be made to the whole skin. Data obtained from examination of histological sections of the epidermis may be assumed to be applicable to all ages as LM examination of skin sections removed from people over the age of 60 years have shown that keratinocytes are unaffected by age (Lavker et al 1989). However, with increasing age, the undulations of the DEJ flatten (Smith 1989), probably due to reduced lateral pressure as mitotic activity lowers. Dermal changes also occur, with the apparently random collagen network changing to a more linear lattice (Schuster et al 1975).

Thomas et al (1985) described a thickening of the granular layer and a slight increase in mitotic figures in the basal layer of callused skin. EM studies have shown some structural differences in the lipid bilayers of callus (Mackenzie 1983, Phillips 1992), compared with normal plantar skin. LM examination of normal and callused plantar skin sections may elucidate some of the differences between the normal and pathological state. It may also be possible to identify features in callus which are evident in other hyperkeratoses such as parakeratosis (Graham-Brown and Burns 1990), thus leading to a better understanding of their aetiology. Observations on plantar

skin callus structure may be useful in explaining some of the clinical and viscoelastic features of this cutaneous lesion.

3.12.1 Materials and Methods

Instrumentation (see section 3.6)

Plantar skin sections were removed from people who had died from acute conditions, within the previous 4 days and on whom a post-mortem examination was to be carried out. Both normal plantar and callused skin sections were excised from the forefeet of 5 cadavers.

Skin sections were placed in 10% formalin, fixed in paraffin, stained with H and E and 0.9 micron thick microtome sections cut. Thickness measurements of each skin layer were recorded in millimeters or cell layers and a count of basal cells was made for each skin site (n = 10).

3.12.2 Results of light microscopy studies

3.12.2.1 Stratum corneum

The stratum corneum of normal plantar skin showed evidence of numerous eccrine glands along with their ducts and syringia. This epidermal skin layer was thicker and more dense when compared with hairy skin and no cell organelles were evident.

Vertical light and dark bands in this epidermal layer in normal plantar skin indicated varying uptake of the basophilic H and E stain (figure 3.12.2.1). The darker bands corresponded frequently to eccrine glands, their ducts or syringiae. The use of a monoclonal antibody for sweat duct keratin (Ae1) led to the demonstration of the same feature (Dykes 1992).

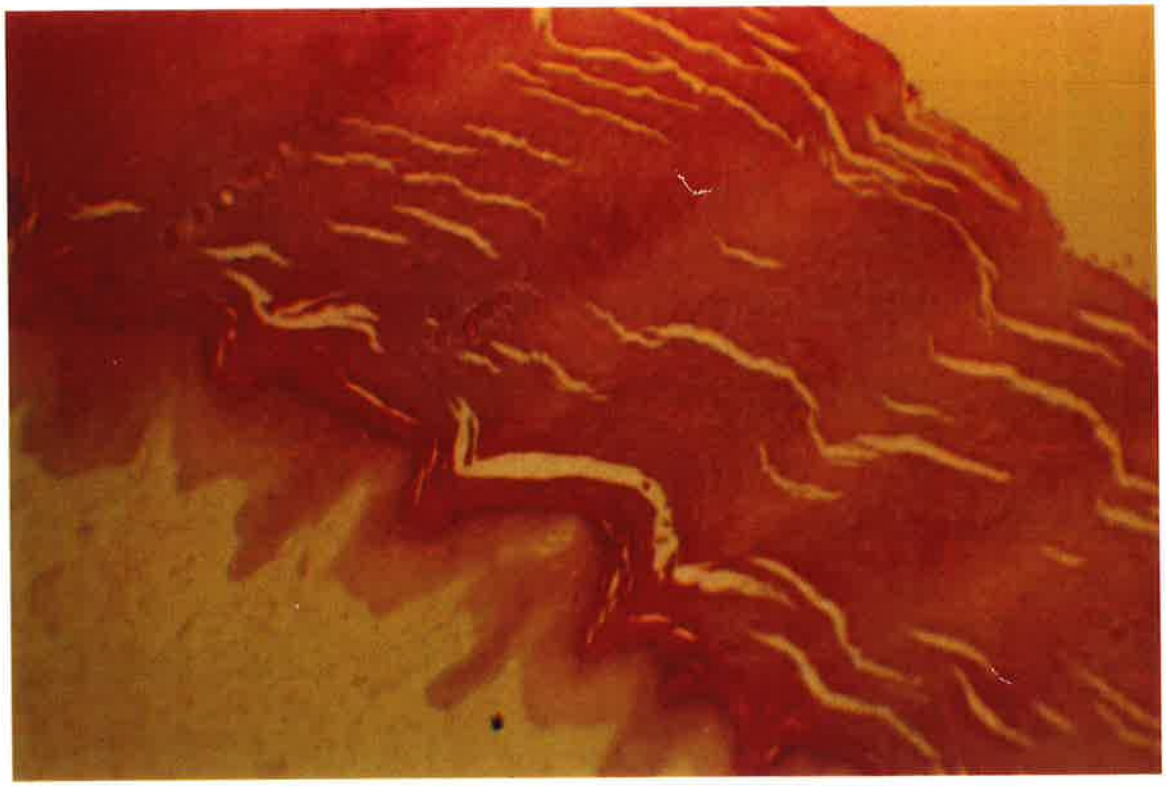

Figure 3.12.2.1
Normal plantar skin stained with H and E. The uneven uptake of this basophilic dye can be seen as vertical bands in the stratum corneum. The darker stained bands align frequently with eccrine sweat glands, ducts and syringae. (x 40)

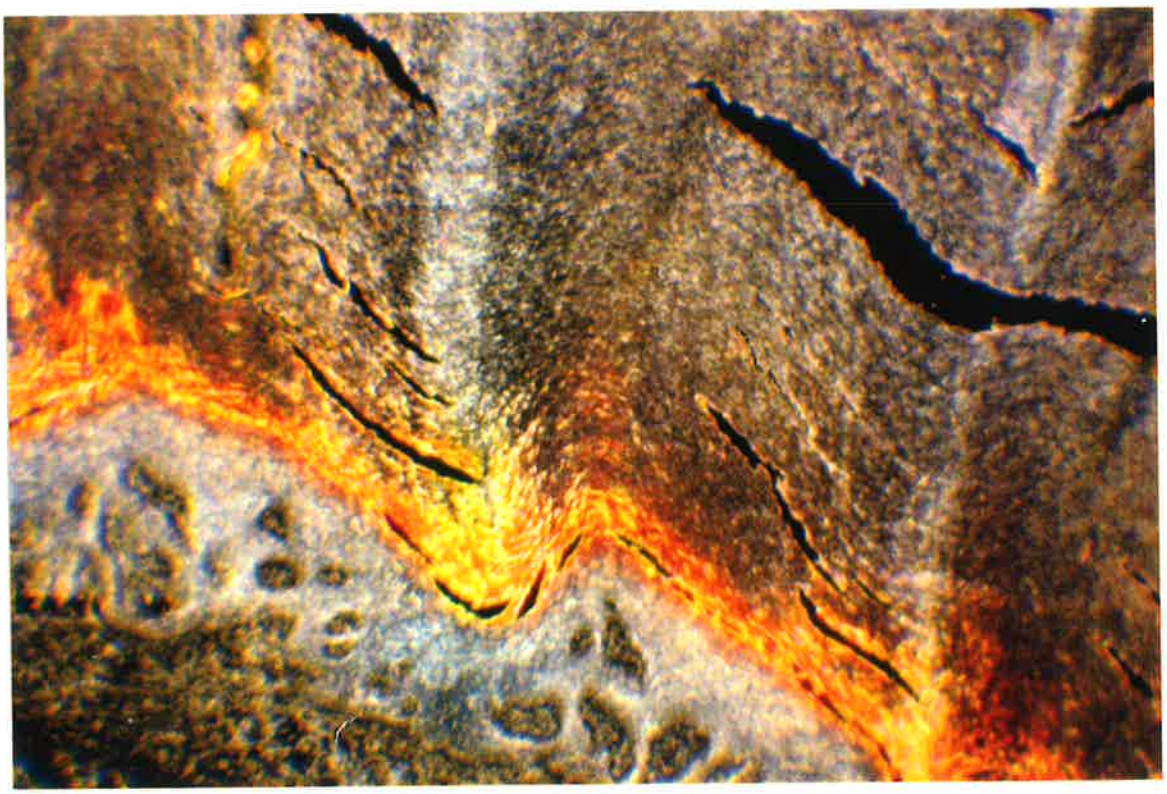

Figure 3.12.2.2
Normal plantar skin with dark field illumination showing refraction of light from the stratum compactum. The section is stained with H and E. (x 40)

Measurements made of normal stratum corneum thickness are recorded in table 3.12.1. As callus had to be removed from the lesion surface to facilitate microtoming, it was considered inappropriate to record its thickness.

When illuminated in a dark field, refraction of light from the stratum compactum region of this layer was marked in both normal plantar skin (figure 3.12.2.2) and callus.

Plantar callus stratum corneum had very few eccrine ducts and syringia visible. This layer was very thick and dense with a marked and extended stratum compactum region visible under dark field illumination. The vertical banding seen in normal plantar stratum corneum was not evident.

Callus stratum corneum, uncomplicated by clinically evident corns, showed no parakeratosis when nuclear material remnants are stained with H and E. In places which corresponded to some disruption of the granular layer, the keratinocytes tended to appear vacuolated or alternatively the intracellular contents appeared very pale when compared with adjacent cells. Parakeratosis was occasionally observed in callus when the stratum granulosum was present though it was grossly disrupted at these sites. In contrast, parakeratosis was consistently evident throughout the stratum corneum in both dorsal and plantar corns.

3.12.2.2 Stratum granulosum

In normal plantar skin, this 2 - 3 thick cell layer contained darkly staining granules. No other characteristics were evident up to x400 magnification. In callus this layer was 3 - 4 cells thick and at some sites appeared disrupted, consisting of cells with poorly stained granules (figure 3.12.2.4 and 3.12.2.5).

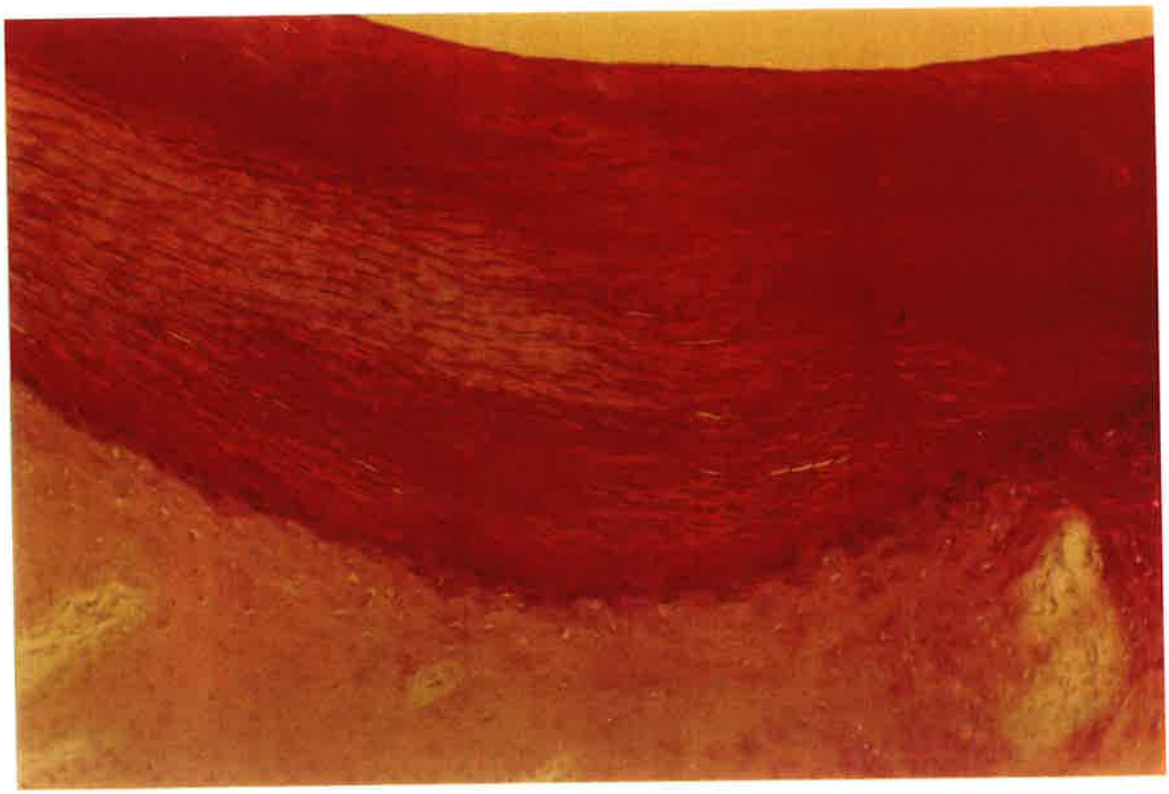

Figure 3.12.2.3
Plantar callus, stained with H and E. The granular layer is 3 - 4 cells thick, the stratum corneum is thick and does not demonstrate the banding of normal plantar skin. (x 100)

Figure 3.12.2.4

Stratum granulosum of callus stained with H and E showing disruption and disintegration of this layer. (x 100)

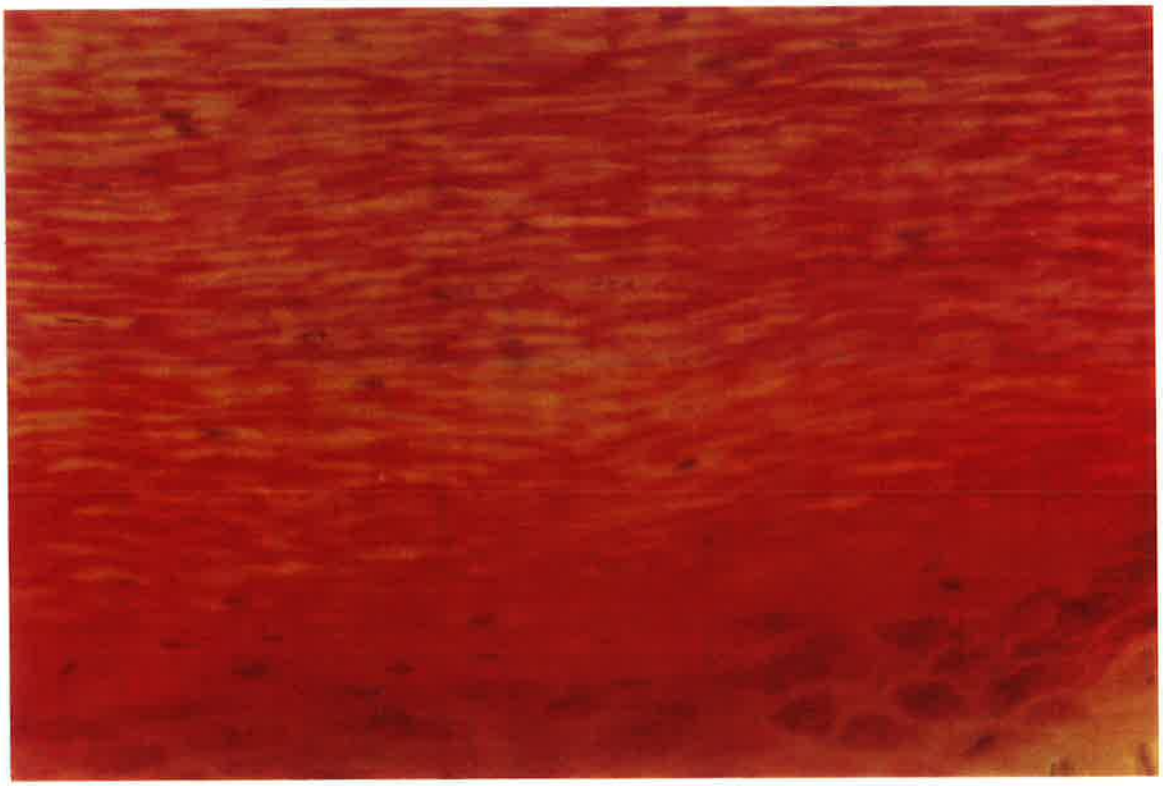

Figure 3.12.2.5
Disruption and disintegration of the granular layer and associated parakeratosis of the stratum corneum. (x 400)

Under the stratum corneum of corns (where parakeratosis was evident), the granular layer was absent or very poorly staining.

3.12.2.3 Stratum spinosum

There was no variation evident from the normal characteristic polyhedral cell shape in both normal and callus keratinocytes and the mean thickness of this layer was measured and is recorded in table 3.12.1. The undulations of the DEJ caused a wide range in values obtained. The nucleus was evident in the cells of this layer but magnification up to x400 showed no other cellular structures.

		Stratum corneum	Stratum granulosum	Stratum spinosum	Basal layer
Skin site		(mm)	(cell layers)	(mm)	(cell layers)
Normal plantar skin	mean SD range	0.647 0.054 0.52-0.71	2.43 0.504 2 - 3	0.55 0.16 0.25-0.78	1 0
Callus	mean SD range	**	4.125 0.686 3 - 5	0.8 0.715 0.8-2.6	1
Plantar corn	mean SD range	**	absent	0.5 0.165 0.28-0.82	1 0
Dorsal corn	mean SD range	N/A	absent	0.548 0.165 0.48-0.61	1 0

Table 3.12.1 Thickness measurements of the epidermis of normal plantar skin, callus, one plantar and one dorsal corn. Mean of 10 measurements taken at 10µm intervals along the histology section for each tissue.

3.12.2.4 Basal layer

The cuboidal epithelial cells were packed tightly in a single layer in normal plantar skin. In plantar callus, cells within this layer appeared to overlap and a streaming effect was evident starting from the base of some pinched-looking rete pegs.

Skin site	Mean (n = 10)	SD	Range
Anterior thigh	5.8	1.13	4 - 8
Abdomen	5.6	0.60	5 - 7
Dorsal foot	6.1	0.73	5 - 7
Dorsal corn	8.0	0.66	7 - 9
Normal plantar skin	7.8	1.03	6 - 9
Plantar callus	10.4	1.26	8 - 12
Plantar corn	9.0	1.16	7 - 10

Coefficient of variation = 22.98%

chi squared value of all tissues studied = 10.143, p = 0.071
critical value (0.05) = 11.07

Table 3.12.2. Count of basal cells along a 2 micron length of basal layer for each skin type studied. (x40 magnification).

No significant difference in the degree of hyperplasia (chi squared = 10.143, p = 0.071) was apparent in the basal layer of plantar callus compared with normal plantar skin. This observation was supported by Marks (1992). The count of basal cells along a 2 micron length of basal layer for each skin type studied is listed in table 3.12.2.

3.12.2.5 Dermo-epidermal junction

The DEJ undulations created by dermal papillae and epidermal rete pegs were marked in normal plantar skin giving rise to normal dermatoglyphics but in callused skin these were exaggerated, pinched looking and often convoluted. No further features were detected by LM.

3.12.2.6 Dermis

When the callus lesions were excised from the cadavers's' feet, fibrous adhesions from the skin to deep structures were evident, whereas the normal plantar skin was relatively easy to resect. It was not possible with LM and H and E staining techniques to determine changes in collagen content or type within normal plantar skin and callus. However all dermal fibrous tissue appeared to be orientated parallel to the skin's surface though under callus plaques this arrangement was slightly disrupted.

No characteristics typical of inflammatory exudate were evident under callus plaques and corns (Marks 1992), but an increased number of capillaries were apparent in the reticular and papillary dermis.

3.12.3 Discussion

Thomas et al (1985) reported a number of differences between normal and callused plantar skin and the results presented here are in agreement. In addition, skin sections viewed in this study show a streaming effect of basal cells within pinched rete ridges which may be associated with a slight increase in cell proliferation and an enhanced transit time in response to cytokines released by traumatised keratinocytes, such as interleukin 1 and 8 (Camp et al 1990). Alternatively, they may be an artifact created as a result of oblique microtome sectioning of the skin.

The loss of the epidermal proliferation unit (Orfanos et al 1971) and its overlapping stacked tetrakaidecahedral structure in callus (Dawber et al 1972, Wilkes et al 1973)) was evident under LM examination of the histological sections used in this study. The smooth and serrated types of basal keratinocyte described by Hume (1985) and Wertz and Downing (1989) were not distinguishable under LM.

The rate of desquammation from callus was reported (Thomas et al 1985) as being greater than that from normal plantar skin, however it is not clear whether this calculation took into account the increased number of the smaller callus keratinocytes compared with normal skin. Also, the rate of cell entry into the stratum corneum, though faster than normal exceeded shedding so that gradually stratum corneum bulk will increase creating a callus plaque.

Mackenzie (1983) reported that friction stimulated mouse ear keratinocytes arrived in the stratum corneum sooner than in normal skin. Thomas et al (1985) also suggested that mechanically damaged human keratinocytes do not stay in the epidermis long enough to differentiate fully. Bernerd et al (1992) proposed a mechanism of delayed cell differentiation in psoriasis, a concept which may be transferable to plantar callus. However, with either interpretation of data (fast transit rate or delayed cell differentiation) the end product will be the same, namely immature corneocytes will enter the stratum corneum. The process of keratinisation with destruction of cell organelles, formation of keratin and biochemical maturation of the cell envelope (in which transglutaminase plays a part, and appears to occur within the stratum corneum (Michel et al 1988)) cannot then be completed. These young, immature keratinocytes present in callus stratum corneum have a mosaic-like, convoluted and villous surface, and closely interdigitate with each other (Orfanos et al 1971, Elias and Fritsch 1983)). This feature, seen also in psoriasis and icthyosis (Dawber et al 1972, Heilman et al 1983), might be expected to have an influence in intercellular cohesion.

The desmosomal degradation of desmoglein I (Lundstrom and Torbjorn 1990) may be reduced in callus skin as the early arrival of keratinocytes in

the skin (Thomas et al 1985, Mackenzie 1983) precludes completion of the biochemical and biophysical changes which occur during keratinisation. It is difficult to speculate on the desmosomal plaque status without resorting to EM studies which would be an interesting sequel to the current study. Desmosomal degradation has been reported in the stratum corneum of normal hairy skin (Wertz and Downing 1989). Lundstrom and Torbjorn (1990) noted a considerable fraction of intercellular space was occupied by desmosomal plates in normal plantar and palmar stratum corneum and a malfunction in desmosomal degradation processes in callus would prevent normal desquammation which would help to explain the inequality between cell entry into the stratum corneum and cell loss.

LM examination of sections cannot reveal the structure of the lipid bilayer in callus (Wertz and Downing 1989). EM has shown numerous MCG's occupying large sac-like dilations in the extracellular space (Mackenzie 1983). The refraction of light noticeable at the stratum compactum of callus under a dark field illumination may reflect the alteration of the lipid lamellae of this layer such that the interface between squames provides a marked contrast. Information on the lipid distribution within normal and callus stratum corneum would help to explain the viscoelastic behaviour and aetiology of calluses.

This study disputes a minor observation made by Orfanos et al (1971), that no stratum disjunctum is apparent in TEM of callus. Whilst the stratum disjunctum in callus is not as obvious as in hairy or normal plantar skin, darkfield LM examination of this region demonstrates a similar refraction of light at the surface of callus histology sections. Darkfield illumination of corns shows little contrast occurring superficial to the viable epidermis and homogeneity throughout the stratum corneum. Further observations under

polarized light may provide further information. Parakeratosis was identified in the stratum corneum of corns, both plantar and dorsal, in the skin sections obtained in this study. Parakeratosis was invariably associated with an absent, diminished or disrupted stratum granulosum (figures 3.12.2.3 and 3.12.2.4).

A series of sections from one cadaver showed parakeratosis to be apparent only in the superficial layers of the stratum corneum above an apparently normal stratum granulosum. While the medical history of the donor of the cadaver sections was known, the details of any management of the mortal condition was not available. It is possible that the absence of new parakeratotic tissue being formed may have been due to removal of the stimulus, ie: the patient may have become bed-bound.

Mackenzie (1983) reported parakeratosis to occur in association with friction stress in mouse ear studies and noted, under low power TEM, that keratohyaline granules were situated more superficially in the stratum granulosum and were larger than in normal skin. This feature was considered indicative of an increased degree of synthetic activity as keratohyaline granules are involved in keratin fibril formation in a manner not yet identified.

One explanation for the presence of large masses of keratohyaline more superficially in the stratum granulosum than usual may be the rapid transit time for keratinocytes through mechanically stressed skin (Thomas et al 1985) when cells had not yet achieved the maturity usually commensurate with this layer.

Although LM in conjunction with H and E staining can lead to the identification of keratohyaline granules in human skin, it is neither possible to quantify the keratohyaline nor to comment upon its distribution within the stratum granulosum. Nor, unfortunately, can current technology identify the occurrence of friction stress at the skin's surface during gait and therefore determine whether this is the primary mechanical stress associated with callus and corn formation. However, animal experiments (Mackenzie 1983) suggested that such stress is indeed implicated in the aetiology.

If the quantity and siting of keratohyaline granules is indicative of increased synthetic activity in the epidermis (Mackenzie 1983), then the increased number and change in appearance of the stratum granulosum cell layers in callus may also result in a variation in keratin fibril formation. In hyperproliferative states, such as psoriasis, where there is a rapid transit time for keratinocytes, proteolytic enzymes may be involved in keratin formation, or alternatively there may be incomplete filament assembly *in situ* (Mackenzie 1983). In psoriasis, keratin filaments are relatively short but frequently thicker than normal (Steinert and Cantieri 1983). These characteristics may be secondary manifestations of other abnormal features of psoriasis and may not relate to the intracellular ultrastructure of callus keratinocytes.

In TEM studies of callus, Orfanos et al (1971) described the intracellular framework of callus as being reticulated and less frequently built up in fibrils. Two types of stratum corneum cell in callus were described, one lighter coloured with a homogeneous inner structure with no keratin pattern, and the other darker looking with a filamentous inner structure showing an inverse alpha-keratin pattern. Garson et al (1990) also described callus keratin as being an alpha-type keratin more in line with the hard keratins of wool and nail. It is not yet clear what the role cytokeratin 9, a cytoskeletal protein

Figure 3.12.3.1
TEM of plantar callus. Ruthenium tetroxide has been used to stain the lipid lamellae intercellulary. These structures appear complete in some areas and less so in other parts of the section. The series of white bands correspond to the headgroups of the ceramide molecules of the lipid lamellae. (Phillips 1992) (x 60000).

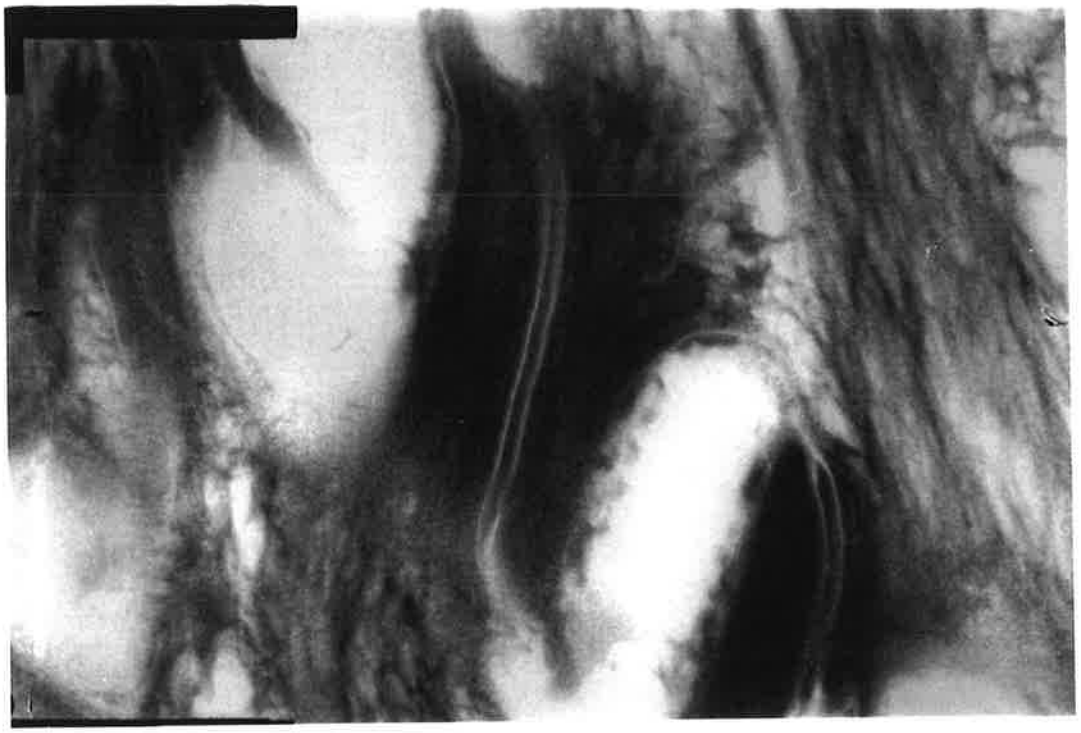

Figure 3.12.3.2
TEM of corn tissue. The lipid bilayers normally surrounding keratinocytes appear to be absent, or alternatively there is poor uptake of the ruthenium tetroxide used to stain these structures (Phillips 1992). (x 60000)

involved in the formation of intermediate-size filaments of keratin, has in plantar and palmar skin (Knapp et al 1986).

The morphological difference between corns and callus is noticeable. Corns show parakeratosis in the stratum corneum and the stratum granulosum is absent. The presence of parakeratosis in the stratum corneum implies cell immaturity and as this invariably occurs when the stratum granulosum is absent, this latter epidermal layer must be a transit rate limiting structure where keratinocytes would normally have time to differentiate.

The increased number of cell layers of the stratum granulosum in callus and its absence in corns presents a dilemma. Possibly the change in thickness of this layer in callus is a precursor to its disruption, when abnormal cell envelopes (Michel et al 1988) and lipid lamellae (Mackenzie 1983) may be formed. There is some evidence for this hypothesis in the skin sections investigated (figure 3.12.2.4) where disintegration of the stratum granulosum within an otherwise typical layer can be seen. Also, TEM of callus stratum corneum identified some lipoid granules characteristic of parakeratosis while other ultrastructural features of parakeratosis were not evident (Orfanos et al 1971). TEM studies of corn and callus tissue, (Phillips 1992) fixed with ruthenium tetroxide (figures 3.12.3.1 and 3.12.3.2), confirm changes in the lipid bilayer structure described by Mackenzie (1983) and support the hypothesis that formation of the lipid bilayer is incomplete when compared with normal plantar skin.

Further support is provided by LM examination of the squames of some callus sections which showed a pale internal structure which might be indicative of a recently disintegrated nucleus. With an increased transit rate in callus (Thomas et al 1985, Mackenzie 1983), these keratinocytes will not have

completed their differentiation entirely and the space occupied by the cell nucleus would remain relatively unfilled by intracellular keratin fibrils and matrix giving rise to the slightly vacuolated appearance. As discussed previously, it is possible that this feature is a LM manifestation corresponding to the lighter and darker callus cells described by Orfanos et al (1971).

CHAPTER 4

Normal plantar skin and callus hydration levels.

4.1 Introduction

Callus samples, removed from patients whose gait was also studied, were stored for later investigation of their viscoelastic characteristics. The force plates used to measure gait parameters were geographically too distant from the rheometer which was to be used for this study. Prompt analysis of the skin callus samples was therefore impractical and suitable methods of storing and equlibriating these samples were needed. It has been suggested that water content represents a suitable parameter that can be used to compare fresh and re-equilibriated callus sections *in vitro* and the technique of Fourier Transform Infrared Spectroscopy (FTIR) has been shown to be a suitable method of assessing callus water content under differing conditions (Potts et al 1985).

4.2 Methods of storage for skin tissue

Hill (1991) reported that desiccation of skin tissue permitted 3 months successful storage but it was considered that it would not always be possible to measure skin callus viscoelasticity within this period. Alternative methods of storage such as paraffin fixation were considered to be unsuitable as the solvents used are known to affect the breaking strength of the stratum corneum (Wildnauer et al 1971). The long-term storage method used by most other workers is that of freezing as described for example, by Caputo and Gasparini (1985), where the tissue is immediately immersed in liquid nitrogen. However, each research group has found it necessary to develop its own protocol, some complex and some simple (Hill 1991). Freezing of

skin callus with immediate immersion in liquid nitrogen was therefore considered the most suitable method and was selected for the current study.

4.3 Effects of freezing skin tissue

The effect of freezing on skin tissue is not well documented. Freezing and thawing effects may modify skin properties and behaviour, however these are likely to be minimal in the case of stratum corneum which has a low water content, normally between 10 and 20%, (Blank 1952, Spencer 1976). A drug permeation study (Harrison et al 1984) showed the rate of percutaneous absorption of a drug through a skin section to be the same before and after freezing, and, by implication, the corneocyte and lipid bilayers can be assumed not to be markedly affected by the freezing process.

In previous studies, there appears to have been little need to investigate the effects of freezing on skin tissue. For example, workers using freeze-fracture techniques to study skin structure have no requirement to look at thawed sections, their interest being in structure of cellular components (Hill 1991) rather than results of cryoturbation. However, effects evident as artifacts in freeze-fracture studies (Caputo and Gasparini 1985) include inter- and intra-cellular disruption due to ice crystal formation. Should such ice crystal formation develop in the callus sections following freezing and subsequent equilibriation in the present study, then the viscoelastic behaviour may be different from that of fresh callus.

Keratin is a tough, fibrous protein (Wertz and Downing 1989) and artifacts due to an inappropriate freezing process are likely to be minimal. The water concentration gradient through the stratum corneum increases with depth

(Bomannan et al 1990), the outermost layers containing least water. The maximum water content in these outermost layers of callus can be assumed to be 10 - 20% due to their distance from the viable layers (Thomas et al 1985). As the water content throughout this biological tissue is small, its integrity is likely to be unaffected by the effects of freezing and thawing.

4.4 Equilibriation techniques for frozen callus sections

There is inconsistency in the existing data on the appropriate relative humidity and time at which frozen stratum corneum should be equilibriated since the few studies on skin equilibriation conditions after storage refer to hairy skin. Ferguson (1980) investigated the equilibriation time of normal stratum corneum at 22°C and RH82%, and after immersion for 45 minutes in distilled water. Skin sections were taken from the abdomen, volar surface of the arm, sternum and anterior thigh. His results showed that prolonged periods of incubation in the test environment did not change the values for the mechanical characteristics of human stratum corneum in a consistent manner and therefore overnight re-equilibriation was selected. Wildnauer et al (1971) reported re-equilibriation of forearm skin took as little as 24 hours yet Middleton (1968) found up to 5 days were required for rehydration of hairy skin.

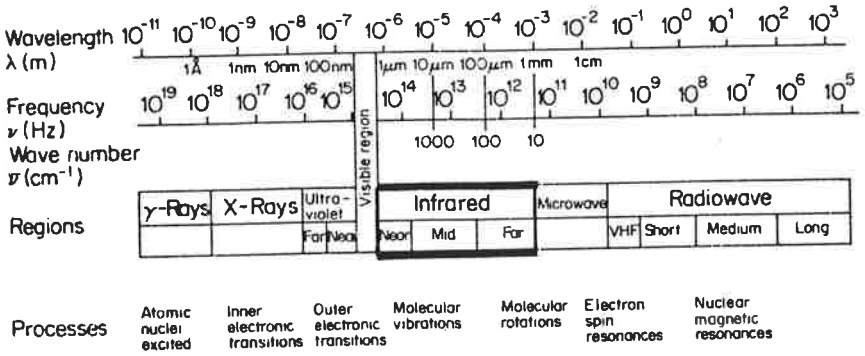

Figure 4.5.1

The electromagnetic spectrum (from George and McIntyre 1987)

4.5 Principles of Infrared Spectroscopy

A number of non-invasive methods exist that can measure hydration of the stratum corneum (Potts et al 1985, Triebskorn et al 1983), including measurement of electrical resistance, capacitance, TEWL, and microwave and spectroscopic techniques. The advantage of the latter, especially Fourier Transform Infra-red Spectroscopy (FTIR), is that the relationships between specific parameters and water content have been identified (Potts et al 1985). Although, Triebskorn et al (1983) noted contradictory results between electrical resistance data and infrared (IR) spectra with hydrated skin, a number of other workers (Potts et al 1985, Walling and Dabney 1989, Roberts and Walker 1993) considered the FTIR technique the most suitable for the quantification of the water content of skin.

Fourier Transform Infrared Spectroscopy (FTIR) permits examination of both inorganic and organic substances, both *in vitro* and *in vivo.* As Fourier Transform mathematics permit all frequencies to be analysed simultaneously, this technique provides a reproducible, quick measurement of the infrared spectra of a substance, with good resolution ((Miller and Stace 1972) and, since it is also non-invasive then it is particularly suited for *in vivo* studies.

Infrared spectroscopy utilises the full range of the IR spectrum from $4000cm^{-1}$ at the high frequency end to $625cm^{-1}$ at the low frequency end (Williams and Flemming 1980). The position of the IR spectra within the electromagnetic spectrum is illustrated in figure 4.5.1.

The IR beam when passed through a sample of the substance to be studied shows transitions which are due to molecular vibrations involving stretching or bending of bonds (Sternhill and Kalmar 1986). The IR light is absorbed when an oscillating dipole moment (due to a molecular vibration) interacts with the oscillating electric vector of the IR beam emitted by the light source (Williams and Flemming 1980). The frequency of absorption of a particular vibrational mode of a molecule is determined by the bond strength and the masses of the atoms concerned (George and McIntyre 1987). Generally a large number of bonds exist in molecules, and as each bond may have several IR-active vibrational modes, IR spectra have many features. Thus IR spectroscopic examination of keratin, for example, will show absorbence in a number of regions of the IR spectrum. As a typical fibrous protein the bonds are expected to include N-H, C=O, carboxyl, disulphide and sulphydryl. However the potential complexity of IR spectra absorbence is simplified because the frequencies of many vibrations lie outside the normal scanning range of FTIR instruments and not all vibrations give rise to strong absorption while others are IR inactive.

The entire IR spectrum may be split into four regions (George and McIntyre 1987) (figure 4.5.2). In the region 4000 - 2500cm^{-1}, the fundamental vibrations can be attributed to X - H stretching, whereas the region 2500 - 2000cm^{-1} contains triple bond stretching absorptions. In the double bond region (2000 -1500cm^{-1}), the strong bands are associated with the C = C and C = O stretch with a strong band due to N - H bending in amines occurring between 1630 - 1500cm^{-1}. This latter feature is a specific amino acid marker. Below 1500cm^{-1} very similar molecules give different absorption patterns

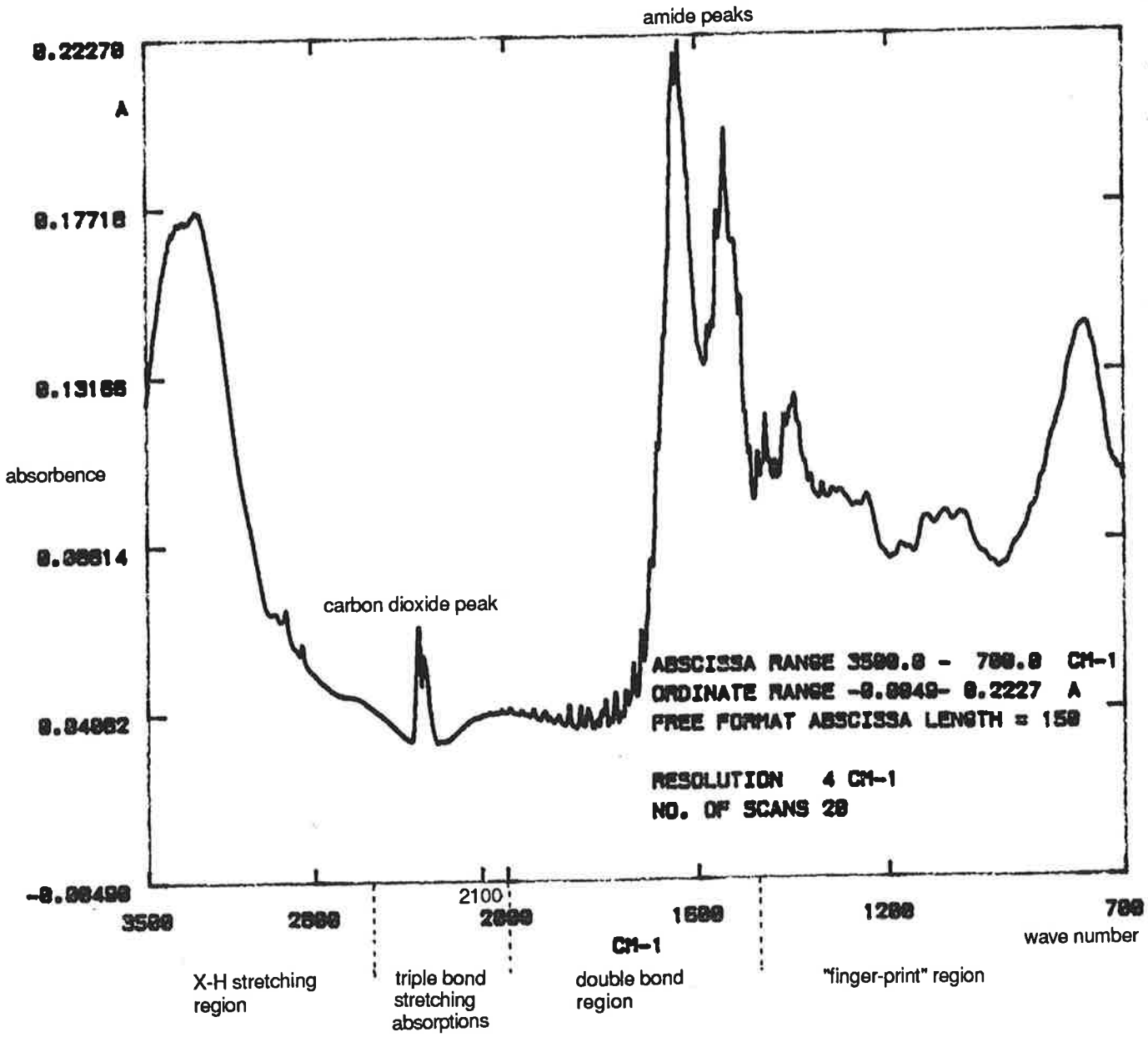

Figure 4.5.2

Absorbence spectra of normal forearm skin using a Fourier Transform Infrared Spectrometer, divided into regions of interest.

and many useful bands exist in the "fingerprint" region down to $650cm^{-1}$, for example C - O stretching between 1000 and $1400cm^{-1}$.

Complicating factors in the interpretation of spectral data include overtone and combination bands, Fermi resonance, hydrogen bonding and other inter-molecular interactions as well as transitions which are difficult to assign (George and McInTyre 1987). This means that the spectrum may show overtone and combination bands which are harmonics of the fundamental absorption frequency at twice the wave number, although they are weak in comparison with the fundamentals. The Fermi resonance may create two bands close together when only one is expected. Spectra of the same substance under different conditions (for example with increased water) may show a shift in absorption bands due to the effect of hydrogen bonding at different sites. Many vibrations are modified by electronic effects which lead to large shifts in band wave number particularly in the $1500\text{-}650cm^{-1}$ region which consequently, can be difficult to assign.

IR spectra may be calibrated in wavelength (micrometers) or frequency related wave numbers (cm^{-1}) which are reciprocals of wavelengths (Sternhill and Kalman 1986). The majority of publications refer to wave number (cm^{-1}).

4.6 The Fourier Transform Infrared Spectrometer

A diagram of a typical Fourier Transform Infrared Spectrometer and light path is shown in figure 4.6.1. Light from an IR source is focussed by a system of mirrors on to the entrance slit of a monochromator which contains an optical mirror system. This in turn focuses the entrance slit onto the exit slit. A

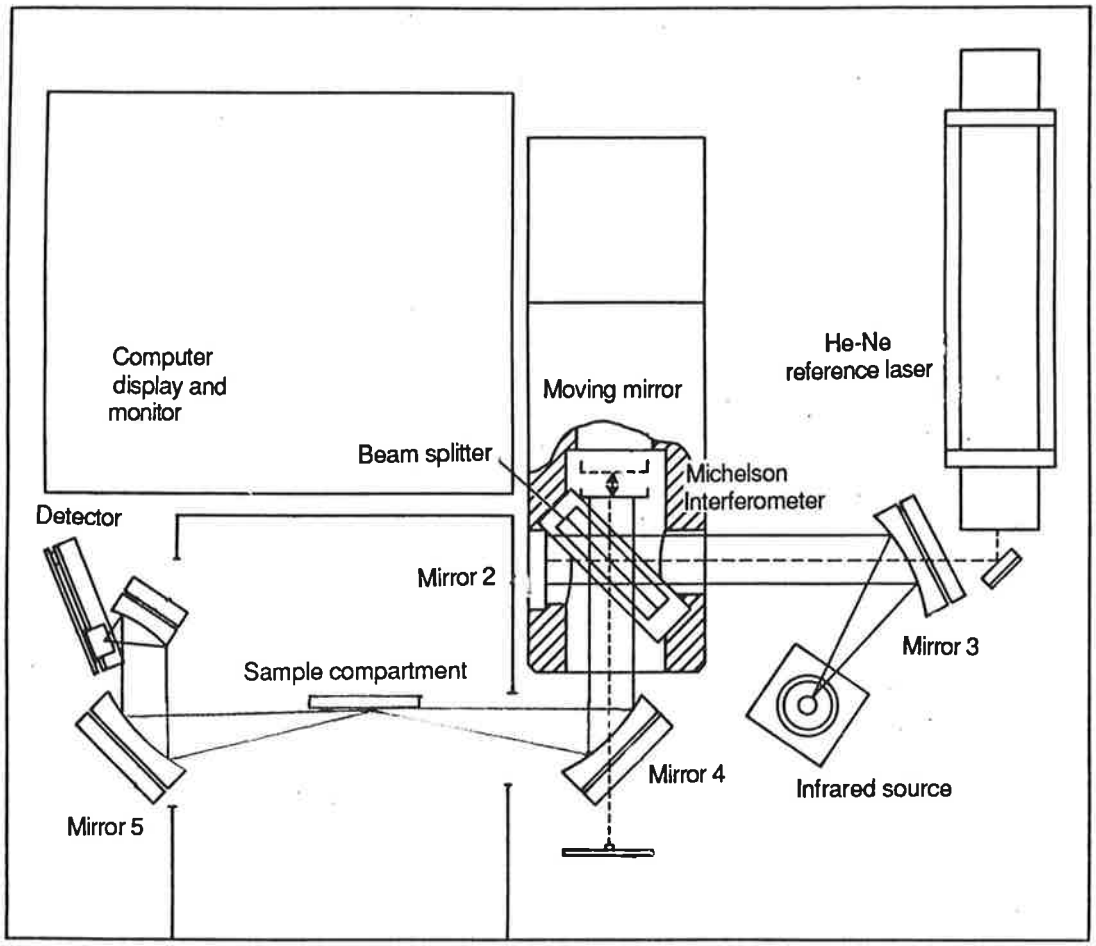

Figure 4.6.1
Fourier Transform Infrared Spectrometer: optical pathway

dispersing device (prism or grating) spreads this image out into a spectrum in the exit slit. Movement of the dispersing device scans the spectrum across the exit slit.

The Michelson Interferometer (figure 4.6.1) consists of two perpendicular mirrors, one of which is stationary whilst the other moves at a constant velocity. A beam splitter is placed between the two mirrors dividing the incoming beam which is re-combined after a path difference has been introduced between the two beams. One light path passes to the internal reflectance element (IRE). The interference pattern in the re-combined beam is registered by the detector which produces an electrical signal proportional to the incident radiation intensity. A helium neon reference laser is used to monitor the position of the moving mirror for greater accuracy.

The detector signal, or interferogram, contains information on the intensity of each frequency in the spectrum which can be calculated by a mathematical manipulation known as a Fourier Transform allowing all frequencies to be integrated simultaneously.

The substance or tissue to be studied using FTIR is placed on an IRE which must be transparent to IR light, and for example, germanium, thallium bromo-iodide or zinc selenide are used. The position of the IRE in the FTIR light path is illustrated in figure 4.6.1.

In order to allow for any extraneous transitions in the spectra, an interferogram with and without a sample in the beam must first be recorded. The ratio of the spectra of the source minus sample and source plus sample

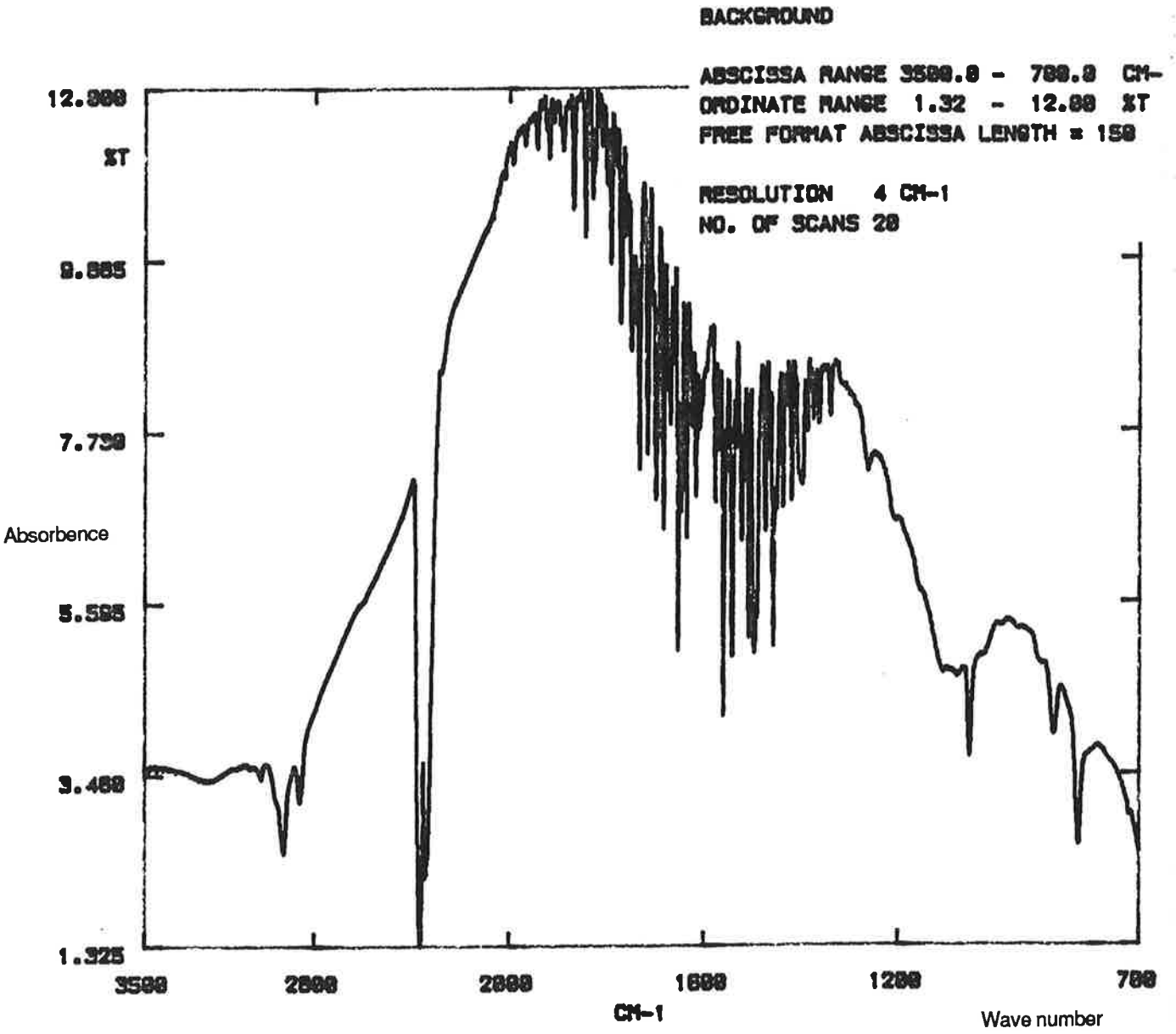

Figure 4.6.2

A background interferogram of the environment. This spectral scan, expressed as a ratio of the sample spectra, effectively cancels out any extraneous transitions in the sample spectra.

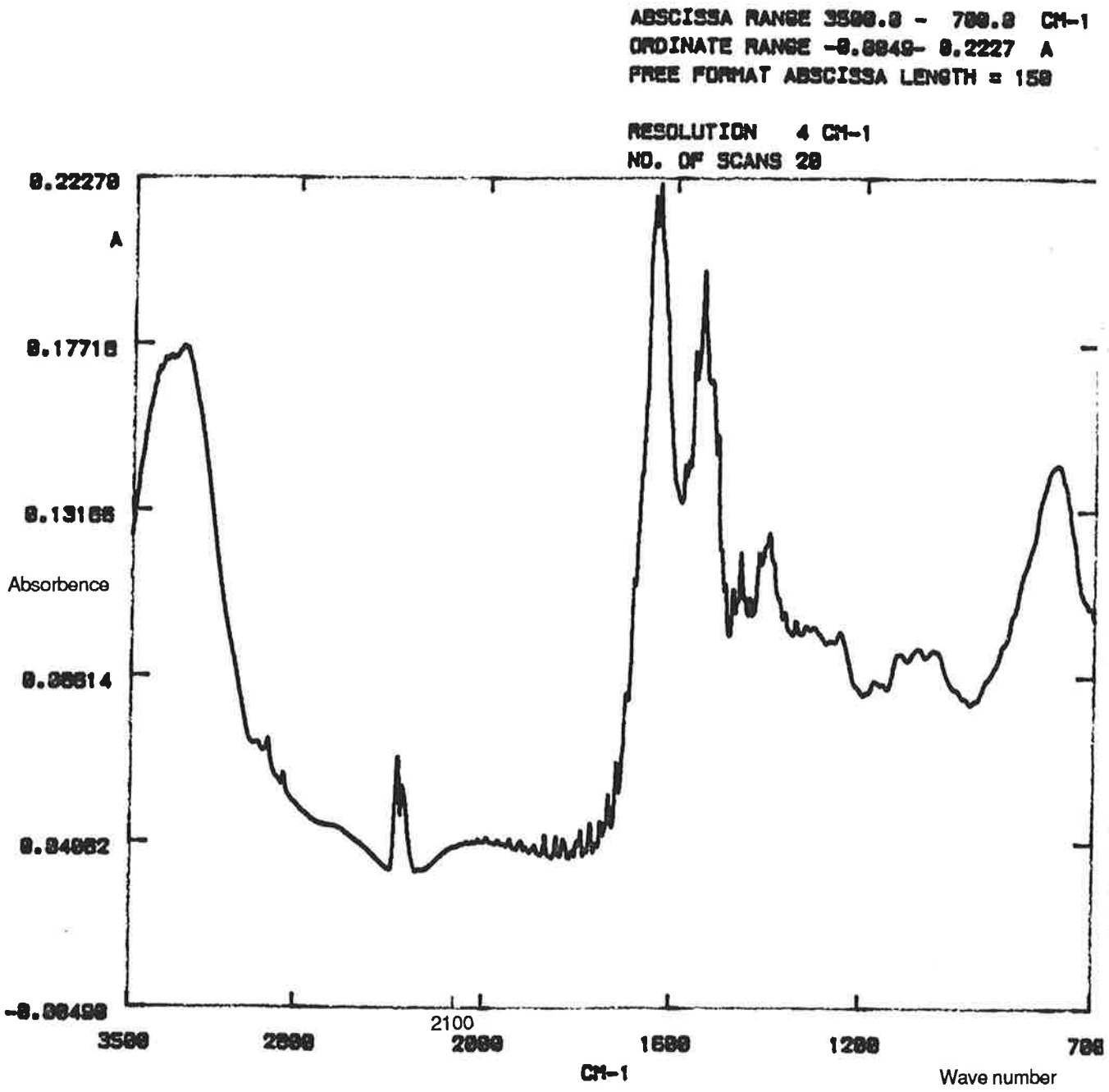

Figure 4.7.1

FTIR absorbence spectra of normal plantar skin. The calculated absorbence ratio of the 2100cm^{-1} peak was used to quantify skin hydration levels.

corresponds to a double beam dispersive spectrum (George and McIntyre 1987). It is the ratio of this spectral scan of the environment to the sample spectra that effects the cancellation and this interferogram (figure 4.6.2) is referred to as the "background".

4.7 Quantification of water content in skin using FTIR

Potts et al (1985), using FTIR identified a 2100cm^{-1} absorbence peak in the IR spectrum which was used by these workers to quantify water content in skin (see figure 4.7.1). This peak was chosen because of its distance from the other peaks produced both by stratum corneum and commonly applied substances (for example soap and emollient creams). This same technique was applied in the current study to quantify callus equilibriation from the frozen state.

4.7.1 Materials and methods

Cryotubes, Nunc Cryosystem, Denmark.

Dewar flask filled with liquid nitrogen.

Potassium bromide disc, Specac, Kent

A Perkin-Elmer infrared spectrometer (model 1720X FTIR, Perkin-Elmer, Beaconsfield, Buckinghamshire, UK) was used. This has a helium-neon reference laser, with a wavelength of 633nm, and a beam focus of 8mm and resolution 2 - 64cm^{-1} . The scan speed was set at 4cm^{-1}, so that during a contact period of 0.3 minutes, 20 scans were recorded and output in the form of absorbence to both disc and plotter.

A mercury cadmium telluride detector was cooled with liquid nitrogen. Room temperature ranged from 22 to 28ºC and relative humidity (RH) 52% to 66%, well within the optimum operating limits for the instrument.

The sample/contact cell was a horizontally mounted thallium bromo-iodide IRE which has a high refractive index (2.37 at 1000cm^{-1}) and in *in vitro* studies, a potassium bromide disc (Specac Ltd, Orpington, Kent, UK) was used to provide contact between the callus samples and the IRE.

The technique used to calculate the water content of stratum corneum from FTIR spectra in this study followed that described by Potts et al (1985). Lines were drawn parallel to the y axis on the plotted FTIR spectra, at the arbitrarily selected values of 1900cm^{-1} and 2300cm^{-1} (figure 4.7.1.1). A further line was drawn between the points of intersection of the lines drawn at 1900cm^{-1} and 2300cm^{-1} on the spectrum.

The area contained within these lines (the area above the baseline, also referred to as the baseline area) is proportional to scattered radiation which is primarily due to the optical properties of the stratum corneum. The area between the upper line and 2100cm^{-1} absorbence peak is proportional to total water content (Potts et al 1985). A ratio of the upper to lower areas under the 2100cm^{-1} absorbence curve provides a quantitative value for stratum corneum water content, independent of stratum corneum/IRE contact (Potts et al 1985).

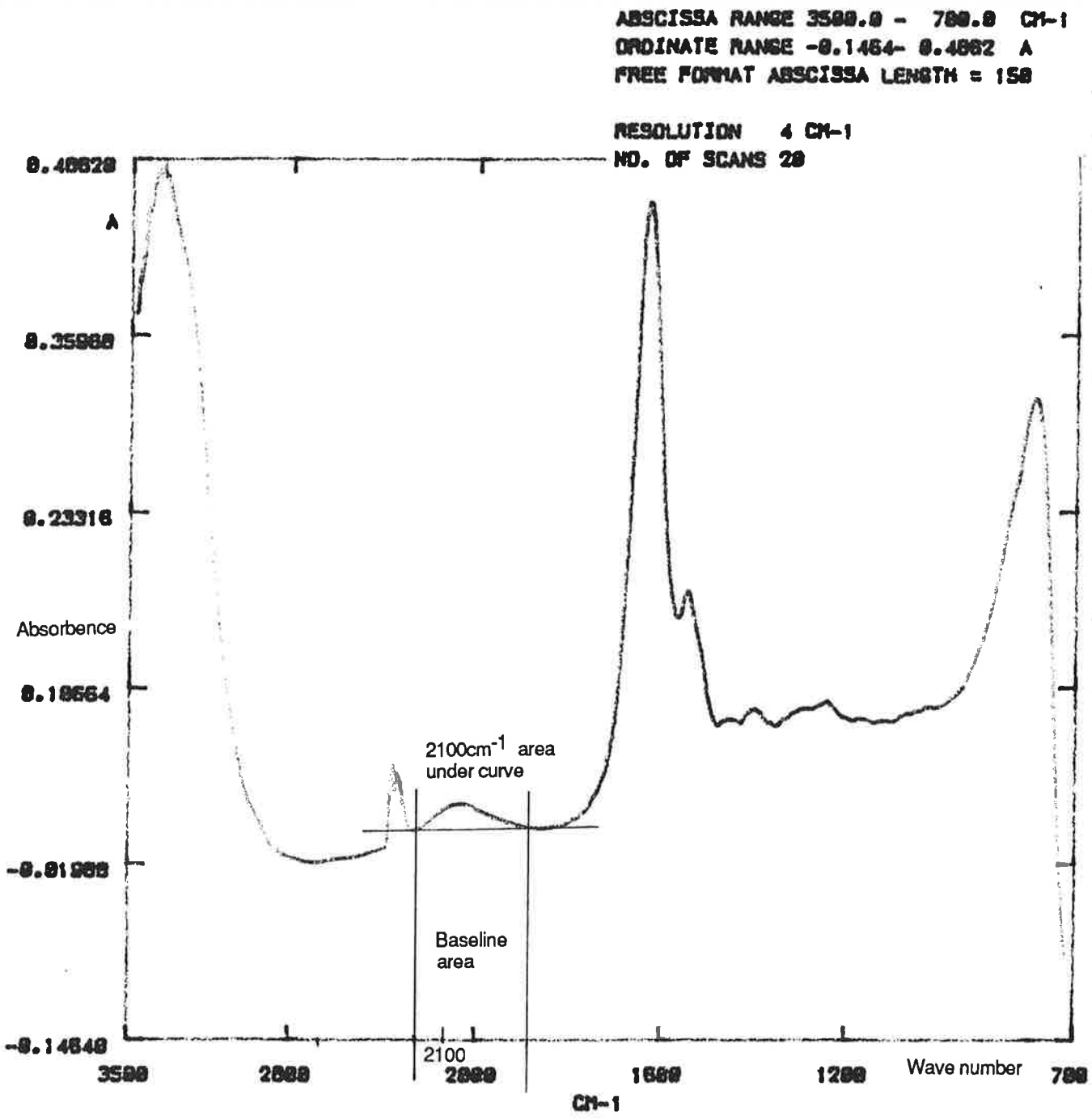

Figure 4.7.1.1

FTIR absorbence spectra where the area under the 2100cm^{-1} curve and area between the base of the curve and base line (baseline area) have been isolated.

Following excision, callus sections were placed in small, labelled cryotubes which were immersed immediately in liquid nitrogen in a Dewar flask used to transport the callus sections to a -80°C deep freezer.

Seventeen, consenting subjects (8 male, 9 female) with a mean age of 39 years (age range 28 - 51 years) with mechanically induced plantar calluses took part in this study. Their general health was good and none were taking a medication which might have affected their skin. Subjects were instructed to wash their feet in water, applying no soap or other aids, on the morning of data collection. Three separate areas of investigation were carried out, *in vivo* and *in vitro* , so that the *in vivo* water content and rate of dehydration *in vitro* of plantar callus could be established. The hydration levels of fresh and frozen callus sections were also studied.

First, for the *in vivo* study, a background spectrum of the environment was obtained using the FTIR, then 9 healthy, agile volunteers with plantar callus were selected. They were asked to sit on a chair resting on a table, the footwear was then removed and the skin wiped with a paper tissue. The foot with the callus was placed on the IRE and positioned firmly so that the absorbence spectra of the callus plaque only was obtained, the procedure was then repeated for normal plantar skin. The agility required of subjects taking part in this section of the investigation meant this group had to be younger than those for whom data was obtained in the rest of the study.

Secondly, investigations into the dehydration rate of callus samples *in vitro* investigations were then commenced. A background interferogram was again recorded. The normal skin samples were then removed from the foot of

one, and later a second, third and fourth subject using a scalpel. Absorbence spectra of the first skin samples were obtained immediately using the FTIR as described previously. The skin sample was left exposed to the ambient conditions on the IRE (RH55%, temperature 24°C) and FTIR spectra recorded at 30 and 60 seconds. This sequence was repeated for the callus sample. The same procedure was carried out for the second, third and fourth subjects.

To compare hydration levels of fresh and equilibriated frozen callus samples, the same 9 subjects from the previous experiment and a further four were selected. A scalpel was used to remove callus samples from each subject's foot in turn after the foot had been wiped with a dry paper tissue to remove surface debris. A background interferogram was recorded and the absorbence spectra of the callus samples was recorded.

To investigate optimal equilibriation conditions, callus sections were removed from the freezer and allowed to thaw and equilibriate in a desiccator at the four relative humidities and temperatures described below for a maximum of 48 hours. Callus sections were removed from the controlled environment at 3, 6, 24 and 48 hours, FTIR spectra were recorded for each callus section, which were then returned promptly to the appropriate controlled environment.

The required relative humidities were provided by the following solutions:

a) RH 84%. Saturated solution of potassium chloride

b) RH 91%. Saturated solution of potassium nitrate

c) RH 100%. Capillary mat soaked in distilled water

d) RH 55% by exposure to ambient conditions at 24°C.

Large skin callus sections were removed from four further subjects and absorbence spectra recorded. The callus samples were large enough to divide into two and were frozen as described previously. One half of each sample was then equilibriated under RH 84%, and the other, later, under RH 91%, both at 30°C. Absorbence spectra for each section were recorded at 3, 6, 24 and 48 hours.

The ratio of the area under the 2100cm^{-1} absorbence peak to baseline area for each set of data was calculated as described previously (figure 4.7.1.1) and the results compared using the paired t-test.

4.7.2 Results

Callus *in situ* on the foot has a lower water content than that of normal plantar skin. However, the difference between these two skin types is not significant ($t = 1.2$, $p = 0.45$).

Table 4.7.2.1 shows the calculated absorbence ratios of callus sections equilibriated for 3 and 6 hours at RH 55% and 100%. Callus sections equilibriated at RH 100%, 30°C show a marked increase in water content whilst those equilibriated at ambient conditions (20°C and RH 55%) show a marked reduction in water content when compared with the fresh state. No further data were therefore collected at these two relative humidities.

A) Sample	0	3	6 hours at RH 100%, 30°C
1	0.018	0.143	0.38
2	0.047	0.14	0.18
B) Sample	0	3	6 hours at RH 55%, 24°C
1	0.18	0.04	0.034
2	0.182	0.036	0.028

Table 4.7.2.1. Calculated FTIR absorbence ratios of area under 2100cm^{-1} curve to baseline area of callus sections, excised from the same subject on different days and equilibriated at A) RH 100% and 30°C, and B) RH 55% and 24°C.

Table 4.7.2.2 and figure 4.7.2.1 show the dehydration rates of normal plantar skin and callus. As seen in figure 4.7.2.1, there is a marked reduction of water content in both normal and plantar skin. Callus and normal plantar skin sections dehydrated to similar values in 60 seconds.

Callus	0	30	60 (s)
Mean	0.181	0.067	0.063
SD	0.008	0.016	0.013
Range	0.17-0.19	0.091-0.64	0.046-0.074
Normal plantar skin			
Mean	0.418	0.048	0.05
SD	0.12	0.019	0.022
Range	0.295-0.57	0.0270.067	0.036-0.083

Table 4.7.2.2. Calculated values for normal and callus section FTIR spectra, proportion of area under 2100cm^{-1} curve and baseline area, on exposure to 24°C and RH 55%, when dehydration of tissue occurs. (n = 5)

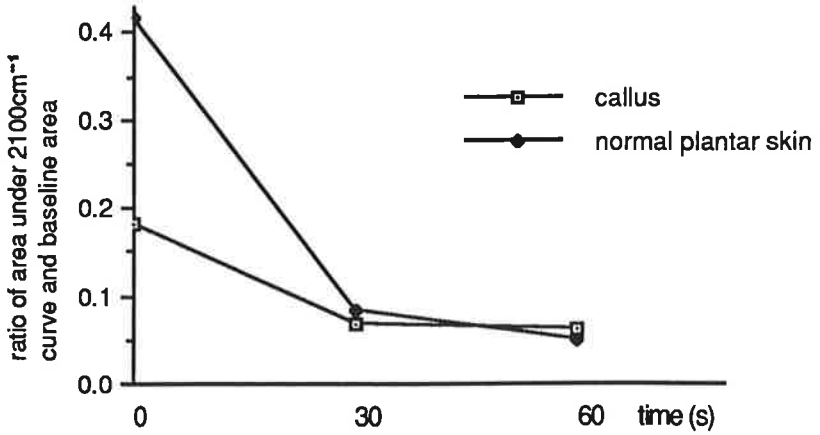

Figure 4.7.2.1
Dehydration of normal and callus skin sections (in vitro) with time at RH 55%, 24°C. Values plotted are calculated FTIR absorbence spectra ratios of area under the 2100cm^{-1} curve to baseline area.

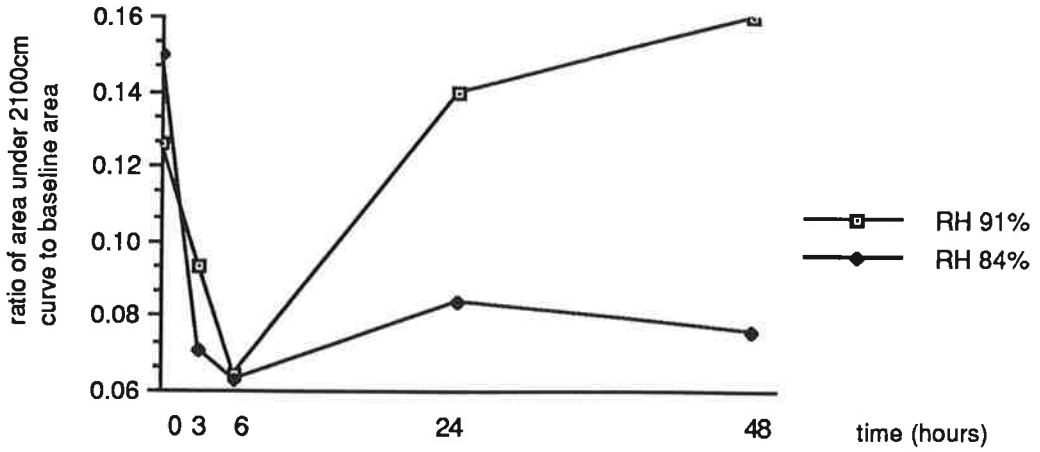

Figure 4.7.2.2
Variation in callus section hydration at RH 84% and 91%, 30 C as a function of time. Values plotted are calculated FTIR absorbence ratios of area under 2100cm curve to baseline area

Callus	fresh	3	6	24	48 hours
Mean	0.15	0.72	0.63	0.084	0.072
SD	0.04	0.9	0.051	0.1	0.83
Range	0.01-0.384	0.01-0.205	0.009-0.11	0.01-0.32	0.018-0.27

Table 4.7.2.3. Calculated absorbence ratios of area under the curve of the 2100cm^{-1} peak to baseline area of the FTIR spectra for callus samples hydrated at RH 84% and 30°C. (n = 8)

At RH 84%, 30°C, callus samples equilibriated for 48 hours were found to have a water content less than that observed with freshly excised callus (table 4.7.2.3). Figure 4.7.2.2 illustrates the calculated absorbence ratios of the area under the 2100 cm^{-1} curve to baseline areas for callus sections at 3, 6, 24 and 48 hours compared with the fresh callus absorbence spectra. The reduction in water content under these conditions when compared with the fresh callus sections at 0 hours is shown. After 24 hours at RH 84% there was no significant difference (paired t-test) between the calculated absorbence ratios of the fresh callus sample FTIR spectra ($t = 0.826$, $p = 0.218$). At 48 hours again there was no significant difference between the fresh and re-equilibriated callus sample FTIR spectra ($t = 1.31$, $p = 0.117$) (table 4.7.2.3 and figure 4.7.2.2). Five callus samples equilibriated at RH 84% were not studied as they were too dry to contact the IRE satisfactorily.

At RH 91% and 30°C, (table 4.7.2.4 and figure 4.7.2.2) there is no significant difference (paired t-test) between the calculated absorbence ratios of the fresh callus and that equilibriated for 24 hours ($t = 0.208$, $p = 0.419$), and after 48 hours re-equilibrium there is again no significant difference ($t = 1.12$, $p = 0.14$) between the fresh and equilibriated callus.

Callus	fresh	3	6	24	48 hours
Mean	0.126	0.093	0.064	0.14	0.16
SD	0.167	0.048	0.052	0.25	0.19
Range	0.01-0.55	0.003-0.52	0.014-0.18	0.02-0.32	0.01-0.67

Table 4.7.2.4 Calculated absorbence ratios of area under the curve of the 2100cm^{-1} peak to baseline area of the FTIR spectra for callus samples hydrated at RH 91% and 30°C.

Comparison of callus sections equilibriated at RH84% and 91%, for both 24 and 48 hours showed no significant difference in values obtained ($t = 0.6544$ and $p = 0.266$; $t = 1.0$ and $p = 0.1753$ respectively).

The four callus samples large enough to allow division into two sections and equilibriation at RH 84% and RH 91% respectively, show no significant difference between fresh and equilibriated callus at RH 84% after 24 hours (RH 84%; 24 hours $t = 1.72$, $p = 0.09$), and a small, but insignificant difference at RH 84%; 48 hours ($t = 1.625$, $p = 0.1$) (figure 4.7.2.3). When equilibriated at RH91% for 24 hours a significant difference between fresh and equilibriated callus sections was evident ($t = 3.203$, $p = 0.03$), although there was no significant difference after 48 hours ($t = 2.8$, $p = 0.246$). These results vary from those in tables 4.7.2.3 and 4.7.2.4 only in the significant difference in values for callus equilibriated at RH91% for 24 hours.

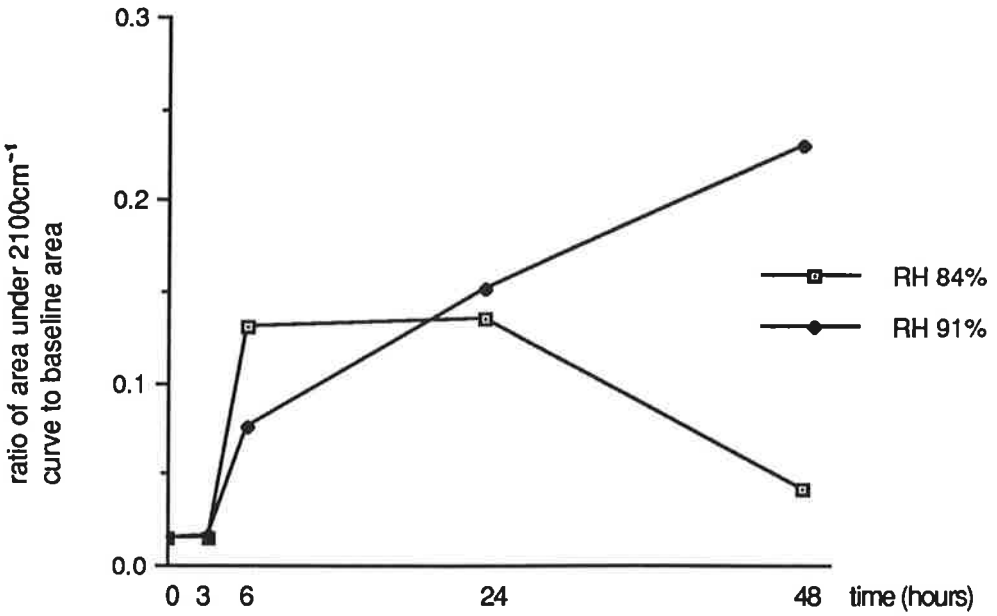

Figure 4.7.2.3
Calculated absorbence ratios of area under the curve of the 2100cm^{-1} peak to baseline area of the FTIR spectra for callus samples. Each sample was divided and equilibriated at RH 84% and 91%, 30°C.

Callus samples	RH	0	3	6	24	48 hours
Mean	84%	0.015	0.015	0.13	0.136	0.0415
	91%	0.015	0.0176	0.076	0.152	0.233
SD	84%	0.01	0.0058	0.1309	0.1357	0.0345
	91%	0.01	0.0221	0.0437	0.0809	0.1602
Range	84%	0.01-0.03	0.01-0.02	0.02-0.09	0.02-0.32	0.01-0.039
	91%	0.01-0.03	0.0003-0.05	0.069-0.24	0.069-0.24	0.21-0.4

Table 4.7.2.5. Calculated absorbence ratios of area under the 2100cm^{-1} curve and base line area of large, divided callus samples hydrated at RH 84% and RH 91% at 30°C.

4.7.3 Discussion

The results from tables 4.7.2.4 and 4.7.2.5 indicate that either an 84% and 91% relative humidity at 30°C for 24 or 48 hours are a suitable environment and times for the equilibriation of frozen callus samples prior to investigation of their physical characteristics, providing that on removal from that environment they are tested promptly. However, some data for equilibriation of callus samples at RH84% was not studied for reasons discussed below. The data illustrated in figure 4.7.2.3 show the calculated absorbence ratios for both RH 84% and 91% increasing with time until 24 hours when samples equilibriated at RH 84% suddenly dehydrate to values commensurate with those established for fresh callus samples. This is probably due to a prolonged exposure of the batch of callus samples to ambient conditions, however there was no statistical difference in callus samples equilibriated at both relative humidities used. As either RH 91% or 84% had been shown to be suitable equilibriation environments, a relative humidity of 91% was then arbitrarily selected to equilibriate callus samples removed from the feet of

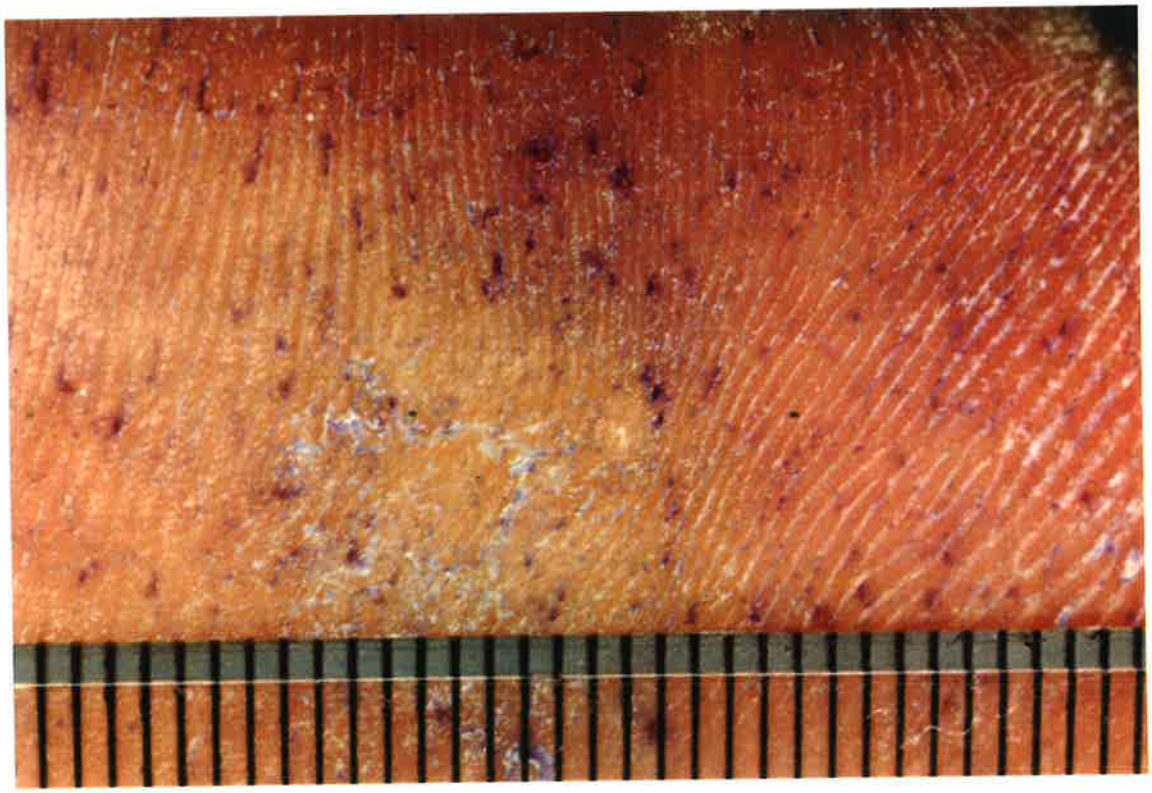

Figure 4.7. 3.1
Bromophenol blue with maize starch has been used *in vivo* to show active sweat ducts in a callus plaque and adjacent normal skin. The few ducts in callus compared with normal skin can be seen clearly.

patients for whom force plate data was available, prior to testing the viscoelasticity of the callus sample.

In practice, conditions of humidity within shoes will vary according to the fabric of manufacture. Ambient temperature changes will also influence foot sweating and therefore the skin water content will change accordingly. It was difficult to control these parameters prior to callus removal from a patient's foot. The sweat duct density in normal plantar skin and callus (figure 4.7.3.1) may also influence stratum corneum hydration and factors such as sweating rates and shoe fabric may contribute to the variation in results.

The equilibriation environment of RH 84% or 91% at 30°C is likely to reflect the *in vivo* state of normal plantar skin. The physiological barrier of the normal hairy skin stratum corneum experiences a relatively low ambient external relative humidity (averaging 64% RH in the UK) and high internal moisture content. Transepidermal water loss (TEWL) therefore provides moisturisation of the stratum corneum layers in the form of a gradient with the lowest water content being at the surface (Bomannan et al 1990, Tagami 1988). In callus the distance of the outer layers from the viable, moist layers of the epidermis is greater than in normal plantar skin (Thomas et al 1985). Therefore the moisture gradient found in normal skin (Bomannan et al 1990, Tagami 1988) is likely to be amplified in callused plantar skin, ie. the callus surface layer will have a lower water content than normal plantar stratum corneum.

This reasoning may explain the lower water content of fresh callus compared with fresh normal plantar skin as identified in the current study. A reduced

water content in callus may result in it becoming less pliable and more rigid (Spencer 1976, Potts et al 1986) when compared with normal skin. The concept of callus having a reduced water content is consistent with clinical observation as this tissue in some patients is effectively brittle and fracture planes seem to exist, parallel to the skin's surface.

At RH 100% and 30ºC after 3 and 6 hours, the callus sections were highly hydrated, fissured easily and compressed. (It is not clear why callus samples studied under this RH were different at t = 0 minutes from those measured at RH 55% (table 4.7.2.1)). Whether callus samples are in contact with liquid water or water vapour to obtain RH 100% equilibriation conditions would appear unimportant. Elden (1971) considered the relative effects of water vapour and liquid water on stratum corneum. He concluded that stratum corneum is less resistant to liquid water than water vapour but the experimental technique resulted in liquid water possibly contacting the samples. *In vivo* , foot skin, encased in a shoe which limits TEWL, will be in contact with both water vapour and liquid water, thus the selection of either water vapour or liquid water to equilibriate callus can both be said to reflect the *in vivo* state. However, 100% RH has been shown in the current study to hydrate skin callus to a higher level than that found *in vivo* and was therefore considered inappropriate for the purposes of equilibriating frozen callus sections.

In stratum corneum containing less than 10% water, the latter is avidly bound to the polar sites of the proteins. This primary water of hydration (Spencer 1976, Potts 1986) accounts for the normal pliability of hairy skin. Secondary water of hydration (10 - 40% w/w) is less avidly bound (probably hydrogen

bonded to the primary hydration water) and is present as the relative humidity increases above 60% (Spencer 1976). Above 50% w/w water, the tertiary water of hydration absorbed by hairy skin stratum corneum has a higher mobility and at RH 100% the skin is mechanically weak because of the matrix being highly hydrated (Spencer 1976). It may be deduced from the relative humidity (91%) required to equilibriate plantar callus to the hydration levels found in freshly removed *in vitro* callus sections that all three types of water of hydration are present in normal plantar skin and callus when encased in footwear. Hairy skin at RH 100% is mechanically weak (Spencer 1976), yet plantar skin must be tough and is habitually encased in footwear where, it can be surmised, a high RH is attained. As normal plantar skin functions satisfactorily under these conditions, this explanation suggests that the biomechanics of plantar skin may be different from that of hairy skin.

Garson et al (1990) using EM studies reported the keratin of plantar skin callus to be closer to the alpha-type keratin of wool and human hair, which explains the observation made by Hey (1978) that water behaves in a very similar fashion in wool fibres, human hair and human callus. If the keratin structure of normal and callused plantar skin is different then the effect of water of hydration on these two keratin types may also be different. Such differences may result for example, in slow clinical maceration of callus on hydration compared with adjacent normal skin. However, this effect is more likely to be due to differences in hydration of the lipid bilayers of the stratum corneum (Potts et al 1990).

The relative dryness of plantar callus compared with normal plantar skin, may be explained further by considering callus keratinocyte maturity, the rapid

transit time for keratinocytes in callus, the development of the lipid lamellae intercellularly and the influence of water on skin lipids. In studies on the influence of RH on normal and extracted human skin, Wildnauer et al (1971) observed that fracturing of the skin structure occurred intercellularly leaving internal corneocyte structures intact. These workers considered that water affected the structures intercellularly, *viz* the lipid bilayers, such that they weakened, while the keratin filaments and cell envelope of the corneocyte remained unaffected.

In vivo skin callus which has become macerated due to occlusion with strapping or affected by a topical drug such as 20% or 40% Salicylic Acid, cleaves apparently superficially to the viable epidermis, probably at the base of the stratum corneum, in the stratum compactum. Histological preparations also show artifactual splitting at this level. While this effect may be mechanical due to fissuring at the interfaces in this composite tissue (Vincent 1982), it is also likely that the integrity of the lipid bilayers is being disrupted such that cleaving occurs.

The rapid transit time of squames through plantar callus (when compared with normal plantar skin) (Mackenzie 1983, Thomas et al 1985) may mean that squames have not matured sufficiently (Michel et al 1988) on reaching the stratum compactum to produce the strong covalent bonds between the ceramide molecules of the lipid bilayers and cell envelope (Phillips 1992). Hydration of tissue of this immaturity may result in mechanical weakness between layers due to changes in bond types between molecules. This zone is also the site at which stress (Vincent 1982) results in induced longitudinal shear failure (chapter 5). Such stresses may be mechanical or induced by

hydration gradients, as occurs in histological fixation processes or *in vivo* with occlusion of the skin.

The FTIR *in vivo* studies comparing normal plantar skin with intact plantar callus in the current study indicate that callus has a lower water content than normal plantar skin. However data collection was marred due to the patient's difficulty in placing their foot with only its callus plaque over the IRE. The dehydration rate of the skin's superficial layers while the patient climbed into the position over the IRE appropriate for data collection was impossible to predict, particularly as the viable skin layers contribute to stratum corneum hydration (Bomannan et al 1990).

In vitro callus sections were demonstrated to have a lower water content than normal plantar skin on removal from the patient's foot. This observation is compatible with the trend found *in vivo*. When dehydration rates were examined both callus and normal plantar skin sections dehydrated to similar values in 60 seconds, which confirms the clinical assumption that water loss may account in part for the stiff texture of excised callus tissue. These results support the converse observation of the high rate of water sorption by human callus (Hey 1978).

The texture of callus samples equilibriated at RH 91% was similar to that noted clinically on removal of the callus samples from the patient. However, even with prompt FTIR analysis, the texture of the callus samples were perceived to change and become less pliable. Although the scan time of the sample on the FTIR crystal was only 0.3 minutes, the time taken in preparation for this data to be collected (30 - 60 seconds) was sufficient for

samples to dehydrate which appears to take place over a few seconds. A possible but relatively inaccessible solution to this experimental difficulty which could influence results, would be to construct a chamber around the IRE whereby the RH could be maintained during preparation and data collection.

Room temperature and relative humidity, though constant for collection of each set of data, were unfortunately not controllable. However, the temperature and relative humidity were within a range where the effect on skin water content would be expected to be minimal (Spencer et al 1975, Potts et al 1985). A further source of error may occur with the change in refractive index which occurs on hydration of the skin (Bomannan et al 1990). Normal skin refractive index can be considered to be between 1.33 (that of water) to 1.55 (that of dry, scaly stratum corneum). However, Bomannan et al (1990) indicated even when maximum error was introduced, results are not significantly affected.

Contact of the sample with the FTIR IRE created a particular experimental difficulty. The drier callus sections showed a noisy monitor display due to poor contact with the IRE. This could be improved by hydrating the callus tissue, which would obviously negate the purpose of the study. Three callus samples which were to be used for the RH 84% study had to be discarded and the fresh, *in vitro* , callus sections were too dry to obtain a suitable FTIR spectrum even though they had just been removed from the subject's foot. The reason for the dryness of the samples is not clear, but the distance of the callus surface from the moist, viable layers of the epidermis may have been greater in these patients, and the water gradient more marked.

Further variation in results may be due to the influence of age on the stratum corneum; the number of corneocytes and quantity shed increases (Leveque et al 1984) and the DEJ flattens (Smith 1989) although the keratinocyte structure remains unchanged (Lavker et al 1989). The experimental method required subjects to be reasonably agile, thus necessity dictated these *in vivo* FTIR studies be carried out on an younger age group (mean age 39 years) than the patient group selected for the rest of the current study.

Although Gloor et al (1980) specified no washing of the skin test site for at least three days prior to data collection, it was noted that feet readily became coated with substances which may affect FTIR data. Therefore the feet were washed in tap water on the morning of data collection and wiped with a dry paper tissue just prior to callus removal for FTIR spectra collection so that minimal distortion of skin hydration levels occurred which would have caused spurious data.

It would be interesting to carry out investigations into the effects of variations in RH of plantar skin callus. TEWL is restricted when callus is occluded with a dressing such as adhesive plaster and maceration of the stratum corneum develops. On removal, an occlusive dressing often pulls away the macerated callus exposing a zone which may be the stratum compactum (Patients removing these dressings occasionally tear off adjacent, normal skin.) Once the conditions for hydration of the callus plaque are known whereby it is made pliable yet remains intact (possibly RH 91% or higher), then dressings with appropriate occlusion values may be designed to recreate that required RH. Such dressings would not, of course, treat the cause of the callus, nor

control its development, but might manage the symptoms. Much of the discomfort associated with callus appears to be due to its rigidity as well as its bulk, but if it is softened and made more pliable, then stress on sub- and adjacent skin might be reduced and consequently the low grade, chronic tissue irritation which is assumed to occur within and under callus plaques (section 3.12.3) could resolve along with much of the discomfort experienced by the patient (Springett 1987).

4.8 Conclusions

Plantar skin callus, when investigated using FTIR (Potts et al 1985), has been shown to be significantly drier both *in vivo* and *in vitro* compared with normal skin. This confirms a clinically held assumption about callus characteristics.

A RH 84% or 91%, 30°C have been shown to be suitable a equilibriation environment for excised and stored plantar callus sections, and either of these relative humidities may mimic that found *in vivo*.

There was some experimental difficulty in creating an effective contact of dry callus tissue with the IRE.

CHAPTER 5

The rheology of plantar skin callus

5.1 Introduction

Clinically, it appears that the texture of callus plaques is responsible for many of the symptoms about which patients complain. A soft, macerated callus lesion for example, seems to cause less pain than a dense, non-pliable plaque. Normally skin must be able to conform to external forces. The dermis and epidermis must be deformable to a greater or equal extent as underlying tissue (Ferguson 1980) in order to prevent separation of layers, to prevent fissuring or puncturing so that it can retain its integrity and remain as the body's primary barrier to the environment (Wilkes et al 1973). The stratum corneum achieves its conformability in a number of ways (Ferguson 1980, Potts and Breuer 1981) which allow the skin to extend under load. In the foot, the skin's ability to withstand load yet be able to conform to the supporting surface is of major importance for pain-free, efficient locomotion. Plantar callus lesions are often painful, probably due to the abnormal biomechanical behaviour of this pathological tissue, and may be seen, clinically, to inhibit normal gait.

The clinical characteristics of a callus plaque are distinctly different from those of normal plantar skin (figure 1.4.1). Also the water content of callus tissue has been shown, in the present work, to be lower than that for normal plantar skin (section 4.7), probably due to the altered volume and quality of the stratum corneum intercellular lipid lamellae (Mackenzie 1983, Phillips 1992). Callus keratin ultra-structure has been shown to vary from normal plantar skin (Mackenzie 1983, Garson et al 1990) in a similar way to that of other hyperkeratoses such as psoriasis and ichthyosis vulgaris.

In these skin conditions, keratin fibril formation has been claimed to be shorter and wider, or shorter and narrower respectively than normal (Steinert and Cantieri 1983). In callus, keratin fibrils are shorter but of normal diameter (Mackenzie 1983). The LM histological characteristics of callus are also different from those of normal plantar skin as illustrated in the current work (section 3.12.2). All these features of plantar skin callus tissue may affect the viscoelastic behaviour of normal skin. Any inability of callus tissue to conform to external forces and restore normal configuration will stress the adjacent structures and the potential for damage may be created. This type of induced mechanical trauma may be an adequate stimulus to enter the skin site into the cycle of callus formation. It has become clear from the present study, that the empirical assumption that callus plaque dermatoglyphics may indicate prevalence of a particular force vector is simplistic and further investigations into callus plaque characteristics are required to explain their formation and clinical appearance.

5.2 Proposed function of plantar skin callus

It is interesting to ponder over Nature's reasons for the development of plantar callus. This tissue contains an alpha-keratin similar to that found in hair and nails (Garson et al 1990). The latter have many uses, including fighting, scratching, digging, protection for the sensitive finger and toe-tips, and an aid to dexterity (Samman 1986). However, it is difficult to understand the reasons for the development of this form of keratin in callus, other than for protection (Adams et al 1989). Barefoot peoples develop protective, continuous and uniform callus over the soles of their feet enabling them to walk over almost any terrain. Such feet often show deep fissuring at the margins between non-weight bearing and weight bearing areas (such as around the heel) suggesting there is loss of conformability in the callus tissue.

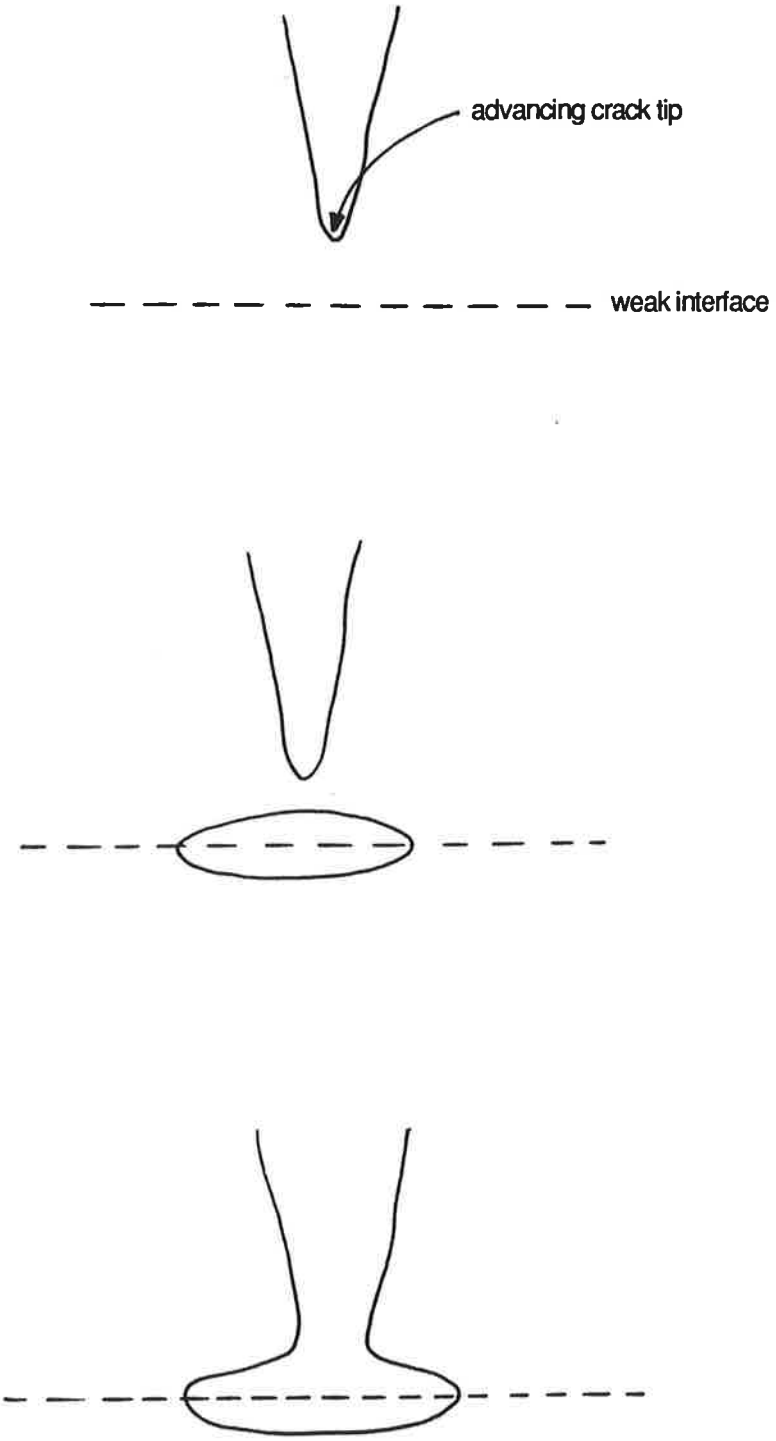

Figure 5.2.1
Vertical fissuring in composite materials often translate into horizontal, thus limiting the damage of mechanical stress. The Cook-Gordon model for blunting of a crack tip at a weak interface (from Vincent 1982)

These fissures may be in the form described by Vincent (1982) where widening of the base of the fissure transfers load laterally, halting further ingression of the fissure (figure 5.2.1). Fraser and Macrae (1980) considered that the composite nature of keratin incorporated within the intracellular matrix of keratinocytes, should tend to distribute any applied stress evenly over the filaments of keratin, thus preventing propagation of cracks from local imperfections or points of ruptures. However, the structure of hairy skin keratin was studied by these workers and the keratin-dense squames of plantar and palmar skin were not considered.

Callus formation in shod people may be the legacy of normal plantar skin protective response to the stimulus of mechanical stress which occurs in barefoot walking. These lesions seem to become a problem when a change in skin biomechanics occurs and there is a sudden transition from normal, conformable skin to a bulky, stiff lesion, or when callus thickness is uneven, giving rise to differentials in skin tissue response, with time, to mechanical stress. Then both adjacent normal skin and cellular structures within the callus plaque will be affected by the altered skin biomechanics.

The biomechanics of hairy full skin have been studied extensively (Potts and Breuer 1981, Manschott and Brakkee 1986, Vogel 1988, Wilkes 1973) together with that of the dermis (Daly and Odland 1979, Daly 1989). Epidermal and specifically stratum corneum biomechanics are relevant to the present work. Christensen et al (1977) demonstrated that the stiff (elastic) elements, necessary for restoration of the skin's resting configuration, reside principally in the stratum corneum (Christensen et al 1977), however the properties of the dermal elastin are likely to be of paramount importance. Further study of stratum corneum biomechanics showed that water content affected stratum corneum extensibility (Christensen et al 1977, van Duzee

1978, Potts and Breuer 1981) and a three phase curve could be created *in vitro.* For a water content (measured as a percentage of dry weight) of between 0 - 10%, the force-extension curve was found to be Hookean, at 20% it was curvilinear, and at 125% water content, extension was shown to be linear leading to fracture (Ferguson 1980). The water content of the lipid lamellae of the stratum corneum also appears to affect it's molecular configuration (Potts et al 1990), thence its intercellular mobility which will influence stratum corneum biomechanical properties.

Stratum corneum, as a partially plasticised polymer composite may be expected to display viscoelastic behaviour (Wilkes et al 1973). To study stratum corneum biomechanics *in vitro*, Laden and Morrow (1970) used an oscillating torsion pendulum to monitor changes in callus stiffness with changing relative humidity. The callus remained relatively stiff until 60% RH when it was reported to "soften" rapidly. These workers proposed that at high RH (over 80%) slippage between keratin chains had occurred and no further movement was possible, hence callus exhibited elastic properties.

Low amplitude shear wave propagation has been used to determine the elastic and viscoelastic features of skin *in vitro* (Potts et al 1983, Wilkins and Dorogi 1986, Pereira et al 1991) though polarised opinions exist as to the frequencies which appear to provide information on the properties of the skin's surface. Stress-relaxation studies on human skin (Wilkes et al 1973) showed skin to be elastic, plastic and viscoelastic according to the stress applied, and these features varied with site both within an individual and from person to person.

The viscoelastic behaviour of skin has also been studied using oscillatory stress applied with a sinusoidal waveform (Vincent 1982, van Duzee 1978, Jemec et al 1986). Although, comparison of the Lissajous loops so obtained

was considered by Wilkes et al (1973) to provide inaccurate data, contemporary studies have utilised more advanced mathematics and software to manipulate the data (Vincent 1982, Hennenberg and Silbererg 1984) and greater accuracy has resulted.

It is difficult to separate the interplay between the biomechanics of the dermis and the epidermis. In age, the viscoelastic behaviour of full skin changes (Vogel 1988), yet that of the keratinocyte appears unaltered (Lavker et al 1989, Smith 1989). However, as dermal morphology changes with increasing age, so epidermal biomechanical behaviour may be affected. Skin tensile strength decreases with age (Duck 1990) and in disease (Wilkes et al 1973, Leveque et al 1984) in part probably due to the flattening of the DEJ (Smith 1989) which is then no longer able to extend under load, and change from the apparently random dermal collagen fibre orientation (Leveque et al 1984) to a more rigid lattice.

Load can be taken up by the healthy stratum corneum in a number of ways. Surface undulations of the cell envelope of young squames flatten on taking load, the overlap between squames may be increased, skin folds extend and, at the physiological limits of strain, the desmosomes and intracellular keratin fibrils take up load (Ferguson 1980). Cycles of tension and relaxation can result in preconditioning, where there is a progressive reduction in stress in the tissue (Duck 1990) as it retains its new configuration and develops structural changes to support this re-organisation (viz Wolf-Davies law with regard to tendon and ligamentous tissue). The micro-relief of the skin's surface extends when stressed and may undergo certain deformations without stressing the DEJ or over-stretching the stratum corneum (Leveque et al 1984). It is possible that the dermatoglyphics of palmar and plantar skin not only aid grip (Buchholz et al 1988) but permit this form of deformation in

response to stress, although Higuchi and Tillman (1965) found no difference between callus samples tested with striations placed horizontally or vertically.

A complication to be considered when studying the viscoelasticity of plantar callus is that of the rapid transit rate of cells through the epidermis (Mackenzie 1983, Thomas et al 1985). It is postulated in the current study that the stratum corneum of callus has insufficient time to mature and to develop normal intercellular structures important in intercellular cohesion. Consequently the viscoelastic behaviour of this tissue may show variation commensurate with the maturity of its squames.

The intracellular ultrastructure is also altered in callus tissue (Mackenzie 1983) so again, the viscoelastic behaviour of the callus keratin:matrix composite may be affected. The main factors which determine the mechanical properties of a filament:matrix composite as found in stratum corneum squames include (Fraser and Macrae 1980):

- the mechanical properties of the keratin filament
- filament length
- the orientation and packing of the filament in the matrix material
- the mechanical properties of the matrix material
- the proportion of the matrix
- adhesion of the matrix to the filaments (via van der Waals' forces, H-bonds, ionic interactions and covalent disulphide bonds)

In hairy skin stratum corneum, keratin filaments occur in bundles with preferred plane of orientation parallel to the skin's surface. In normal plantar skin, the orientation of the keratin bundles is not seen (Frazer and Macrae 1980), nor is the ordered stacking of the squames (Mackenzie 1983) as seen in mouse ear LM sections. The significance of keratin content and fibril packing in the electron-light and dense keratinocytes (Mackenzie 1983) seen

in plantar skin is not known. The packing arrangement of keratin fibrils in plantar callus also is not known, however, it would appear that keratin fibrils are shorter in callus compared with those for normal plantar skin (Mackenzie 1983) which may influence callus biomechanics. However, as discussed previously, the water content of the stratum corneum within the lipid lamellae, is particularly influential in skin biomechanical behaviour and this variable can be controlled under experimental conditions, whereas selection of tissue of similar maturity and ultrastructure is not feasible.

5.3 Rheology

Rheology may be defined as the study of the response of materials, with time, to an applied force (Besancon 1985). Rheologists are proud of their associations with the ancient Hebrew prophetess, Deborah, the fourth judge of the Israelites who long before the 5th century BC sang "the mountains flowed before the Lord" in celebrating the victory of Barak over the Canaanites (Judges 5:5).

Biorheology, a branch of physics established in the middle of this century, is defined as the study of the deformation and flow of biological materials in their biological context (Scott-Blair 1974). In the field of biorheology, a number of different biological tissues have been studied including muscle, bone, hair, skin, mucus and blood. An understanding of the viscoelastic behaviour of full skin has, for example lead to a change in surgical skin closure techniques (Scott-Blair 1974) where the wound is closed manually allowing tissues to conform to their new orientation prior to closure, thus reducing stress at the suture site. Identification of the critical abnormalities in skin biomechanics has led to remedial therapies and effective evaluation of drugs used in disease (Wilkes et al 1973). Research into the biorheology of mucus has provided helpful information in the management of cystic fibrosis

(Marriott et al 1990).The aspect of biorheology specifically relevant to the current study is that of measurement of viscoelasticity of skin callus which is considered in the next section.

5.4 Viscoelasticity in biological tissues

The vast majority of biological tissues are viscoelastic and frequently function at 50% strain or more. The behaviour is often non-linear and models for viscoelasticity may be considered invalid under these conditions, therefore assumptions must be made because linear small strain models are being applied to non-linear large strain tissues (Vincent 1982).

Perfectly elastic materials can be deformed and will restore to their original shape almost immediately once the force is removed. Viscosity is defined as the ratio of shearing stress to velocity gradient (Newton's law) and viscous substances will flow on deformation. (The shear modulus is defined as the ratio of shear stress to strain.) Viscoelastic materials will restore with time once the deforming force is removed. Materials such as flexible clays may exhibit a plastic behaviour where shape is not restored after removal of the load. Figure 5.4.1 illustrates these different types of behaviour of materials under load.

Viscoelastic materials exhibit viscous and elastic properties simultaneously. During application of stress, the molecular structure of a viscoelastic material will undergo changes which permit the change in configuration and some later restoration. Stretching of primary valency bonds and rupture of weak bonds (eg: van der Waals') allows extension of the material (Marriott 1992), as proposed by Laden and Morrow (1970) and this occurs in skin callus.

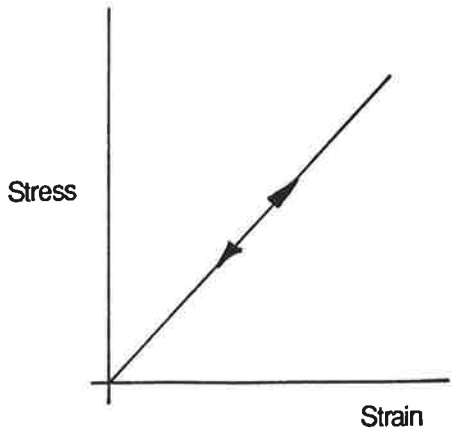

An elastic material

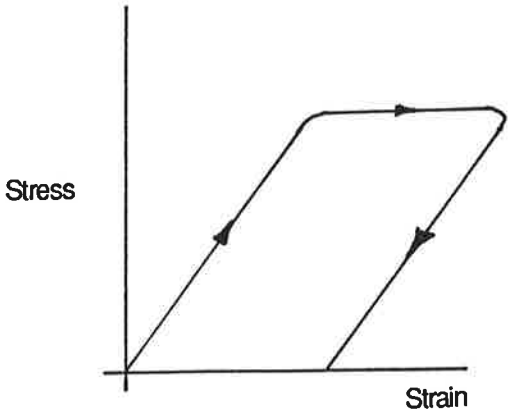

An elastic-plastic material

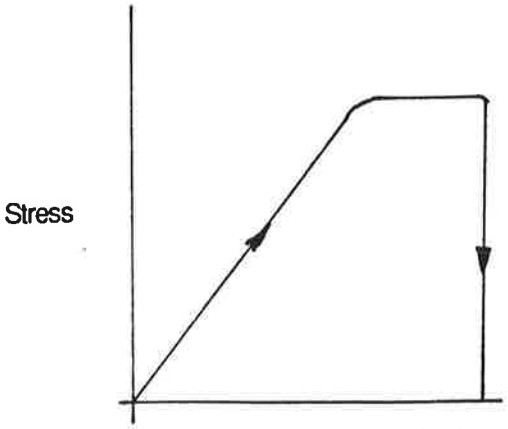

A plastic material

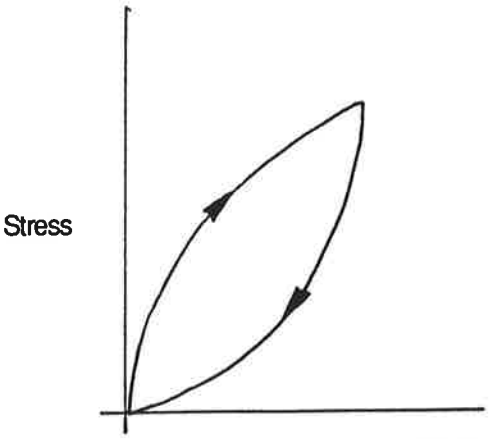

A viscoelastic material

Figure 5.4.1
Stress-strain curves illustrating different types of material behaviour under load (Vincent 1982)

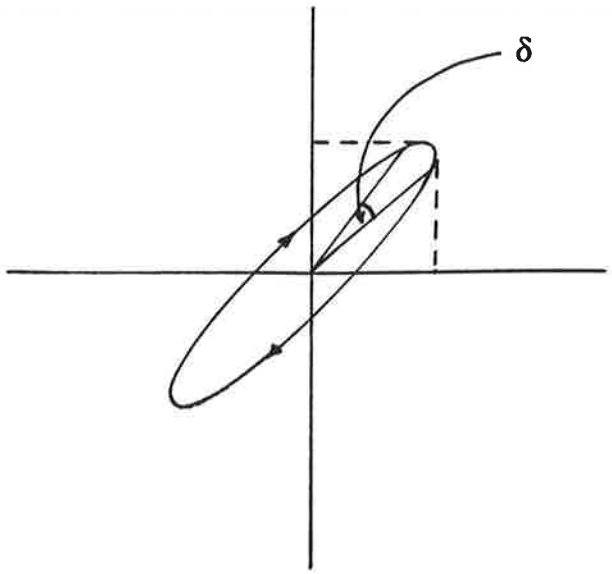

Figure 5.4.2

A Lissajous figure - a vector diagram of a viscoelastic material undergoing dynamic testing.

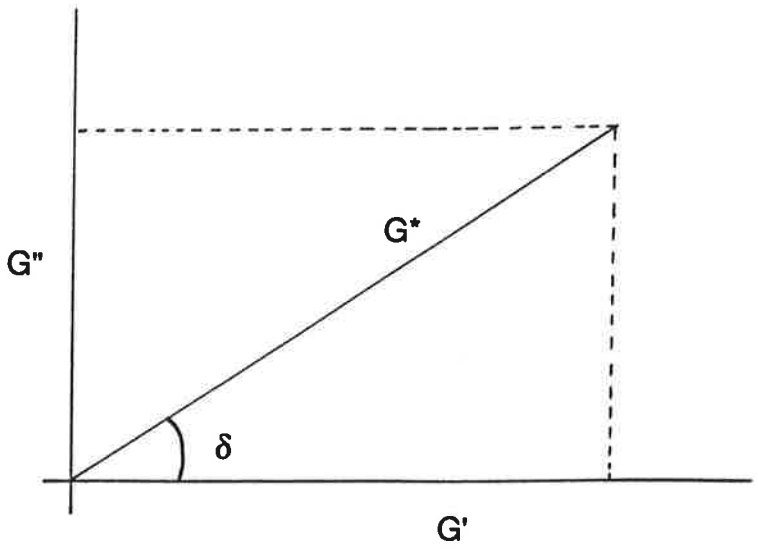

Figure 5.4.3
Geometric resolution of the complex modulus G* into its components G', G" and delta.

Both transient (elongation or shear deformation of a material and its response) and dynamic (where stress or strain is varied cyclically and sinusoidally) experiments can be made on biological tissues (Vincent 1982).

Dynamic testing is versatile and has become, in the field of biorheology, an established method of investigating tissue viscoelasticity (Scott Blair 1974). To avoid the difficulty mentioned previously of linear, small strain models being applied to large, non-linear materials or tissues, small strains are generally applied to the tissue being tested, and dynamic testing is particularly suited in this instance (Vincent 1982).

The response of a viscoelastic tissue to a sinusoidally varying stress or strain may be plotted as a Lissajous figure (figure 5.4.2) or more conveniently, data may be manipulated using the equation 5.4.1 and illustrated as a vector diagram demonstrating the relationship between G*, G' and G" (figure 5.4.3).

$$\sigma_o = e_o G^* \sin(\omega t + \delta) \qquad \text{Equation 5.4.1}$$

where:

δ denotes stress
ω denotes frequency
e denotes one dimensional strain
t denotes time
G* is the complex modulus of G' and G"
G' is the dynamic storage modulus (the amount of energy stored during each cycle upon deformation).
G" the dynamic loss modulus (the amount of energy lost to viscous dissipation).

Tan delta is the ratio of viscous response to elastic response which reaches a maximum when the various relaxation mechanisms of the tissue are activated. It can therefore be used as an indicator of the presence, position and relative magnitude of transitions. The smaller the value for tan delta, the more elastic the tested substance will be, and conversely, as the substance becomes more viscous, so the value for tan delta increases.

If the material sample tested were soft and elastic, then the curve plotted of the frequency applied by a suitable instrument to the displacement would be the same and the two wave forms would be "in phase" (Scott Blair 1974). A viscous substance would result in the two waveforms being completely out of phase when the phase angle would be 90°. For a linear viscoelastic system, the stress curve will also be sinusoidal and the phase angle will lie between 0° and 90°. Measurement of viscoelasticity should be carried out in the linear viscoelastic region so that permanent deformation of the material or tissue can be avoided. As the frequency of the imposed oscillations increases, so the structural molecules of the tissue fail progressively to adjust themselves in the time allowed by the frequency of the oscillations (Vincent 1982). The interval of time when tissues fail to adjust (the lag) may be used as an indicator of the viscoelastic characteristics of the tissue.

As instruments designed for industrial applications had to be adapted for smaller biological samples, a number of techniques were developed to measure flow and deformation of biological tissues (Scott-Blair 1974). These include the microcapillary viscometer, the cone-plate viscometer and a rheometer which applies sinusoidal frequencies to the sample. This latter instrument has become an established method of measuring viscoelasticity in biological tissues (Scott Blair 1974, Vincent 1982, Marriott et al 1990) and will be used in the current work.

5.5 Materials and methods

Rheometrics Dynamic Spectrometer, Rheometrics, New Jersey, USA

Parallel plates, diameter 0.25cm

Scalpel handle and blades

Potassium nitrite (saturated solution) within a desiccator was used to obtain a relative humidity of 91% at 25°C.

Figure 5.5.1.1
The Rheometrics Dynamic Spectrometer

5.5.1 Rheometrics Dynamic Spectometer

The Rheometrics Dynamic Spectrometer (rheometer) is capable of measuring both elastic (G') and viscous (G") components of a material or tissue and software options permit selection of the parameters to be computed and recorded (figure 5.5.1.1). Moduli are recorded in dyn/cm^2 and data has been converted, in the current work, into SI units (N/m^2).

Torque was applied by a motor to the upper plate causing it to oscillate in a pre-determined log sequence of sinusoidal frequencies recorded in radians/second which were converted to Hertz for convenience. (Frequency range 0.63 - 63 rad/sec or 0.1 - 10Hz). These waveforms initiated through the upper plate are transmitted through the sample which is placed between the upper and lower plates. The resulting deformation of the sample is measured by a low compliance transducer beneath the lower plate, strain and deformation are amplified, digitised, manipulated by the instrument's software and displayed in hard copy (appendix 2).

5.6 Validation of use of Rheometric Dynamic Spectrometer to study plantar skin callus viscoelasticity

Samples of callus were removed from the feet of consenting patients to ascertain the range of values which may be obtained when investigating callus viscoelasticity before relating this to the clinical appearance of the lesions.

All patients were healthy, age range 30 - 80 years, and were taking no medication which may have affected their skin. A scalpel was used to remove callus samples of diameter greater than 0.25cm, from their feet. Although a dermatome would have provided a constant sample thickness, it

was not possible to use this on patients without causing damage to the viable skin.

Preliminary studies using the rheometer demonstrated that callus samples removed and exposed to ambient conditions were too dry to allow effective contact with the rheometer plates. Samples slipped when torque was applied thus data obtained was spurious. A low value strain (5%) was arbitrarily selected and used on all samples. Callus samples hydrated in RH 91% provided satisfactory data initially, but when further samples were removed from the same desiccator, ambient conditions altered the enclosed atmosphere and dried the remaining samples.

Consequently, callus samples were immersed in water in ambient conditions for 5, 10, 30 and 50 minute intervals before testing to ascertain the optimum period of time for each sample to become uniformly hydrated. Ten minutes of hydration allowed good contact of the sample with the rheometer plates. However a wide coefficient of variation (c.o.v. 80.38%) was obtained in the data. Also the level of hydration in callus sections of different thickness was not controllable.

As the water content of the skin has been shown to affect stratum corneum biomechanics (Laden and Morrow 1970, van Duzee 1978, Potts and Breuer 1981), callus samples were again hydrated to a consistent, controlled level in RH 91%, 25°C for 48 hours. On this occasion however, four callus samples were placed in six small desiccators so that the effects of drying when samples were removed for testing were minimised.

The coefficient of variation is a descriptive method of allowing the SD to be expressed as a proportion or percentage of the mean (Armitage 1980).

5.6.1 Method

Having rationalised the experimental method, callus samples, each from different patients (n = 24), were tested using the rheometer. Three repeat determinations were carried out on each sample. A 5% strain was selected on the instrument, calibration carried out and all dials set to zero. The micrometer ratchet settings obtained were not altered, so that the load on each callus sample remained constant. The callus sample was then placed between the upper and lower plates of the rheometer and the thickness of each sample measured. This value was input into the instrument's software. A coating of silicone oil was applied over any exposed parts of the callus sample to inhibit dehydration. The sample was left in place for the three runs when the sinusoidal frequencies applied to the tissue ranged from 1Hz to 10Hz. The upper and lower plates of the rheometer were cleaned meticulously after each experiment.

The vast volume of data generated by the instrument was reduced by sampling data at 0.1, 0.3992, 2.519 and 10Hz (0.6302, 2.508, 15.83 and 63.02 rad/sec respectively). The coefficient of variation was then determined for each of these four sample frequencies.

As plantar skin callus samples from patients had been archived frozen, comparison of viscoelastic behaviour was made between the equilibriated and fresh callus samples obtained as described above. The frozen samples were placed in the small desiccators to equilibriate and their viscoelastic behaviour recorded in the same manner as that described above for fresh callus samples. ANOVA (different sample sizes) was carried out to compare data for frozen and fresh callus samples.

One sample of normal plantar skin was excised using a scalpel and its viscoelasticity tested using the rheometer. Its viscoelastic profile may provide

an indicator of the features of normal plantar skin, in general, and a comparitor for callus viscoelasticity.

5.6.2 Results

The results demonstrate that plantar skin callus is, as expected, a viscoelastic tissue (figure 5.6.2.1). Viscous behaviour dominates at the lower frequencies, when the values for tan delta are greatest (between 0.1 and 0.3992Hz). As the applied frequency increases so elastic behaviour dominates, and the values for tan delta lessen between the frequencies of 2.519 to 10Hz. For comparison, figure 5.6.2.2 illustrates the viscoelastic behaviour of one sample of normal plantar skin, where the plot profile can be seen to be similar to that of plantar skin callus. However, the values for tan delta between 0.1 and 0.3992Hz are less than that seen in plantar skin callus indicating this tissue does not exhibit the same marked elastic response upon deformation, although a transition similar to that for plantar callus, to a more viscous response to deformation, occurs at higher applied frequencies (between 0.3992 and 2.519).

The coefficient of variation for the three runs of all samples is large (table 5.6.1). There is, generally, no significant difference (t-test) in values for each of the four sample frequencies between the first and third runs (table 5.6.2) suggesting that dehydration probably did not occur during the testing. Three sets of data were discarded as irregularities in data obtained suggested the sample slipped during testing. These samples appeared slightly domed in profile and would therefore not contact the rheometer plates adequately.

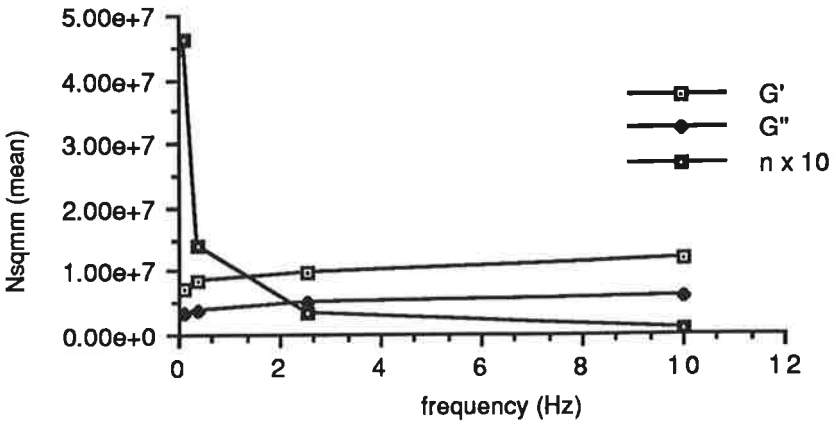

Figure 5.6.2.1
Plot of G', G" and η indicating change in plantar callus viscoelastic properties with variation in sinusoidal frequency.
η = poise

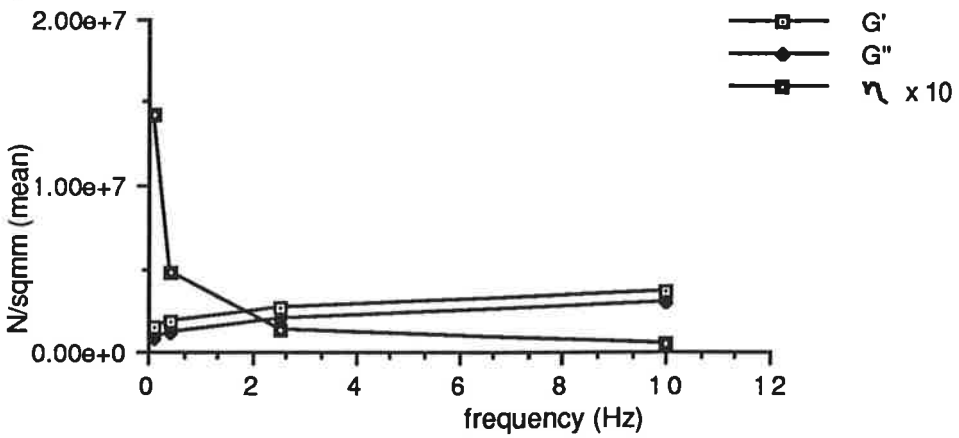

Figure 5.6.2.2
Plot of normal plantar skin change in viscoelastic behaviour with change in sinusoidal frequency (n = 1).

Frequency (n = 21)	Mean (N/mm^2)	SD	Range	Coefficient of Variation (%)
G' run 1 0.1 Hz	5.82^{06}	9.56^{06}	3.91^{05}-3.48^{07}	164.19
G' run 2	8.13^{06}	1.57^{07}	1.49^{05}-6.8^{07}	193.86
G' run 3	7.57^{06}	1.5^{07}	3.13^{05}-6.68^{07}	198.91
G' run 1 0.3992 Hz	8.23^{06}	1.5^{07}	1.07^{05}-6.21^{07}	182.38
G' run 2	8.89^{06}	1.76^{07}	1.06^{05}-7.75^{07}	198.43
G' run 3	7.89^{06}	1.55^{07}	3.54^{05}-6.87^{07}	197.28
G' run 1 2.519 Hz	1.1^{07}	2.19^{07}	2.02^{05}-9.7^{07}	198.37
G' run 2	1.03^{07}	2.09^{07}	3.89^{05}-9.36^{07}	448.64
G' run 3	8.58^{06}	1.71^{07}	3.11^{05}-7.62^{07}	199.42
G' run 1 10.00Hz	7.7^{07}	1.09^{07}	2.5^{05}-4.33^{07}	211.64
G' run 2	1.21^{07}	2.5^{07}	4.54^{05}-1.13^{07}	206.27
G' run 3	1.03^{07}	2.05^{07}	3.51^{05}-9.05^{07}	197.75
G" run 1 0.1Hz	2.94^{06}	5.79^{06}	1.59^{05}-2.6^{07}	196.57
G" run 2	3.25^{07}	7.09^{06}	1.45^{05}-3.27^{07}	217.79
G" run 3	3.4^{06}	7.41^{06}	1.21^{05}-3.4^{07}	217.70
G" run 1 0.3992Hz	3.61^{06}	7.46^{06}	1.5^{05}-3.39^{07}	206.41
G" run 2	3.84^{06}	8.79^{05}	1.38^{05}-4.06^{07}	228.47
G" run 3	3.84^{06}	8.63^{06}	1.4^{05}-3.98^{07}	222.36
G" run 1 2.519Hz	4.79^{06}	1.16^{07}	1.57^{05}-5.38^{07}	241.85
G" run 2	5.05^{06}	1.2^{07}	1.66^{05}-5.6^{07}	239.16
G" run 3	4.99^{06}	1.12^{07}	1.28^{05}-5.09^{07}	226.62
G" run 1 10Hz	6.08^{06}	1.51^{07}	1.08^{05}-7.04^{07}	249.14
G" run 2	6.21^{06}	1.54^{07}	1.78^{05}-7.18^{07}	248.75
G" run 3	6.02^{06}	1.41^{07}	1.53^{05}-6.45^{07}	235.60

Table 5.6.1 Values obtained when investigating plantar callus viscoelasticity using the Rheometrics Mechanical Spectrometer were sampled at four frequencies (0.1, 0.3992, 2.519 and 10Hz). The coefficient of variation for these values is given.

(n = 21)		t	p
G' run 1:run 3	0.1 Hz	1.128	0.136
G' run 1:run 3	0.3992 Hz	0.56	0.28
G' run 1:run 3	2.519 Hz	2.21	0.0193
G' run 1:run 3	10 Hz	1.79	0.0445
G" run 1:run 3	0.1 Hz	0.9119	0.1863
G" run 1:run 3	0.3992 Hz	0.515	0.3058
G" run 1:run 3	2.519 Hz	0.131	0.4486
G" run 1:run 3	10 Hz	0.7187	0.24

Table 5.6.2 Statistical analysis (paired t-test) of values obtained using the Rheometrics Dynamic Spectrometer when investigating plantar skin callus viscoelasticity. Data sampling at four frequencies has been made in each of the first, second and third runs for G' and G".

(n = 11)		Mean (N/mm^2)	SD	Range	Coefficient of Variation (%)
G' run 1	0.1 Hz	8.54^{06}	6.62^{06}	4.26^{05}-3.25^{06}	77.5
G' run 2		7.71^{06}	4.39^{06}	9.32^{05}-4.5^{07}	56.97
G' run 3		7.69^{06}	4.4^{06}	8.54^{05}-1.38^{07}	58.43
G' run 1	0.3992 Hz	1.24^{07}	9.37^{07}	8.26^{05}-4.61^{07}	75.4
G' run 2		9.11^{06}	5.08^{06}	1.13^{06}-1.66^{07}	55.74
G' run 3		8.46^{06}	5.09^{06}	9.3^{05}-1.63^{07}	60.23
G' run 1	2.519 Hz	1.63^{07}	1.11^{07}	1.4^{06}-4.8^{07}	68.35
G' run 2		1.1^{07}	6.35^{06}	1.41^{06}-2.11^{07}	57.53
G' run 3		1.03^{07}	6.11^{06}	1.07^{06}-2.06^{07}	58.91
G' run 1	10.00Hz	2.04^{07}	1.42^{07}	1.83^{06}-6.95^{07}	69.66
G' run 2		1.35^{07}	7.79^{06}	1.78^{06}-2.65^{07}	57.65
G' run 3		1.21^{07}	7.81^{06}	1.3^{06}-2.58^{07}	64.2

Table 5.6.3a Values for stored, frozen callus samples, hydrated at RH 91% for 48 hours, 25°C. Values for G' are given.

(n = 11)	Mean (N/mm^2)	SD	Range	Coefficient of Variation (%)
G" run 1 0.1Hz	4.56^{06}	3.48^{06}	2.65^{05}-1.58^{07}	76.27
G" run 2	3.66^{06}	2.080^{06}	4.94^{05}-7.22^{06}	56.8
G" run 3	3.92^{06}	2.29^{06}	5.7^{05}-7.73^{06}	58.59
G" run 1 0.3992Hz	6.56^{06}	4.91^{06}	4.04^{05}-2.47^{07}	74.89
G" run 2	4.57^{06}	2.79^{06}	6.26^{05}-9.39^{06}	60.93
G" run 3	4.63^{06}	2.86^{06}	7.33^{05}-9.75^{06}	60.56
G" run 1 2.519Hz	9.16^{06}	6.28^{06}	8.27^{05}-3.12^{07}	68.57
G" run 2	6.18^{06}	3.78^{06}	1.16^{06}-1.31^{07}	61.2
G" run 3	5.92^{06}	3.83^{06}	9.75^{05}-1.31^{07}	64.75
G" run 1 10Hz	1.13^{07}	7.22^{06}	1.22^{06}-3.44^{07}	63.3
G" run 2	7.73^{06}	4.84^{06}	1.49^{06}-1.68^{07}	62.62
G" run 3	7.4^{06}	4.98^{06}	1.28^{06}-1.68^{07}	67.35

Table 5.6.3b Values for stored, frozen callus samples, hydrated at RH 91% for 48 hours, 25°C. Values for G" are given.

(n = 11)	F	p
G' runs 1,2,3 0.1 Hz	0.137	0.9832
G' runs 1,2,3 0.3992 Hz	0.027	0.9997
G' runs 1,2,3 2.519 Hz	0.705	0.621
G' runs 1,2,3 10 Hz	0.059	0.9977
G" runs 1,2,3 0.1 Hz	0.083	0.9948
G" runs 1,2,3 0.3992 Hz	0.057	0.997
G" runs 1,2,3 2.519 Hz	0.047	0.9986
G" runs 1,2,3 10 Hz	0.05	0.9984

F alpha (0.05) between 2.37 and 2.29

Table 5.6.4. Comparison (ANOVA) of the means obtained of fresh and frozen, stored callus sample, both equilibriated at RH 91%, 25°C for 48 hours.

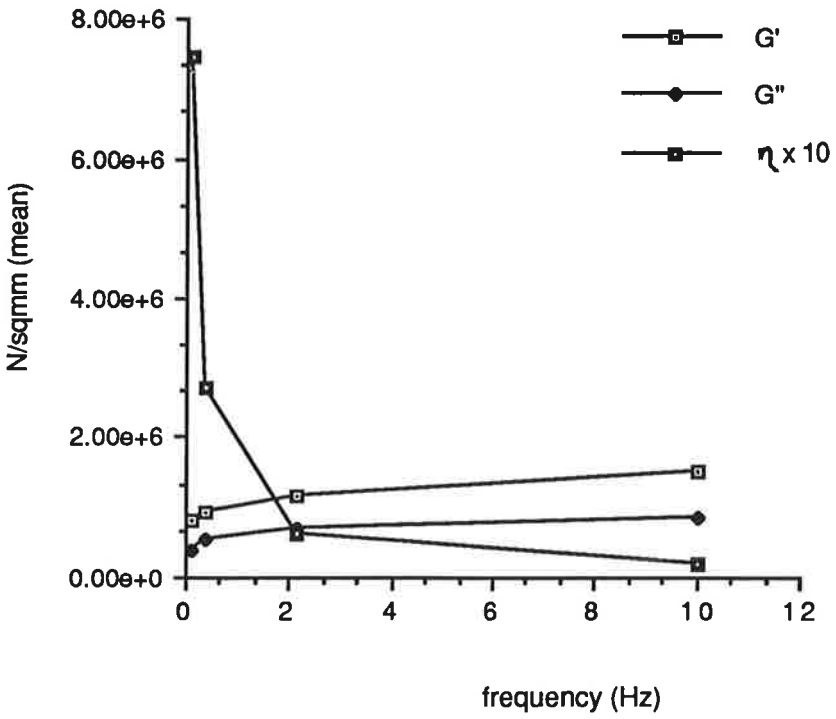

Figure 5.6.2.3
Plot of G', G" and η demonstrates the viscoelastic behaviour of stored, frozen callus sections which were equilibriated at RH 91% for 48 hours.
η = poise

Table 5.6.3 gives the coefficient of variation for frozen, stored callus samples, indicating again a wide range of values similar to that obtained with fresh samples hydrated to RH 91%. Figure 5.6.2.3 shows the change in viscoelastic behaviour of stored callus samples equilibriated at RH 91%, 25°C for 48 hours with increasing applied frequency. There was no significant difference (ANOVA) between the mean values of fresh and frozen, stored callus samples hydrated in RH 91% ($F_{alpha\ (0.05)}$ between 2.37 and 2.29) as shown in table 5.6.4.

5.6.3 Discussion

As expected (Vincent 1982), plantar skin callus exhibits viscoelastic behaviour. The response of the callus tissue following hydration at RH 91% shows an increase in elastic behaviour with increasing frequency. At RH 91% it is possible that differences in keratin bonding upon hydration is such that molecular chain slippage has already occurred and no further movement is possible (Laden and Morrow 1970, Ferguson 1980, Marriott 1992) allowing the callus samples used in the present study to demonstrate features of elasticity. Also, in plantar callus tissue, the quality of the lipid lamellae appears altered (Mackenzie 1983, Phillips 1992) so spacing between the polar head groups of the ceramide molecules of the intercellular lipid lamellae (Seddon 1990) and alteration in chain configuration (Potts 1991) with hydration may not occur as in normal skin, thus skin callus may retain its relatively stiff, semi-crystalline structure (Morris and Shamos 1967).

The large coefficient of variation in the results for callus samples (both fresh and stored) may be considered to demonstrate a wider range in morphology of biological tissues (Ferguson 1980, Wilkes et al 1973) than that expected with non-biological structures, particularly when a pathology is evident. In a pathological state, tissue structure cannot be expected to be consistent as

there can be a marked variation in structure and function from one pathology to another, *viz* malignancy. In plantar skin callus the status of keratinocyte maturity and cohesion, the level of development of the intercellular lipid lamellae (Phillips 1992) and water content (Christensen et al 1977, van Duzee 1978, Potts et al 1983) are all factors which may influence the viscoelastic behaviour of this tissue. The dimensions of skin tissue samples obtained precluded testing by other instruments such as those designed to test linear stress:strain relationships, all of which required larger skin sections either in area or longitudinal section (Duck 1990, Jemec et al 1986, Vogel 1988).

5.7 The viscoelasticity of plantar skin callus samples compared with their clinical appearance.

The morphology of callus, if intended as a protective mechanism, must be such that it can conform to its parent tissue, the viable epidermis, while transmitting applied external force evenly over a large surface area. The water gradient demonstrated to be present in skin (Bomannan et al, 1990) is likely to hydrate the lower layers of the stratum corneum so that it is pliable while the outer layers, being more crystalline (Morris and Shamos 1967) exhibit elastic characteristics. This composite tissue then functions as a viscoelastic material (Christensen et al 1977, Vincent 1982).

Although ordinary engineering theory is not really adequate to cope with the majority of problems in biomechanics (Gordon 1980), many of the principles may be applied. Application of force on a relatively stiff structure will transfer load laterally, and the supporting material tissue will be loaded evenly (Mackey and Chung 1969) (figures 5.7.1 and 5.7.2). Generally, it would appear that diffuse plantar callus of uniform thickness (seen in barefoot races) fulfils this function and only at the periphery of this load-bearing

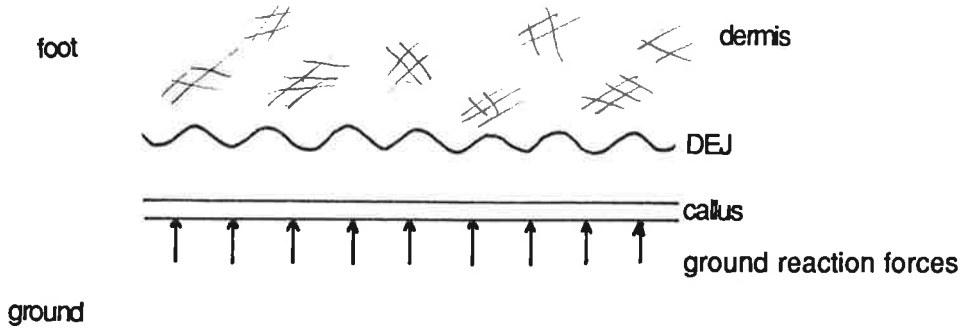

Figure 5.7.1
Loading (N) of a large stiff structure supported by a soft material/tissue results in even transmission of load.

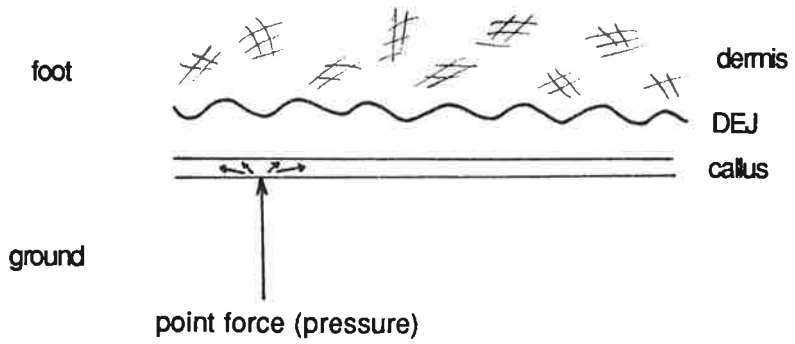

Figure 5.7.2
Point loading of a stiff structure transfers laterally, and subjacent structures take load evenly (Hooper 1984)

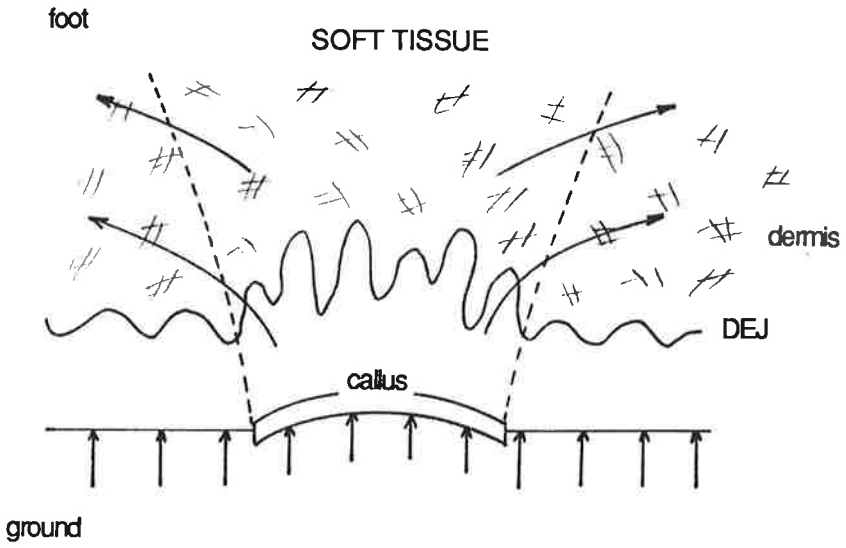

Figure 5.7.3
Variation one
Loading of a small semi-stiff structure which deforms under load is accompanied by deformation of underlying soft tissue (applied from Tomlinson 1986). The callus plaque may bow on loading due to the characteristics of the underlying tissue. As ground reaction forces cause the callus plaque to be indented into the tissue of the foot, so dermal and subcutaneous tissues are stressed in the direction of the arrows.

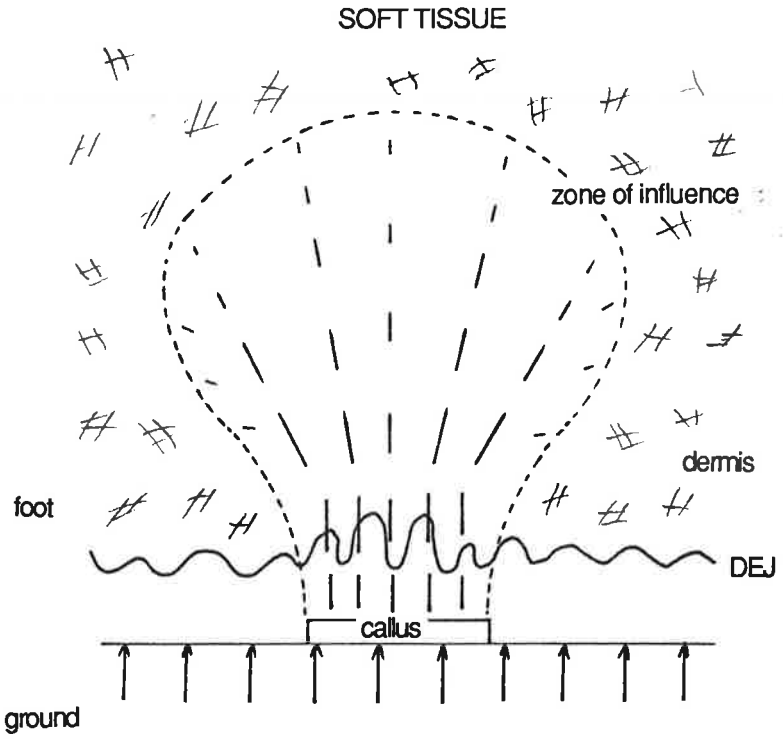

Figure 5.7.4
Variation two
Loading of a callus plaque which does not deform on loading. The bulk of the callus plaque indents into the foot tissues in response to ground reaction forces causing a zone of influence as indicated (applied from Mackay and Chung 1969, and Tomlinson 1986).

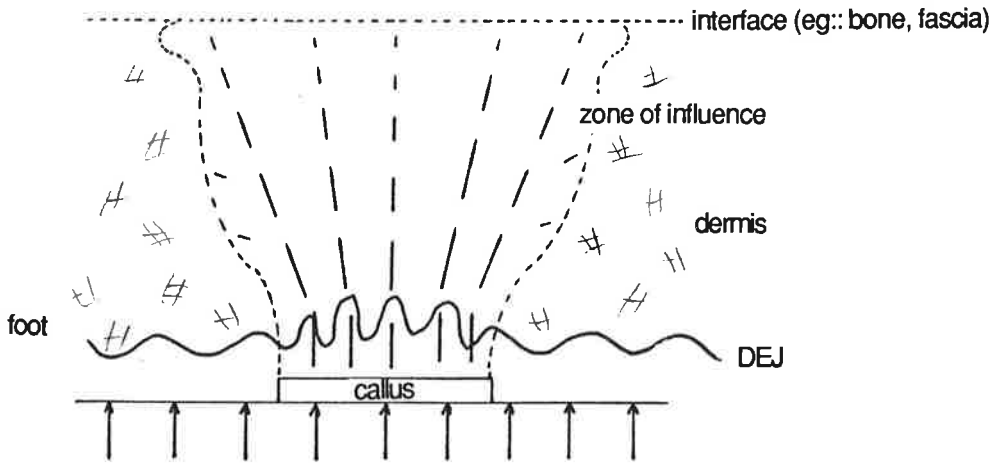

Figure 5.7.5

Loading of a callus plaque with the effect of an interface (eg: bone) shown (applied from Mackay and Chung 1969, and Tomlinson 1986)
Variation three

Figure 5.7.6
Salicylic acid plaster applied to this corn has hydrated the tissue surrounding the corn nucleus. The tissue surrounding the corn has flowed, with time, on application of mechanical stress leaving the corn standing proud.

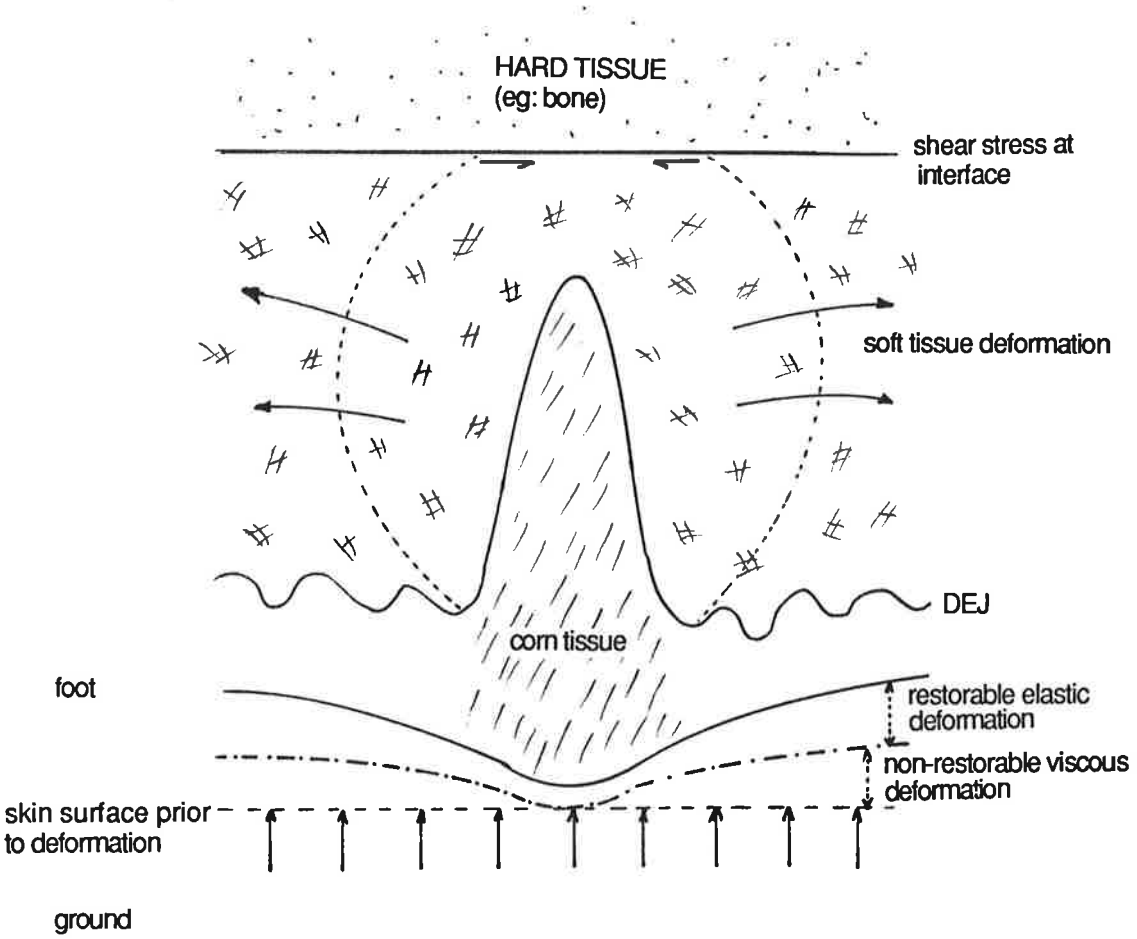

Figure 5.7.7
A stiff, elastic structure restores on release of load. A viscous tissue cannot restore to normal contours. Callus (and corn) tissue, although still viscoelastic, appears to demonstrate more elastic properties than normal plantar skin. The normal skin surrounding such a lesion may be relatively more viscous than callus or corn tissue and be able to flow on deformation (applied from Mackay and Chung 1969, and Tomlinson 1986). This feature can be seen clinically, particularly when the skin is hydrated having been occluded with a dressing.

structure does application of force during gait manifest, frequently as fissuring around the margins of the foot.

In pathological callus plaques about which patients complain, it would seem that this mechanism of load transfer via the small callus lesions merely succeeds in traumatising the skin and deeper structures (figures 5.7.3, 5.7.4 and 5.7.5). This concept is illustrated clinically in figure 5.7.6 where application of salicylic acid to a corn has hydrated surrounding skin which may have become viscous or plastic, allowing it to flow (figure 5.7.7), with time, on application of force. The corn tissue which hydrates to a lesser extent has remained a stiff, elastic structure resisting force, retaining its integrity.

The clinical appearance of a callus plaque has been thought, empirically, to indicate the predominance of a force vector acting on the foot during gait but results from the present work suggest this assumption appears to be simplistic. The biomechanics of callus stratum corneum will be investigated and then related to the clinical appearance of the lesion in the present work.

5.7.1 Method

As described previously (section 5.5), callus samples removed from each patient were hydrated at RH 91% for 48 hours at 25°C and their viscoelastic behaviour tested using the Rheometrics Dynamic Spectrometer. The large quantity of results obtained was reduced in the manner described in section 5.6.1.

Comparison was made first (ANOVA different sample sizes) of the viscoelastic behaviour of callus sections from each of the lesion types (accentuated, flattened, tortuous dermatoglyphics, or a combination of these characteristics). The viscoelastic profile of each callus sample and its clinical

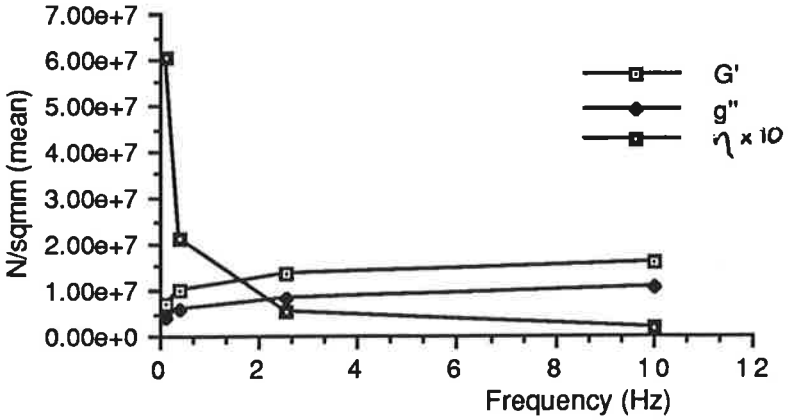

Figure 5.7.2.1
Plot illustrates the viscoelastic behaviour of callus samples removed from a callus lesion with accentuated dermatoglyphics.
η = poise

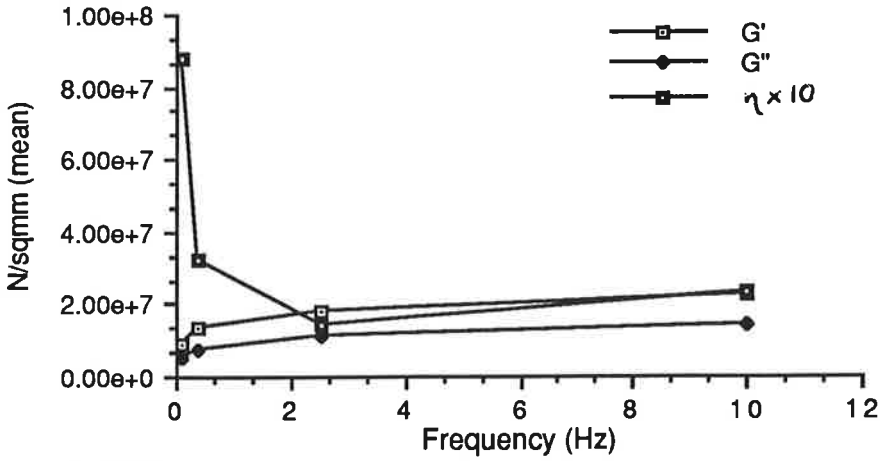

Figure 5.7.2.2
Plot illustrates the viscoelastic behaviour of callus samples removed from a callus lesion with flattened dermatoglyphics.
η = poise

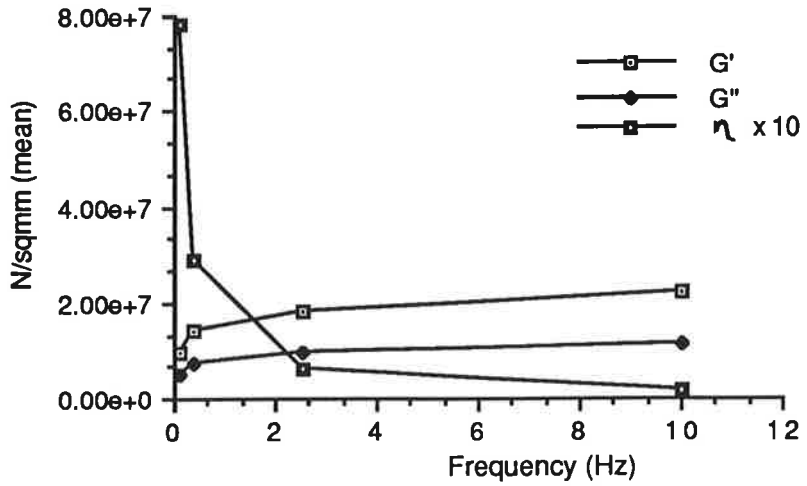

Figure 5.2.7.3
Plot to illustrate the viscoelastic behaviour of callus sections removed from a lesion with flattened, tortuous dermatoglyphics.
η = poise

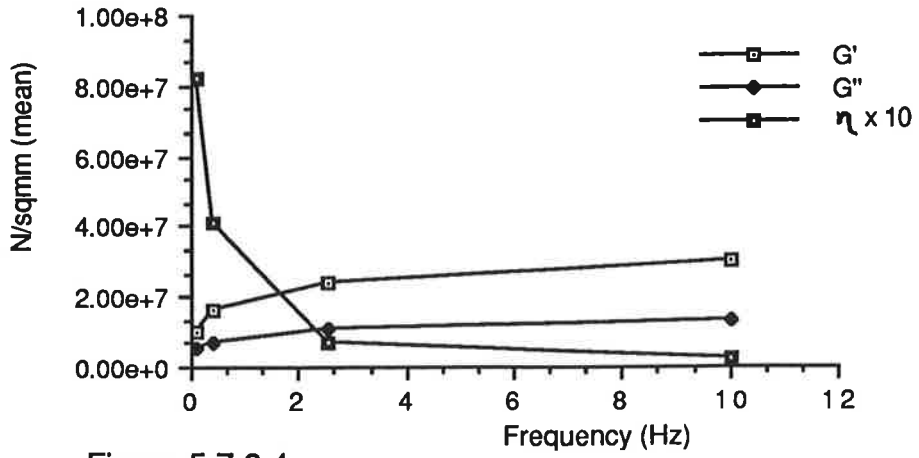

Figure 5.7.2.4
Plot to illustrate the viscoelastic behaviour of callus sections removed from a lesion with accentuated, flattened dermatoglyphics. η = poise

appearance was then related to the patient's locomotor pathomechanics which was collected when patients gait characteristics were investigated using the two linked force plates (Musgrave and Kistler).

5.7.2 Results

Results showed there is no significant difference (ANOVA different sample sizes) between any of the callus lesion types (table 5.7.2.1) (accentuated (n = 16), flattened (n = 6), flattened and tortuous (n = 8) or accentuated and flattened (n = 5) dermatoglyphics). It would appear therefore, that the viscoelastic behaviour of callus plaques with different dermatoglyphics is not significantly different. The mean coefficient of variation for all frozen, stored callus samples is large (64.65%).

Figures 5.7.2.1, 5.7.2.2, 5.7.2.3 and 5.7.2.4 illustrate the viscoelastic profile for callus plaques which show accentuated or flattened dermatoglyphics or a combination of these. The transition from a large to lesser tan delta value occurs within the same sample frequency band (0.3992 and 2.519Hz) for all callus sample types.

(n = 11)	Frequencies sampled	F	p
G'	0.1 Hz	0.451	0.718
	0.3992 Hz	0.63	0.601
	2.519 Hz	1.041	0.338
	10 Hz	1.251	0.308
G"	0.1 Hz	0.225	0.878
	0.3992 Hz	0.343	0.794
	2.519 Hz	0.497	0.686
	10 Hz	0.615	0.61

F alpha (0.05) = between 2.83 and 2.92

Table 5.7.2.1. ANOVA (different sample sizes) of the viscoelastic behaviour of all callus lesions with different clinical appearance (accentuated, tortuous, flattened (or a combination of these) dermatoglyphics).

5.7.3 Discussion

The results obtained do not provide any indication of viscoelastic behaviour being associated with callus lesion dermatoglyphics. LM histology indicates that there are parakeratotic areas within a callus plaque surrounded by orthokeratin implying variation in keratinocyte maturity may occur in callus plaques, (figure 3.12.2.3) , though it is difficult to equate these with the clinical, macroscopic appearance as histological section preparation distorts these features.

The differentials in viscoelastic properties of each of these small areas may cause invagination of epidermal tissue into the dermis (as proposed within this section) to different degrees giving rise to the clinical appearance of these lesions (figure 2.9.3.1). Ground reaction forces acting on tissue of different stiffness with varying load transfer capacities may cause stress to be distributed unevenly through to deeper structures resulting in contouring at tissue interfaces such as the DEJ (figure 5.7.3.1). This feature is clinically evident especially in corns (figure 5.7.6). Further conjecture in this direction as to the cause, of flattening, accentuation and convolution of the DEJ will be difficult to support without access to punch biopsy of callus tissue. A request for such an *in vivo* study is unlikely to be granted Ethical Committee approval and also suitable cadaver sections are not readily available.

Selection of dermatoglyphics as a method of callus lesion classification and indication of biomechanical behaviour does not appear, therefore, to be particularly helpful. Clinically appreciable textural differences may provide a better predictor of callus biomechanics and hence potential discomfort for the patient.

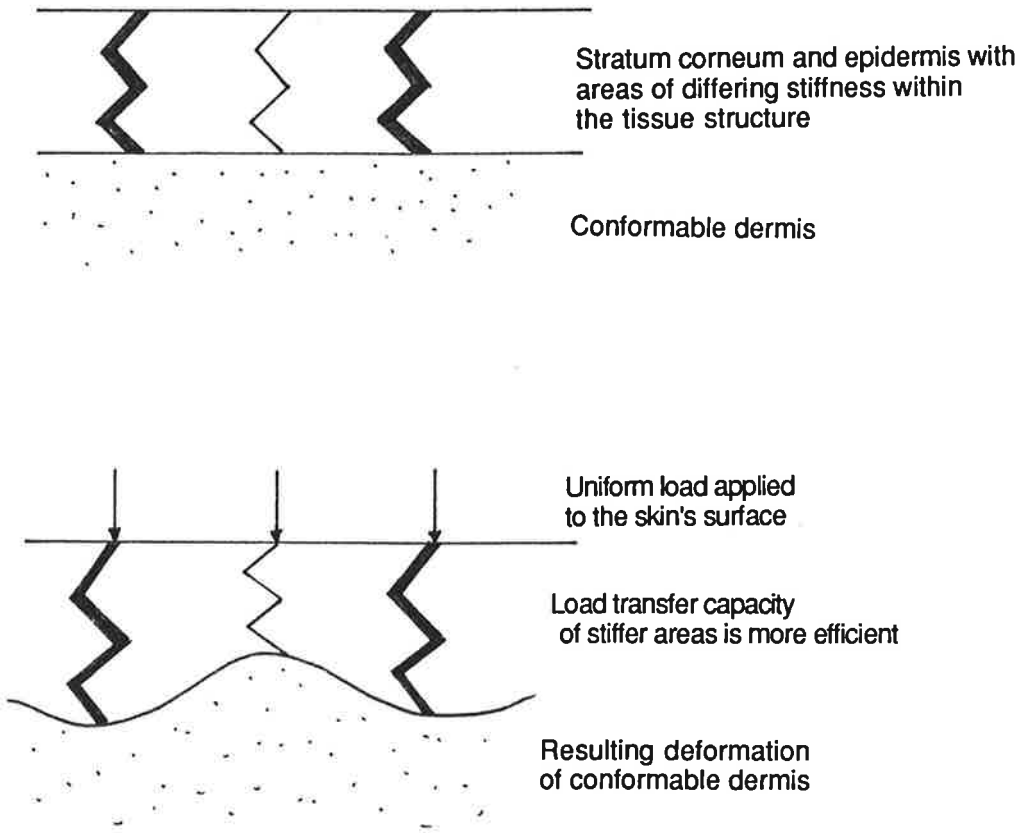

Figure 5.7.8
Diagram of transfer of a uniform load via a tissue which has differing stiffnes within its structure, onto a conformable tissue. This results in distortion of a flat interface. It is possible that the structure within a callus plaque may have this effect on the underlying dermis.

The variations in callus stratum corneum morphology may also affect deeper structures but the interplay between dermis, DEJ and epidermis is difficult to separate. However there is some evidence of plantar callus plaque influence on deeper structures. Abnormal formation of the lipid lamellae in callus (Mackenzie 1983, Phillips 1992) (figures 3.12.3.1 and 3.12.3.2) and their ability to hydrate may prevent intercellular dissipation of force and viscous flow of the tissue on application of force. Compression of the superficial blood plexus is evident clinically under a callus plaque in compromised skin tissues where dermal biomechanical characteristics are also altered, and ulceration is a common sequel (Adams et al 1989). Laser Doppler imaging (figures 2.9.2.2 and 2.9.2.3) of non-calibrated blood flux under a callus plaque before and after weight-bearing indicated changes in flow under the lesion compared with adjacent, normal plantar skin. It is probable that a hyperaemic response occurs subsequent to the transient ischaemia induced by the foot taking load. However, inter-subject variation and instrument over-sensitivity to slightly varying ambient conditions precludes a more definitive conclusion as yet.

It is probable that the complex interaction of all the soft tissues of the foot with the skeleton contribute to the features of these lesions.

It would be interesting to compare normal plantar skin biomechanics with plantar callus in a range of relative humidities, however, the current work was designed to indentify any relationship between plantar callus viscoelastic features with the clinical appearance of its source lesion.

5.8 Conclusions

Plantar skin callus exhibits viscoelasticity and there is no statistically significant variation in viscoelastic behaviour with the different callus lesion types, although there is a wide range in values which may be considered commensurate with a pathological tissue. Further studies are required to compare these results with those for normal plantar skin, as the current work was not designed to encompass these investigations within its remit.

It is probable that a combination of complex interaction with all soft and bony tissues gives rise to the different clinical appearances of these lesions. Structure variation within the callus plaque is likely to create differentials in response of this tissue to force leading to formation of the differences in DEJ dermatoglyphics. Further, in depth work into the epidermal causes of changes in dermatoglyphics is probably not of any great value and efforts should be directed towards elucidating the effect of dermal morphology on these lesions.

Classification of callus lesion by textural difference may be more helpful in predicting the lesion biomechanical behaviour and potential pathogenesis than observation of lesion dermatoglyphics.

CHATPER 6

Discussion of investigations undertaken within the scope of this thesis.

A number of areas of investigation, some novel, have been studied in the current work to study the aetiology and pathology of plantar callus, and their relationship to the clinical features of the lesion. A detailed interpretation and discussion of these investigations completed each chapter. This section will consider the main findings of the five fields of study in the current work, in relation to the formation of plantar callus plaques and their clinical characteristics. The five areas of investigation were:

- reactive forces exerted on the foot during gait
- A-scan ultrasound imaging of skin and the callus lesion
- LM histological scrutiny of callus tissue
- FTIR *in vivo* and *in vitro* of plantar skin callus tissue
- rheology of callus tissue *in vitro*

The findings of the studies undertaken in the current work have been synthesized and compiled into a proposed model for plantar callus formation (figure 6.1). The biochemistry of plantar callus tissue was not studied but a review of relevant papers permitted cogent inferences to be drawn on the likely influences of cytokines (Wright 1983, Camp et al 1990, MacKay and Leigh 1991) in callus formation, although the effects of the retinoids on cell differentiation were not considered.

It was proposed initially, that the dermatoglyphics of plantar skin calluses were likely to be indicative of the aetiological mechanical forces generated during gait (Adams et al 1989). Study of the forces exerted on the foot at the time of lesion loading showed that no prevalent

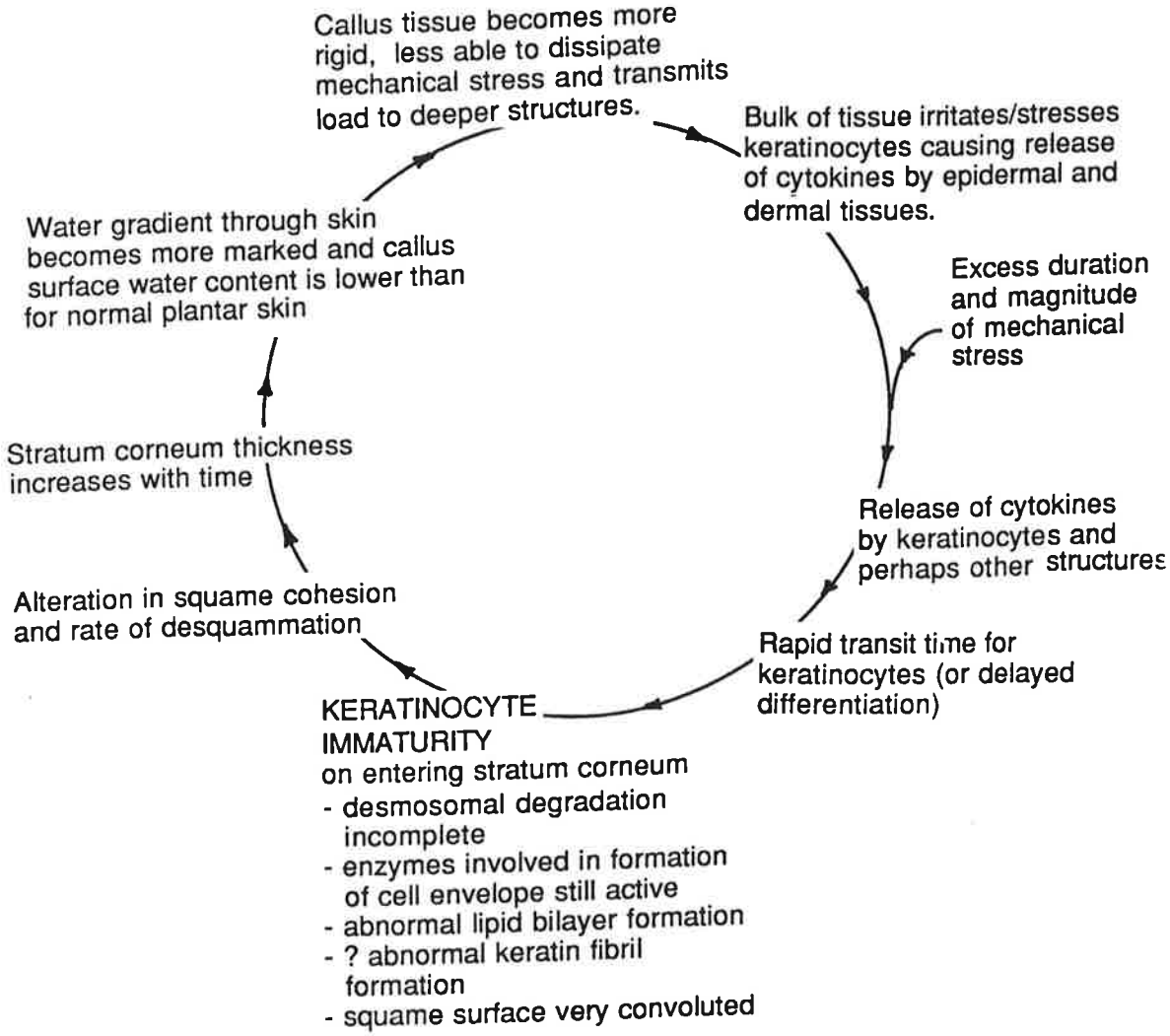

Figure 6.1
A proposed model for callus formation. (The role of retinoids and the influence of the dermis are not considered.)

reactive force vector was associated with any of the callus plaque dermatoglyphic variations (sections 2.7 and 2.8). However, data from the Musgrave pressure plate demonstrated that the lesion site was subjected to greater pressure than adjacent tissues and it should be recalled that the pressure measured by this instrument includes vertical forces as well as the vertical components of forces exerted on the foot in the other planes (for example shear stress has a vertical, as well as horizontal, component), although forces measured by the Kistler force plate can be resolved into the component planes.

Force plate results also showed that the duration of loading of the lesion site was significantly extended when compared with normal forefoot loading and it is likely that this factor contributes greatly to the effect of mechanical stresses acting at the lesion site. Preliminary investigations of blood flux (figures 2.9.3.2 and 2.9.3.3) under the callus plaque show changes compared with normal plantar skin and further studies are required to demonstrate whether or not ischaemia occurs under the lesion, to quantify its duration, and to assess its influence on dermal and epidermal response to this form of trauma.

It was found that the Musgrave pressure plate and Kistler force measurement plate can be linked to provide novel information on foot loading characteristics at a particular time. However, future development of in-shoe force measurement instruments capable of recording 3D forces at any site should permit quantification of mechanical stresses at the lesion site. The successful development of such instruments may help to resolve the controversy that exists concerning the wide range in values for force and load measured under the metatarsal heads and lesions in the current work, and by other

workers using a variety of instruments (Miller and Stokes 1979, Gross and Bunch 1988, Cavenagh et al 1992).

Edwards et al (1986) reported the two main layers of the skin could be measured using ultrasound techniques and it was hoped that a 3D contour map of callus lesions could be created in the present work, so that the clinical characteristics of the lesion could be quantified. Unfortunately, as discussed in detail in section 3.10, A-scan ultrasound imaging of the callus lesion was not successful, probably due to the limited output power of the instrument used (DDD) rather than unsuitability of the technique in general.

US measurements made *in situ* of cadaver skin, epidermal and full skin thickness, were validated against histological measurement. Fluctuation was found in values obtained using these techniques and some variation in results were also found in comparison with those of other workers (Tan et al 1985). The reasons for the variation in measurements, and the results of the comparison of the DDD with another US skin imaging instrument (Dermascan C) have been discussed fully in chapter 3. US imaging of the skin will be of value to podiatric clinical practice, as it is in dermatology (Nessi et al 1991), for example when searching for foreign bodies embedded in the tissues, evaluating healing rates of ulcers (Rippon et al 1991) or assessing the regression of plantar warts. Further work using US skin imaging techniques in this manner could have potential rewards.

It has become evident, as the present work has progressed, that podiatric classification (Tollafield 1985) of callus lesions requires revision. It would be useful to have an elegant method by which the different callus lesions can be catalogued and classified. Although, US

imaging using the DDD has been shown to be unsatisfactory, preliminary attempts using an A-scan US instrument (Dermascan A) with a more powerful output than the DDD to measure plantar callus characteristics are encouraging. The assessment of the texture of the callus tissue on excision may also be a helpful method of differentiating between the various callus lesion types (section 5.7) although a quantifiable, clinical technique for this method of assessment is not readily available.

The histological features of plantar skin callus sections were similar to those reported by other workers (Thomas et al 1985). The interpretation of the histological features and comparison with the results of other studies of callus plaque epidermis, using both LM and EM (Mackenzie 1983, Phillips 1992), suggests that the process of differentiation is either delayed (Bernerd et al 1992) or the transit rate of keratinocytes through the epidermis is faster than normal (Dawber et al 1972, Thomas et al 1985). With either interpretation, the end product is the same, that is immature keratinocytes enter the stratum corneum of callus lesions, as demonstrated in section 3.12.3. The immature squames, it is proposed, will not have time to complete the process of keratinisation: the lipid bilayer will show anomalies (Mackenzie 1983, Phillips 1992) and cell cohesion characteristics will be altered from normal, desmosomal degradation will be insufficiently advanced (Lundstrom and Torbjorn 1990), and squame surface contours will be marked (Ferguson 1980). All these anomalies may lead to reduced desquammation and formation of the hyperkeratotic plaque seen in callus. Other hyperkeratoses (ichthyosis and psoriasis) exhibit some of these features (Graham-Brown and Burns 1990).

It is difficult to speculate whether the clinically appreciable textural and histological differences between corns and callus suggest a more fundamental variant other than callus being merely a step along the route to becoming a corn. However, the histological appearance of callus sections which clinically had the potential to become a corn, showed a grossly disrupted granular layer and parakeratotic areas in the stratum corneum, confirming Mackenzie's (1983) comment that there appeared to be a sequential development of these lesions. LM studies using H and E staining cannot solve this problem, and biochemical and EM analysis would be a logical means of extending the present work.

The present work was not designed to investigate the biochemical pathway by which an increased duration and excess mechanical stress during gait stimulates keratinocyte proliferation and speeds the transit rate of cells through the epidermis. It is likely, however, that as the stratum corneum can no longer be considered an inert structure (Leveque et al 1992), the keratinocytes of the stratum compactum will release cytokines (Camp et al 1990) in response to trauma. Thus the cell proliferation cycle will be stimulated. In callus and corns, the keratinocytes entering the stratum corneum can be considered to be immature, as demonstrated in part by the presence (in corns and sometimes in callus) of parakeratosis. It is possible that these immature squames may be more metabolically active than their normal counterparts and are capable of responding to trauma by marked release of cytokines. Hence there follows an enhanced cell proliferation which is not matched by desquammation as cell cohesion is altered in these immature cells, consequently a callus plaque develops. There is no evidence from the LM histology sections of inflammatory infiltrate in the dermis of these lesions (Thomas et al 1985, Marks 1992) although

on excision, there was a definite fibrosing of tissue in these chronic lesions.

As the bulk of hyperkeratinised tissue of a callus plaque develops so the water gradient (Bomannan et al 1990) will become greater and the surface of the callus drier when compared with normal plantar skin. This characteristic was demonstrated using FTIR *in vivo* and *in vitro*. Contact of the callus tissue with the internal reflectance element was difficult owing to the dry nature of these samples and the rapid rate of dehydration on removal from the controlled environment (section 4.7). Considerable time was spent identifying the optimum method for this investigation.

The rate of dehydration for both normal plantar skin stratum corneum and callus samples was shown to be similar. It is difficult to speculate over the relationship between the different forms of water of hydration, the proposed immature status of the lipid bilayers in callus tissue, and the enclosing influence of footwear. Further studies (which it was not possible to include in this study) would have to be carried out in a carefully controlled environment to ascertain dehydration rates of normal and callused plantar skin in relation to all these variables. Such studies would generate interesting information, providing indirect evidence of the presence and quality of the lipid bilayers, though it is unlikely this would be particularly helpful in developing rational management regimes for calluses.

The relatively fast transit time of squames through plantar callus may mean the cells have not matured sufficiently to produce the strong covalent bonds between the ceramide molecules of the lipid bilayers and cell envelope (Wertz and Downing 1989, Haftek et al 1992).

Hydration gradients imposed on tissue of this immaturity may result in mechanical weakness between layers. The zone of greatest mechanical weakness is theoretically (Vincent 1984) likely to be the stratum compactum region as demonstrated by blister (mechanical aetiology) formation (Elias and Fritsch 1983) and the artifactual splitting of histologically prepared samples. It is possible that this is the mode by which salicylic acid paste BP cleaves hyperkeratotic tissue from the remainder of the epidermis but this hypothesis requires confirmation.

The water content of stratum corneum affects its barrier properties as well as its viscoelastic behaviour (Blank 1952, Potts et al 1985, Jemec et al 1986) and callus is, clinically, appreciably drier and stiffer than normal plantar skin. In the present work, when the gait of patients suffering with plantar calluses was recorded with the Kistler and Musgrave plates, callus samples were removed from these patients at that time and stored for later study. Prior to investigation of the viscoelastic behaviour of these samples, a relative humidity of 91% was selected, supported by appropriate FTIR studies (section 4.7), to equilibriate these plantar skin callus samples.

The viscoelastic properties of callus samples were measured using a dynamic oscillatory technique (Scott Blair 1974, Vincent 1984). All callus samples demonstrated an increase in elastic behaviour with increasing frequency. The coefficient of variation in values obtained for both fresh and stored, frozen callus samples equilibriated in RH 91%, 25^{0}C for 48 hours was large (section 5.6.2), which probably reflects its pathological state when inconsistency of formation is likely. LM histology demonstrated some variation in structure of callus epidermis and this may also help to explain the range of values in viscoelasticity reported in the current work.

Callus tissue morphology, its maturity and hydration will affect its viscoelastic behaviour (Christensen et al 1977, Ferguson 1980, Leveque and Rasseneur 1988). It is likely that the callus dermatoglyphics, may result from variation in viscoelastic behaviour within the callus plaque and thence, indirectly represent the maturity of its squames. Thus the stiffer, clinically more dense and glassy callus lesions may contain squames which are less mature than those lesions which are clinically softer. This may be due to the proposed limited presence and immature status of the lipid bilayers in callus tissue (Mackenzie 1983, Phillips 1992), and as discussed previously (and in detail in chapters 4 and 5), the water content of skin and its pliability depends greatly upon the presence of these structures.

As noted previously, it has become evident that current podiatric classification of callus lesions is inadequate. Development of a less ambiguous classification system for the different callus lesion types would be helpful in research and clinically. The current work suggests that the clinical textural stiffness of each lesion may provide an indication of the viscoelastic behaviour which in turn may provides an indirect indication of the maturity of the callus squames. To support this hypothesis, it would be necessary to pursue histological and rheological studies of both glassy and clinically soft callus lesions, to associate the tissue structure of each lesion type with its viscoelastic behaviour. This may represent a more suitable method of lesion classification than exists at present and permit a clinical estimation of the lesion severity and its prognosis. Further studies comparing normal plantar skin viscoelastic response to the application of mechanical stress with that of callus tissue may provide an insight into the load bearing and transfer capacity of callus tissue. The current work suggests theoretical response of skin

using some mechanical engineering concepts, while acknowledging that engineering theory is not really adequate to deal with the complexities of biological structures (Gordon 1980).

The stiff, dry nature of calluses and adjacent more viscous normal plantar skin will, it is proposed, interact such that the dermis will deform as described in detail in section 5.7. If the superficial structures of the skin are not pliable enough to conform to mechanical trauma and then restore to normal configuration, then the effects of this mechanical stress must be accommodated in other tissues. The transmission of mechanical force to adjacent and deeper structures, rather than dissipation of stress and by the structures of the stratum corneum may provide an explanation for some of the clinically notable symptoms patients exhibit with stiff plantar calluses, such as peri-lesion stinging or pain. Dermal morphology will influence epidermal biomechanics (Wood and Bladon 1986, Potts and Breuer 1981), and further studies, possibly using models, should elucidate this relationship in the pathology of plantar callus.

A number of points exist in the proposed cycle of callus formation (figure 6.1) where podiatric management may intervene. Development of topical drugs, which influence the release and effect of cytokines, may be helpful to the clinician in preventing the alteration in keratinisation which appears to occur in corns and calluses. The effect of therapeutic modalities, such as low level laser therapy (LLLT), on these lesions should be investigated. It is thought that cellular activity and the sequence of cellular events is maximised by the effect of LLLT (Dyson 1992). Thus, the duration of events which lead to formation of hyperkeratotic tissue may possibly be reduced. The duration of release of cytokines may be reduced and stimulus for the slight hyperplasia and

rapid keratinocyte transit time through the epidermis (Thomas et al 1985) subsequently similarly reduced, so that it takes longer for a callus lesion to develop.

The pliability of callus tissue in relation to its water content has been discussed in chapter 5. Restoration of a level of hydration similar to that of normal plantar skin may alter callus tissue biomechanics so that the lesion becomes more pliable and less uncomfortable for the patient. The podiatrist may be able to achieve this result by application of suitable dressings, such as the hydrocolloid wafers used in wounds. A further area of study is that of removal of the bulk of callus tissue which the podiatrist achieves using a scalpel, in such a way that trauma is minimal, although some keratinocytes must be damaged by the cutting blade. The optimum frequency of removal of this tissue is not known and frequent operating in this manner may be sufficient to cause traumatised keratinocytes to release cytokines, thus perpetuating the formation in this manner. Further study is required to ascertain the importance of this possibility.

CONCLUSION

The dermatoglyphics of plantar calluses do not appear related to a prevalent aetiological force vector when measured using the Musgrave and Kistler plates linked together.

Increased duration of loading of the forefoot and lesion site occurs in those suffering with plantar forefoot calluses.

Callus tissue is drier than normal plantar skin which will cause it to be stiffer and on loading will indent into the more viscous surrounding normal tissue. Alternatively if the stiff callus tissue rests on a firm base (bone), then on application of mechanical stresses, the more viscous adjacent normal tissue will flow, with time, whilst the callus or corn will retain its integrity and stand proud of the skin's surface.

The transit rate for callus keratinocytes is likely to be faster than normal leading to immature squames entering the stratum corneum, which are then unable to fulfil many of the normal epidermal functions, such as desquammation, at a rate commensurate with cell proliferation.

GLOSSARY OF TERMS

3D	three dimensional (forces)
A-scan	ultrasound amplitude scan attenuation of ultrasound, scatter, refraction and reflection
B-scan	ultrasound brightness scan
biorheometry	study of flow behaviour
cadence	walking rhythm + speed
callus	thickened, yellow, non-pliable skin tissue found most frequently on the plantar surface of the foot
corneocyte	see keratinocyte
DDD	Dermal depth detector
DEJ	Dermo-epidermal junction
Dermascan	ultrasound skin imaging instrument
dermatoglyphics	skin ridge patterns (viz finger prints)
dressings	adhesive plaster, gauze, or similar item applied to the skin's surface
FTIR	Fourier Transform infrared spectrophotometry
full skin	dermis and epidermis
gait	normal walking
H and E	haematoxylin and eosin histological staining dye
histometric	measurements made using histological techniques
hyperkeratoses	term includes calluses/callosities, and other hyperproliferative skin disorders including ichthyosis, and psoriasis
IR	infrared
keratinocyte	the epidermal cell which undergoes the process of keratinisation to form the skin barrier
Kistler	Kistler force plate utilises piezoelectic transducers to measure forces in three dimensions and moment
laterality	right:left handedness/footedness and influence of dominant side
LLLT	low level laser therapy

macerate	soggy, white appearance of the skin's surface which maceration develops when it is covered for a few days or more
MCG	membrane coating granules/cementasomes in stratum granulosum of the epidermis
mpj	metatarso-phalangeal joint
Musgrave	Musgrave force plate utilises pressure sensitive transducers
orthokeratin	normal keratinised stratum corneum
parakeratosis	seen in histological sections where keratinocytes of the stratum corneum can be seen under LM to have cell nuclear remnants.
pathomechanics	the study of pathological locomotor biomechanics
PVDF	polyvinylidine fluoride - piezo electric material frequently used in transducers
RH	relative humidity
SEM	scanning electron microscopy
SI units	systeme internationale
squames	the flattened, differentiated keratinocytes seen on the skin's surface
TEM	transmission electron microscopy
TEWL	transepidermal water loss
US	ultrasound

LIST OF TABLES

3.10.4 Direct (light microscopy) and US measurements (DDD and Dermascan C) of epidermal and full skin thickness of samples from different body sites, measured in millimeters. Body sites measured - anterior thigh, outer and inner forearm, abdomen, calf, dorsal foot, normal plantar and forefoot callused skin and corn.

3.12.1 Thickness measurements of the epidermis of normal plantar skin, callus, one plantar and one dorsal corn. Mean of 10 measurements taken at 10μm intervals along the histology section for each tissue.

3.12.2 Count of basal cells along a 2 μm length of basal layer for each skin type studied (x40).

4.7.2.1 Calculated FTIR absorbence ratios of area under $2100cm^{-1}$ curve to baseline area of callus sections equilibriated at (a) RH 100% and $30^{o}C$, and (b) RH 55% and $24^{o}C$.

4.7.2.2 Calculated values for normal and callus section FTIR spectra, ratio of area under $2100cm^{-1}$ curve to baseline area of callus sections on exposure to RH 55% and $24^{o}C$, when dehydration of tissue occurs.

4.7.2.3 Calculated FTIR absorbence ratios of area under $2100cm^{-1}$ curve to baseline area of callus sections hydrated at RH 84% and $30^{o}C$.

4.7.2.4 Calculated absorbence ratios of area under the curve of the $2100cm^{-1}$ peak to baseline area of the FTIR spectra for callus samples equilibriated at RH 91% and $30^{o}C$.

4.7.2.5 Calculated absorbence ratios of area under the $2100cm^{-1}$ curve and baseline area of large, divided callus samples hydrated at RH 84% and 91% at $30^{o}C$.

5.6.1 Values obtained when investigating plantar callus viscoelasticity using the Rheometrics Mechanical Spectrometer were sampled at four frequencies (0.1, 0.3992, 2.519 and 10Hz). The coefficient of variation for these values is given.

5.6.2 Statistical analysis (paired t-test) of values obtained using the Rheometric Dynamic Spectrometer when investigating plantar skin callus viscoelasticity. Data sampling at four frequencies has been made in each of the first, second and third runs for G' and G".

5.6.3 Coefficient of variation in values for stored, frozen callus samples, hydrated at RH 91% for 48 hours, $25^{o}C$. Values for G' and G" are given.

5.6.4 Comparison (ANOVA) of the means obtained of fresh and frozen, stored callus samples, both equilibriated at RH 91%, $25^{o}C$ for 48 hours.

5.7.2.1 ANOVA (different sample sizes) of the viscoelastic behaviour of all callus lesions with different clinical appearance (accentuated, tortuous, flattened (or a combination of these) dermatoglyphics).

List of Figures

Figure 5.7.7 A stiff, elastic structure restores on release of load. A viscous tissue cannot restore to normal contours. Callus (and corn) tissue, although still viscoelastic, appears to demonstrate more elastic properties than normal plantar skin. The normal skin surrounding such a lesion may be relatively more viscous than callus or corn tissue and be able to flow on deformation. This feature can be seen clinically, particularly when the skin is hydrated having been occluded with a dressing.

Figure 5.7.2.1 Plot illustrates the viscoelastic behaviour of callus samples removed from lesions with accentuated dermatoglyphics.

Figure 5.7.2.2 Plot illustrates the viscoelastic behaviour of callus samples removed from lesions with flattened dermatoglyphics.

Figure 5.7.2.3 Plot to illustrate the viscoelastic behaviour of callus samples removed from lesions with flattened and tortuous dermatoglyphics.

Figure 5.7.2.4 Plot to illustrate the viscoelastic behaviour of callus samples removed from lesions with accentuated and flattened dermatoglyphics.

Figure 5.7.8 Diagram of transfer of a uniform load via a tissue which has differing stiffness within its structure, onto a conformable tissue. This results in distortion of a flat interface. It is possible that the structure within a callus plaque may have this effect on the underlying dermis.

Figure 6.1 A proposed model for callus formation. (The role of retinoids and the influence of the dermis are not considered.)

Appendix 1
(section 2.8.2)
(figures 2.8.2.4/5/6/7)
Reactive force vectors and moment resultant recorded under the forefoot of patients and normal subjects at 0, 20, 40, 60, 80, and 100% of forefoot contact time. (L = left foot, R = right foot, Mr = moment resultant)

Foot and force vector measured	Patients			Normal subjects		
	Mean	SD	Range	Mean	SD	Range
0% of fore-foot contact						
LFx	17.65	21.84	-38.57-48.4	26.22	9.6	14.65-34.9
LFy	51.48	32.79	-27.59-102.05	28.18	24.14	-4.39-57.37
LFz	566.18	121.89	235.84-710.94	492.87	93.69	437.99-659.67
LMr	42.96	24.61	10.07-110.07	28.1	10.8	15.94-36.6
RFx	-21.36	16.29	-46.88-17.5	-37.47	28.22	-101.32--10.74
RFy	38.38	41.27	-34.67-156.74	47.6	53.27	-0.98-152.1
RFz	585.96	113.23	314.45-730.47	583.59	141.2	423.34-840.82
RMr	80.65	144.517	0.54-684.2	37.77	25.36	16.52-72.23
20% of fore-foot contact						
LFx	22.58	13.85	-2.93-48.3	22.99	9.56	11.20-35.16
LFy	30.07	28.77	-31.98-71.53	-0.78	18.91	-27.10-20.51
LFz	585.58	93.02	312.5-719.24	49.27	38.53	416.02-514.16
LMr	32.02	16.99	4.14-66.62	27.19	16.44	10.64-43.53
RFx	-24.69	16.29	-49.9-14.4	-36.37	28.81	-107.18--6.59
RFy	12.04	28.19	-44.68-74.71	11.35	35.27	-27.83-84.23
RFz	579.12	97.98	362.79-761.72	539.64	95.82	418.95-696.29
RMr	40.11	16.57	10.74-71.53	32.5	6.56	27.66-41.86

Appendix 1 continued

Foot and force vector measured	Patients			Normal subjects		
	Mean	SD	Range	Mean	SD	Range
40% of fore-foot contact						
LFx	19.67	12.78	-5.13-41.75	23.24	9.33	13.92-33.69
LFy	-3.54	20.59	-54.20-22.71	-32.52	24.96	-63.48--1.46
LFz	581.59	86.38	393.55-686.04	486.13	43.55	427.25-524.9
LMr	29.92	16.43	2.89-59.79	30.94	14.23	16.86-45.31
RFx	-24.41	15.92	-52.73-9.03	-27.39	19.97	-68.85-0.0
RFy	-12.42	23.89	-72.75-40.28	-29.92	21.60	-78.37-2.69
RFz	596.75	98.62	421.88-826.66	578.07	128.20	434.57-812.5
RMr	28.96	10.84	3.6-51.03	34.19	7.88	26.1-44.51
60% of fore-foot contact						
LFx	16.08	12.29	-11.47-35.4	26.07	13.23	5.86-38.09
LFy	-46.74	24.32	-92.29-28.56	-73.73	28.46	-96.68--27.83
LFz	593.87	80.76	465.33-763.18	531.54	60.87	456.05-601.07
LMr	26.08	13.70	4.63-54.05	33.40	7.91	25.17-40.96
RFx	-26.62	19.08	-61.52-18.55	-28.40	22.45	-73.73-0.98
RFy	-55.27	25.07	-110.84--20.75	-87.64	31.97	-144.29--44.19
RFz	638.93	113.85	435.06-885.25	620.28	100.68	482.19-750.98
RMr	27.25	10.07	4.28-48.06	36.36	9.59	26.53-49.32
80% of fore-foot contact						
LFx	16.75	17.39	-17.58-41.99	19.14	14.64	4.15-39.31
LFy	-108.67	21.59	-55.522--32.23	-102.53	37.59	-151.61--59.81
LFz	587.66	135.79	181.64-791.99	445.89	132.40	222.17-545.41
LMr	24.07	12.38	1.62-45.33	23.89	2.66	21.03-26.31
RFx	-21.53	17.97	-58.35-11.47	-26.82	24.21	-73.73-10.99
RFy	-104.41	32.12	-163.09--19.78	-151.15	56.88	-272.71--86.18
RFz	545.56	146..02	74.71-743.16	593.64	110.53	452.64-791.5
RMr	23.83	12.37	0.73-50.24	33.39	8.73	24.15-45.22

Appendix 1 continued

Foot and force vector measured	Patients			Normal subjects		
	Mean	SD	Range	Mean	SD	Range
100% of fore-foot contact						
LFx	-3.88	10.46	-33.94-15.14	-5.12	7.92	-14.65-2.44
LFy	-29.69	27.88	-91.8-4.64	-41.32	41.44	-96.68--0.49
LFz	102.22	80.63	9.28-290.53	115.11	93.81	7.81-227.54
LMr	3.54	3.27	0.00-13.36	5.35	6.87	0.49-10.21
RFx	-0.07	8.57	-16.11-18.8	3.58	8.68	-7.57-17.82
RFy	-20.27	30.94	-98.94-30.76	-52.11	37.47	-123.05--10.5
RFz	70.09	71.41	-18.55-234.38	145.34	91.06	17.58-320.31
RMr	2.16	1.85	0.00-6.27	12.79	5.71	5.72-17.84

Appendix 2
(section 2.9.2)
Forces exerted on the foot during the time of lesion loading, related to the clinical appearance of each callus type. (Mr = moment resultant).

		Dermatoglyphic patterns			
		(n = 14) Accentuated	(n = 14) Flattened	(n = 10) Accentuated + flattened	(n = 4) Flattened + tortuous
40% forefoot contact time Fx	Mean	14.85	23.0	30.3	28.75
	SD	13.02	13.2	10.85	5.5
	Range	-5-42	5-53	15-52	21-34
40% forefoot contact time Fy	Mean	-6.42	-22.28	11.8	26.5
	SD	19.2	22.95	14.3	9.81
	Range	-54-20	-73-13	-11-40	-35--18
40% forefoot contact time Fz	Mean	525.35	612.85	628.1	622.5
	SD	108.5	83.06	33.39	19.97
	Range	393-675	540-827	578-686	605-644
40% forefoot contact time Mr	Mean	23.85	28.92	31.4	43.75
	SD	16.19	10.01	10.4	14.9
	Range	3-59	8.51	10-48	27-60
60% forefoot contact time Fx	Mean	13.7	24	28.5	30.5
	SD	11.57	14.6	15.05	17.7
	Range	-11-35	2-56	8-62	8-47
60% forefoot contact time Fy	Mean	-47.5	-63.2	-17.8	-34.7
	SD	30.19	26.31	42.66	17.05
	Range	-92-41	-111--24	-61-57	-58--21
60% forefoot contact time Fz	Mean	588.92	641.85	620.2	601.75
	SD	120.51	100.6	65.2	92.33
	Range	435-763	533-885	498-694	467-671
60% forefoot contact time Mr	Mean	25.21	26.0	29.5	26.5
	SD	16.04	10.09	10.94	6.55
	Range	4-54	7-38	5-42	20-35

Appendix 2 continued		Accentuated	Flattened	Accentuated + flattened	Flattened + tortuous
80% forefoot contact time Fx	Mean	13.78	19.71	30.9	18.25
	SD	11.7	17.4	13.32	13.64
	Range	-5-39	-7-44	16-58	0-33
80% forefoot contact time Fy	Mean	-115.14	-105.71	-111.5	-67.5
	SD	26.56	36.1	12.84	25.06
	Range	-163--75	-154--20	-140--99	-91--32
80% forefoot contact time Fz	Mean	544.64	551.85	642	460.5
	SD	129.95	168.63	44.28	199.49
	Range	375-743	75-792	567-700	182-656
80% forefoot contact time Mr	Mean	23.85	21.85	30.8	14.25
	SD	12.98	9.96	12.88	2.75
	Range	5-46	1-36	2-50	11-17
100% forefoot contact time Fx	Mean	1.35	1.28	-1.5	2.5
	SD	9.8	6.7	15.1	2.38
	Range	-23-19	-10-15	-34-16	1-6
100% forefoot contact time Fy	Mean	-33.4	-26.07	-31.3	3.5
	SD	25.2	27.6	31.39	2.38
	Range	-92--3	-84-4	-99--4	0-5
100% forefoot contact time Fz	Mean	89.64	93.28	93.4	9.75
	SD	53.64	106.24	78.39	4.27
	Range	25-203	75-291	19-223	4-13
100% forefoot contact time Mr	Mean	2.28	3.07	3.8	1.5
	SD	1.77	3.02	3.64	0.57
	Range	0-6	0-11	1-13	1-2

REFERENCES

Abenhaim, L. and Suissa, S. (1987) Importance and economic burden of occupational back pain: a study of 2,500 cases presenting in Quebec. J. Occup. Med. 29. pp. 670-674.

Adams, I. Whiting, M. Savin, J. Branford, W. (1989) Skin and subcutaneous conditions. In: Adams, I. and Neale, D. eds. Common Foot Disorders. London, Churchill Livingstone. pp. 85-114.

Arcan, M. and Brull, M.A. (1976) A fundemental charateristic of the human body and foot, the foot - ground pressure pattern. J. Biomech. 9. pp. 453-457.

Armitage, P. (1980) Statistical methods in medical research. Oxford, Blackwell Scientific Publications.

Baker, M.R. Bader, D.L. Hopewell, J.W. (1988) An apparatus for the testing of the mechanical properties of skin in vivo: its application to the assessment of normal and irradiates pig skin. J. Bioeng. and skin vol 4. Milwaukee meeting pp. 87-103.

Bamber, J.C. and Hill, C.R. (1979) Propagation speed in mammalian tissue as a function of temperature. US. Med. Biol. 5 . pp. 149-157.

Bamber, J.C. Hill, C.R. King, J.A. Dunn, F. (1979) Ultrasound propagation through fixed and unfixed tissue. US. Med. and Biol. 5. pp. 159-165.

Bernerd, F. Magnaldo, T. Darman, M. (1992) Delayed onset of epidermal differentiation in psoriasis. J. Invest. Dermatol. 98. (6). pp. 902-910.

Bescancon, R. ed. (1985) Encyclopaedia of physics. NY, R van Norstrad Co Reinhold.

Betts, R.P. Frankes, C. Duckworth, T. Burke, J. (1980) Static and dynamic foot pressure measurement in clinical orthopaedics. Med. Biol. Eng. Comput vol 18 pp. 647-684

Blank, I. (1952) Factors which influence water content of stratum corneum. J. Invest. Dermatol. 18 pp. 433-408.

Bobbert, M. and Schamhardt, H. (1990) Accuracy of determining the point of force application with piezoelectic force plates. J. Biomech vol. 23. (7). pp. 705-710.

Bomannan, D. Potts, R.O. Guy, R.H. (1990) Examination of stratum corneum barrier function in vivo by infra red spectroscopy. J. Invest. Dermatol. 4 pp. 403-408.

Bransby-Zachary, M. Stother, I. Wilkinson, R. (1990) Peak pressure in the forefoot. J. Bone Joint Surg. (Br) 72B. pp. 718-721.

Buchholz, B. Frederick, L. Armstrong, T. (1988) An investigation of human palmar skin friction and the effects of materials, pinch force and moisture. Ergonomics. 31. (3) pp. 317-325.

Camp, R. (1991) Personal communication.

Camp, R. Fincham, M.J. Ross, R.J. (1990) Cytokines in skin lesions of psoriasis Cytokine. 2. (1). pp. 68-75.

Caputo, R. and Gasparini, G. (1985) Freeze fracture replication technique in studies of the skin. In: Methods in Skin Research eds Skerrow, D. and Skerrow,C.J. Chichester, John Wiley and Sons. pp. 37-70.

Cavenagh, P. Rodgers, M. Iibashi, A. (1987) Pressure distribution under symptom free feet during barefoot standing. Foot and Ankle 7 (5) pp. 262-276.

Cavenagh, P.J. Hewitt, F.G. Perry, J.E. (1992) In-shoe plantar pressure measurement: a review. The Foot 2 (4) pp. 185-194.

Cernacek, J. and Jagr, J. (1972) Posture, vision and motor dominance Aggressologies vol 13 C pp. 101-105.

Christensen, M.S. Hargen, C.W. Nacht, S. Gans, E.H. (1977) Viscoelastic properties of intact human skin: instrumentation, hydration effects and contribution of the stratum corneum. J. Invest Dermatol 69 (3) pp. 282-286.

Daly, C. and Odland, B. (1979) Age related changes in the mechanical properties of human skin. J. Invest Dermatol 73 (1) pp. 84-87.

Daly, C. and Wheeler, H. (1971) The use of ultrasound thickness measurement in clinical evaluation of soft tissue. Int. Dent. J. 21 pp. 418-419.

Davies, B.M. (1981) Community Health. Preventative Medicine and Social Services. London, Bailliere's Concise Medical Textbooks.

Davies, B.M. (1984) Community Health and Social Services. London, Hoddern and Stoughton.

Dawber, R. Marks, R. Swift, J.A. (1972) Scanning electron microscopy of the stratum corneum. Br. J. Dermatol. 86 pp. 272-281.

de Vita, P. and Bates, B. (1988) Intra-day reliability of ground reaction force data. Human Movement Science 7 (North Holland) pp. 73-85.

Dean John, A. ed (1985) Lange's Handbook of Chemistry 13th edition (New York), McGraw Hill Book Company.

Dines, K.A. Sheets, P.W. Brink, J.A.Hanke, C.W. Condra, K.A. Clendenon, J.L. Goss, S,A. Smith, D.J. Franklin, T.D. (1984) High frequency ultrasound imaging of the skin: experimental results US Imaging 6 pp. 408-434.

Duck, F.A. (1990) Acoustic values of tissues as ultrasonic frequencies in Physical Properties of Tissue London, Academic Press.

Duell, E. and Vorhees, J.J. (1983) Control of Epidermal Growth. In: Goldsmith, L. ed. Biochemistry and Physiology of the skin. New York, Oxford University Press pp. 241-268.

Dykes, P. (1992) Department of Dermatology, University of Wales, College of Medicine. Personal communication.

Dyson, M. (1992) Tissue Repair Research Unit, Guys Hospital. Personal communication.

Edwards, C. (1989) The acoustic properties of the epidermis and stratum corneum. In: Marks, R. Edwards, D. Barston, S.P. eds. the Physical Nature of Skin. Lancaster, MTP. pp. 201-208.

Edwards, C. Al Aboosi, M. Marks, R. (1986) Measurement of ultrasound propagation constants of the component layers of human skin Bioengineering and the skin. Vol 2 p. 138.

Eichner, R. Kahn, M. Capelola, R.J. Gendimenico, G.J. Mezick, J.A. (1992) Effects of topical retinoids on cytoskeletal proteins: implications for retinoids on epidermal differentiation J Invest Dermatol 98 (2) pp. 154-161.

Elden, Harry R. (1971) In: Biophysical Properties of Skin Chichester, Wiley Interscience.

Elftman, H.O. (1930) A cinematic study of the distribution of pressure in the human foot. In: Lord M (1981) Foot pressure measurement: a review of methodology. J. Biomech. Eng 3. pp. 91-99.

Elias, M. and Fritsch, P.D. (1983) Exfoliation and pathogenesis of blister formation. In: Goldsmith, L. ed. The biochemistry and physiology of the skin. Oxford, Oxford University Press. pp. 1037-1055.

Evans, D.H. McDicken, W.N. Skidmore, R. Woodcock, J.P. (1989) Doppler US in Physics, instrumentation and clinical application Chichester, John Wiley and Sons.

Ferguson, J. (1980) Structural and mechanical properties of human stratum corneum Doctoral thesis. University of Strathclyde.

Fleischer, A.C. and James, A.E . (1980) Introduction to diagnostic sonography Chichester, John Wiley.

Fok, W.C. (1988) Static force measurement of the human foot. Experimental techniques vol 2. pp.16-17.

Fraser, R.D.B. and Macrae, T.P. (1980) Molecular structure and mechanical properties of keratins. In: The mechanical properties of biological materials Symposia of the Society for experimental biology no XXXIV. Cambridge, Cambridge University Press pp. 211-229.

Garson, J.C. Doucot, J. Tsoucaris, G. Leveque, J.L. (1990) Study of lipid and non-lipid structures in human stratum corneum by Xray diffraction J Soc Cosm Chem 41. pp. 347 - 358.

George, B. and McIntyre, P. (1987) Analytical Chemistry by Open Learning: Infrared Spectroscopy. Chichester, John Wiley and Sons.

Gillott, H. (1985) Quantifying the fit of a hand orthosis. Care 1(1). pp. 12-17.

Gloor, M. Willebrandt, U. Thomas, G. Kupferschmid, W. (1980) Water content of the horny layer and skin surface lipids. Arch. Dermatol. Res. 268. pp. 221-223.

Gordon, J.E. (1980) Biomechanics: the last strong-hold of vitalism. In: The mechanical properties of biological materials. Symposia of the Society for experimental biology no XXXIV. Cambridge, Cambridge University Press. pp. 1 - 14.

Graham-Brown, R. and Burns, T. (1990) Lecture notes on dermatology. London, Blackwell Scientific Publications.

Greer. N, Hamill, J. Campbell, K. (1988) Ground reaction forces in childrens' gait. J. Biomech. vol 21. pp.879.

Grieve, D.W. (1980) Monitoring gait. Br. J. Hosp.Med 24 (13) pp.198-204.

Gross, T. and Bunch, R.P. (1988) Measurement of discrete in-shoe stress with piezoelectric transducers. J. Biomed. Eng. 10 pp. 261-264.

Haftek, M. Serre, G.M. Mils, V. Thivolet, J .(1991) Immunocytochemical evidence for a possible role of cross-linked keratinocyte envelopes in stratum corneum cohesion. J. Histochem-cytochem. 39 (11) pp. 1531-1538.

Hancock, R. ed. (1987) Illustrated Encyclopaedia of science and technology 6th edition vol 17 New York, McGraw Hill.

Harkiss, K. (1985) Cheaper in the long run. Pharmaceutical J. 31 pp. 268 -269.

Harris, R.I. and Beath, T. (1947) Army foot survey. An investigation of foot ailments in Canadian soldiers. In: Lord, M. (1981) Foot pressure measurement: a review of methodology J. Biomed. Eng. 3 pp. 91-99.

Harrison, S.M. Barry, B.W. Dugard, P.H .(1984) Effects of freezing on human skin permeability J. Pharm. Pharmacol. 36 pp. 261-262.

Heilmann, B.B. Rychmanns, F. Plewig, G. (1983) SEM of human corneocytes. In: Marks, R. Plewig, G. eds. The Stratum Corneum Berlin. Springer-Verlag. pp 134-145.

Hennenberg, M. and Silberberg, A. (1984) Kinetorheological aspects of biorheology. Biorheology 21 pp. 437-443.

Henig, E.M. and Rosenbaum, J. (1991) Pressure distribution patterns under the feet of children in comparison with adults. Foot and ankle 11(5) pp. 306-311.

Henig, E.M. Cavenagh, P.R. Albert, H.T. Macmillan, N.H. (1982) A piezoelectric method of measuring vertical contact stress beneath the human foot. J. Biomed. Eng. vol 4 pp. 213-221.

Hey, M.J. Taylor, D.J. Derbyshire, W. (1978) Water sorption by human callus Biochimica et Biophysica Acta 540. pp. 518-533.

Heylings, D.J. (1988) Observations on a static footprint using the Musgrave foot print apparatus. The Chiropodist vol 43 (5) pp. 81-87.

Higuchi, T. and Tillman, W.J. (1965) Stress-relaxation of stretched callus strips Arch. Environ. Health vol 11. pp. 508-521.

Hill, J. (1991) Unilever. Personal communication.

Hughes, J. (1988) The assessment of patients with foot problems using the pedobarograph. Clinical Rehab vol 2. pp. 51-60.

Hughes, J. Clark, P. Jagoe, J.R. Gerber, C. Klenerman, L. (1991) The pattern of pressure distribution under the weight bearing forefoot, The Foot vol 1 (3) pp.117-124

Hume, J. (1985) Keratinocyte proliferative hierarchies confer protective mechanisms in surface epithelia. Br. J.Dermatol. 112. pp. 493-502.

Hutton, W.C. and Dhanedran, M. (1981) The mechanics of normal and abnormal hallux valgus feet - a quantitative study. Clin. Orthop. 157 pp. 7-13

Inman, V. Ralston, H. Todd, F. (1981) Human walking. Baltimore and London, Williams and Wilkins.

Jemec, G. Jemec, B. Serup, J. (1986) The effect of superficial hydration on the rheology of human skin in vivo. Bioengineering and the Skin vol 2 p. 194.

Johanson, D.C. and Maitland, A.E. (1981) Lucy: the beginnings of humankind. London, Granada.

Kaliszer, M. O'Flanagan, S. McCormack, B. Mulhall, J. Heavey, A. Shehan, J. (1989) Setting the baseline parameters for clinical assessment of foot to ground contact using the Musgrave pressure plate system. J. Biomech. Eng. vol 11 pp. 30-34.

Kemp, J. and Winkler, T. (1983) Problems a foot: need and efficiency in foot care. London, Disabled Living Foundation.

Knapp, A.C. Franke, W.W. Heid, H. Hatzfeld, M. Jorcano, J.L. Moll, R.. (1986) Cytokeratin no. 9, an epidermal type I keratin characteristic of a special programme of keratinocyte differentiation displaying body site specificity. J. Cell Biol. 103 pp. 657-667.

Krebs, B.E. Eldelstein, J.E. Fishman, S. (1985) Reliability of observational kinematic gait. Physical Therapy 65 pp. 1027-1033.

Laden, K. and Morrow, R. (1970) Torsional measurements in skin. J. Soc. Cosmet. Chem. 21 pp. 417-425.

Laforest, Nicholas Laurent (1782) L'Art de Soigner les Pieds (*The art of caring for the feet.*) Ch 8. 2nd edition. Paris.

Lang, L.M.G. (1990) A longitudinal study of lower limb growth in infants. Doctoral Thesis, CNAA.

Lavker, R.M. Zheng, P.S. and Dong, G. (1989) Morphology of aged skin Clin. Geriatr. Med. 5 (1) pp. 53-67.

Leveque, J.L. Corcuff, P. de Rigal, J. Agache, P. (1984) In vivo studies of the evolution of physical properties of the human skin with age. Int. J. Dermatol. vol 23 (5) pp. 322-329.

Leveque, J.L. and Rasseneur, L. (1988) Mechanical properties of stratum corneum: influence of water and lipids. In: Marks, R. Edwards, C. and Barton, C. eds. The Physical Nature of Skin Lancaster, MTP pp. 155-162.

Leveque, J.L. (1991) Presentation at conference. Non-invasive skin measurement. Royal Marsden Hospital. MRI and skin imaging.

Leveque, J.L. Ribaud, C. Garson, J.C. (1992) (Biophysical characteristation of the stratum corneum. Relationship between structure and properties. Pathol. Biol. (Paris) 40 (2). pp. 95-108.

Lord, M. (1981) Foot pressure measurement: a review of methodology J. Biomed. Eng. 3 pp. 91-99.

Lundstrom, A. and Torbjorn, E. (1990) Evidence that cell shedding from plantar stratum corneum in vitro involves endogenous proteolysis of the desmosomal protein desmoglein I. J. Invest. Dermatol. 94 (2) pp. 216-220.

McKay, I.A . and Leigh, I .M. (1991) Epidermal cytokines and their roles in cutaneous wound healing. Br.J .Dermatol. 124. pp 513-518

Mackenzie, I.C. (1983) Effects of frictional stimulation of the structure of the stratum corneum. In: Marks, R. and Plewig, G. eds. The Stratum Corneum Berlin-Heidelberg, Springer-Verlag pp. 153-160.

Mackey, S. and Chung, T.K. (1969) Considerations in the analysis of raft foundations. Civil Engineering and Public Works Review. September pp. 877-885.

Manabe, M. Sanchez, M. Sun, T.T. Dale, B.A. (1991) Interaction of filaggrin with keratin filaments during advanced stages of normal human epidermal differentiation and in ichthyosis vulgaris. Differentiation 48 (1) pp. 43-50.

Mandy, P. (1988) An investigation into the effect of peripheral vascular disease on skin thickness. Bioengineering and the skin 4 pp. 323-332.

Manschott J and Brakkee A (1986) The measurement and modelling of the mechanical properties of human skin in vivo. I The measurement. J. Biomech. 19 (7) pp. 511-515.

Marks, F. Bertsch, S. de Brave, M. Furstenberger, G. (1981) Studies on the trigger mechanism of epidermal hyperplasia. In: Marks, R. and Christophers, E. eds. The Epidermis in Disease. Lancaster, MTP Press Ltd pp. 193-210.

Marks, R. (1992) University of Wales, College of Medicine. Personal communication.

Marriott, C. (1992) Kings College London. Personal communication.

Marriott, C. (1990) The role of mucous glycoproteins in the rheologic properties of cystic fibrosis sputum Am. Rev. Respir. Dis. 142 (5) pp. 1053-1058.

Messenger, N. and Bowker, P. (1986) The role of gait analysis in clinical medicine: a survey of UK centres Eng. Med. vol 16 no 4 pp. 221 - 227.

Michel, S. Schmidt, R. Shroot, B. Reichert, U. (1988) Morphological and biochemical characterisation of the cornified envelopes from human epidermal keratinocytes of different origin J. Invest. Dermatol. 91 (1) pp. 11-15

Middleton, J.D. (1968) The mechanism of water binding in stratum corneum Br. J. Dermatol. 80 pp. 437-450

Miller, G.F. and Stokes, I.A.F. (1979) A study of the duration of load bearing under different areas of the foot. Eng. Med. vol 8 (3) pp. 128-132

Miller, R.G.J. and Stace, B.C. eds (1972) Laboratory Methods in Infrared Spectroscopy. London, Heyden and Son Ltd.

Morris and Shamos (1967) Piezoelectricity as a fundamental property of biological tissue. Nature 21 pp. 267-269.

Morton, D.J. (1930) Structural factors in stasis disorders of the foot. In: Lord M (1981) Foot pressure measurement: a review of methodology. J. Biomed. Eng. 3 pp. 91-99.

Morton, D.J. (1935) The Human Foot. New York, Columbia University Press.

Nakamura, A. Crowninshield, R. Cooper, R. (1981) An analysis of soft tissue loading in the foot; a preliminary report. Bull. Prosth. Res. vol 18 (19) pp. 10-35.

Nessi, R. Blanc, M. Bosco, M. Dameno, S. Venegoni, A. Betti, R. Bencini, P.L. Crosti, C. Uslenghi, C. (1991) Skin ultrasound in dermatologic surgical planning. J. Dermatol. Surg. Oncol. 17 (1) pp. 38-43.

Neville, A. (1990) University of Kent. Personal communication.

Neville, A. (1991) Doctoral thesis. Development of an in-shoe gait analysis instrument University of Kent.

Nigg, B. and Skleryk, B. (1988) Gait characteristics of the elderly. Clin. Biomech 3 pp. 79-87.

O'Brien. (1981) Quantitative acoustical assessment of wound maturation and acoustic microscopy J. Acoustic Soc. Amer. 69 pp. 575-579.

Querleux, B. Yassine, M.M. Darasse, L. St Jalmes, H. Sauzade, M. Leveque, J.L. (1986) Magnetic Resonance Imaging of the skin. A comparison with the US technique. Bioengineering and the skin p. 136.

Orfanos, C.E. Mahrle, G. Ruska, H. (1971) Callus and its keratin before and after treatment with acid sodium thioglycolate Br. J. Dermatol. 85 pp. 437-449.

Payne, P.A. (1985) Medical and industrial applications of high resolution US J. Phys. Sci. Instrum. 18 pp. 465-472.

Payne, P.A. (1985) Application of ultrasound in dermatology Bioengineering and the Skin 1 pp. 293-320.

Payne, P.A. (1988) Skin imaging a comparison of available techniques in: Marks, M. Barton, S.P. Edwards, C. eds. The Physical Nature of Skin Lancaster, MTP pp. 31-46.

Peters, M. and Durding, B. (1979) Footedness of left- and right handers Am. J. Psychol. vol 42 (1) pp. 133-142.

Phillips, G. (1992) University of Brighton. Personal communication.

Potter, M. (1992) University of Brighton, personal communication.

Potts, R.O. Breuer, M. (1981) The mechanical spectrum of skin. I The experimental technique and measurements at room temperature. J. Soc. Cosmet. Chem. 32 pp. 339-353.

Potts, R.O. Chrisman, D.A. Buras Jr, E.M. (1983) The dynamic mechanical properties of human skin in vivo. J. Biomech. vol 16 (6) pp. 365-372.

Potts, R.O. Guzek, D.B. Harris, R.R. McKie, J.E. (1985) A non-invasive, in vitro, technique to quantitatively measure water content of the stratum corneum using attenuated total reflectance infrared spectroscopy. Arch. Dermatol. Res. 277 pp. 489 - 495.

Potts, R. (1986) Stratum corneum hydration: experimental techniques and interpretation of results J. Soc. Cosmet. Chem. 37 pp. 9-33.

Potts, R.O. and Francoeur, M. (1990) Lipid biophysics of water loss through the skin Proc. Nat. Acad. Sci. USA 87 pp. 3871-3873.

Potts, R.O. (1991) Presentation at MMM meeting Southampton Lipid -free volume fluctuations, permeant size and stratum corneum permeability.

Radin, E. Yang, K. Whittle, M. Jefferson, R. O'Connor, J. (1987) The generation and transmission of the heel strike transient and the effects of quadricepts paralysis. In: Conference Procedings. Gait analysis and medical photogrammetry. Oxford, Oxford Orthopaedic Engineering Centre, pp. 34-35

Ranu, H.S. (1989) A quantitative method of measuring the distribution of forces under the different regions of the human foot during normal and abnormal gait Eng in Med and Biol Sc 11th Annual International Conference. Biomechanics of upper and lower extremity.

de Rigal, P. Escoffier, G. Querleux, B. Leveque, J.L. (1989) Skin thickness versus age: a comparative approach. Bioeng. and Skin 3 pp. 160.

Rippon, M. Springett, K. Walmsey, M. (1991) Presentation at Second International Congress. Ultrasound and the skin.

Roberts, M. and Walker, M. (1993) Water. The most natural penetration enhancer. In: Transdermal Drug Delivery systems - series of books. NY, Marcel Dekker. Awating publication.

Root, W. Weed, G. and Orien, R. (1977) Biomechanical examination of the foot Los Angeles, Clinical Biomechanics Corporation.

Rose, N. Lawrence, A.F. Cracchiolo, A. (1992) A method for measuring foot pressures using a high resolution computerised insole sensor: the effect of heel wedges on plantar pressure distribution and centre of force. Foot and Ankle vol 13 (5) pp. 263-270.

Ross, H. and Romrell, L.M. eds (1989) Histology. Text and Atlas. London, Williams and Wilkins.

Roy, K.J. (1988) Force pressure and motion measurements in the foot: current concepts. Clin. Pod. Med. Surg. 5 (3) pp. 491-508.

Saleh, M. and Murdock, G. (1985) In defence of gait analysis: observation and gait assessment. J. Bone Joint Surg.(Br.) 67 (2) pp.237-241.

Salter, D. Hodgeson, R.J. Hall, L.D. Carpenter, T.A. Ablett, J. (1992) Moisturisation processes in living human skin studied by Magnetic Resonance Imaging Microscopy. Presentation at Non-invasive imaging of the skin meeting, Royal Marsden Hospital, London.

Samman, P. and Fenton, D. (1986) The nails in disease 4th edition. London, Heinemann Medical Books

Savage, A. and Jordan, C. (1986) Are hydrogel dressings here to stay? Br. J. Pharmaceutical Practice pp. 258 - 264.

Shuster, S. Black, M. McVitie, E. (1975) The influence of age and sex on skin thickness, skin collagen and density. Br. J. Dermatol. 93 pp. 639-643.

Scott-Blair, G.W. (1974) An introduction to Biorheology. Amsterdam, Elsevier Scientific Publishing Co.

Scranton, P.E. and McMaster, J.H. (1970) Momentary distribution of forces under the foot. J. Biomech. vol 9 pp. 45-48.

Seddon, John. M. (1990) Structure of the inverted hexagonal (H 11) phase and non-lamellar phase transitions of lipids. Biochimica et Biophysica Acta 1031 pp. 1-69.

Serup, J, (1991) Gentofte Hospital, Copenhagen, Denmark. Personal communication.

Silvino, N. Evanski, P. Waugh, T. (1980) The Harris and Beath foot printing mat: diagnostic validity and clinical use. Clin. Orthop. 151 pp. 265-269.

Simkin, A. and Stokes, I.A.F. (1982) Characterisation of the dynamic vertical force distribution under the foot Med. Biol. Eng. Comput. 20 pp. 12-18.

Simmonite and Scholl PLC (1992) University of Brighton. Personal communication.

Smith, L. (1989) Histopathologic characteristics and ultrastructure of ageing skin. Cutis 42 (5) pp. 414-424.

Soames, R.E. Blake, C.D. Stott, J.R.P. Goodbody A, Brewerton DA (1982) Measurement of pressure under the foot during function. Med. Biol. Eng. Comput.30 pp. 489-495.

Spencer, T.S. Linamen, C.E. Akers, W.A. Jones, H.E. (1975) Temperature dependence of water content of stratum corneum. Br. J. Dermatol. 93 pp. 159-164

Spencer, T. (1976) Water and the horny layer. J. Soc. Cosmet. Chem. 27 pp. 63-72

Sperryn, P.N. and Williams, J.G.P. eds (1982) Sports Medicine. London, Edward Arnold,

Springett, K. (1987) Corns and calluses Mims Magazine March 1 pp. 26 - 30

Steinert, P. and Cantieri, J. (1983) Epidermal keratins. In: Goldsmith, L. ed. Biochemistry and Physiology of the skin. Oxford, Oxford University Press pp 135-169

Sternill, S. and Kalmar, J.R. (1986) Organic structures from spectra. Chichester, J Wiley and Sons

Stewart, T.P. and Grove, M. (1989) Interface pressure sensor systems and correlation of one with another. Eng. Med. Biol. Sc. 11th Annual International Conference Rehab Engineering.

Stokes, I.A.F. (1975) An analysis of the forces on normal and pathological feet. Doctoral thesis. CNAA.

Stubbs, D.A. (1982) Back problems in work and leisure. Physiotherapy 68 (6) pp. 174-176.

Tagami, H. Iwase, Y. Yoshikuni, K. Inoue, K. Yamada, M. (1988) Water sorption-desorption test of stratum corneum of the skin. In: Marks, R. and Plewig, G. eds. The Stratum Corneum. Berlin, Springer-Verlag.

Tan, C.Y. Marks, R. Payne, P.A. (1981) Comparison of xeroradiographic and ultrasound detection of corticosteroid induced dermal thinning. J. Invest. Dermatol. 76 pp. 126-128.

Tan, C.Y. Statham, B. Marks, R. Payne, P.A. (1982) Skin thickness measurement by pulsed ultrasound, its reproducibility, validation and variability. Br. J. Dermatol. 106 pp. 657-667.

Tappin, J.W. Pollard, J. Beckett, A. (1980) A method of measuring shearing forces on the sole of the foot. Clin. Phys. Physiol. Meas. 1 (1) pp. 83-85.

Thomas, S. (1987) University of Wales, College of Medicine. Personal communication.

Thomas, S. Dykes, P. Marks, R. (1985) Plantar hyperkeratosis: A study of callosities and normal plantar skin. J. Invest. Dermatol. 85 pp. 394-397.

Tollafield, D.R. and Price, M. (1985) Hallux metatarsophalangeal joint survey related to post-op surgery analysis. The Chiropodist vol 40 (9) pp. 284-288.

Tomlinson, M.J. (1986) Foundation Design and Construction. 5th ed. Harlow, Longman Scientific and Technical.

Triebskorn, A. Gloor, M. Greine, F, (1983) A comparative investigation of the water content of the stratum corneum using different methods of measurement. Dermatologica 167 pp. 64-69.

Spencer, T.S. Linamen, C.E. Akers, W.A. Jones, H.A. (1975) Temperature dependence of water content of stratum corneum. Br. J. Dermatol. 93 pp. 159-164

van Duzee, B. (1978) Influence of water content, chemical treatment and temperature on the rheological properties of stratum corneum. J. Invest. Dermatol. 71 (2) pp. 140-144.

Vincent, J. (1984) Structural Biomaterials. London, Macmillan Press.

Vogel, H.G. (1988) Age dependant mechanical and biochemical changes in the skin. Bioeng. Skin 4 pp. 75-81

Walling, P. and Dabney, J. (1989) Moisture in skin by near IR reflectance spectroscopy. J. Soc. Cosmet. Chem. 40 pp. 151-171.

Wells, P.N.T. (1979) Ultrasound in clinical diagnosis. London, Churchill Livingstone pp. 111-117.

Wertz and Downing (1989) The stratum corneum. In: Hadgraft, J. and Guy, R. eds. Transdermal Drug Delivery systems. New York, Marcel Dekker. pp. 1 - 22.

West, S. (1987) A review of methods of obtaining foot loading data during walking. The Chiropodist 42 pp. 84-95.

Whiting, M.F. (1987) Survey of corn and callus incidence in the working population of Eastbourne (employees of the areas largest organisation). Protected data, Scholl PLC.

Wildnauer, R. Bothwell, J. Douglass, A. (1971) Stratum corneum biomechanical properties 1. Influence of relative humidity on normal and extracted human stratum corneum J. Invest. Dermatol. 56 (1) pp. 72-78.

Wilkes, G.L. Brown, I.A. Wildnauer, R.H. (1973) Biomechanical properties of skin CRC critical reviews in Bioengineering August. pp. 453-495.

Wilkins and Dorogi (1986) Snake skin/gelatin model for interpretation of viscoelasticity measurements on human skin. Bioeng. skin p 129.

Williams, Dudley H. and Flemming, I. (1980) Spectroscopic methods in organic chemistry . UK. McGraw- Hill Book Company Ltd.

Wood, E.J. and Bladon, P.T. (1987) The Human Skin. Studies in Biology no. 164 London, Edward Arnold.

Wright, N.A. (1983) The cell proliferation kinetics of the epidermis. In: Goldsmith, L. ed. The biochemistry and physiology of the skin. Oxford, Oxford University Press pp. 203-229.